PREDICTING THE ANCIENT OCCURRENCE OF EVAPORITES USING PALEOCLIMATE MODELLING

by

AMIRATU YAMUSAH

Presented to the Faculty of the Graduate School of

The University of Texas at Arlington in Partial Fulfillment

of the Requirements

for the Degree of

MASTER OF SCIENCE IN GEOLOGY

THE UNIVERSITY OF TEXAS AT ARLINGTON

December 2011

DEDICATION

This work is dedicated to my parents Mr. and Mrs. Yamusah for their unflinching support, love and encouragement throughout my life. To my brothers Ramzi and Salma Yamusah for the inspiration they gave me throughout the writing process. To my husband Robert Sarkodee for being patient while I pursued my dream and to my dear daughter Evaflorence for bringing along the motivation I needed to complete this research. I love you all dearly.

ACKNOWLEDGEMENTS

I would first of all like to thank God for giving me the wisdom needed to pursue this degree, for good health throughout the years and for peace of mind. Dr. Christopher Scotese, my supervisor has been of great help throughout my research and writing process. I can't thank him enough for all the knowledge I have acquired with regards to climate and evaporites while working with him. I would like to thank Tom Moore for his help in getting this research up and running by providing valuable information.

I would also like to thank Arghya Goswami for his help and support with my many GIS and programming questions. A big thank you goes to my parents for their financial, physical and emotional support throughout these years especially my mum who is my rock and my grandmother Gladys Newman. Lastly, I would like to thank my husband Robert for putting up with the many months that I was away from home, his continual encouragement and support. This research would not have been possible without all of your support. Thank you.

November 21, 2011

ABSTRACT

PREDICTING THE ANCIENT OCCURRENCE OF EVAPORITES

USING PALEOCLIMATE MODELLING

Amiratu Yamusah, M.S.

The University of Texas at Arlington, 2011

Supervising Professor: Christopher Scotese

Evaporites are climatic indicators that depend on two main variables: mean annual temperature and mean annual precipitation. This study constructs a model that predicts the localities of ancient evaporites based on paleo- temperature and paleo- precipitation data. A climate envelope, a bivariate plot of temperature and precipitation, is constructed by intersecting the modern temperature and precipitation with climate data obtained from Fast Ocean Atmosphere Model (FOAM). Modern evaporites have a limited extent hence in this research, the Yermosols- Solonchak soil type was used as a proxy. The predictions were made for 16 time intervals. These were plotted on paleogeographic reconstructions obtained from the PALEOMAP Project. The predicted locations of evaporites were compared to the distribution of ancient evaporites.

The statistical results observed show that there was a good agreement between the predicted and the observed distribution of evaporites. This may suggest that the climate envelope technique makes good predictions for the Cenozoic Era, Mesozoic Era and for some of the intervals of the Paleozoic Era. It was observed that the distribution of evaporites for these time intervals coincided with the climates that existed at these times.

TABLE OF CONTENTS

LIST OF ILLUSTRATIONS

LIST OF TABLES

CHAPTER 1

EVAPORITES

1.1 Introduction

1.1.1 Formation of Evaporites

Evaporites are important sedimentary rocks that have been studied extensively through time. They typically form in arid to semi- arid climatic settings and require a surface or near surface brine body (marine or non- marine) that is saline enough to precipitate out this salt rock. They form as a result of the evaporation of the brine. This means that there are two important factors that contribute to evaporite formation: temperature and precipitation. Most evaporites are found within two main belts known as desert belts. These desert belts occur between 15 - 45° North (N) and South (S) of the equator (Figure 1.1). They form largely as a result of the atmospheric circulation of the Hadley cells. The location of subtropical dry zones and tropical/subtropical deserts of the globe are determined by the subsiding branches of the Hadley cells (Lu et al, 2007). Most evaporites occur beneath the cold dry descending air masses of the subsiding branches of the Hadley cells (Crowley and North, 1991). Climate is the underlying factor when it comes to evaporite deposition (Ziegler et al, 1981). Therefore the distribution of evaporites through time should provide a key to the history of aridity on the globe (Frakes, 1979).

Evaporites began forming as early as the Precambrian time period, were most abundant during the Permian and Triassic time periods and are still forming today. The Permian and Triassic evaporites account for almost 35% of the world's evaporite deposits (Trappe, 2000). A further study of evaporites shows that ancient evaporites formed more extensively than modern evaporites are forming presently.

1.1.2 Importance of Evaporites

Two types of evaporites have been identified namely primary evaporites and secondary evaporites. Primary evaporites have been defined as those that mainly form as a result of evaporation from brines at the earth's surface and secondary evaporites are defined as those that form in the shallow subsurface (Warren, 2006). Evaporite minerals are important industrially with some evaporite minerals being used in the production of fertilizer and explosives. Halite is an example of an evaporite mineral that is used in most households and is also known as common salt. Other examples of evaporite minerals include gypsum, fluorite, sylvite and trona.

Evaporites also form an integral part of the petroleum system, because they act as highly effective seals. A lot of the world's oilfields are sealed by evaporites (Grunau, 1987). In the Middle East, Ghawar the world's largest oil field is sealed by bedded evaporites of the Arab formation and the overlying Hith Anhydrite seal (Warren, 2006). Halite formations are famous for their ability to form diapirs which produce ideal locations for trapping petroleum deposits. This makes evaporites very relevant in the petroleum industry (Gordon, 1975). This means that if evaporites can be predicted based on climate data then the existence of possible petroleum deposits that have been sealed by these evaporites can be located.

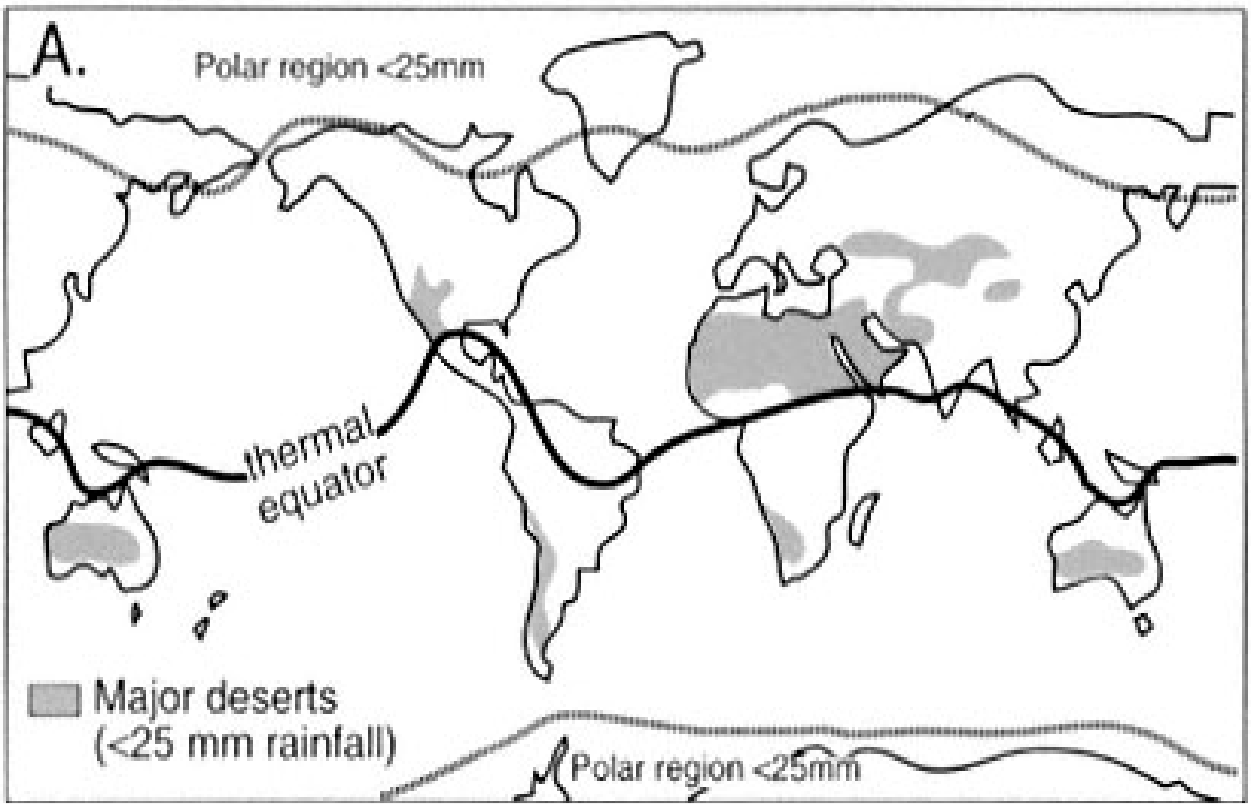

Figure 1.1: World distributions of modern deserts (Warren, 1999).

Therefore the purpose of this study was to predict the possible location of these evaporites across geologic times (Late Cambrian – Late Miocene). The locations of evaporites were predicted using the climate envelope tool (Moore, 2007) and temperature and precipitation data for the various time periods obtained from FOAM global climate model. The prediction was tested by comparing the predicted location of evaporites with that of the observed evaporite occurrence in the rock record (Boucot et al, in press). Both the predicted and the observed evaporites were plotted out on paleoreconstructions obtained from the PALEOMAP Project (Scotese, 2000). A quantitative statistical analysis was used to determine the goodness of fit between the predicted evaporites and the observed evaporites. Only continental evaporites were

analyzed in this research since the observed evaporite data compiled by Boucot et al, in press does not include data from the deep ocean.

Modern day evaporites have a more limited extent than ancient evaporites so in order to create the climate envelope for the evaporites, the Yermosol- Solonchak soil type (Zobler, 1986) was used as a proxy for the conditions under which evaporites are forming in the modern world. The Yermosol- Solonchak soils are sometimes referred to as aridisols (soils of dry regions). In aridisols, evaporation exceeds precipitation and during most years water percolation is minimal (Boul, 1997). Aridisols are mostly covered by sparse, desert type vegetation and form in the same environment as evaporites (Bell, 1998).

1.2 Previous Work

Ancient evaporites formed more extensively than modern evaporites are forming today and most ancient evaporite deposits have thicknesses and areal extents that are two to three orders of magnitude greater than those of Quartenary deposits (Zharkov, 1981). Large volumes of ancient evaporites can be found in places like the Gulf of Mexico (Late Jurassic), Saskatchewan (Late Devonian), Siberia (Mesozoic), Zechstein (Late Permian), Messinian (Late Miocene) and Atlantic Canada (Late Triassic). The Deep Sea Drilling Project (DSDP) led to the discovery that much of the Gulf of Mexico was underlain by evaporites (Ewing et al, 1969). Basinwide evaporites are the largest accumulation of ancient evaporites and can usually be found in depressions as a result of tectonic activity (Warren, 2006). The greatest Phanerozoic accumulation of evaporites corresponds to the time of assembly and breakup of the Pangean supercontinent.

1.2.1 Distribution of ancient evaporites.

The first detailed data on the volume and distribution of evaporite deposits was compiled by Zharkov (1981, 1984). He published data on the location and distribution of Phanerozoic evaporite deposits (Figure 1.2).

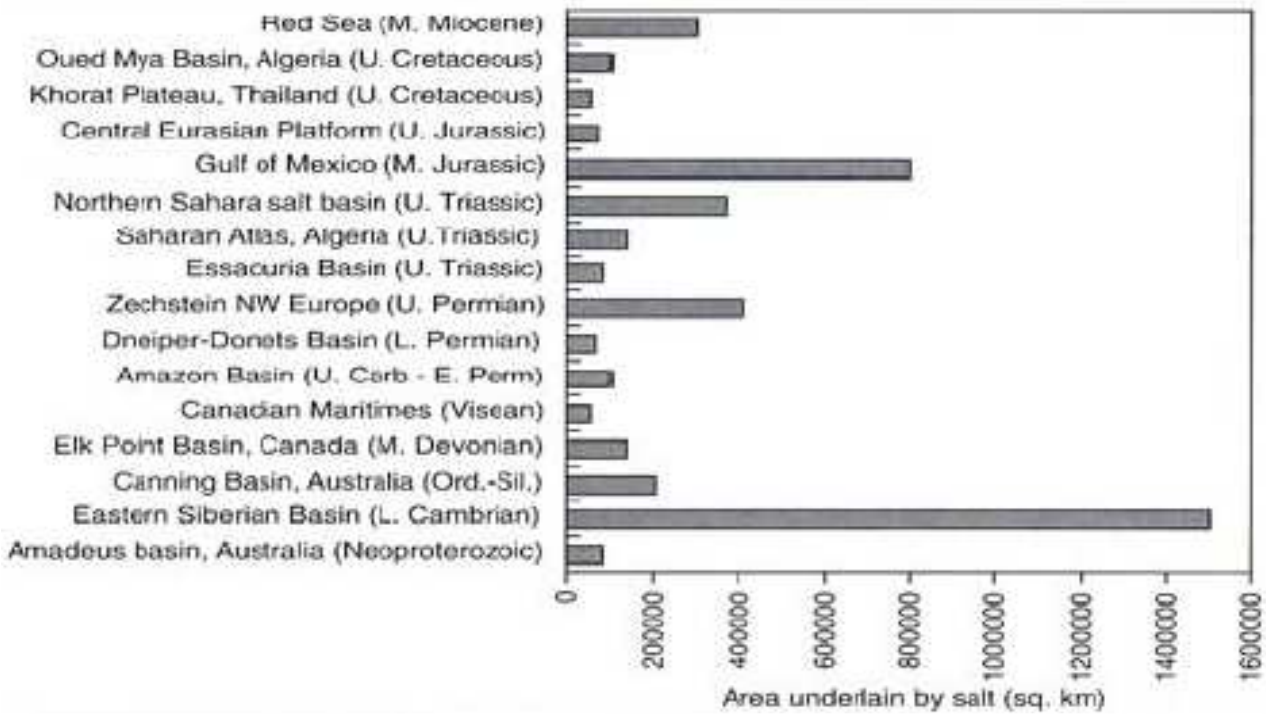

Figure 1.2: This plot shows the areas underlain by salt and various significant evaporite deposits (Zharkov, 1981).

Since Zharkov's compilation of Phanerozoic evaporite deposits, a number of other Phanerozoic evaporite deposits have been described. These include discoveries made on land (in evaporated freshwater lakes) and large deposits of Mesozoic evaporites in the Gulf of Mexico and in the North, Central and South Atlantic and extensive Miocene evaporites underlying broad areas of the Mediterranean, Red Sea and Persian Gulf (Hay et al, 2006). The first comprehensive compilation of evaporite volumes was published by Ronov, 1980 who extracted the data from compilations of sediment volumes and masses for the major geologic intervals of the

Phanerozoic. Hay et al, 2006 noted that the greatest present day volumes of salts are found accumulating within tectonic basins located in the world's desert belts.

Paleoclimatologists have adequately demonstrated over the last twenty years that the distribution of climatically sensitive sediments can be related to present-day climatic zones that are roughly parallel to the latitudes (Parrish et al, 1982). This idea was adapted and used to create the predictions of the evaporite localities using the climate envelope tool. The climate envelope tool is an idea first developed by scientists in the field of ecology and biology where the habitat of a species was defined based a set of climates within which it is believed that an organism can persist (Walker et al, 1991). This idea was adapted by Moore et al, 2007 who defined a climate envelope based on a set of climates within which it is believed that evaporites can persist. He defined his approach as a quantitative technique for describing the occurrence of paleoclimate indicators. Moore's approach was used in this study, using modern day temperature and precipitation values obtained for yermosols and temperature and precipitation values from FOAM to create the climate envelope used for the predictions.

Arghya, Goswami, a student at the University of Texas at Arlington (UTA), assembled some of the data used in this study.

1.3 Presentation of the Data

This study is organized into six chapters. These chapters describe the data used in this research, how the research was performed and the results obtained. ArcGIS together with paleogeographic maps and the results from FOAM paleoclimate model were used to construct and analyze the data. The first part of the study which is Chapter 2 talks about the data and the

methodological approach used. It also explains to the reader the exact steps and data analysis carried out throughout this research.

Chapter 3 briefly outlines the tectonics and climate for the Cenozoic Era and also analyzes the results and statistics obtained. Chapter 4 briefly outlines the tectonics and climate for the Mesozoic Era and also analyzes the results and statistics obtained. Chapter 5 briefly outlines the tectonics and climate for the Paleozoic Era and also analyzes the results and statistics obtained. The final chapter, Chapter 6 discusses the results obtained for each time period. It also discusses the statistics obtained and whether the predictions provide a good fit for the various time periods.

CHAPTER 2

METHODOLOGY

Climate simulations have made it possible to examine the climates of the past and compare the results to modern climates. Since evaporites are indicators of past climates, they can be used to evaluate the results of paleoclimate models. Evaporite deposits are common in the geologic record (Warren, 2006). However, ancient evaporites formed more extensively in the past than they do today. This is largely due to the fact that shallow, epeiric seas were more widespread in the past. Because of the lack of available modern evaporite deposits, in this thesis, yermosols, soils that form in arid conditions were used as a proxy for ancient evaporites. This chapter describes how the yermosol data was acquired, analyzed and how the maps predicting the ancient geographic distribution of evaporites were made for each time period.

2.1. Data Acquisition and Analysis

Information about the modern geographic distribution of arid soils was obtained from the Zobler Soil Database, downloaded from the Oak Ridge National Laboratory Distributed Active Archive Center Oak Ridge Tennessee, USA (Zobler, 1999). The Zobler soil dataset consists of latitude and longitude coordinates (1°x1° grid) for all the identified soil types under the FAO Soil Classification System (26 soil types).

Different soil types form in different climatic regimes. The Yermosol- Solonchak soil type tends to form in arid to semiarid regions (Retallack, 2001) that are characterized by high

temperatures (21°C to 28°C) and low rainfall (0 to 5mm/month). These are the same conditions necessary for evaporite formation.

Temperature and precipitation values for each modern yermosol locality were obtained from the Legates and Willmott Global Climate Database (Legates & Willmott, 1999). Mean annual temperature (MAT) values were calculated from monthly mean temperatures (Figure 2.1). The mean monthly precipitation (MMP) (cm/month) was also calculated in a similar fashion (Figure 2.2). The result was an Excel spreadsheet that contained the following information for each yermosol locality: latitude, longitude, MAT and MMP. We will refer to this dataset as the Yermosol Temperature and Precipitation Dataset (YTPD). A complete listing of the MAT and MMP values obtained from the Legates & Willmott database is given in Appendix A. A complete listing of all yermosol localities and the associated MAP and MMP values is also given in Appendix B.

2.2. Data Analysis in ArcGIS

The yermosol temperature and precipitation data were imported into ArcGIS and plotted in modern geographic coordinates (Figure 2.3) Most of the yermosols are found in the world's desert regions such as North Africa, Australia, Arabia, western North America, southwest South America and in Central Asia (compare Figure 2.3 with Figure 2.4).

A bivariate plot of modern temperature and precipitation is shown in Figure 2.5. The figure on the left (Figure 2.5A) is a scatter plot of the temperature and precipitation values for all yermosols localitites. The figure on the right (Figure 2.5B) shows the relative density of the yermosol data. It should be noted that the highest density contours (red- orange colors) occurs at high temperatures (21°C -28°C) and low precipitation (0-5mm/month).

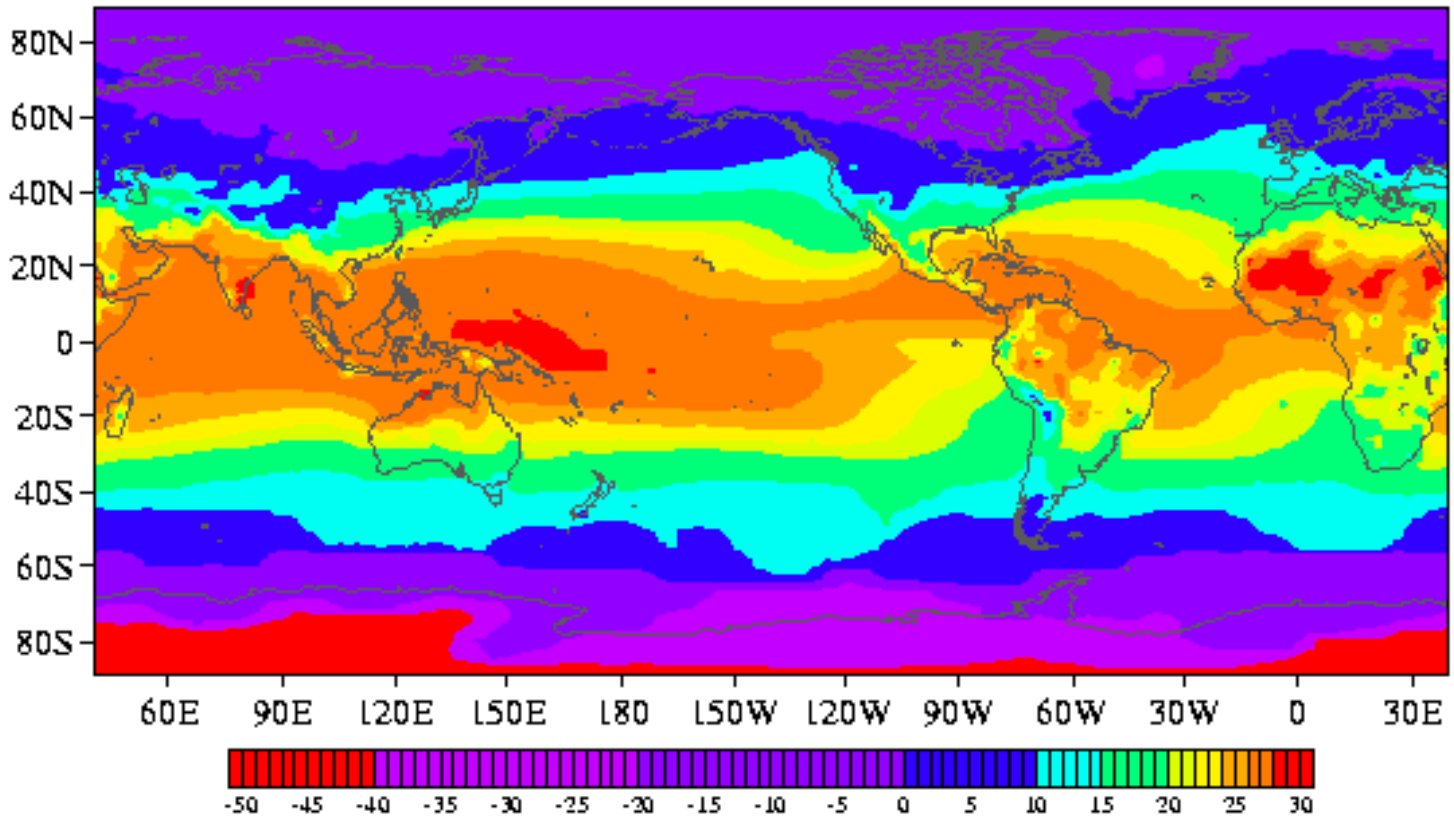

Figure 2.1: Mean Annual Temperatures ranging from < -50°C in Antarctic to < 30°C in the Pacific and Sahara desert regions.
Website: http://jisao.washington.edu/data/legates/

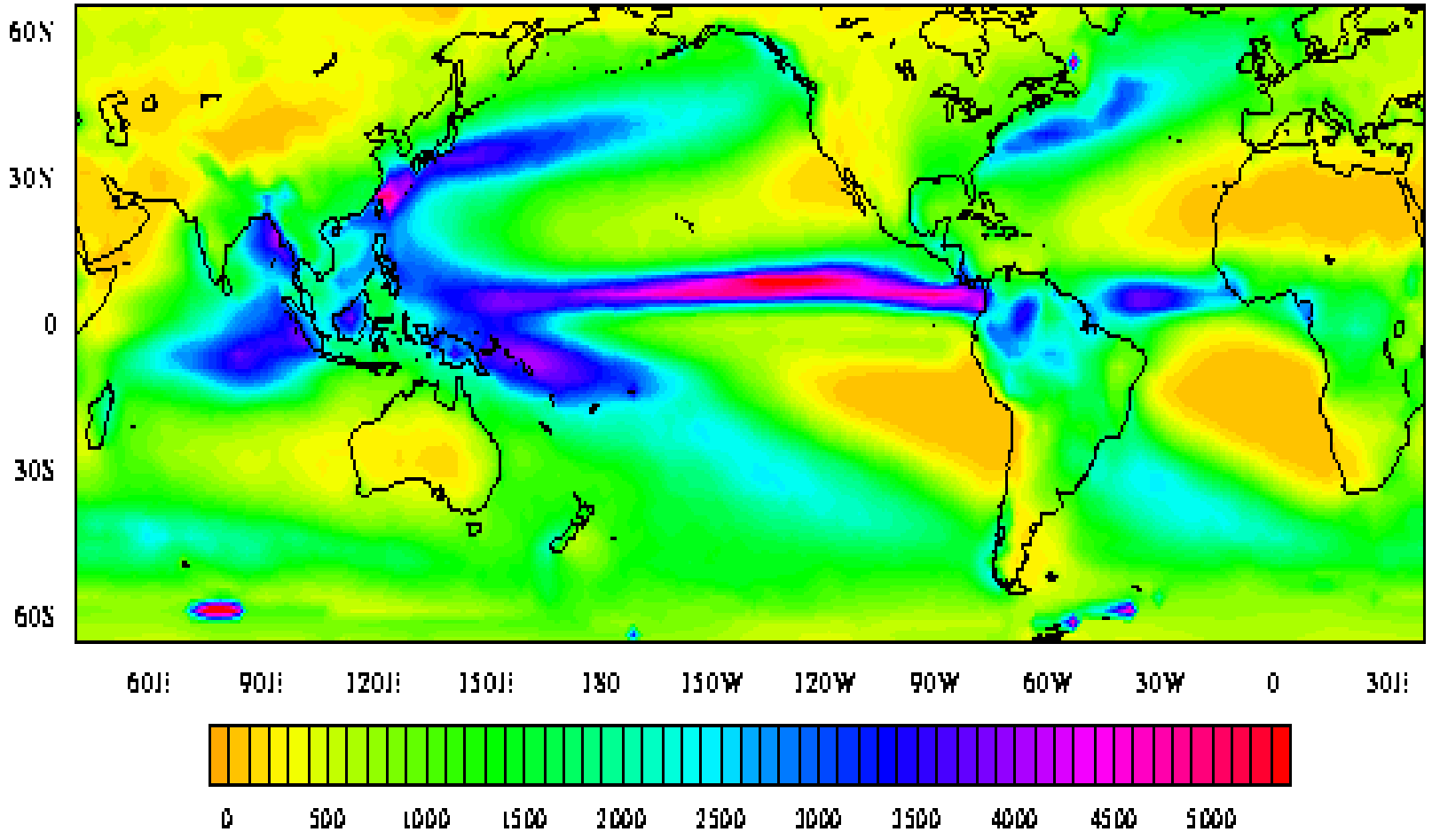

Figure 2.2: Mean Monthly Precipitation ranging from 0 mm/month to < 5000 mm/month.
Website: http://jisao.washington.edu/legates_msu/

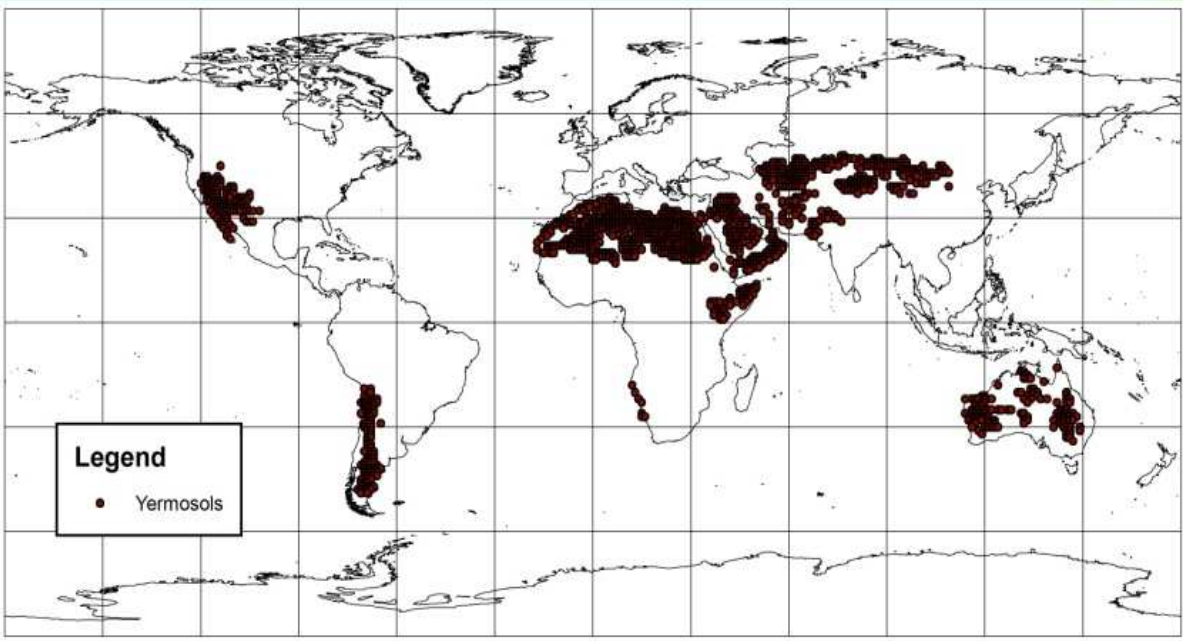

Figure 2.3: This shows the modern day distribution of yermosols (After Zobler, 1999)

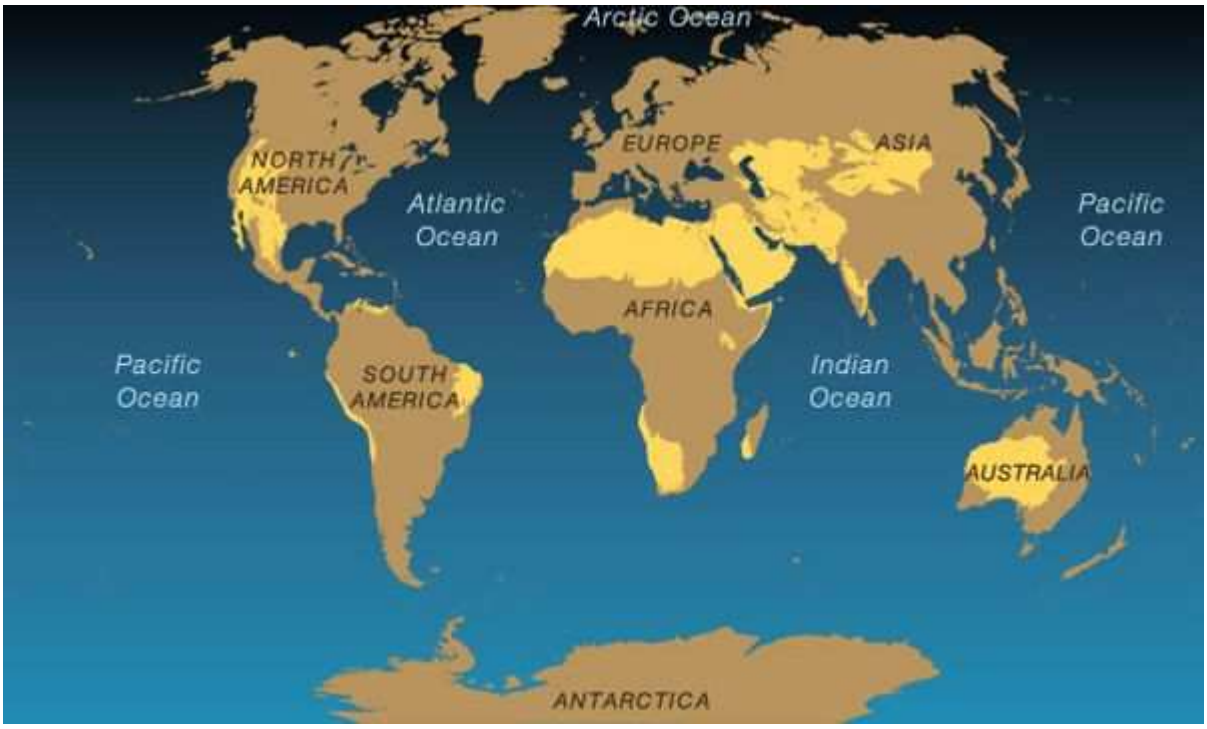

Figure 2.4: World's major desert regions
Website:http://www.worldmapcenter.com/2011/07/map-of-world-deserts/

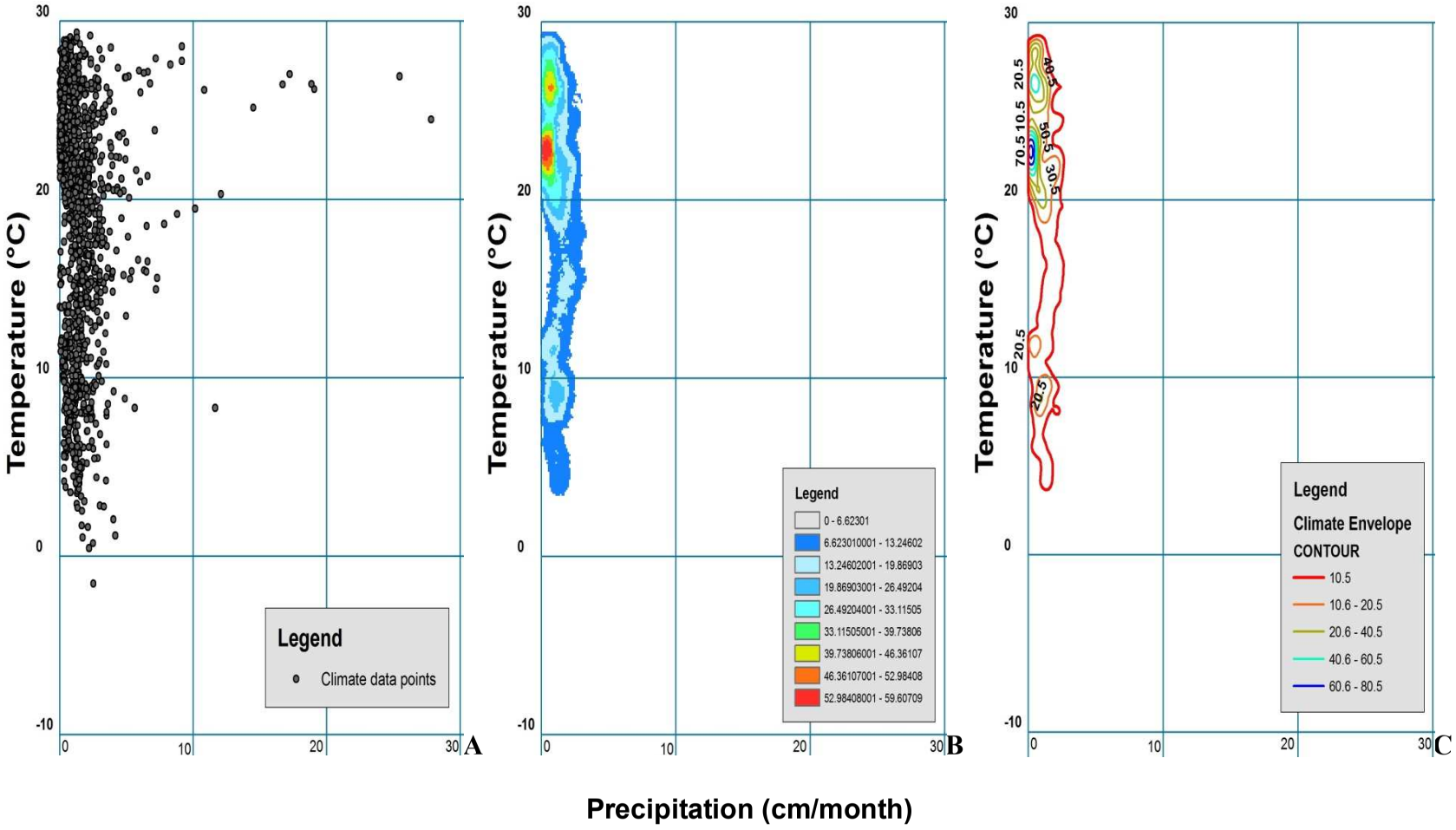

Figure 2.5: Figure A shows the scatter plot of the temperature and precipitation for all yermosols localities while figure B shows the density plot for the yermosols data. Figure 2.5C shows the contour plot for the relative density obtained with the outline for the climate envelope highlighted in red.

The ArcGIS Spatial Analyst tool was used to create a density plot of the yermosol data points (Figure 2.5B). This density plot shows that most yermosol localities occur at high temperatures (21°C-28°C) and low precipitation (0-5 mm/month). Contours were constructed using a gridded raster of temperature and precipitation values. A contour interval of 10 was chosen with a base contour of 0.5 to help smooth out the edges of the contours. The density contour values ranged from 0.5 to 80.5. A contour value of 50, for example, indicates that for any temperature and precipitation value within that contour interval there are on average 50 yermosol localities that exhibit that particular temperature and precipitation.

The outermost contour signifies a data density greater than 10.5 (Figure 2.5C) and has been used to define the yermosol "climate envelope". In other words more than 90% of all yermosol soil localities occur at temperature and precipitation values that fall within the yermosol "climate envelope". In the following section we describe how this climate envelope was used to predict the paleogeographic locations that would most likely favor the formation of ancient evaporite deposits. Because we propose that yermosols are a suitable proxy for evaporites, we will refer to this climate envelope as the Evaporite Climate Envelope.

2.3. FOAM Paleoclimate Simulation Data

Paleoclimate simulations described in this section were produced as part of the GANDOLPH Project (Scotese 2007, 2008, 2009, 2011). In this study the Fast Ocean and Atmosphere Model (FOAM) was used to simulate paleoclimatic conditions for 16 time intervals namely the Late Miocene (10 ma), Oligocene (30 Ma), Middle Eocene (45 Ma), Cretaceous/Tertiary Boundary (70 Ma), Cenomanian/Turonian (90 Ma), Aptian/Albian (120

Ma), Barremian/Berriasian (140 Ma), Late Jurassic (160 Ma), Early Jurassic (180 Ma), Late Triassic (220 Ma), Permo-Triassic Boundary (250 Ma), Early Permian (280 Ma), Mississippian (340 Ma), Late Devonian (360 Ma), Siluro-Devonian (400 Ma) and Late Cambrian (480 Ma).

FOAM is a global climate simulation that uses a dynamic model of the ocean and atmosphere as well as sea-ice, land surface, and river transport models to simulate ancient climates (Jacob et al, 2001). The paleoclimatic variables selected for use in this project were surface temperature (TS1), which measures the top soil layer temperature in Celsius (C), and precipitation (OPREC), which is a measure of the precipitation from the atmosphere (cm/month).

2.3.1. Data Analysis

We will review the procedures for data analysis using the information from the Late Miocene (10 Ma) as an example. A bivariate plot of the temperature (MAT) and precipitation (MMP) data for the Late Miocene (10 Ma) obtained from the FOAM climate simulation is plotted in Figure 2.6. This diagram illustrates all the possible temperature and precipitation values for the Late Miocene. In order to select those localities with MAP and MMP values that might have favored evaporite formation, we intersected the Evaporite Climate Envelope (Figure 2.5C) with the MAT and MMP data for the Late Miocene. The localities that fall within the Evaporite Climate Envelope were selected and are highlighted in Figure 2.7.

In figure 2.8, the localities are plotted on a paleoreconstruction for the Miocene map (Scotese, 2011). These localities represent the predicted location of evaporite formation during the Late Miocene. In order to test these predictions, the actual occurrence of Late Miocene

evaporites were plotted on the same base map and compared to the predicted localities (Figure 2.9).

The predicted evaporite localities are found in the subtropical arid zone 30°N and 30°S of the equator. Majority of the predicted evaporite localities occur in North Africa, the Mideast and northeastern South America.

In comparison, the actual evaporite localities (observed localities) are more widespread occurring in Europe, North Africa, Central Asia, west- central South America and western North America. A quick visual inspection suggests that there is a reasonably good fit between the predicted evaporite localities and the observed evaporite localities; however it is necessary to quantify the goodness of fit. The next section will describe the statistical technique used to estimate how well the evaporite localities predicted by the Evaporite Climate Envelope procedure matches the observed locations of evaporites for each time interval.

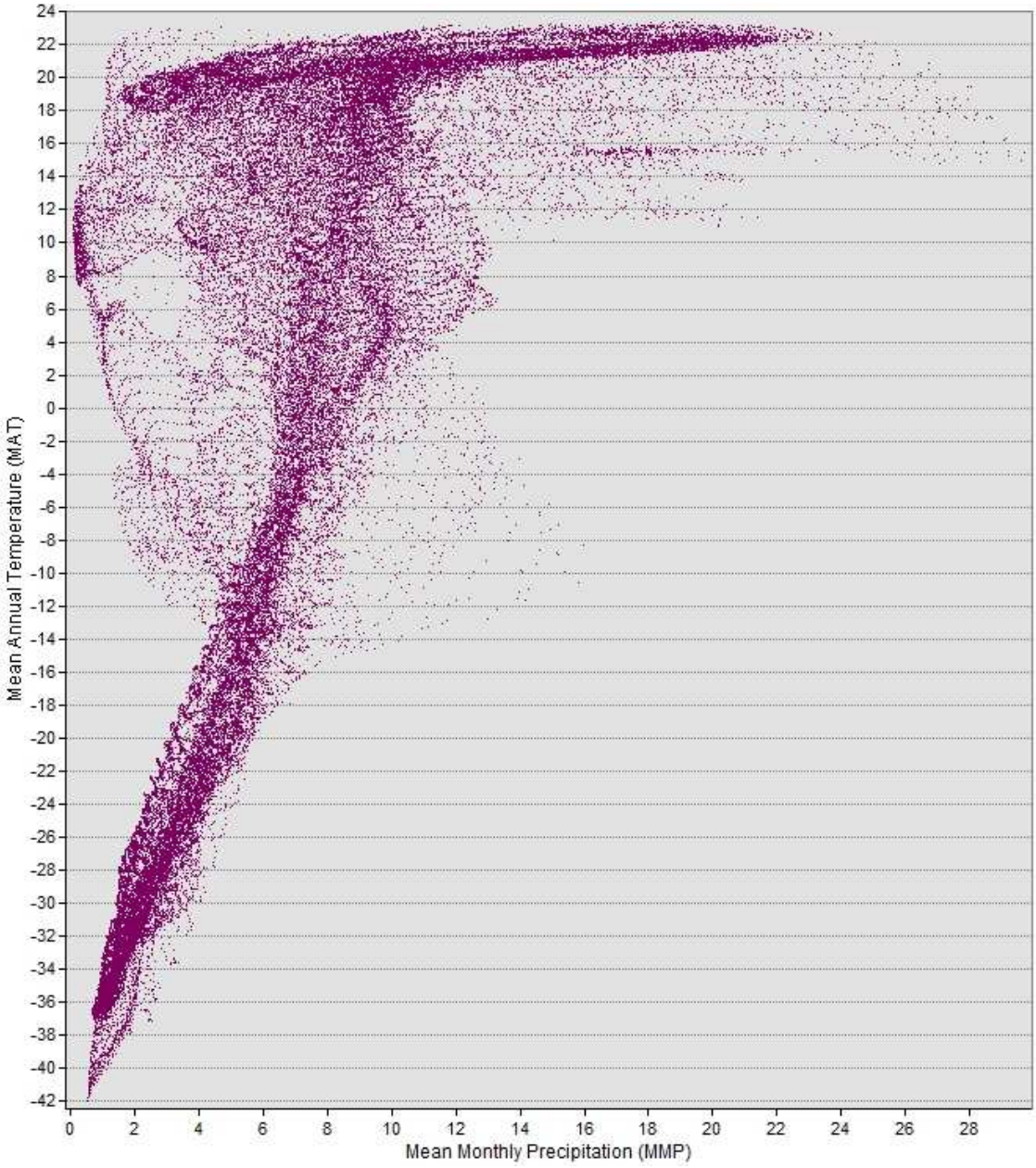

Figure 2.6: This graph is a plot between the temperature and precipitation obtained from the FOAM simulation for the late Miocene. Each dot represents the temperature and precipitation values for a 1°x1° latitude- longitude locality on the Earth.

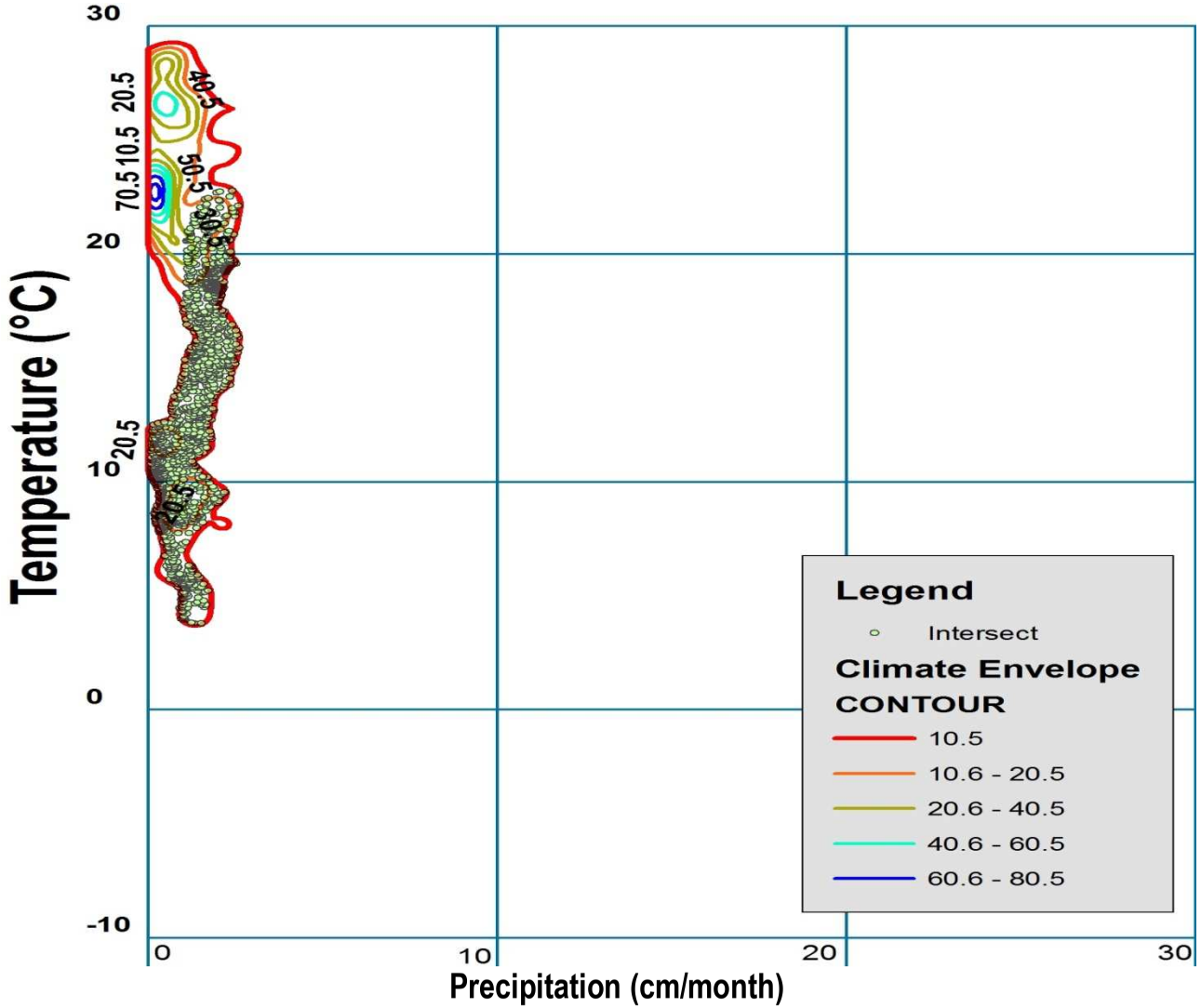

Figure 2.7: This figure shows the intersection between the late Miocene FOAM data and the Evaporite Climate Envelope.

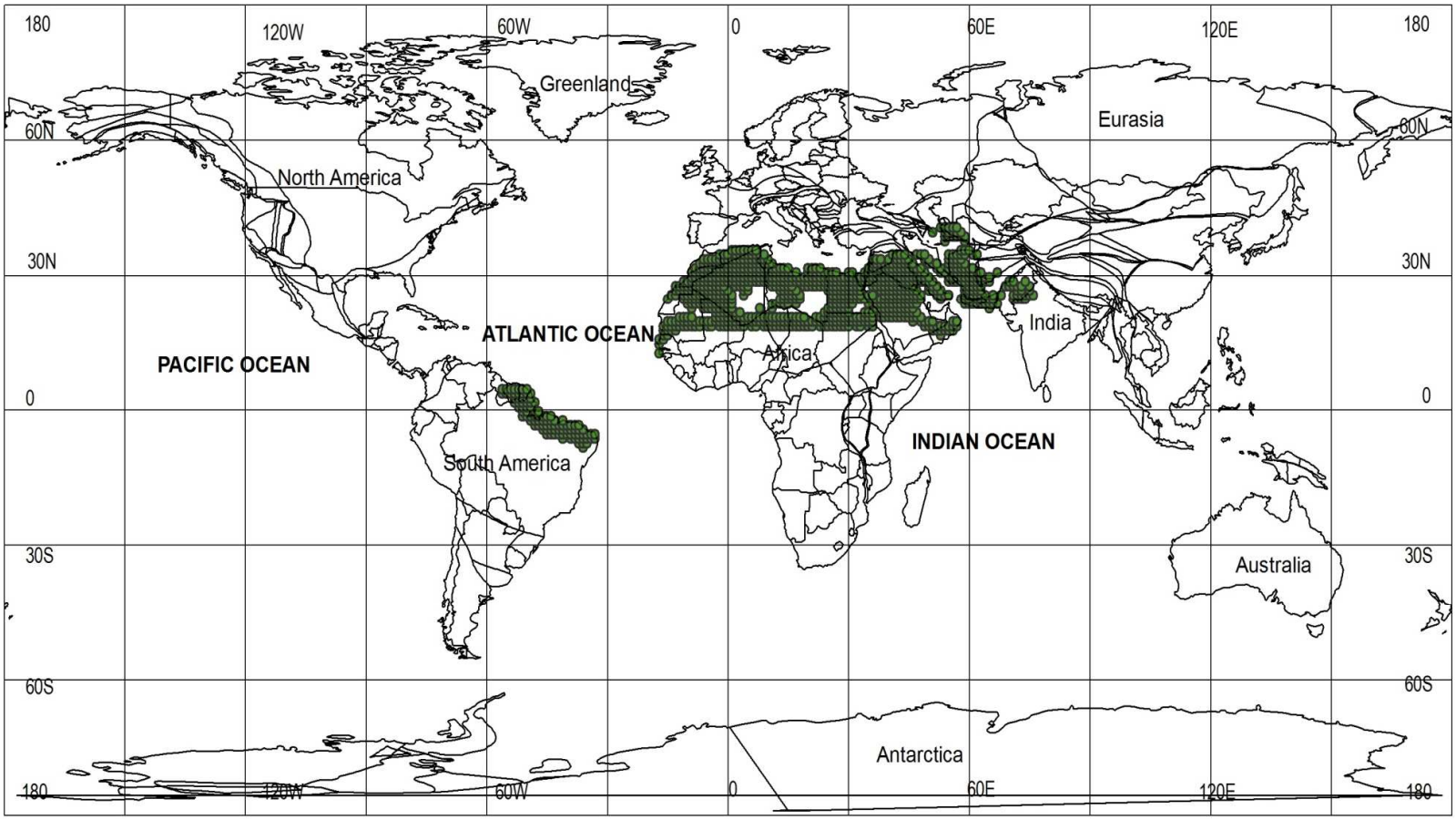

Figure 2.8: This diagram shows where the temperature and precipitation localities that intersected with the Evaporite Climate Envelope plotted on the Late Miocene Paleomap.

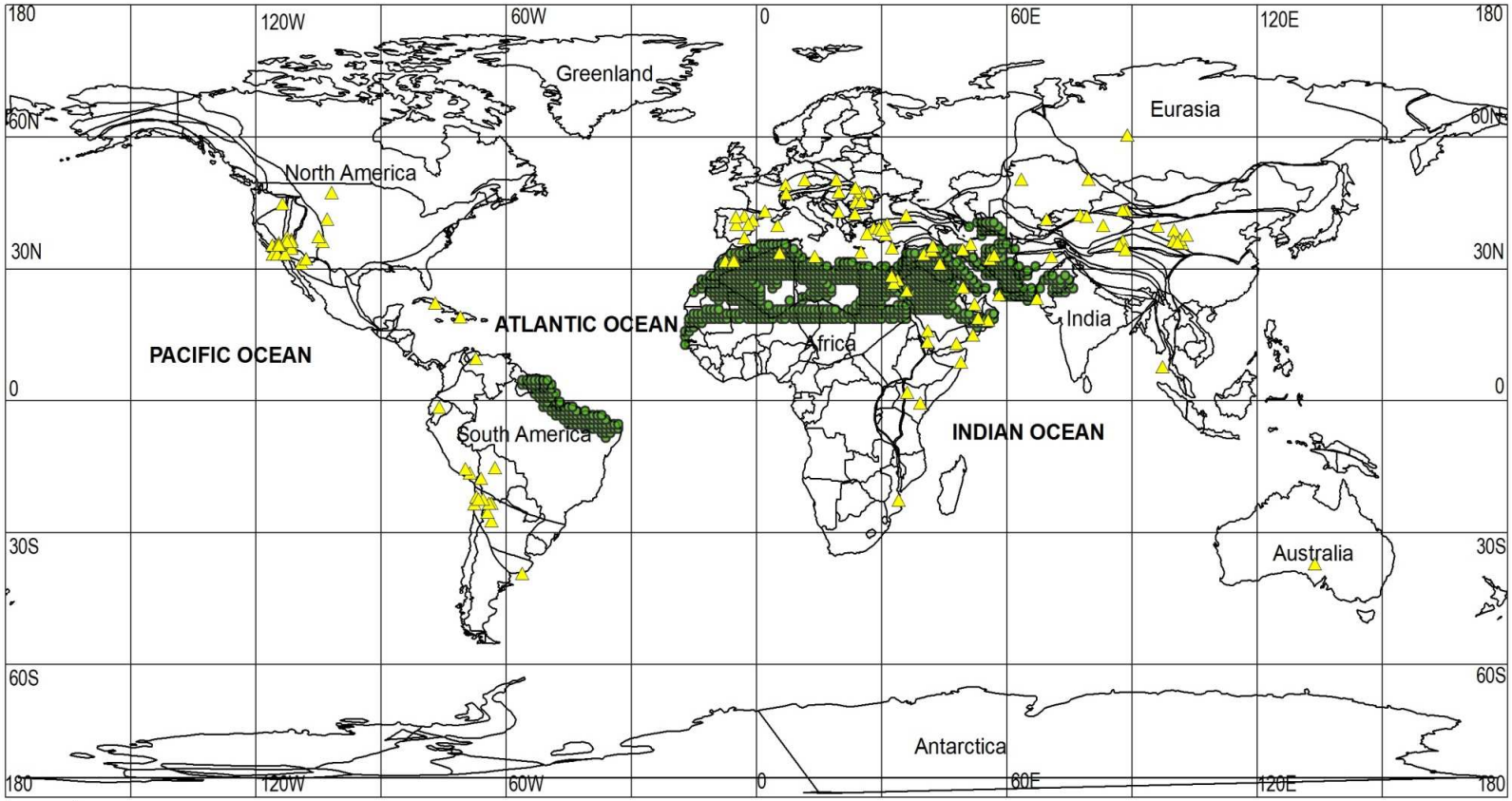

Figure 2.9: The figure shows the geographic distribution of both the predicted and the observed evaporite localities for the Late Miocene.

2.4. Statistical Analysis

2.4.1. Null Hypothesis

A simple statistical procedure was developed in order to test how well the predicted geographic distribution of evaporites matched the observed geographic distribution of evaporites (Figure 2.9). We will review the procedures for statistical analysis using information from the Late Miocene (10 Ma) as our example. The first step in this procedure was to regrid all of the predicted and observed evaporite localities to a common 5°x5° latitude/longitude sample grid. Figure 2.10 illustrates the distribution of evaporites predicted by the climate envelope technique reduced to a 5°x5° grid. Figure 2.11 illustrates the distribution of the observed evaporites reduced to a 5°x5° grid.

In the second step, the number of grid cells that contained both predicted and observed evaporite localities was determined (Figure 2.12). These matches represent the number of successful predictions or "hits". Conversely the number of unsuccessful predictions or mismatches is referred to as "misses".

Table 1 lists the values for all the variables that were used to calculate the statistics for the Late Miocene. The key variables are: total land, the number of predicted evaporites, % total land occupied by predicted evaporites, the number of observed evaporites, predicted number of hits and hits.

The next step was to determine if the number of hits is statistically significant. In other words, if the observed geographic distribution of evaporites is random, then only a small percentage of all observed evaporite localities would be expected to intersect the predicted grid cells. For a random distribution, the expected number of hits should be proportional to the area

represented by the predicted grid cells. For example, if the predicted grid cells represented 25% of the total number of grid cells then, we would expect, on average that 25% of the observed evaporite localities would fall within the predicted grid cells. This is our null hypothesis. Any deviation from the expected number of hits can be assigned a level of significance.

According to the null hypothesis the expected number of hits should be equal to the percentage of the predicted number of evaporites divided by the total number of grid cells. In the case of the Late Miocene, the number of predicted evaporite grid cells was 87 (Figure 2.10, Table 1). The total number of continental grid cells for the Late Miocene was 1434 (Table 1). Therefore, for the Late Miocene 87 of 1434, or 6.07%, of the total number of grid cells are predicted to contain evaporites.

For the Late Miocene 58 "observed" grid cells contained evaporite localities. These observed evaporites are based on actual occurrences of the Late Miocene evaporite deposits (Boucot et al, in press). The null hypothesis predicts that 6.07% of these 58 observed localities or 3.52 localities should register as "hits".

$Hits = E_{obs} * \% E_{pred}$

where,

Hits = grid cells that contain both observed and predicted evaporite occurrences

E_{obs} = number of grid cells representing observed (actual) evaporite localities

%Epred = percentage of grid cells expected to contain evaporite localities

However in actuality, 15 of the observed evaporite localities fall within the predicted grid cells. The occurrence of hits is more than 4 times the number of hits expected from a random distribution (15/3.52 = 4.26). This represents a significant deviation from the number of hits

predicted by the null hypothesis. Intuitively it would seem that the null hypothesis has failed, namely that the distribution is not random but rather highly significant.

2.4.2 Thought Experiment

To better visualize the statistical model for the null hypothesis, imagine the following thought experiment. An experimenter has 2 buckets of ping-pong balls, one bucket is filled with white ping-pong balls and the other bucket is filled with red ping-pong balls. The experimenter then drops 10 white ping- pong balls from a great height into a box that has been divided into a 10 x10 grid of smaller boxes. Assuming each ball has an equal probability of falling into any of the 100 cells, then after 10 balls have been dropped, on average, 10% of the grid cells should be filled.

The experimenter then drops 20 red ping- pong balls onto the grid. After all the red balls have been dropped, the question can be asked, “How many grid cells will contain both red and white ping-pong balls?” The expectation is that since 10% of the grid is filled by white ping-pong balls, then 10% of the red balls (10%* 20 = 2) should fall into the grid cells also occupied by the white ping-pong balls.

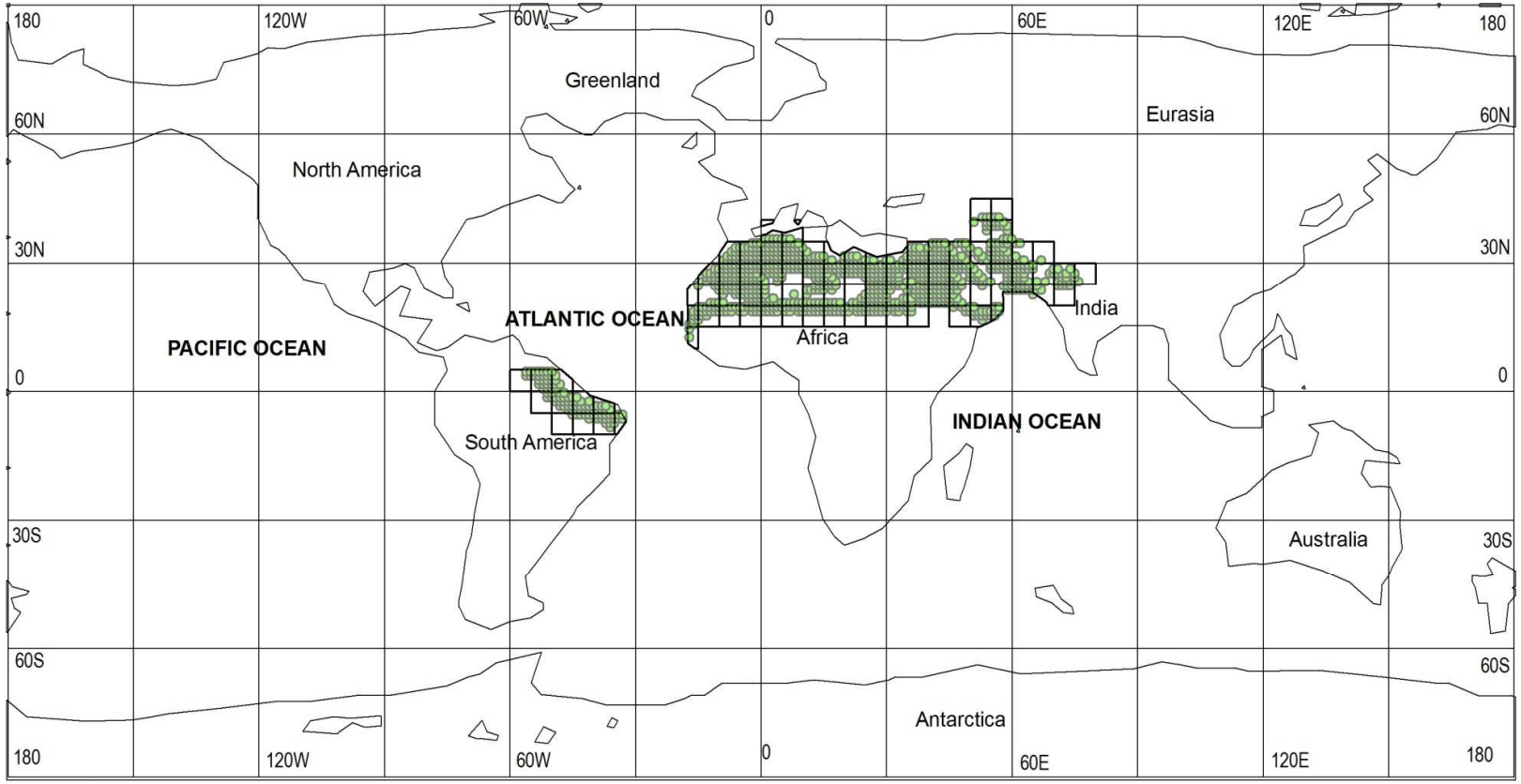

Figure 2.10: This figure shows the 5°x5° latitude- longitude grids (n= 87) obtained for the predicted evaporites.

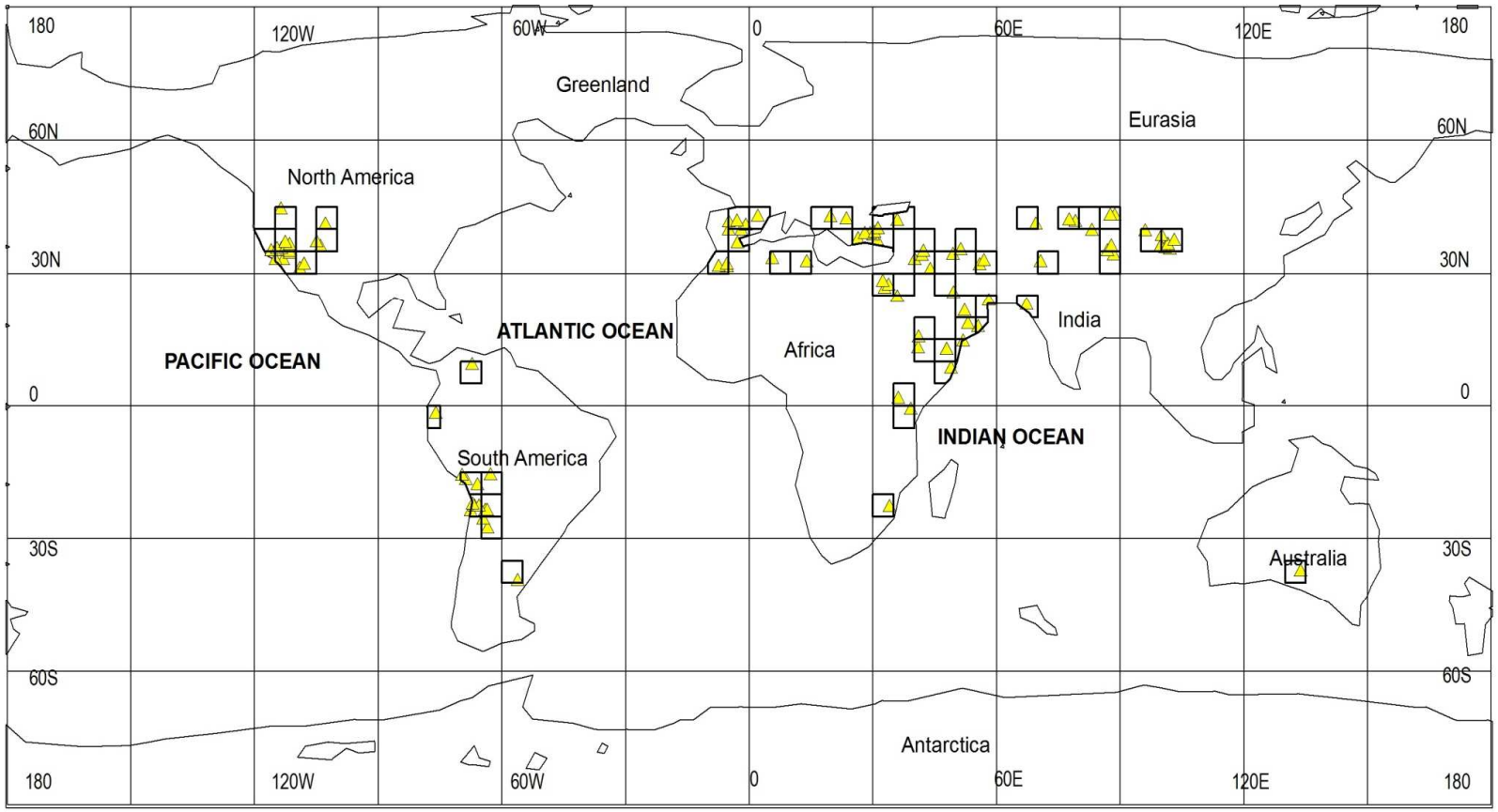

Figure 2.11: This figure shows the 5°x5° latitude- longitude grids (n=58) obtained for the observed evaporites.

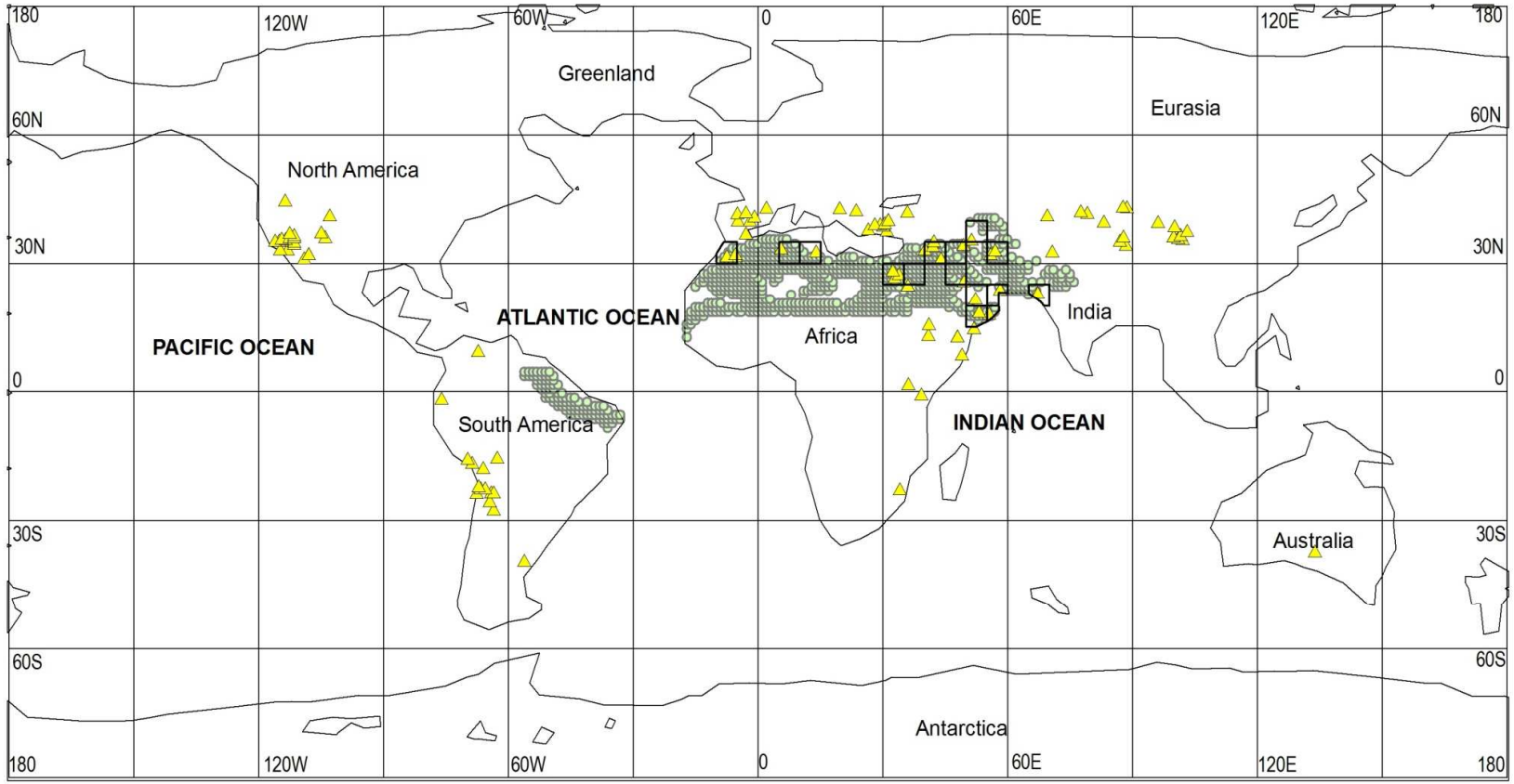

Figure 2.12: This figure shows the "hits" (n= 15) obtained for the Late Miocene.

2.4.3. Probability that observed hits are random

As described in the previous section, our null hypothesis states that the expected number of hits should be proportional to the percentage of predicted evaporite grid cells. The next question one can ask is, "What is the probability that the observed number of hits is due to a random process?" This question can be answered using the Poisson distribution (Downing & Clark, 1989).

The Poisson distribution states that the probability of the frequency of a particular event P(x) can be estimated if the expected frequency of the event (λ) and the observed frequency of the event (K) are known.

Equation (1) $P(x) = (e^{-\lambda}) (\lambda^{K})/ K!$

where,

P(x) = the probability of obtaining a particular number of hits

K= observed frequency of an event (number of observed occurrences)

λ= expected frequency of an event (number of predicted occurrences)

e is the natural log = 2.7183

In the case for the Late Miocene, the expected frequency of the evaporite hits is λ. In this example λ is equal to 3.52 hits. The observed frequency of hits K is 15. Using equation (1) we can solve for P(x), the probability of obtaining a particular number of hits. In this example P(x) = 3.55×10^{-6}. In other words, compared to the expected number of hits, the observed number of hits is very high. This strongly suggests that the observed hits are not random and that the null hypothesis fails.

This statistical procedure was used to calculate the probability for all the other time intervals. The results are given in following chapters: Chapter 3, Cenozoic Era, Chapter 4, Mesozoic Era and Chapter 5, Paleozoic Era and summarized in Tables 3.1- 5.1.

Table 2.1 Statistical Calculation for the late Miocene

Geologic Time Period	Total Land	Number of Predicted Evaporites	%Total Land Occupied by Predicted Evaporites	Number of Observed Evaporites	Predicted Number of Hits	Hits	Misses	Probability that Hits are Random
Late Miocene (10 Ma)	1434	87	6.07	58	3.52	15	43	3.558 x 10-6

CHAPTER 3

CENOZOIC EVAPORITES

3.1 Introduction

The description of the results is organized into three chapters. Chapter 3 discusses the results obtained for the Cenozoic Era. Chapters 4 and 5 discuss the results obtained for the Mesozoic Era and Paleozoic Era, respectively. The global distribution of the observed evaporites for each time period will be compared with the predicted geographic distribution of evaporites. Statistical procedures described in Chapter 2 have been used to test whether the predicted distribution of evaporites passes or fails the null hypothesis.

All paleogeographic maps used in this research were obtained from the PALEOMAP Project (Scotese, 2001). Time periods used in this research match the GANDOLPH time slices for which FOAM paleoclimate simulations were run. The 16 time periods span the Phanerozoic and Late Precambrian. In this chapter we will review the results obtained for the Late Miocene (10 Ma), Oligocene (30 Ma) and Middle Eocene (45 Ma). Chapter 4 will review the results obtained for the Cretaceous/Tertiary Boundary (70 Ma), Cenomanian/Turonian (90 Ma), Aptian/Albian (120 Ma), Barremian/Berriasian (140 Ma), Late Jurassic (160 Ma), Early Jurassic (180 Ma) and the Late Triassic (220 Ma). Finally, Chapter 5 will review the results obtained from the Permo-Triassic Boundary (250 Ma), Early Permian (280 Ma), Mississippian (340 Ma), Late Devonian (360 Ma), Siluro-Devonian (400 Ma) and the Late Cambrian (480 Ma).

3.2. Cenozoic Results

The Tertiary period which begins the Cenozoic Era was characterized by both cool (Ice House) and warm (Hot House) temperatures. The Miocene period experienced cooler temperatures when compared to the Oligocene and Eocene periods. Evaporites for this time period are found in warm arid to semi- arid/warm regions between 30 - 60°N and 30- 60°S (Warren, 2006).

3.2.1 Tectonics and Climate of the Cenozoic Era

The Cenozoic Era has been of increasing interest to many geologists (Raymo et al, 1992; Ruddiman et al, 1991; Barron, 1985; Kraus et al, 2007; Ruddiman and Kutzbach, 1989) with the Early Cenozoic being characterized by a warm and wet climate which was replaced by a much cooler climate in the Late Cenozoic (Ruddiman and Kutzbach, 1991).

Theories that have been suggested to explain these changes in climate include mountain uplift, atmospheric circulation, tectonic activity and orbital variations. The uplift of mountain ranges and plateaus have been suggested to have resulted in drier climates in certain regions which may have been conducive for the formation of evaporites. Mountain uplift may have also contributed substantially to changes in the atmospheric circulation (Ruddiman and Kutzbach, 1991). It is further believed that atmospheric circulation may have been a contributing factor to climate change due to the observation of the build- up and decline of ice sheets (e.g. Antarctica, Crowley and North, 1991). Orbital variations, also known as the Milankovich cycles, have been reported to play a role in Cenozoic climate change as well (Crowley and North, 1991).

Tectonic activity and the way that the continents were distributed have been suggested as a causal factor in global climate change (Kendall et al, 2002). Ruddiman and Kutzbach (1991) reported that the changes in the way that the continents were distributed and the size of the inland seas may have greatly affected climate over long intervals of geologic time.

Climate for the Miocene period has been found to be cooler than other epochs in the Cenozoic but much warmer than today's climate. During the Late Miocene, Africa, Italy, Arabia and India collided with Eurasia, causing the disappearance of the Tethyan Ocean, the upliftment of the Tibetan plateau and the rejuvenation of the Himalayas (Potter et al, 2009, Crowley and North, 1991). The Tethys Ocean is reported to have shrunk to become the Mediterranean Sea which during the Miocene was closed and desiccated leading to the formation of large deposits of evaporites otherwise also referred to as the Messinian salinity crisis (Chamley, 1979; Warren, 2006).

India first collided with Asia in the Eocene and Andes of South America took up most of its present form by the Late Miocene. The North and South Atlantic are known to have widenened and the westward movement of North and South America caused convergence along the west which resulted in the formation of the West Cordillera and Andes mountain chain (Crowley and North, 1991).

Around 50 Ma Australia began to drift northward, opening the Southern Ocean Seaway and establishing the beginnings of the Antarctic Circumpolar Current (ACC). The ACC acted as the barrier that prevented warm currents from reaching the Antarctic coast and may have triggered the growth of the south polar ice cap which began in the Early Oligocene. The

Oligocene period was cool experiencing mostly low temperatures but with a significant warming observed during the Early and the Late Oligocene (Frakes et al, 1979; Zanazzi et al, 2007).

During the Eocene temperatures were relatively warm with high precipitation rates (Rea et al, 1990). The epoch was characterized by an expansion of tropical rainforests. The Eocene experienced low temperatures and Frakes, 1979 reported that this may have resulted in decreased evaporation rates globally. Tectonically, India had started to drift towards Eurasia and there was no connection (Panama Isthmus) between North America and South America. Australia was still very close to Antarctica and Arabia was attached to Africa and the Tethys Ocean still existed.

The climate and the results obtained for this research will be discussed further in Chapter 6. The subsequent sections discuss the predicted and observed evaporite localities and the statistical results obtained for the 3 Cenozoic time periods (Late Miocene, Oligocene and Middle Eocene).

3.3. Late Miocene (~ 10 Ma)

3.3.1 Late Miocene Evaporites

The geographic distribution (Figure 3.1) of predicted evaporites was obtained by intersecting the Evaporite Climate Envelope with precipitation and temperature estimates for the Late Miocene. A total of 1243 1°x1° localities fell within the evaporite climate envelope for the Late Miocene. The predicted evaporite localities occur in Brazil, Morocco, Tunisia, Libya, Egypt, Chad, Eritrea, Senegal, Mauritania, Mali, Niger, Sudan, Ethiopia, Gambia and Western Sahara, Saudi Arabia and India/Pakistan region, Iraq and Iran (Fig 3.1).

The geographic distribution of actual (observed) evaporite localities was obtained from a compilation by Boucot et al (in press). Late Miocene evaporites occur in western North America, Cuba, South America, East and North Africa, Saudi Arabia, India, Pakistan, Iraq, Iran and a few in Australia. A total of 628 observed evaporites are plotted on Figure 3.2.

"Hits" are observed in parts of North Africa, Arabia and Asia. "Misses" are in North America, South America, Europe, Cuba and the interior of Asia (Fig 3.3)

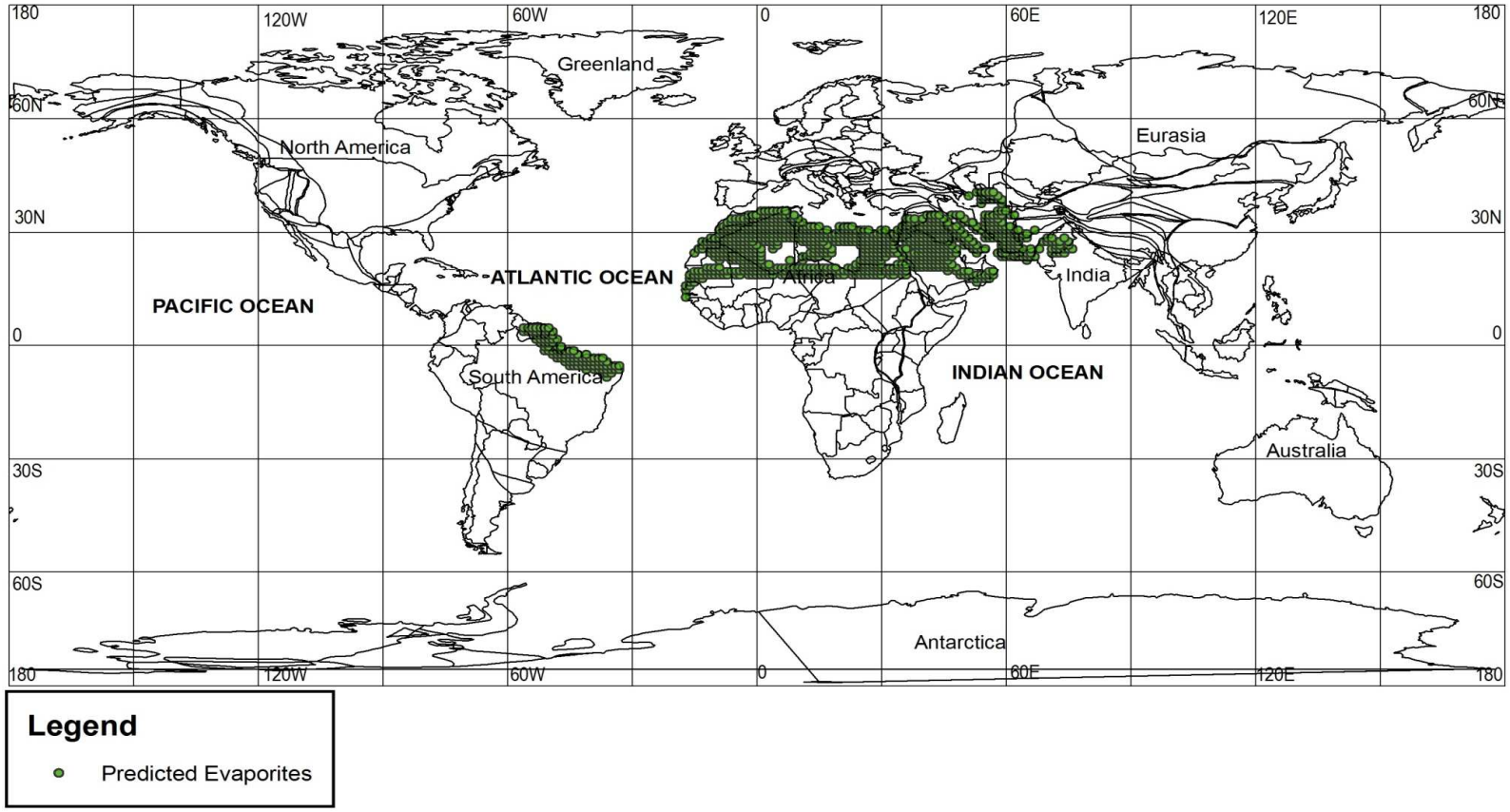

Figure 3.1: A map showing the geographic distribution of the predicted evaporites for the Late Miocene time period.

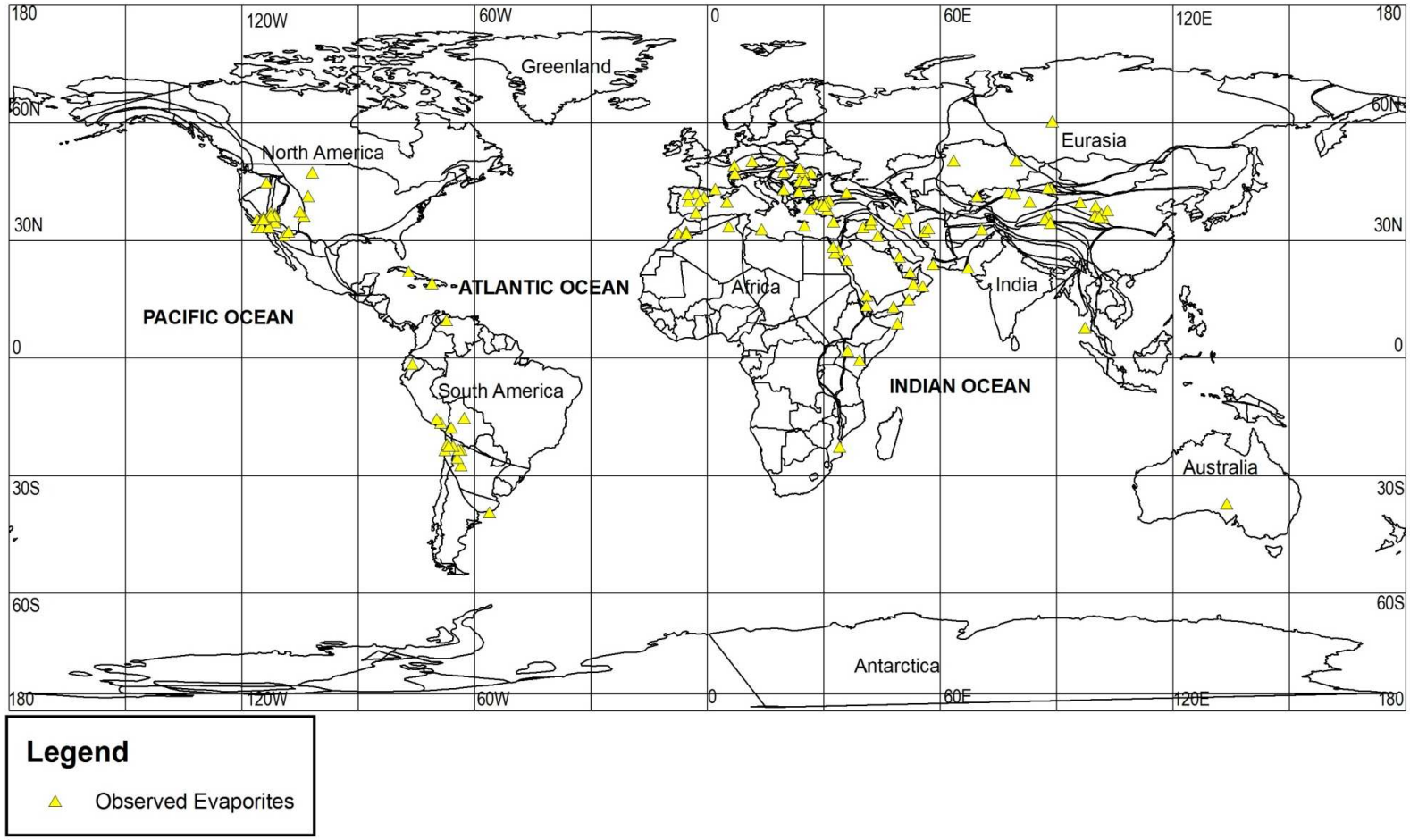

Figure 3.2: A map showing the geographic distribution of the observed evaporites for the Late Miocene time period.

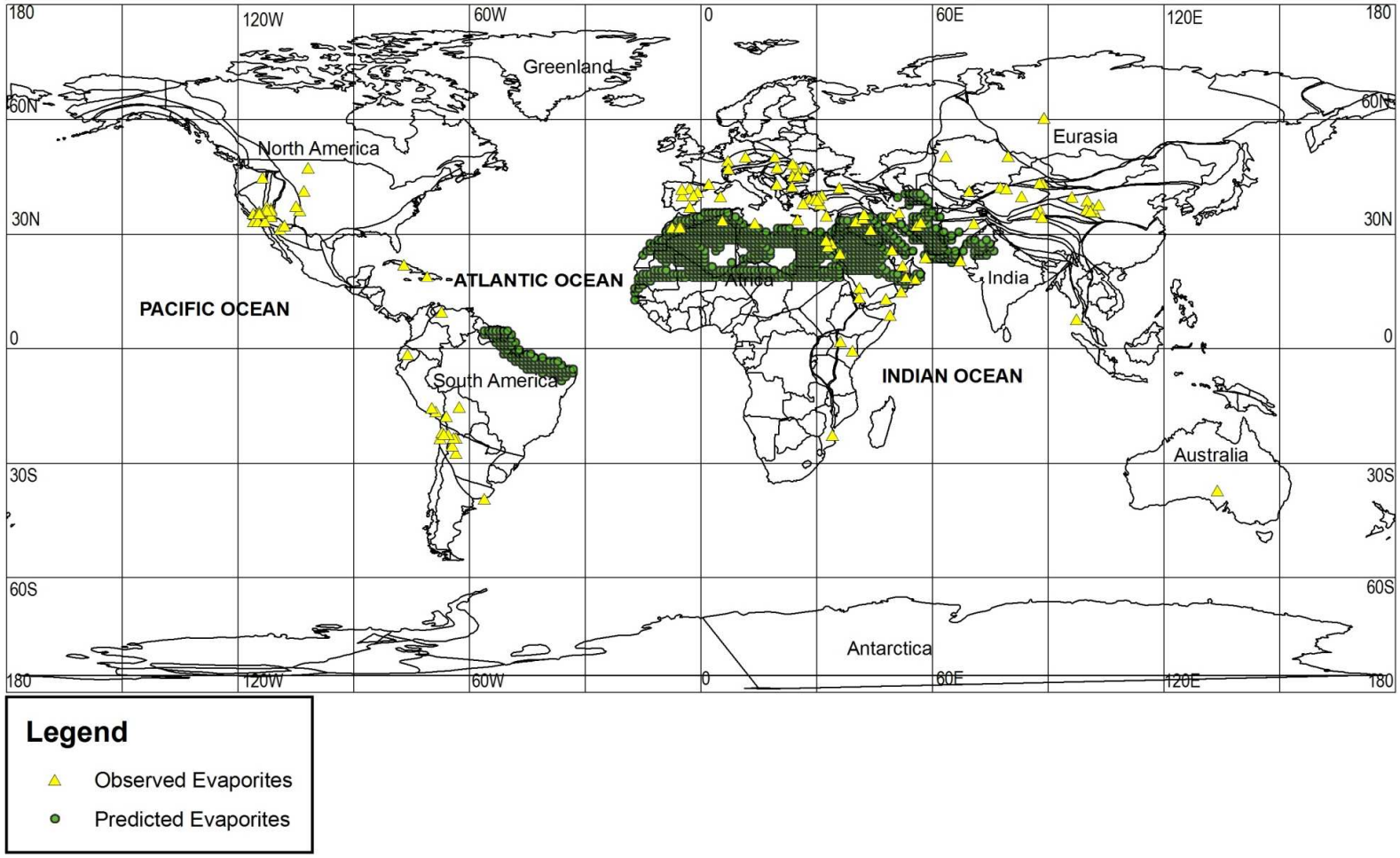

Figure 3.3: A map showing the match between the predicted and the observed evaporites for the Late Miocene time period.

3.3.1.1. Statistical Analyzes for the Late Miocene

A boundary representing the edge of the continental lithosphere for the Late Miocene was mapped and in Figure 3.4 is represented by a 5°x5° set of grid cells. For the Late Miocene, 1434 grid cells were obtained. 87 of these 5°x5° grid cells contained localities for the predicted evaporites. This represents 6.07% of the continental grid cells (Figure 3.5). 58 grid cells contained observed evaporite localities (Figure 3.6). 15 grid cells contained both predicted and observed evaporite localities which are designated as "hits" (Figure 3.7). The variables used in the statistical analysis for the Late Miocene are given in Table 3.1. According to the statistical procedure outlined in section 2.4, since the expected number of hits was 3.52 and the observed number of hits was 15, the probability that the number of hits is due to a random process is 3.55×10^{-6}. This strongly suggests that the observed hits are not random and that the null hypothesis fails.

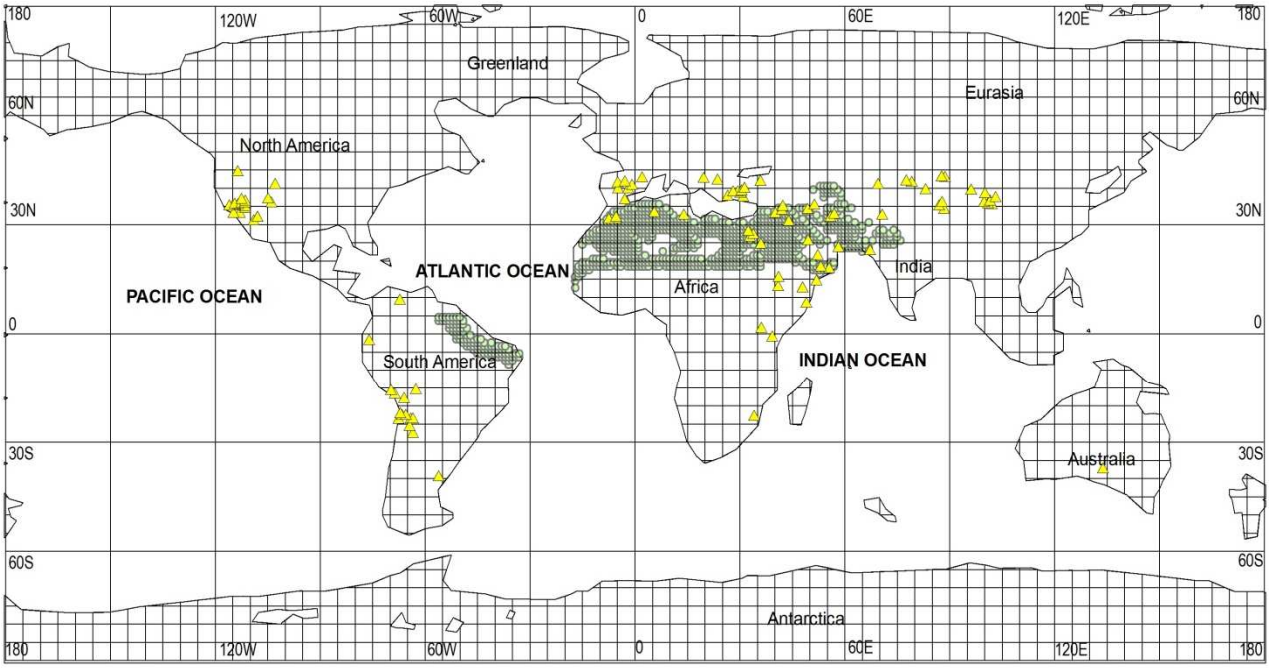

Figure 3.4: This figure shows the 5°x5° latitude- longitude grids drawn for the Late Miocene.

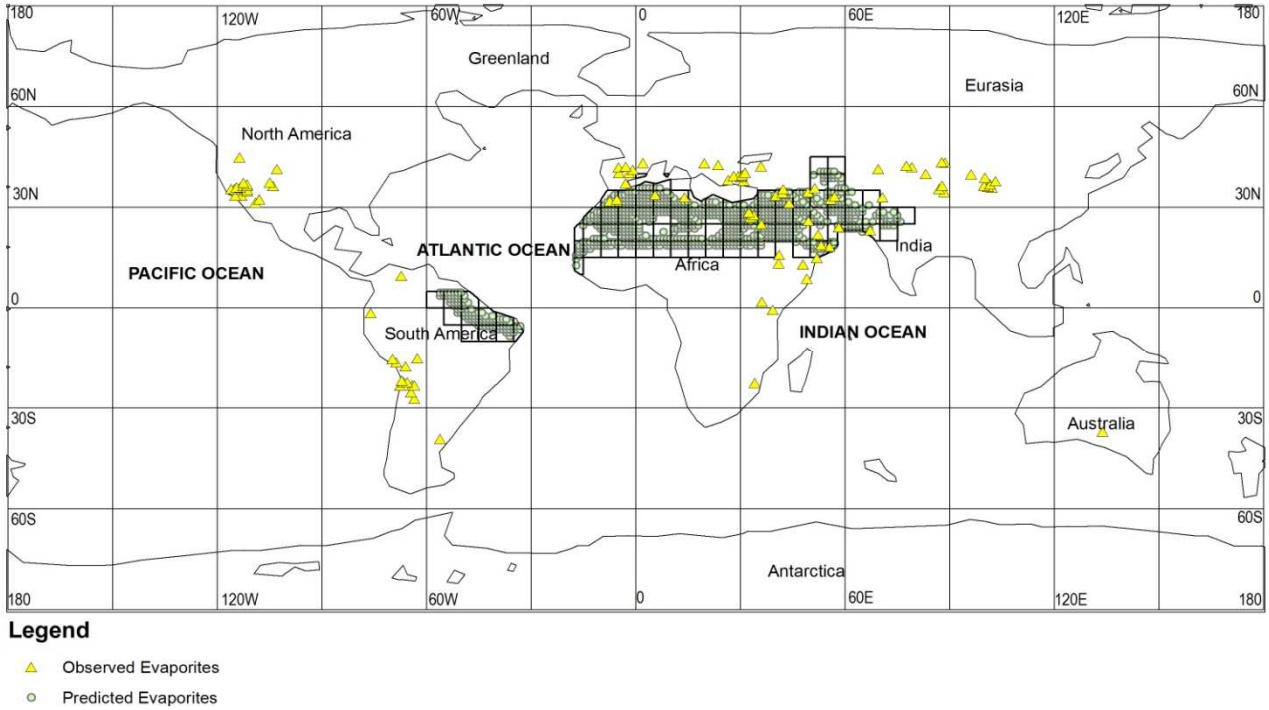

Figure 3.5: This figure shows the 5°x5° latitude- longitude grids for the Late Miocene predicted evaporites.

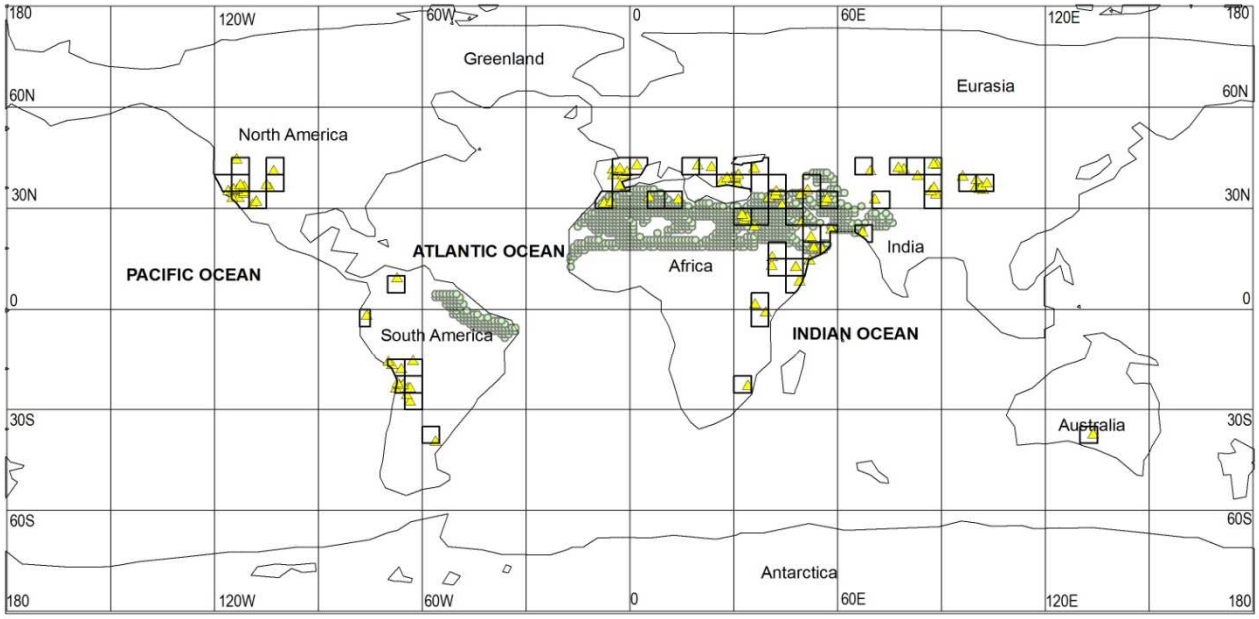

Figure 3.6: This figure shows the 5°x5° latitude-longitude grids for the Late Miocene observed evaporites.

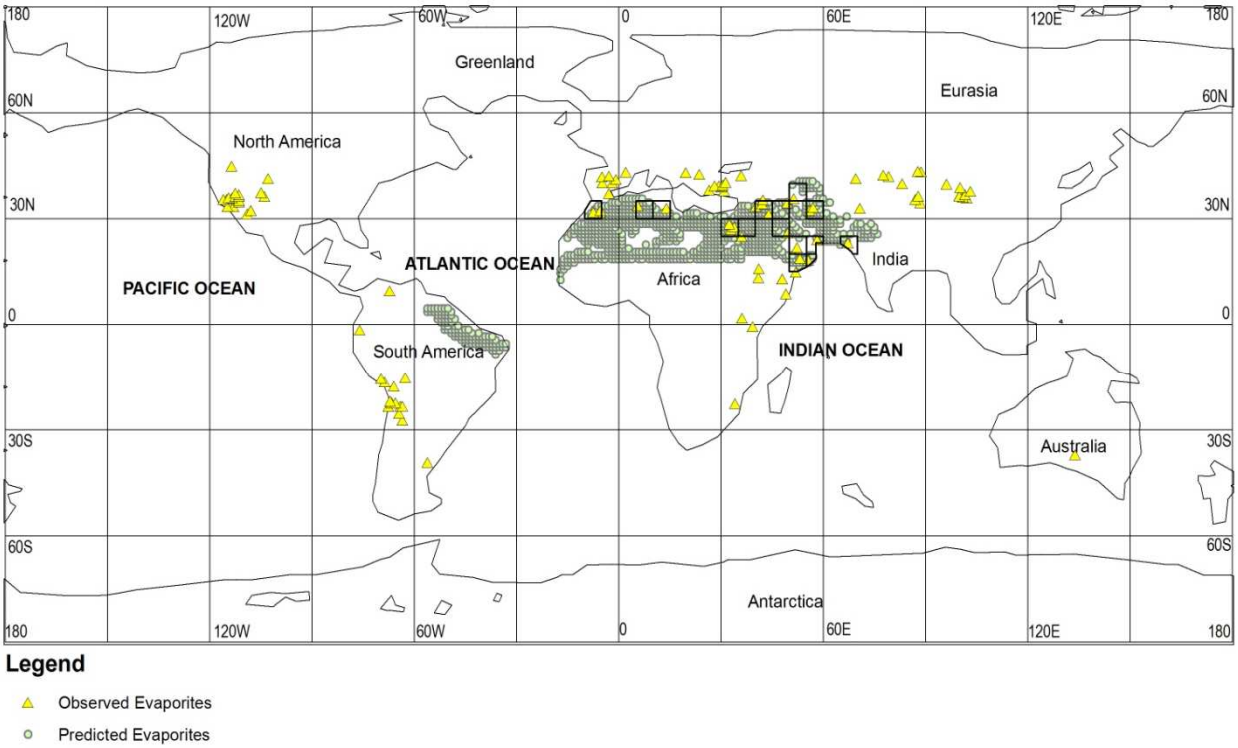

Figure 3.7: This figure shows the "hits" obtained for the Late Miocene time period.

3.4 Oligocene (~ 30 Ma)

3.4.1 Oligocene evaporites

The geographic distribution (Figure 3.8) of predicted evaporites was obtained by intersecting the Evaporite Climate Envelope with precipitation and temperature estimates for the Oligocene. A total of 1049 1°x1° localities fell within the Evaporite Climate Envelope for the Oligocene (Figure 3.8). The predicted evaporites localities could be found in north and South Africa, in south and central Asia and to the north and west of South America.

The geographic distribution of actual (observed) evaporite localities was obtained from a compilation of Boucot et al (in press). The Oligocene evaporites occur in north and South America, and a few plotted out in Cuba and Africa. Majority of the observed evaporites plotted out in Asia and Europe (Figure 3.9). A total of 68 observed evaporites plotted out on the paleomap. “Hits” are seen in Asia and Africa. “Misses” are observed in central South America, northeast South America, South Africa, North Africa, Central and northeast Asia (Figure 3.10).

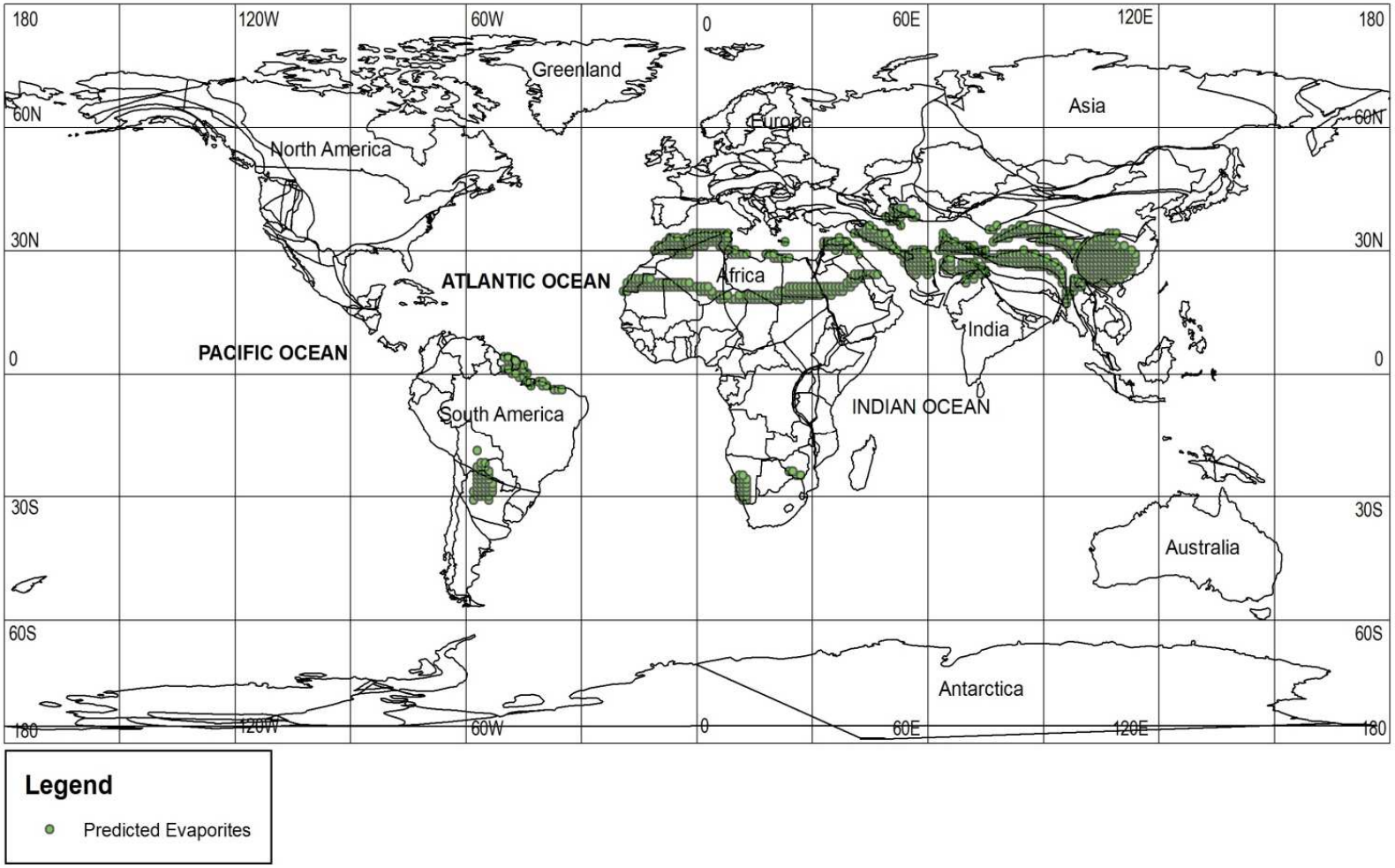

Figure 3.8: A map showing the location of the predicted evaporites for the Oligocene time period.

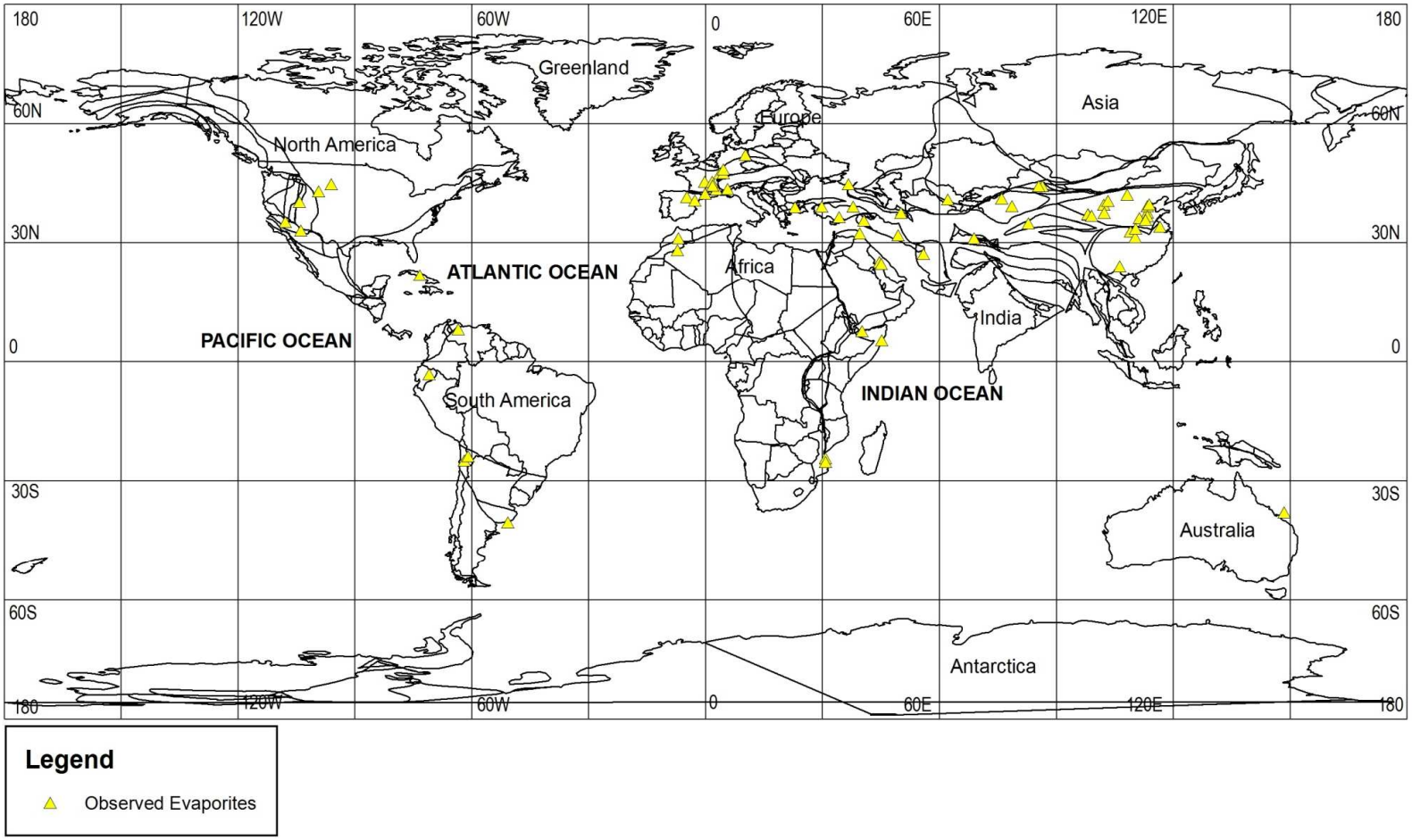

Figure 3.9: A map showing the location of observed evaporites for the Oligocene time period.

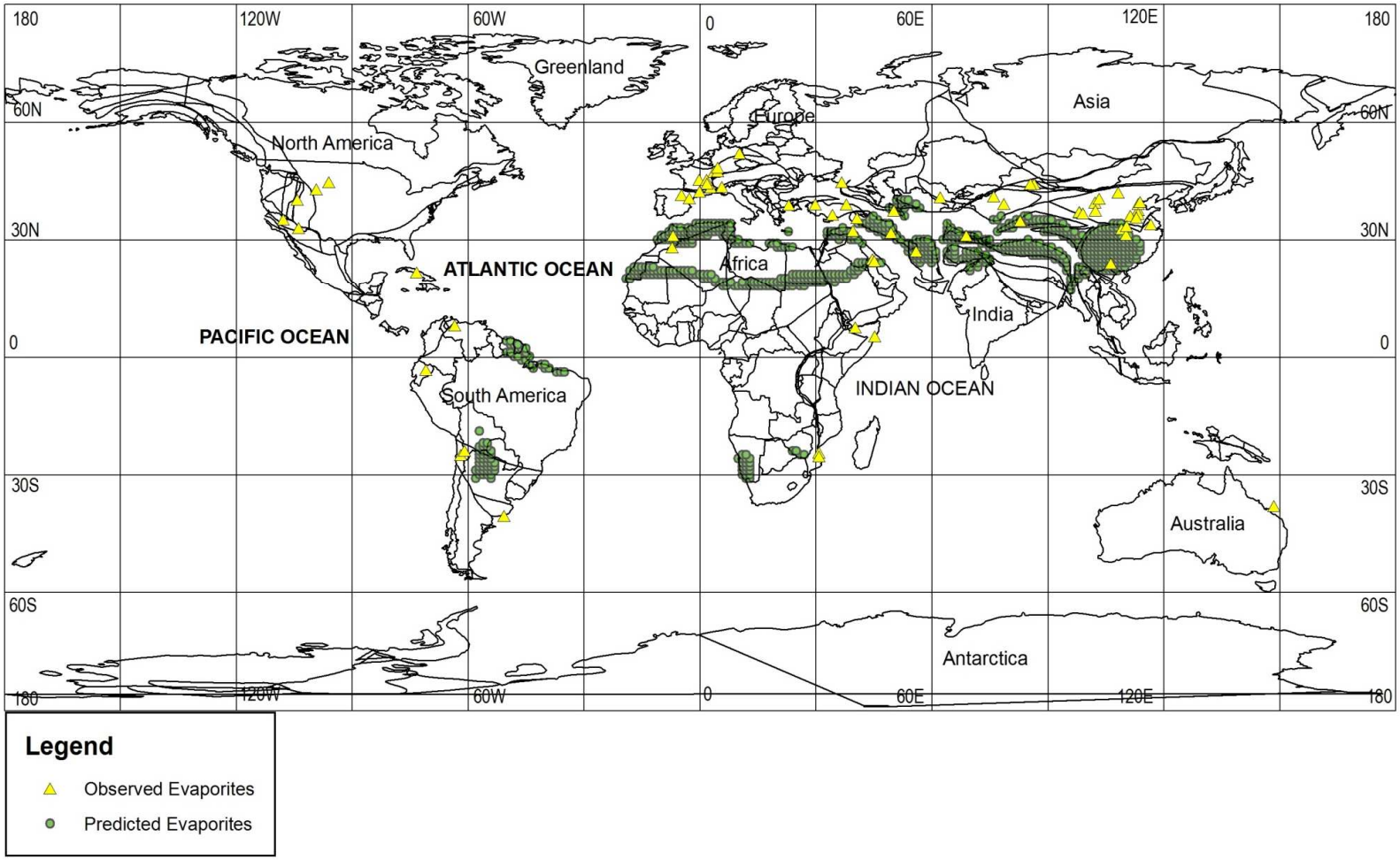

Figure 3.10: A map showing both the predicted and the observed evaporites for the Oligocene time period.

3.4.1.1 Statistical Analyzes for the Oligocene

A boundary representing the edge of the continental lithosphere for the Oligocene was mapped and in Figure 3.11 is represented by a 5°x5° grid cells. For the Oligocene, 1434 grid cells were obtained. 97 of these 5°x5° grid cells contained localities for the predicted evaporites (Figure 3.12). This makes up 6.76% of the continental grid cells. 45 cells contained observed evaporite localities (Figure 3.13). The number of hits between the predicted and the observed evaporites were 15 (Figure 3.14). According to the statistical procedure outlined in section 2.4, since the expected number of hits was 3.04 and the observed number of hits was 15, the probability that the number of hits is due to a random process is 6.502×10^{-7} (Table 3.1). This strongly suggests that the observed hits are not random and that the null hypothesis fails.

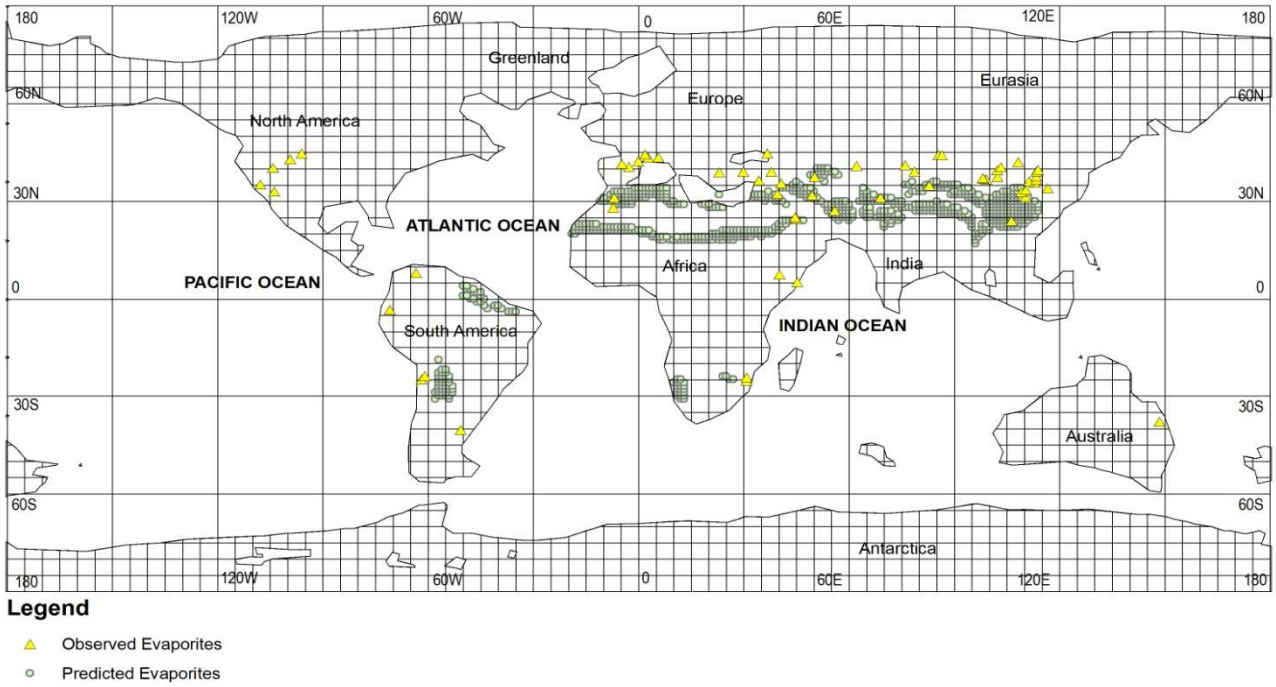

Figure 3.11: This map shows the 5°x5° latitude-longitude for the Oligocene time period.

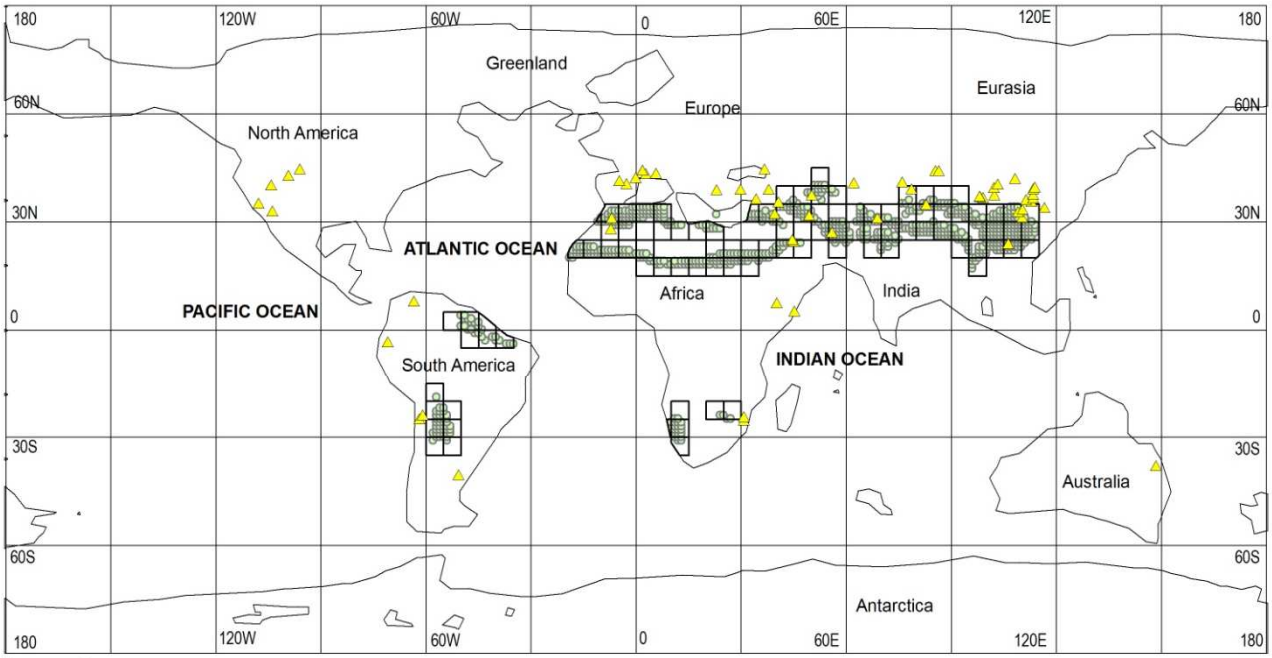

Figure 3.12: This map shows the 5°x5° latitude-longitude for the Oligocene predicted evaporites

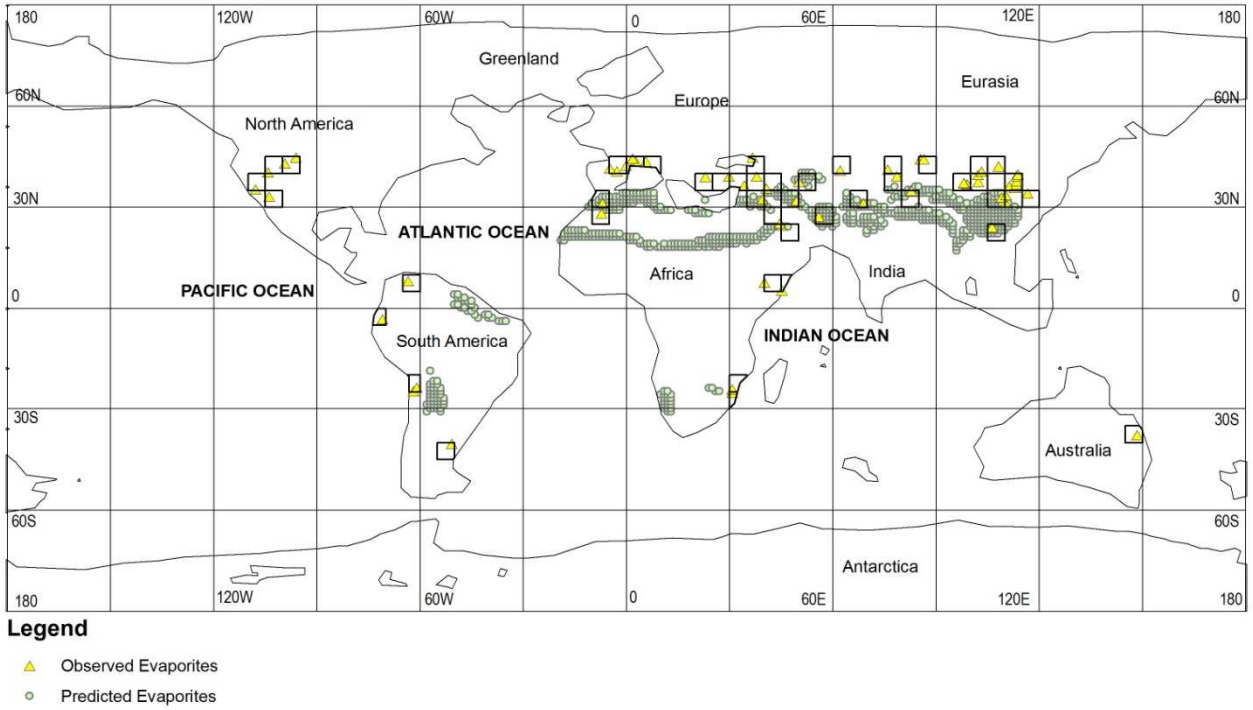

Figure 3.13: This map shows the 5°x5° latitude- longitude grids for the Oligocene observed evaporites.

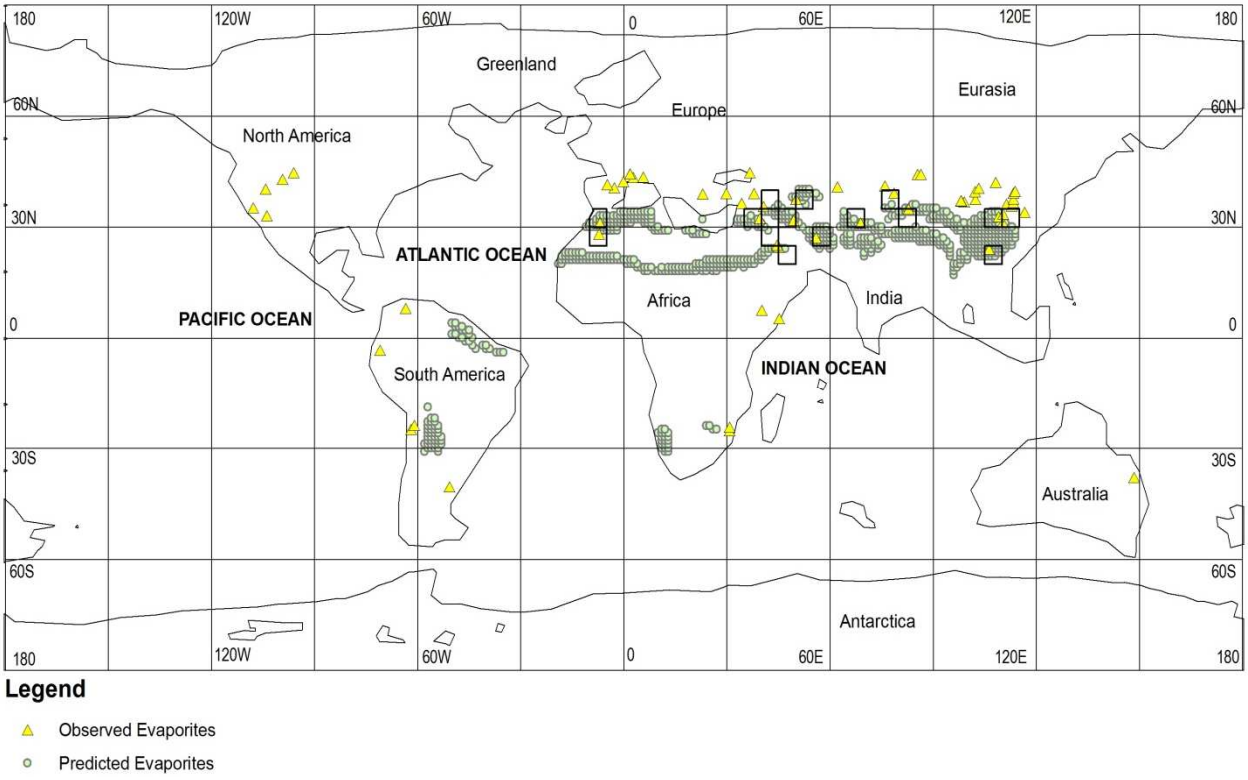

Figure 3.14: This map shows the "hits" obtained for the Oligocene time period.

3.5. Middle Eocene (~ 45 Ma)

3.5.1. Middle Eocene Evaporites

The geographic distribution (Figure 3.15) of predicted evaporites was obtained by intersecting the Evaporite Climate Envelope with precipitation and temperature estimates for the Middle Eocene. A total of 485 1°x1° predicted evaporite localities plotted out on the Middle Eocene paleomap. The predicted evaporites occur in North Africa, Northwest and Central Asia and a few in South Africa. Specifically the predicted evaporites could be found in the Western Sahara, Algeria, Tunisia, Egypt, Namibia and southern Eurasia (Fig 3.15).

The geographic distribution of actual (observed) evaporite localities was obtained from a compilation by Boucot et al (in press). Middle Eocene evaporites occur in West, Central and

eastern Eurasia, few in eastern Africa, North and South America. A total of 26 observed evaporites are plotted on Figure 3.16. “Hits” are observed in North Africa and West and Central Asia. “Misses” are observed in East Africa, North and South America, East Asia and parts of Western Eurasia.

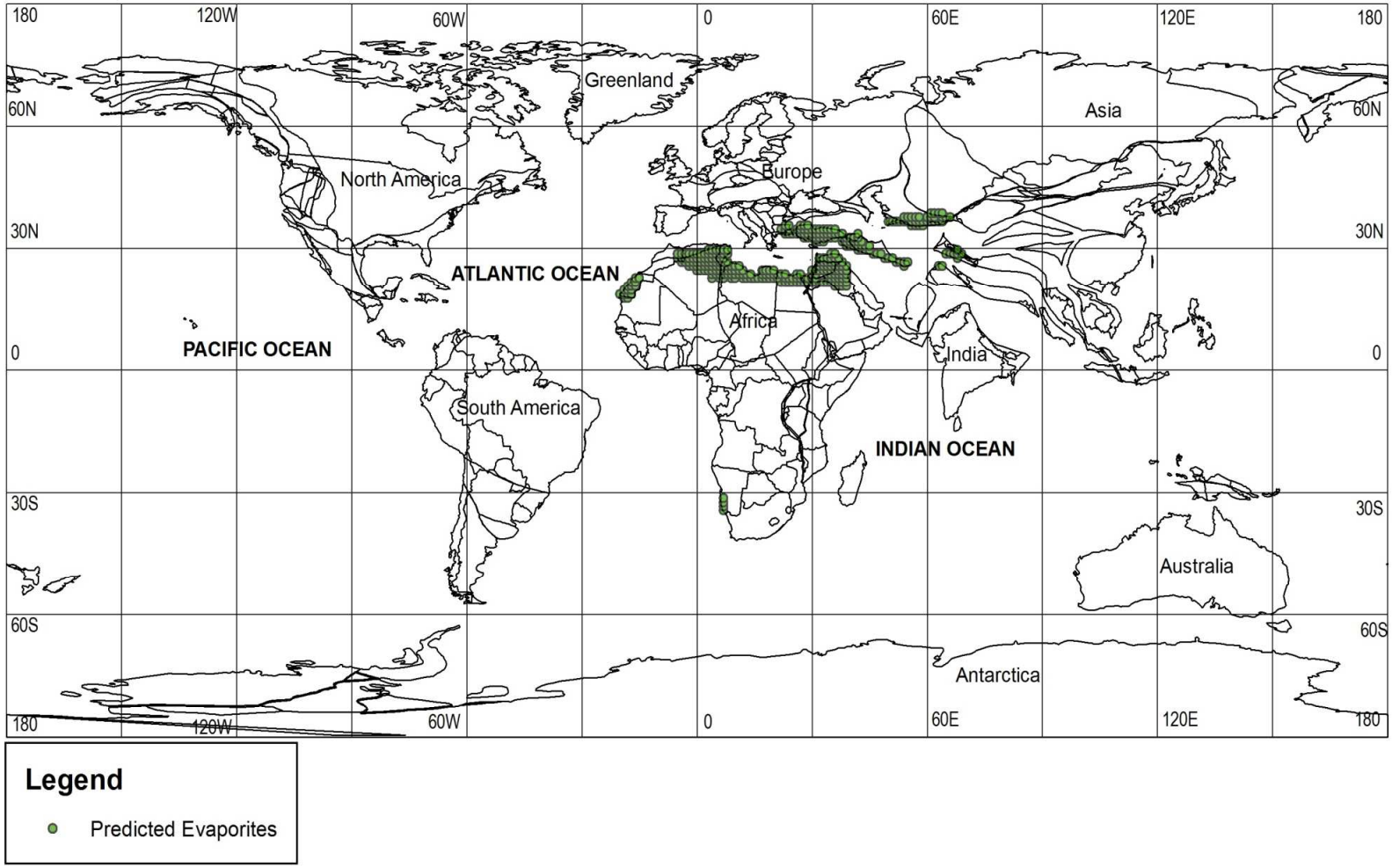

Figure 3.15: A map showing the location of the predicted evaporites for the Middle Eocene time period.

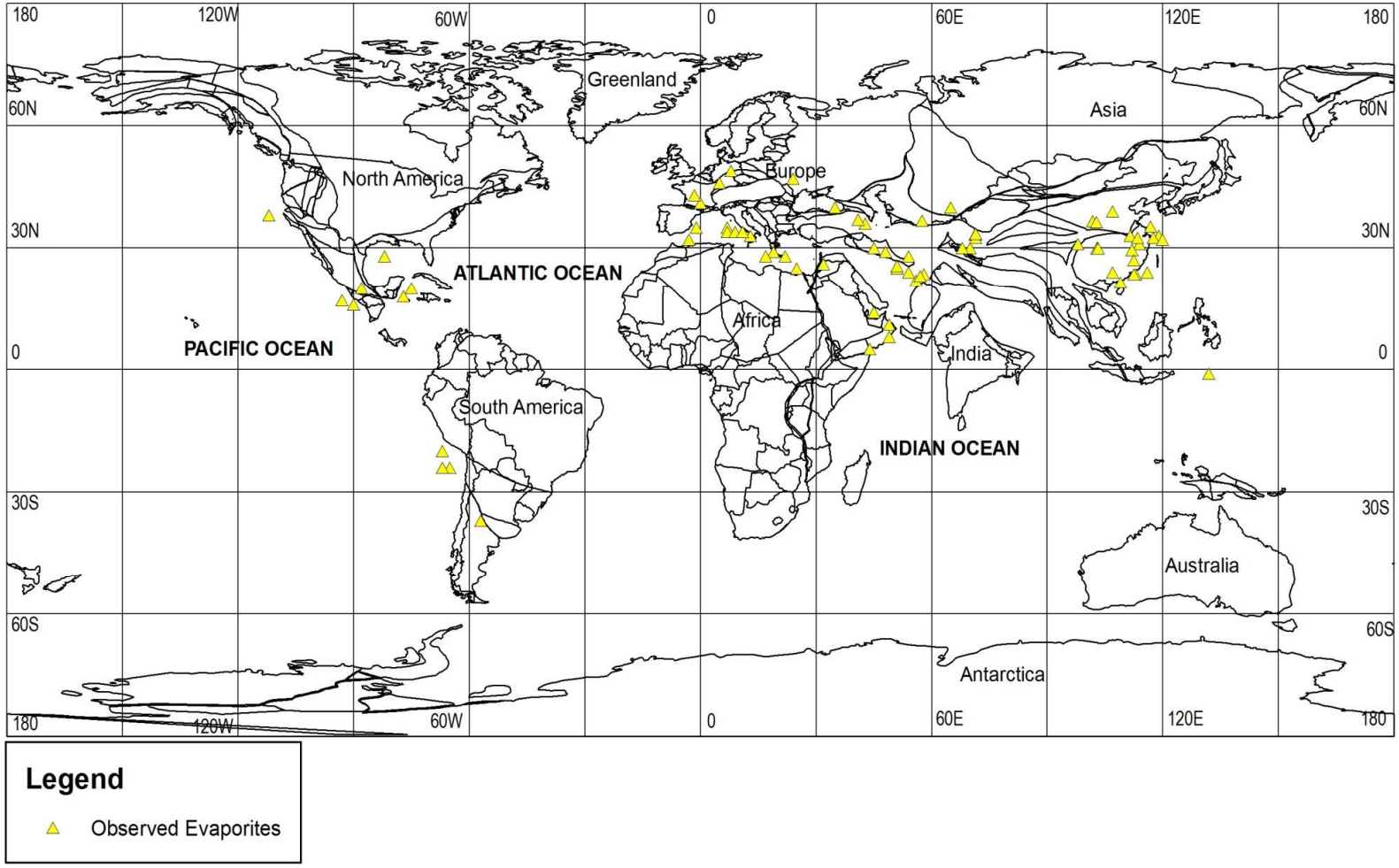

Figure 3.16: A map showing the location of observed evaporites for the Middle Eocene time period.

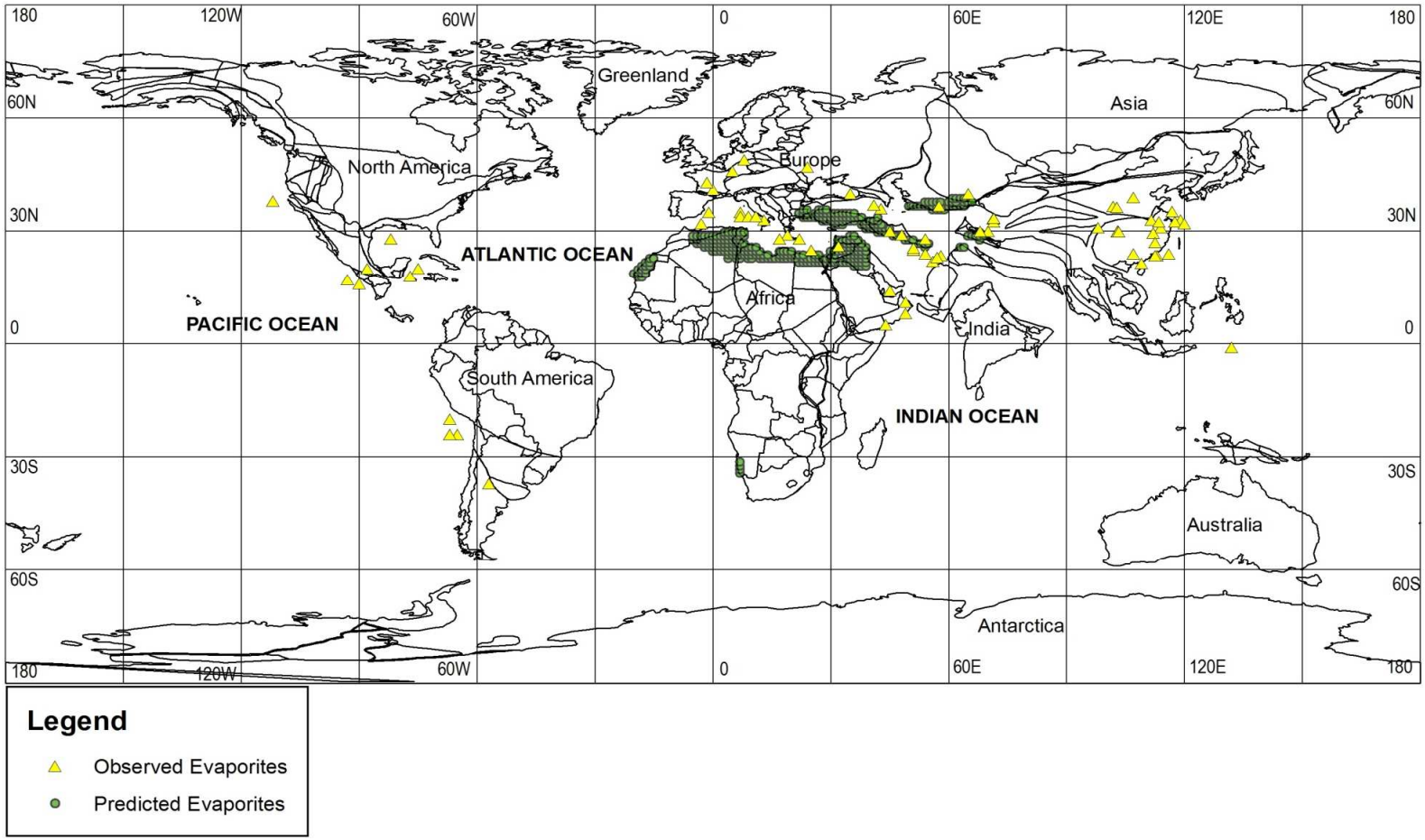

Figure 3.17: A map showing both the predicted and the observed evaporites for the Middle Eocene time period.

3.5.1.1 Statistical Analyzes for the Middle Eocene

A boundary representing the edge of the continental lithosphere for the Middle Eocene was mapped and in Figure 3.18 is represented by 5°x5° grid cells. For the Middle Eocene, 1489 continental grid cells were obtained (Figure 3.18). 37 of these 5°x5° grid cells contained localities for the predicted evaporites. This represents 2.48% of the continental grid cells (Figure 3.19). 44 grid cells contained observed evaporite localities (Figure 3.20). 11 grid cells contained both predicted and observed evaporite localities which are designated as "hits" (Figure 3.21). According to the statistical procedure outlined in section 2.4, since the expected number of hits was 1.09 and the observed number of hits was 11, the probability that the number of hits is due to a random process is 2.17×10^{-8}. The variables used in the statistical analysis for the Middle Eocene are in Table 3.1.

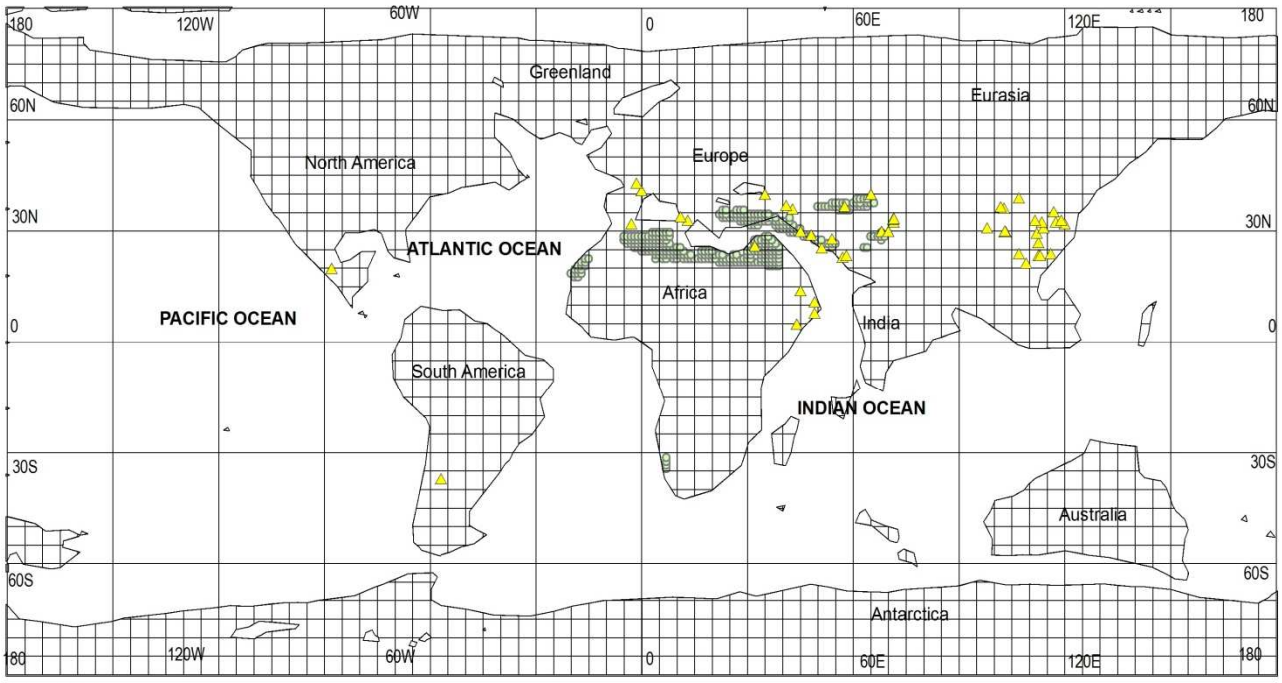

Figure: 3.18: This map shows the 5°x5° latitude- longitude grids for the Middle Eocene time period.

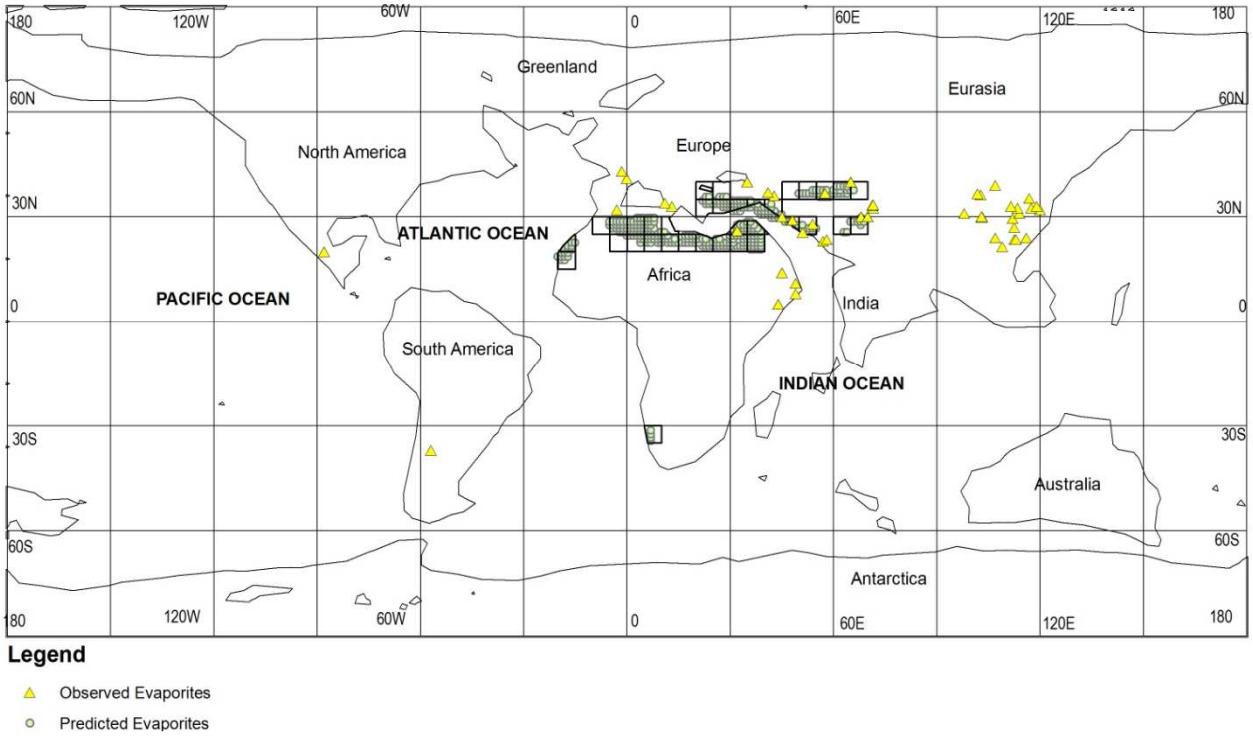

Figure 3.19: This map shows the 5°x5° latitude- longitude grids for the Middle Eocene predicted evaporites.

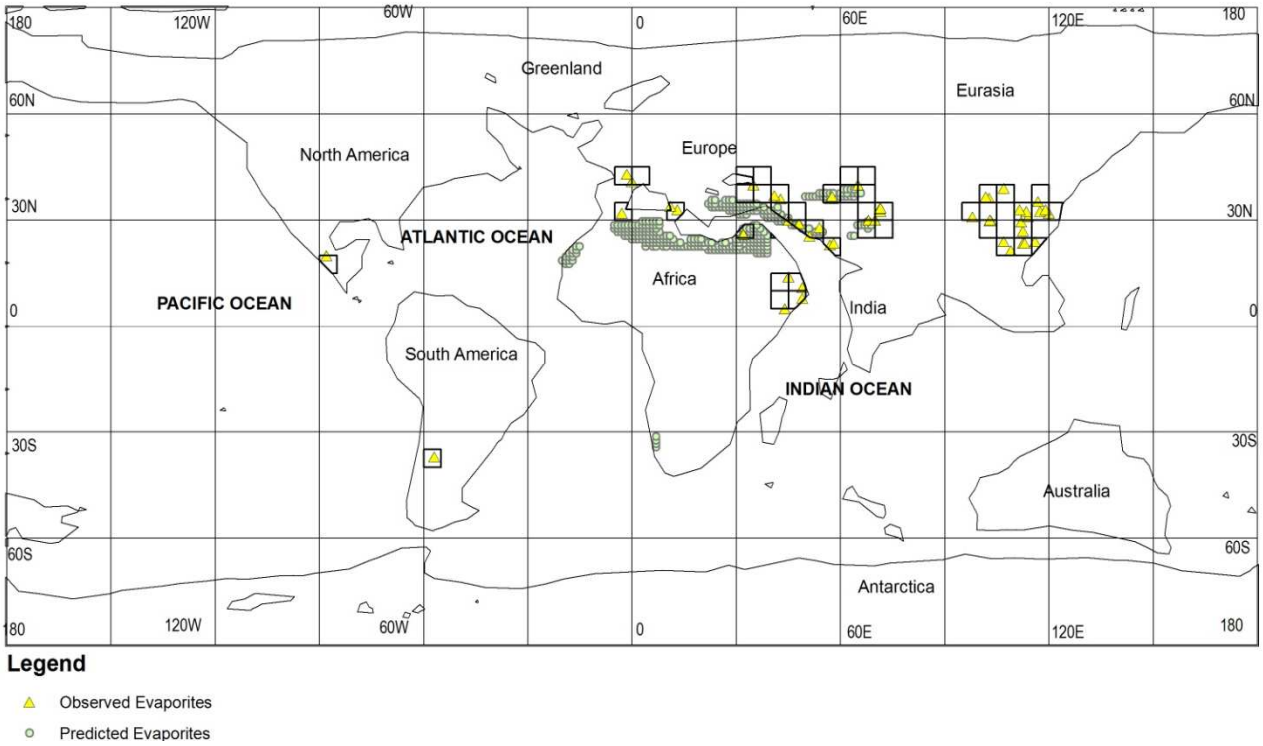

Figure 3.20: This map shows the 5°x5° latitude- longitude grids for the Middle Eocene observed evaporites.

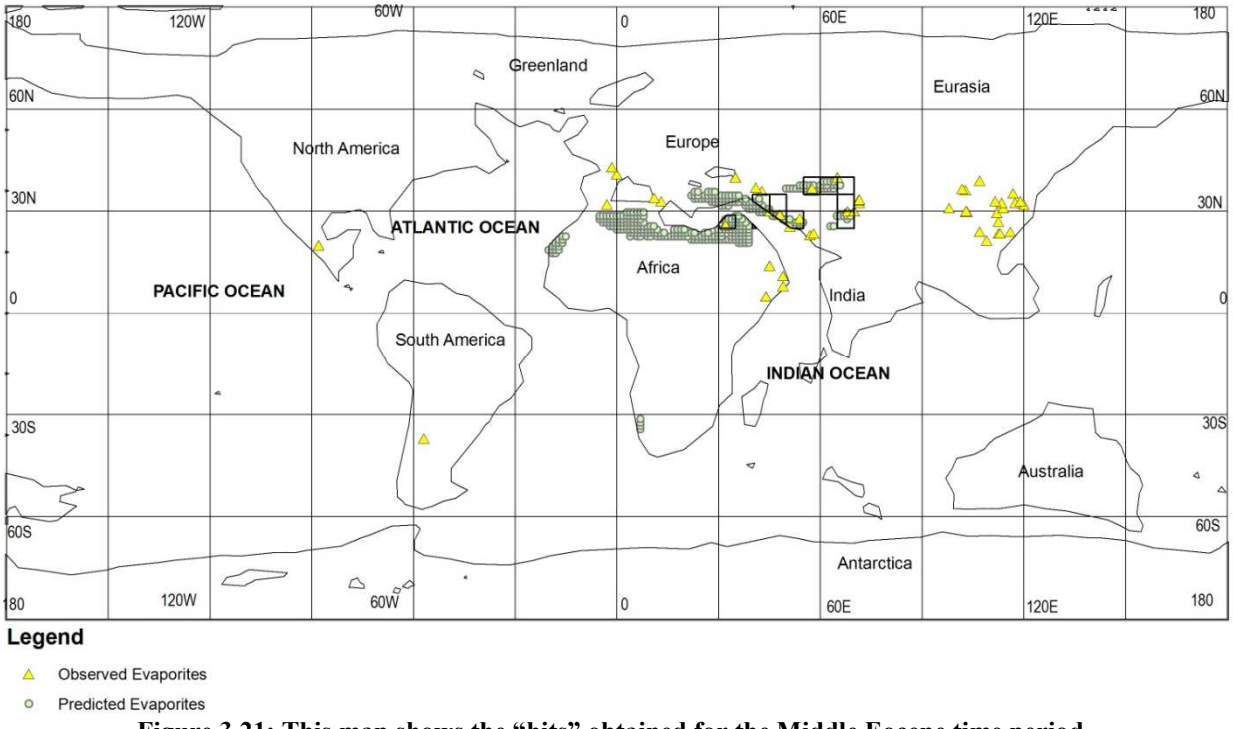

Figure 3.21: This map shows the "hits" obtained for the Middle Eocene time period.

Below is a summary of the statistics obtained for the Cenozoic Era (Table 3.1 and Appendix D). The number of observed predicted evaporites was more for all three time periods than what was expected and hence as can be observed in the table, the probabilities for all three time periods is low which shows that the match between the geographic distribution of the observed and the predicted evaporites is not random.

Table 3.1 Statistical Calculation for the Cenozoic Era

Geologic Time Period	Total Land	Number of Predicted Evaporites	%Total Land Occupied by Predicted Evaporites	Number of Observed Evaporites	Predicted Number of Hits	Hits	Misses	Probability that Hits are Random
Late Miocene (10 Ma)	1434	87	6.07	58	3.52	15	43	3.558×10^{-6}
Oligocene (30 Ma)	1434	97	6.76	45	3.04	15	30	6.402×10^{-7}
Middle Eocene (45 Ma)	1489	37	2.48	44	1.09	11	33	2.173×10^{-8}

CHAPTER 4

MESOZOIC EVAPORITES

4.1 Introduction

The Mesozoic Era is divided into three time periods namely the Cretaceous, Jurassic and the Triassic. The Gandolph time slices for which FOAM paleoclimate simulations were run for the Cretaceous time period includes the Cretaceous/Tertiary boundary, the Late Cretaceous (Cenomanian/Turonian) and two stages from the Early Cretaceous time period: Aptian/Albian and the Barremian/Berriasian. The Jurassic time period includes the Late Jurassic and the Early Jurassic. The Triassic time period is also included and covers the Late Triassic. This chapter will review the climate and tectonics for each time period, the results obtained for both the predicted and the observed evaporites and lastly the statistical results for the match between the predicted and the observed evaporites.

4.2 The Cretaceous

4.2.1 Tectonics and Climate for the Cretaceous period

The Cretaceous period (146Ma- 65.5Ma) has been recorded as one of the warmest Phanerozoic periods with global annual mean surface temperatures 6°C higher than present (Barron, 1983). A weak present pole to equator thermal gradient existed which may have resulted in equable climate (Crowley and Zachos, 2000). The Cretaceous period was

characterized by abrupt greenhouse warming and cooling events (Keller, 2008) with very little glaciations in the Polar Regions (Hay, 2011). The northern Polar Region was covered by ocean and the southern Polar Region by land.

Various methods have been used to record the climatic trends that existed during the Cretaceous the most successful of which has been the oxygen isotope method (Frakes, 1979). Douglas and Savin, 1975 analyzed and recorded $\delta^{18}O$ values for benthic and planktic foraminifera and realized that the Early Cretaceous was characterized by a slight warming and the Late Cretaceous by a marked cooling.

Theories that have been suggested and could possibly explain the warming trend during the Cretaceous include palaeogeography, CO_2 levels and oceanic heat transport (Barron, 1983; Barron et al, 1984; Barron et al, 1993a, 1995). The arrangement of the continents during this time has been considered as a probable cause of the Cretaceous warming (Donn and Shaw, 1977) with the existence of a supercontinent resulting in warm interior climates. The paleogeography of the Cretaceous period included the gigantic landmass Pangea which has been suggested to have had very warm continental climate as a result of its mass (Scotese, 2001). A change in paleogeography would have also led to a change in the oceanic heat transport further increasing the warming trend. An increase in the greenhouse effects would have resulted in an increase in CO_2 levels during this time.

The Cretaceous/Tertiary boundary also known as the K/T boundary is characterized by the extinction of the dinosaurs. This extinction has been attributed to a number of factors some of which include a meteorite impact and an increase in volcanic activity (Kring, 2007). The meteorite impact has been considered as one of the possible theories due to an increase in the

discovery of iridium all over the world by Luis Alvarez and his son. An increase in volcanic activity was also recorded for the Cretaceous/Tertiary boundary (Ruddiman, 2008). It has been suggested that a meteorite impact and/or an increase in volcanic activity would have led to an increase in CO^2 levels and a temporary increase in greenhouse effect (Pope et al, 1997) making climate at the Cretaceous/ Tertiary boundary extremely warm.

At the Cretaceous/Tertiary boundary, North America and South America where not connected and South America was much closer to Africa than it is today. India was drifting towards Eurasia.

During the early Cretaceous, North America was still connected to Europe and South America to Africa. Australia was connected to Antarctica, while India was an island continent located in the South (Crowley and North, 1991). Two oceans existed during this time period namely the Tethys Ocean and the Panthalassic Ocean (Barron, 1980). During the late Cretaceous, the South Atlantic Ocean was opened, Australia was still connected to Antarctica and India was still an island in the southern tropics.

4.2.1.1 Cretaceous/ Tertiary Evaporites

The geographic distribution (Figure 4.1) of predicted evaporites was obtained by intersecting the Evaporite Climate Envelope with precipitation and temperature estimates for the Cretaceous/Tertiary Boundary. A total of 491 1°x1° localities fell within the Evaporite Climate Envelope for the Cretaceous/Tertiary Boundary. The predicted evaporite localities occur in North and South Africa and in the southern parts of Asia and Europe (Figure 4.1).

The geographic distribution of actual (observed) evaporite localities was obtained from a compilation by Boucot et al (in press). Cretaceous/Tertiary Boundary evaporites occur to the south of North America, on the west coast of South America, to the south of Africa and North Africa, Europe and Asia. A few could also be found in India and Australia. A total of 98 observed evaporites are plotted on Figure 4.2.

"Hits" were 6 in total and are observed in North Africa, South Africa, Central Asia and Western Asia. "Misses" are observed to the south of North America, west of South America, Eastern Asia, India, parts of North Africa, West Africa, East Africa, parts of South Africa and western Asia.

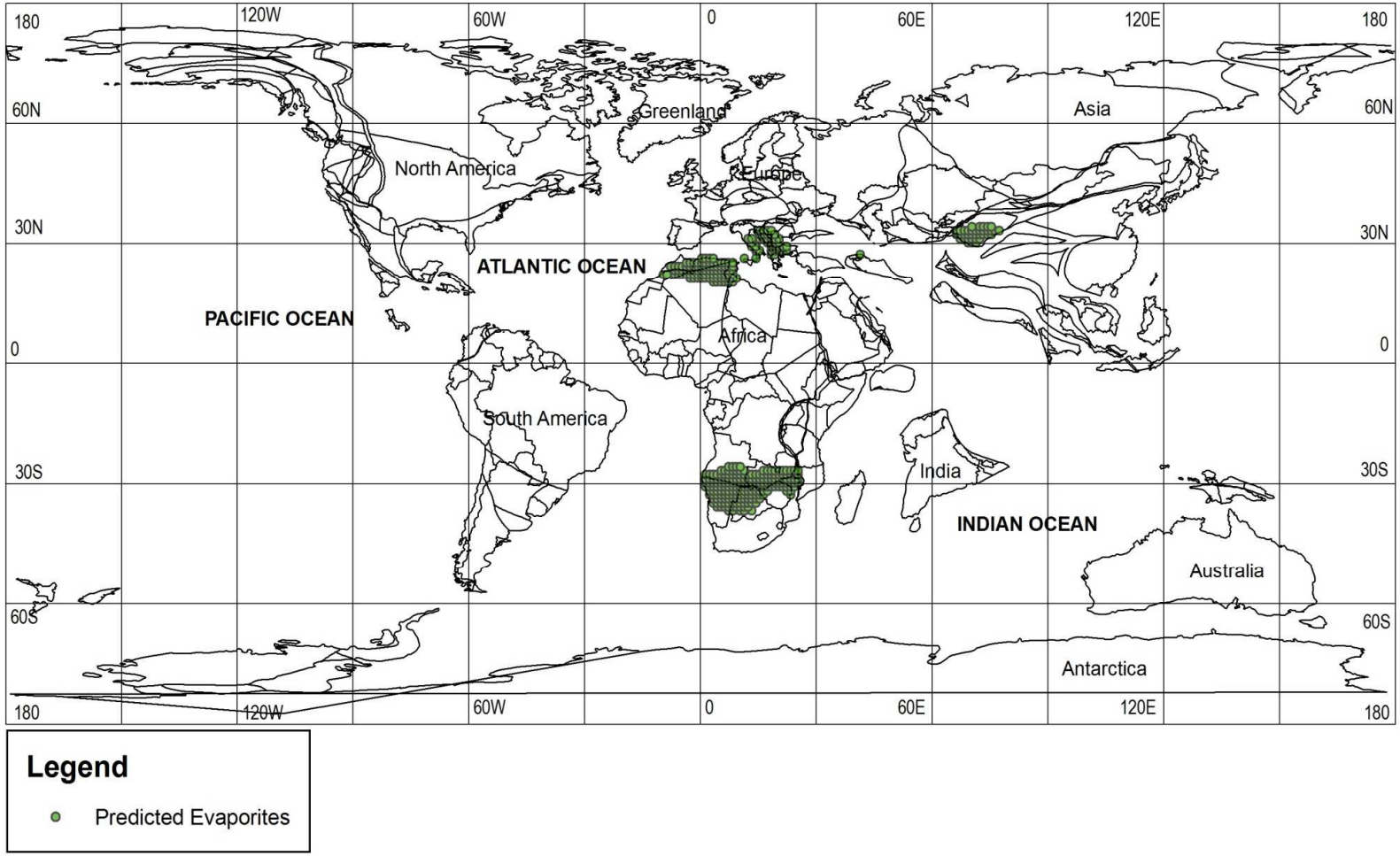

Figure 4.1: A map showing the location of the predicted evaporites for the Cretaceous/Tertiary boundary.

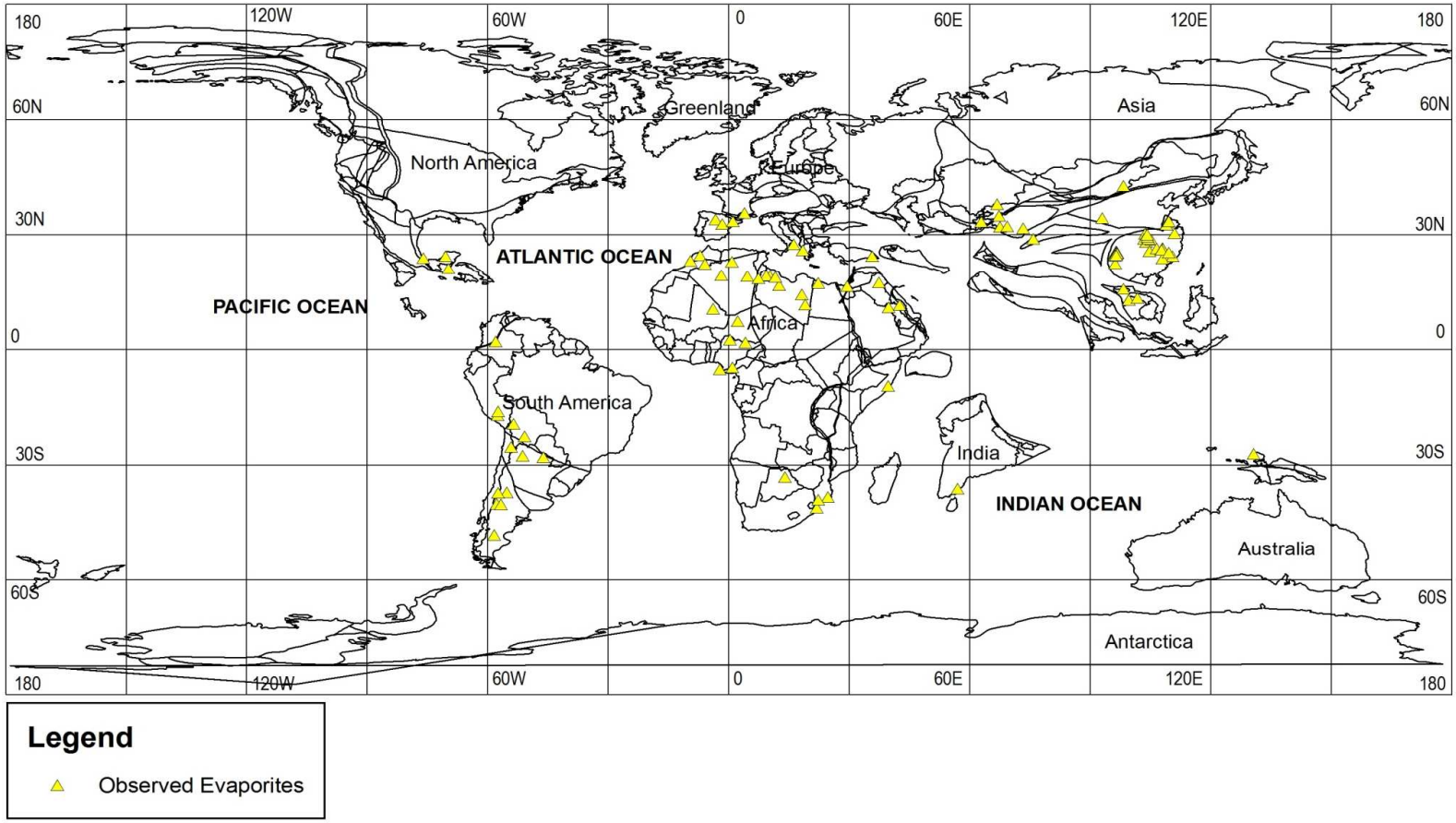

Figure 4.2: A map showing the location of observed evaporites for the Cretaceous/Tertiary boundary.

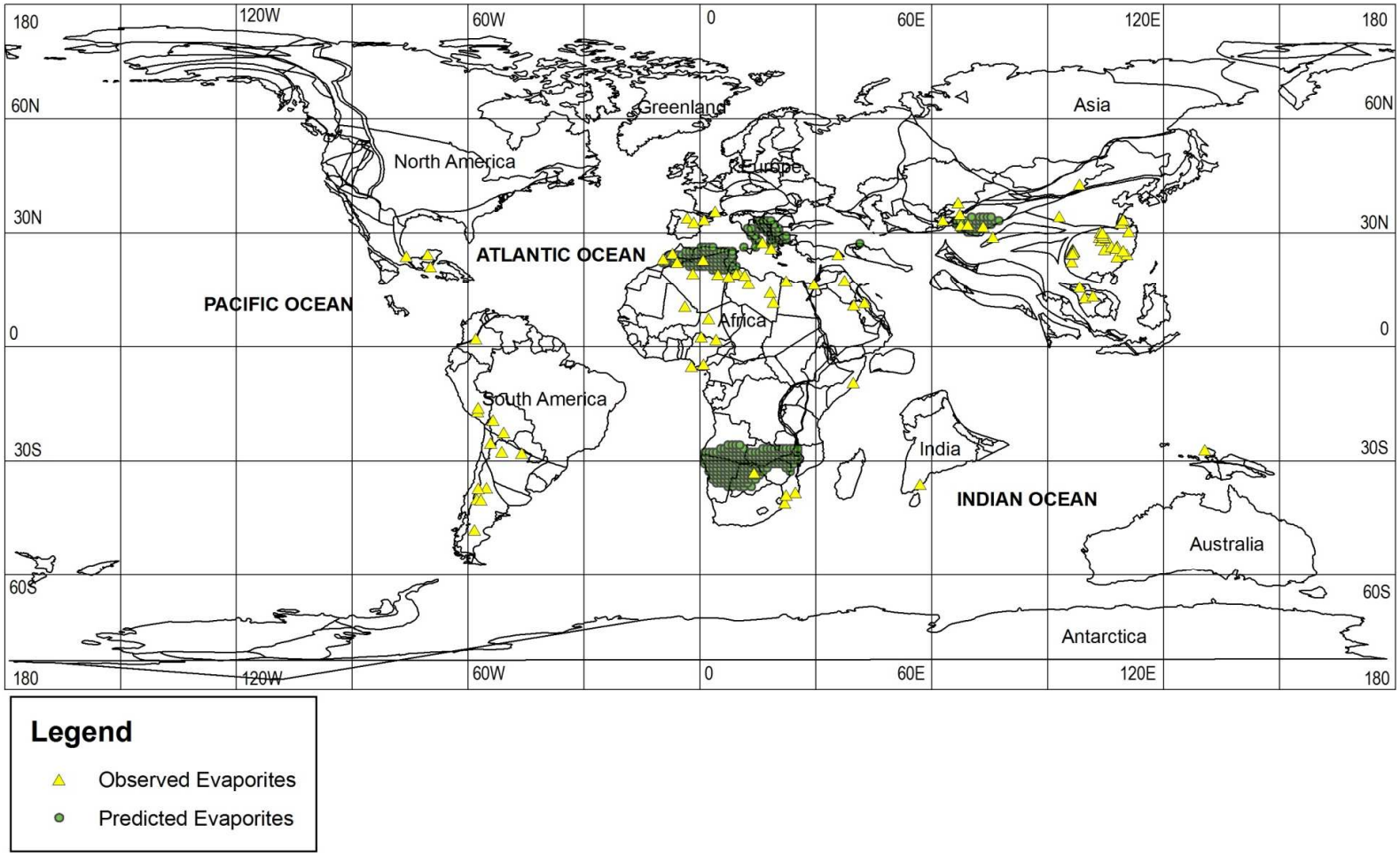

Figure 4.3: A map showing the both the predicted and observed evaporites for the Cretaceous/Tertiary boundary.

4.2.1.1.1 Statistical Analyzes for the Cretaceous/ Tertiary boundary

A boundary representing the edge of the continental lithosphere for the Cretaceous/Tertiary Boundary was mapped and in Figure 4.4 is represented by a 5°x5° set of grid cells. For the Cretaceous/Tertiary Boundary, 1334 grid cells were obtained. 25 of these 5°x5° grid cells contained localities for the predicted evaporites. This represents 1.87% of the continental grid cells (Figure 4.5). 41 grid cells contained observed evaporite localities (Figure 4.6). 4 grid cells contained both predicted and observed evaporite localities which are designated as “hits” (Figure 4.7). The variables used in the statistical analysis for the Cretaceous/Tertiary Boundary are given in Table 4.1. According to the statistical procedure outlined in section 2.4, since the expected number of hits was 0.77 and the observed number of hits was 4, the probability that the number of hits is due to a random process is 0.0068. This strongly suggests that the observed hits are not random and that the null hypothesis fails.

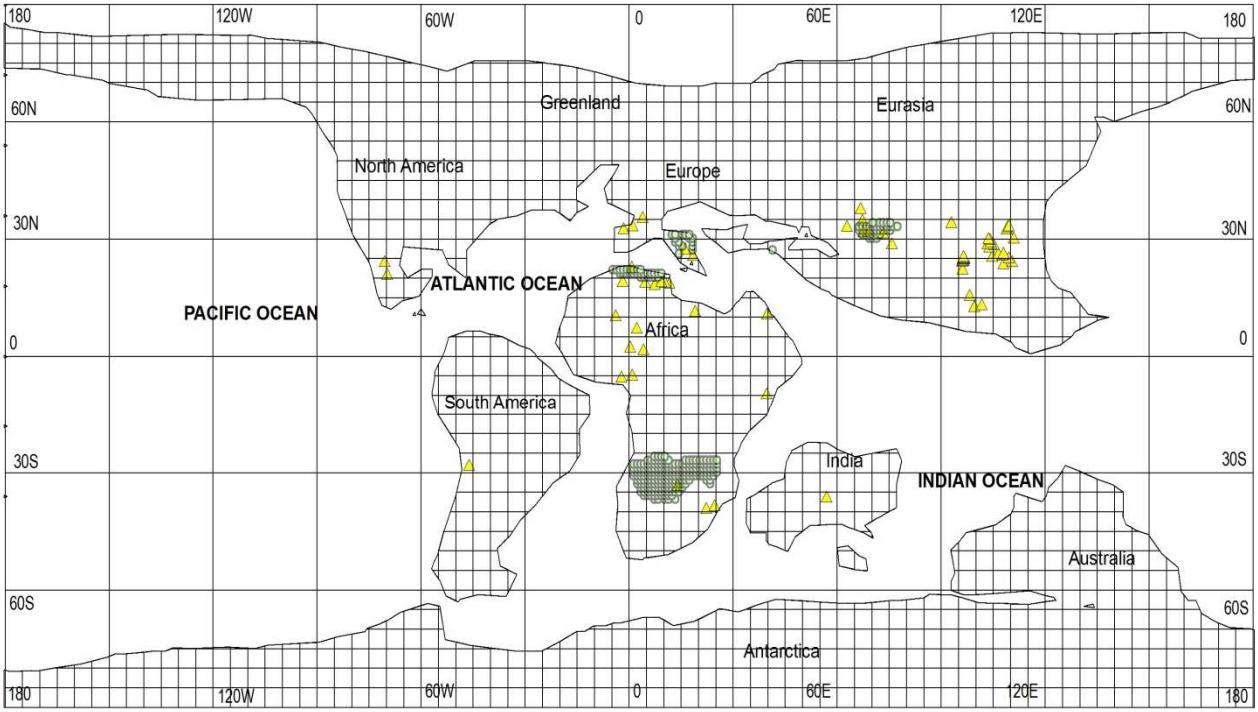

Figure 4.4: This map shows the 5°x5° latitude- longitude grids for the Cretaceous/Tertiary time period.

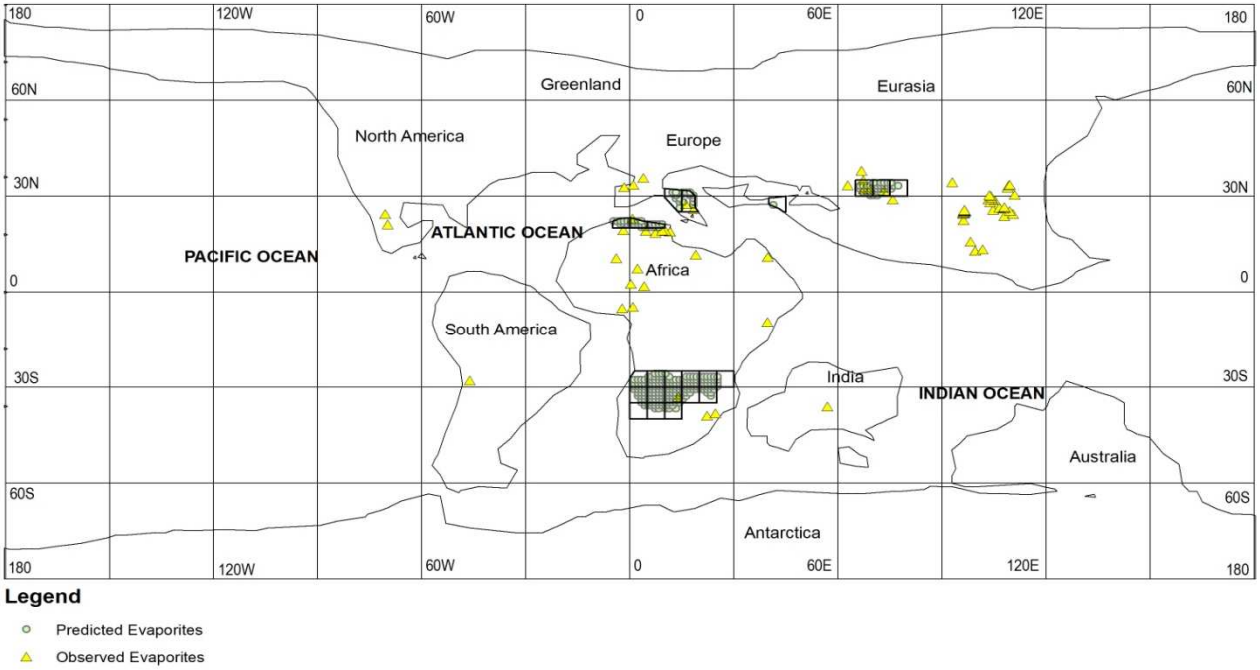

Figure 4.5: This map shows the 5°x5° latitude- longitude grids for the Cretaceous/Tertiary predicted evaporites.

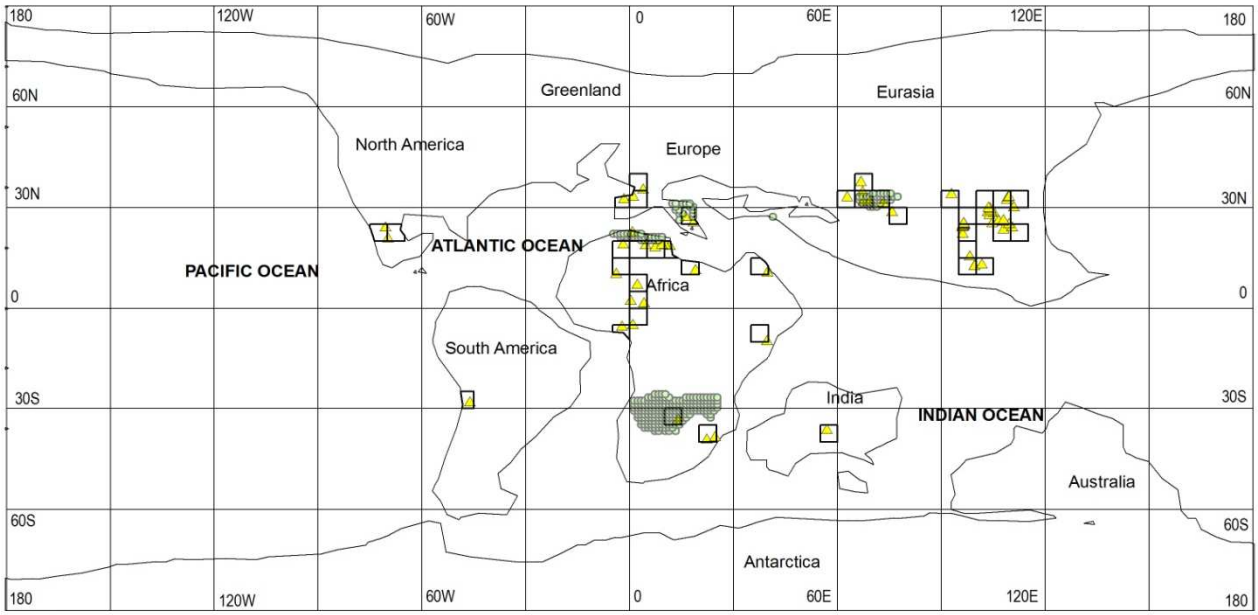

Figure 4.6: This map shows the 5°x5° latitude- longitude grids for the Cretaceous/Tertiary observed evaporites.

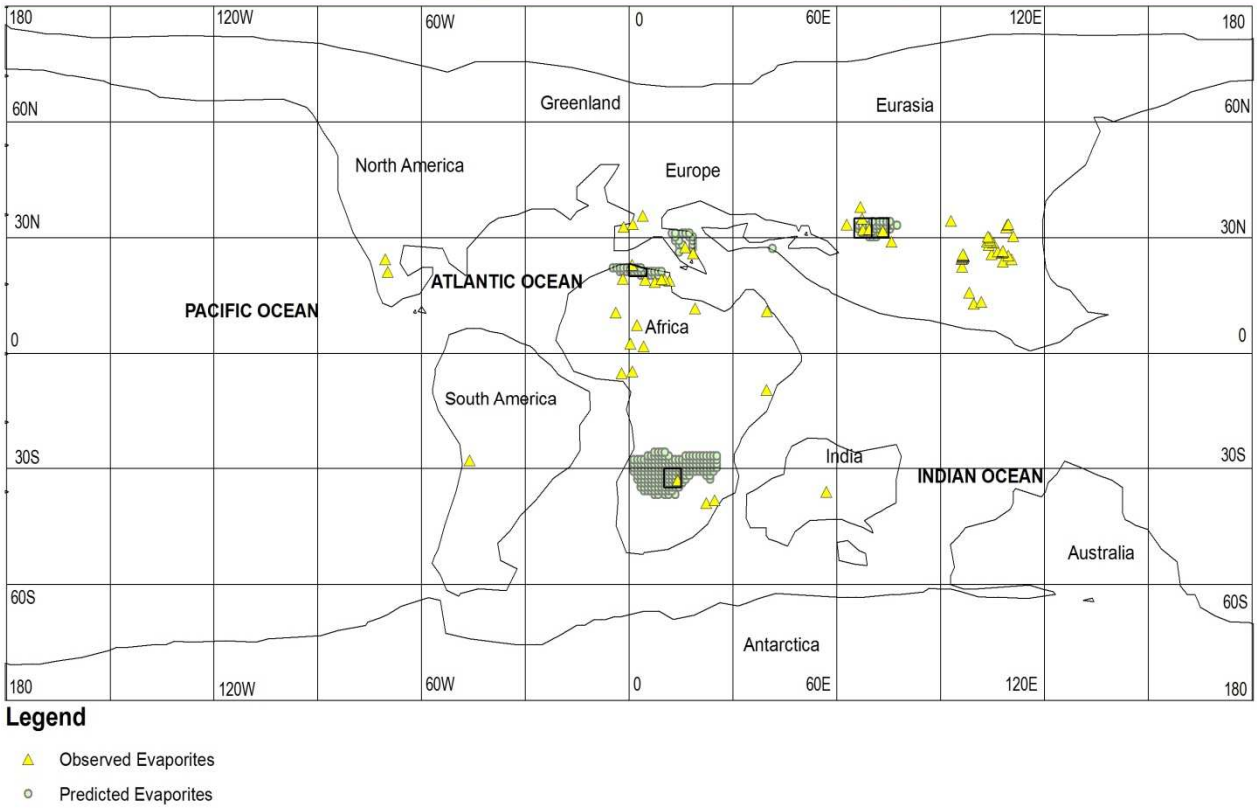

Figure 4.7: This map shows the "hits" obtained for the Cretaceous/Tertiary time period

4.3 Late Cretaceous: Cenomanian/Turonian (~ 90 Ma)

4.3.1 Cenomanian/Turonian Evaporites

The geographic distribution of predicted evaporites was obtained by intersecting the Evaporite Climate Envelope with precipitation and temperatures estimates for the Cenomanian/Turonian Evaporites. A total of 2605 1°x1° localities fell within the Evaporite Climate Envelope for the Cenomanian/Turonian. Majority of the predicted evaporite localities occur in the middle of South America, Africa and in South Asia 0- 45° latitude north and south of the equator. A few could also be found to the south of North America and in North Africa (Figure 4.8).

The geographic distribution of actual (observed) evaporite localities was obtained from a compilation by Boucot et al (in press). Cenomanian/Turonian evaporites occur along the southern coast of North America, eastern North America, north and middle of South America; most of North Africa, South Africa, southern Asia, India and Europe. A total of 105 observed evaporites are plotted in Figure 4.9.

"Hits" are observed in parts of southern North America, western South America, eastern North Africa, and western South Africa, Central and Southern Asia (Figure 4.10). "Misses" are in southern North America, north and south of South America, North Africa, India, Western Asia and Southern Asia.

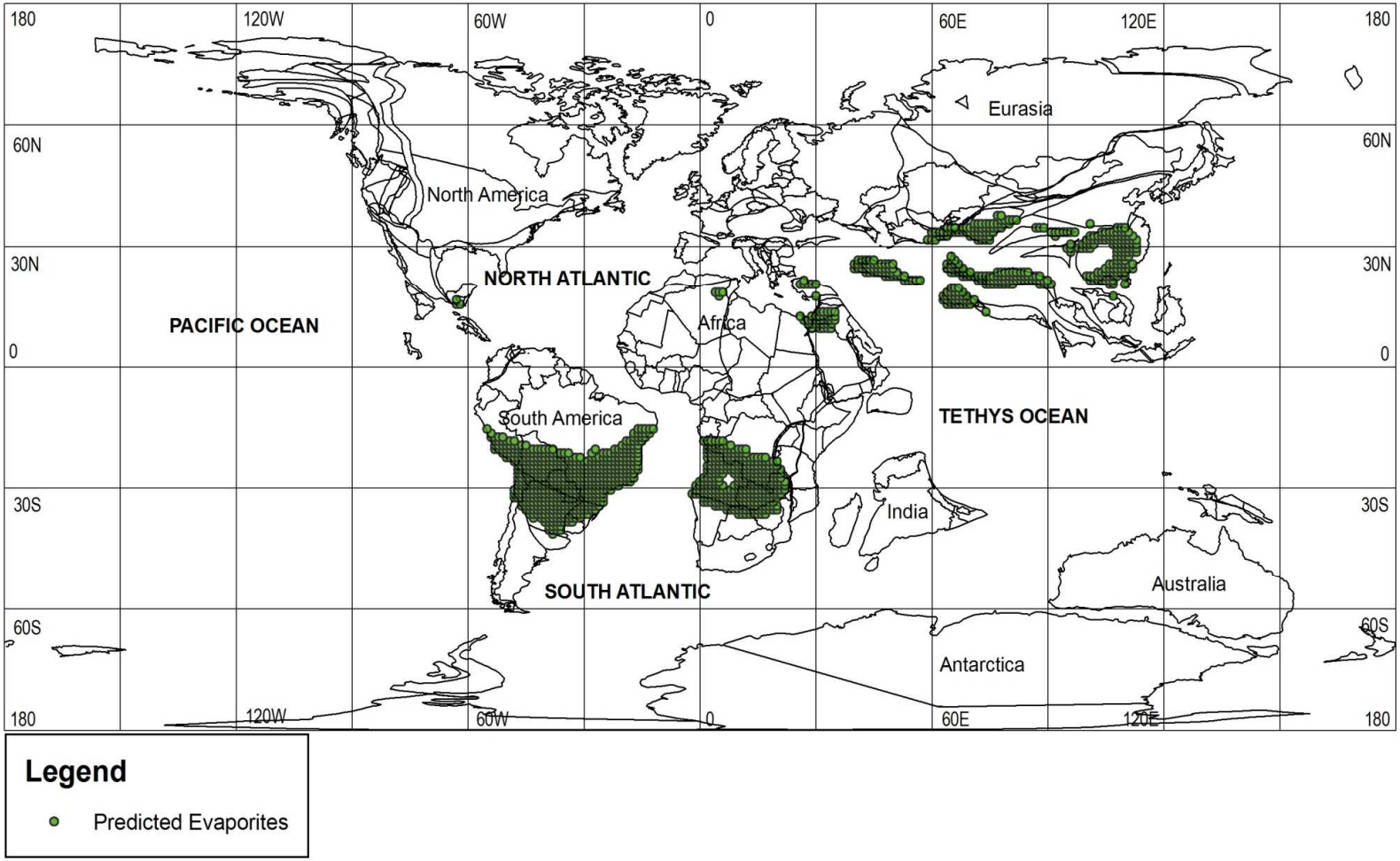

Figure 4.8: A map showing the location of the predicted evaporites for the Cenomanian/Turonian time period.

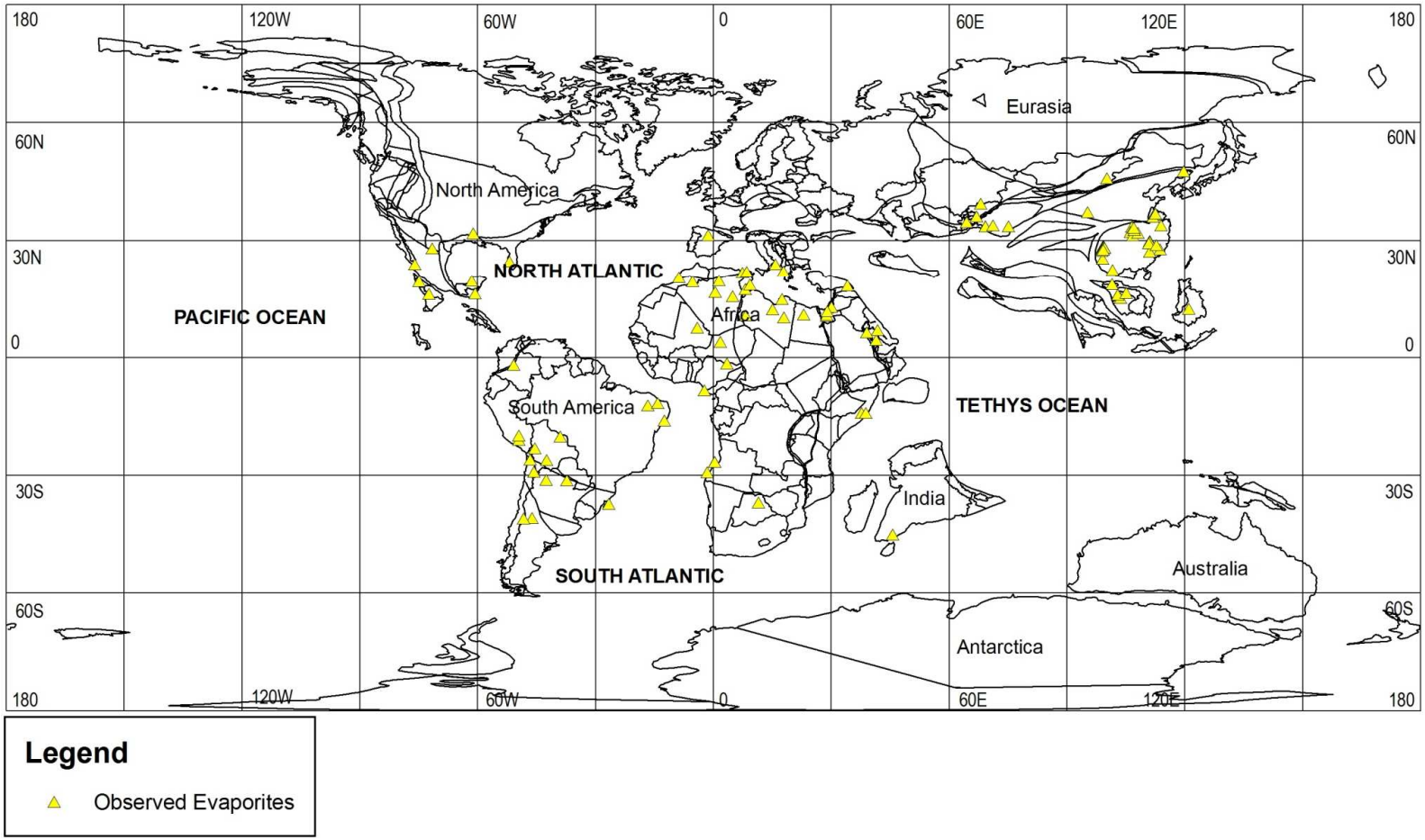

Figure 4.9: A map showing the observed evaporites for the Cenomanian/Turonian time period.

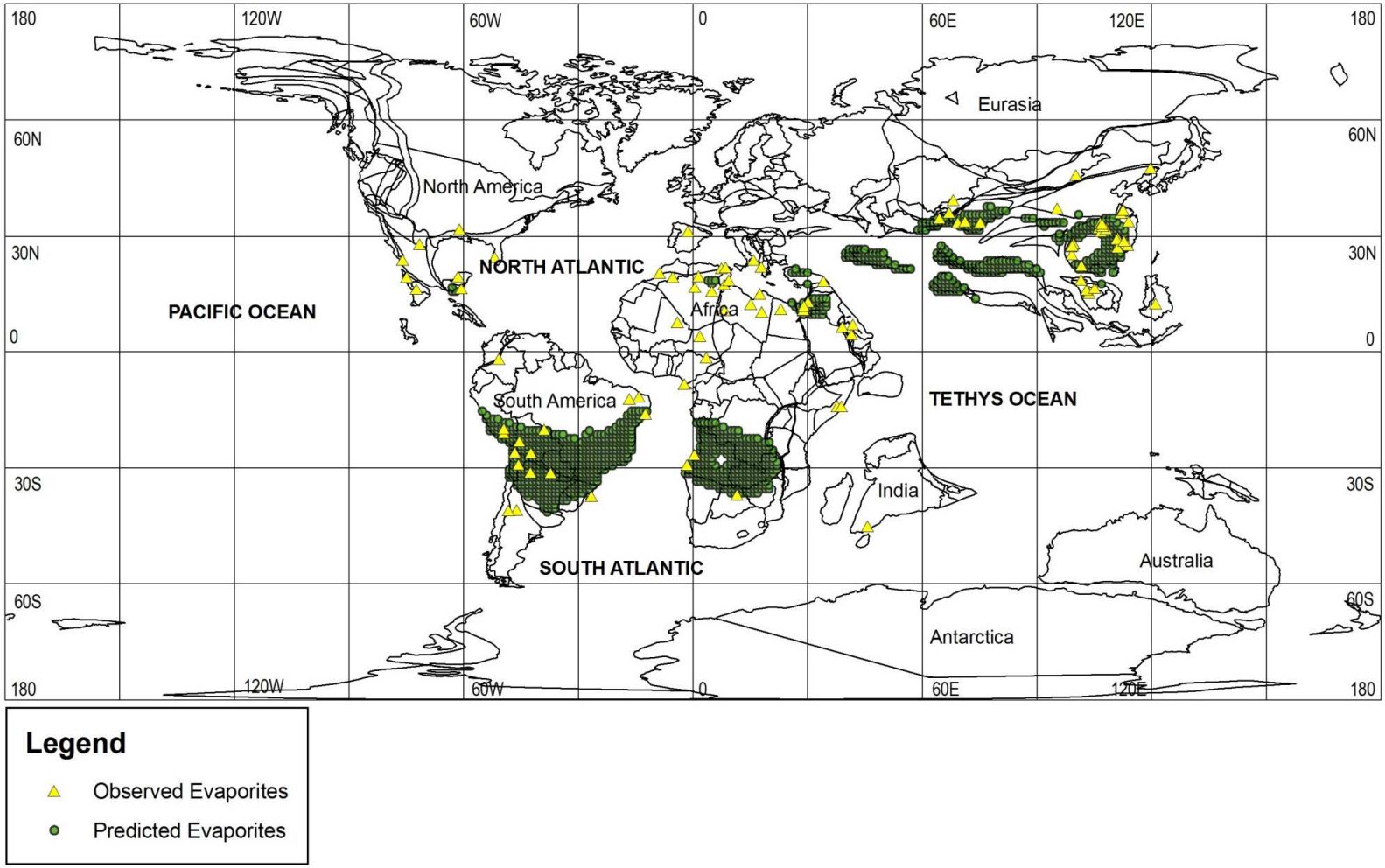

Figure 4.10: A map showing both the predicted and the observed evaporites for the Cenomanian/Turonian time period.

4.3.1.1 Statistical Analysis for the Cenomanian/Turonian

A boundary representing the edge of the continental lithosphere for the Cenomanian/Turonian was mapped and in Figure 4.11 is represented by a 5°x5° set of grid cells. For the Cenomanian/Turonian, 1403 grid cells were obtained. 104 of these 5°x5° grid cells contained localities for the predicted evaporites. This represents 7.41% of the continental grid cells (Figure 4.12). 55 grid cells contained observed evaporite localities (Figure 4.13). 24 grid cells contained both predicted and observed evaporite localities which are designated as "hits" (Figure 4.14). According to the statistical procedure outlined in section 2.4, since the expected number of hits was 4.08 and the observed number of hits was 24, the probability that the number of hits is due to a random process is 1.23×10^{-11} (Table 4.1). This strongly suggests that the observed hits are not random and that the null hypothesis fails.

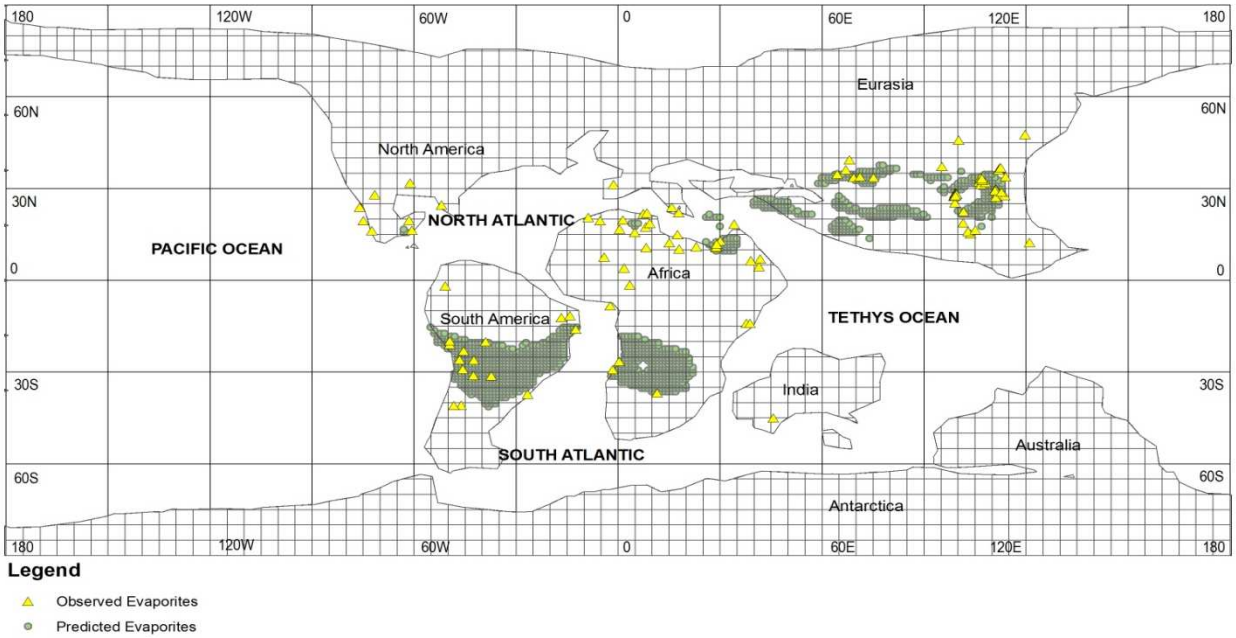

Figure 4.11: This map shows the 5°x5° latitude- longitude grids drawn for the Cenomanian/Turonian time period.

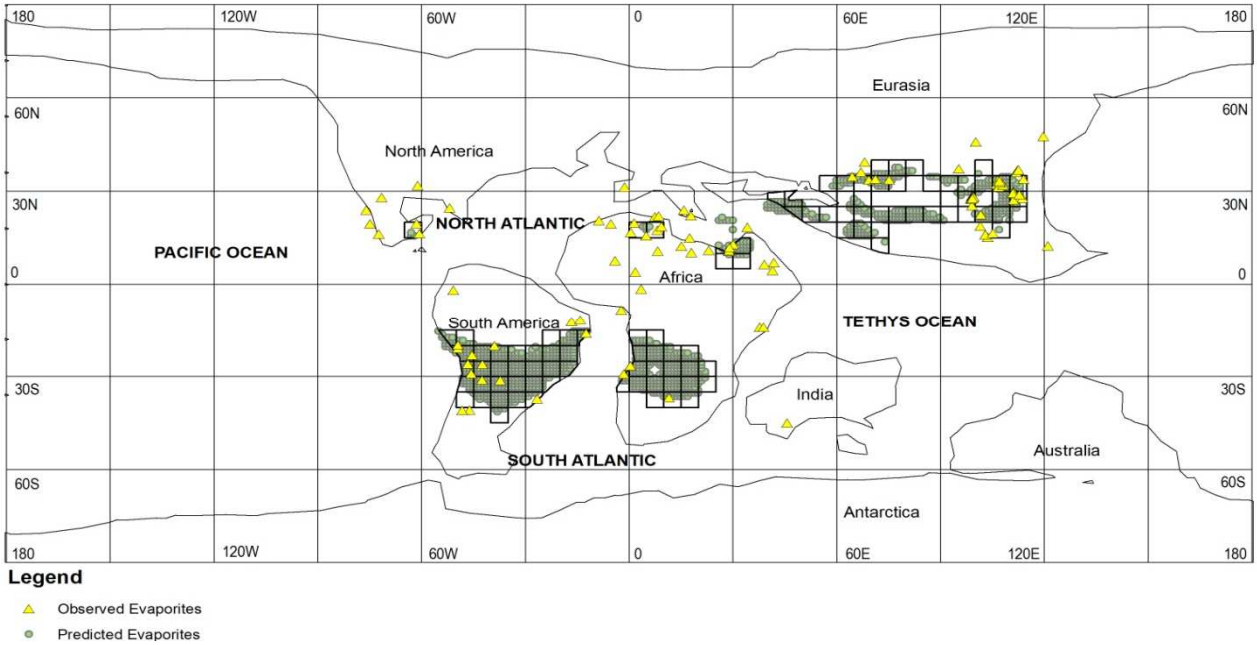

Figure 4.12: This map shows the 5°x5° latitude- longitude predicted grids for the Cenomanian/Turonian evaporite localities.

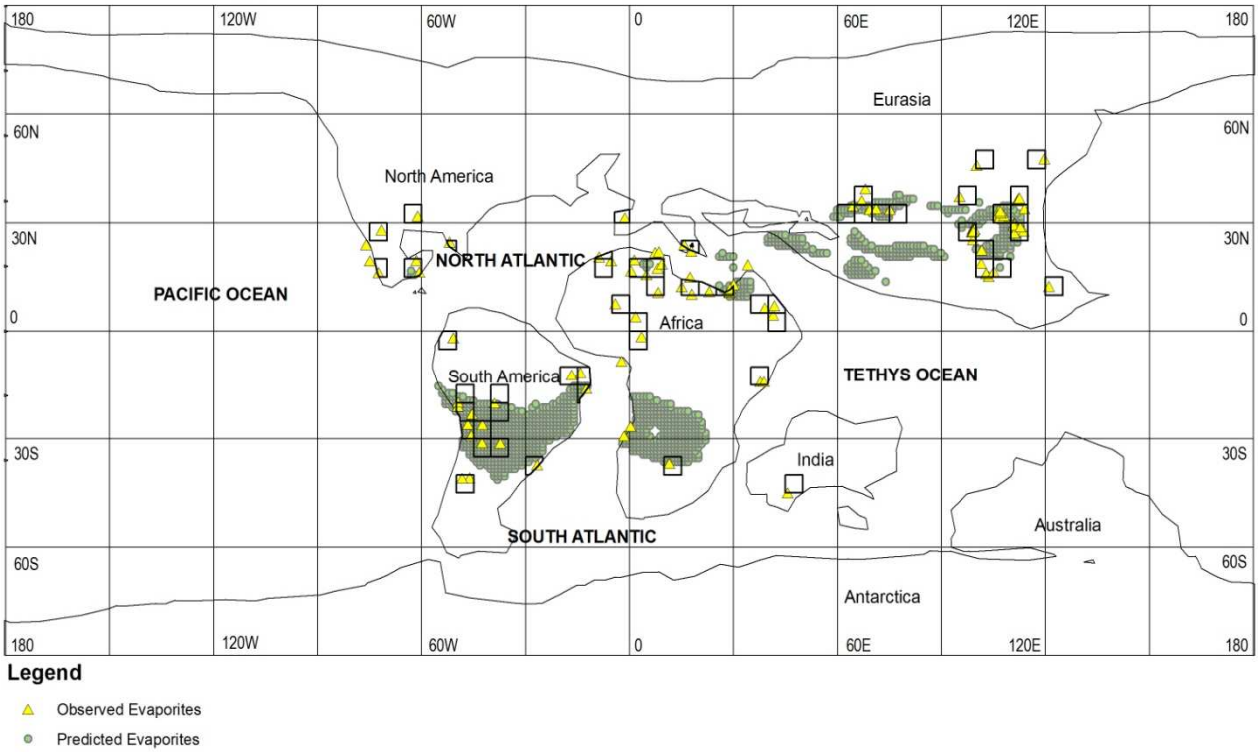

Figure 4.13: This map shows the 5°x5° latitude- longitude for the Cenomanian/Turonian observed evaporite localities.

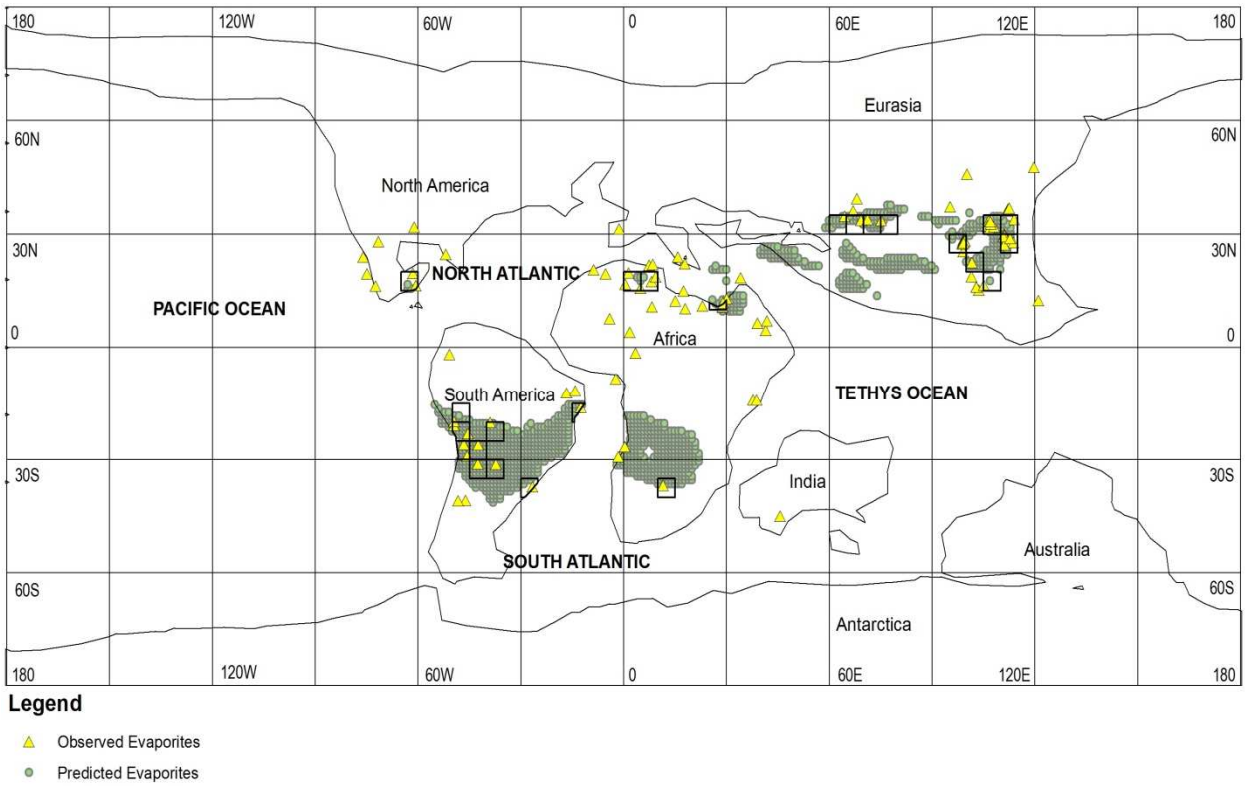

Figure 4.14: This map shows the "hits" obtained for the Cenomanian/Turonian time period.

4.4 Early Cretaceous: Aptian/Albian (~ 120 Ma)

4.4.1 Aptian/Albian Evaporites

The geographic distribution of predicted evaporites was obtained by intersecting the Evaporite Climate Envelope with precipitation and temperature estimates for the Aptian/Albian. A total of 3885 1°x1° localities fell within the Evaporite Climate Envelope for the Aptian/Albian. The predicted localities occur in the middle of South America and Africa forming an evaporite belt across the countries from the west to the east. Other predicted evaporite localities could be found in North America and in Asia (Figure 4.15).

The geographic distribution of actual (observed) evaporite localities was obtained from a compilation by Boucot et al (in press). Aptian/Albian evaporites occur along the coasts of North

America and South America, Europe and Asia. In Europe and Asia, the observed evaporites could also be seen plotting out mainly to the south of the continents and along the coastlines. Other observed evaporites could be found in Africa, India and Australia (Figure 4.16). A total of 103 evaporites are plotted on Figure 4.16.

"Hits" are observed in South Africa, Central Asia, North Africa and central South America (Figure 4.17). "Misses" are in the south of North America, north of South America, North Africa, west of Africa, India, Australia, Western, Eastern and Central Eurasia.

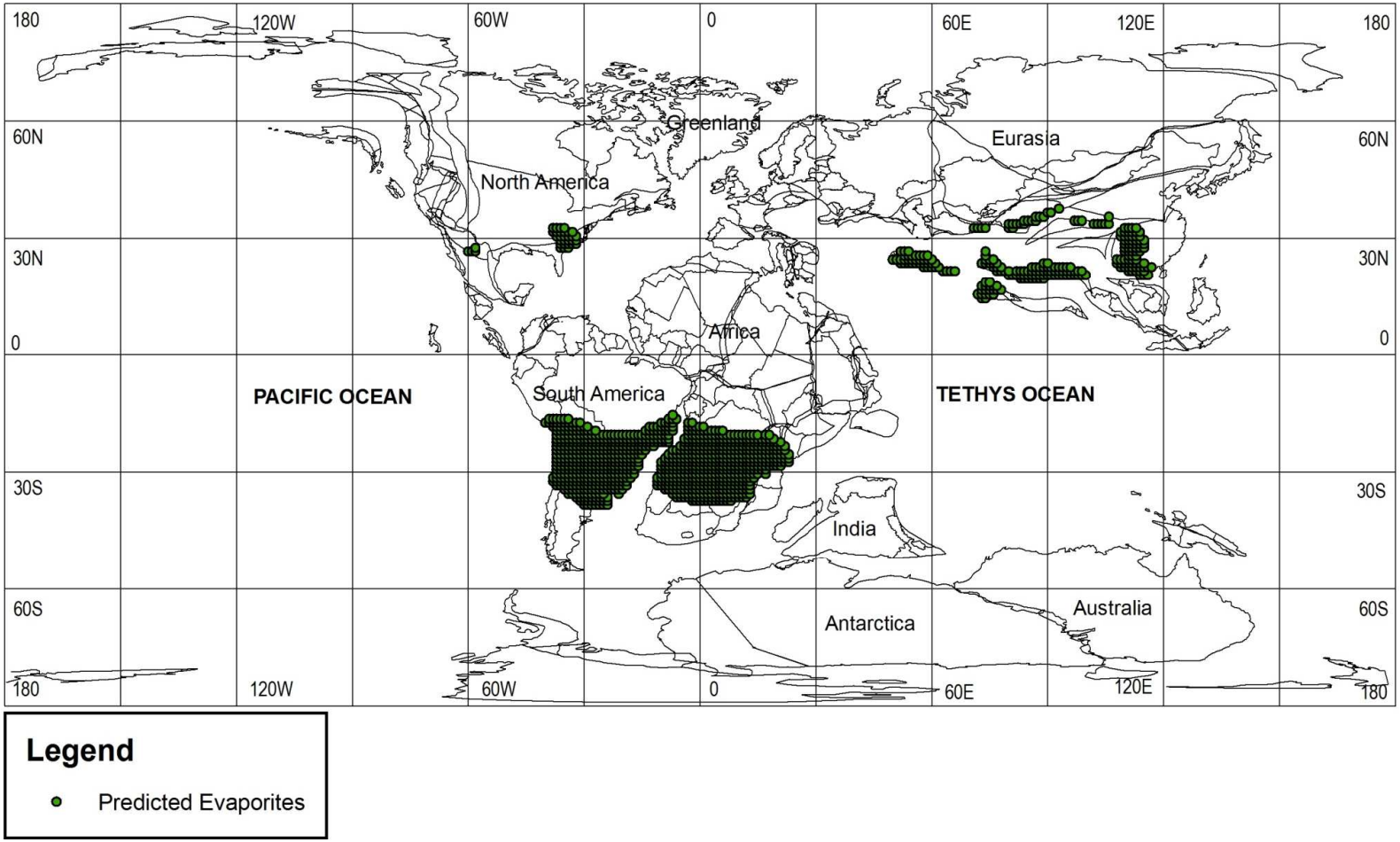

Figure 4.15: Paleoreconstruction showing the location of the predicted evaporites for the Aptian/Albian time period.

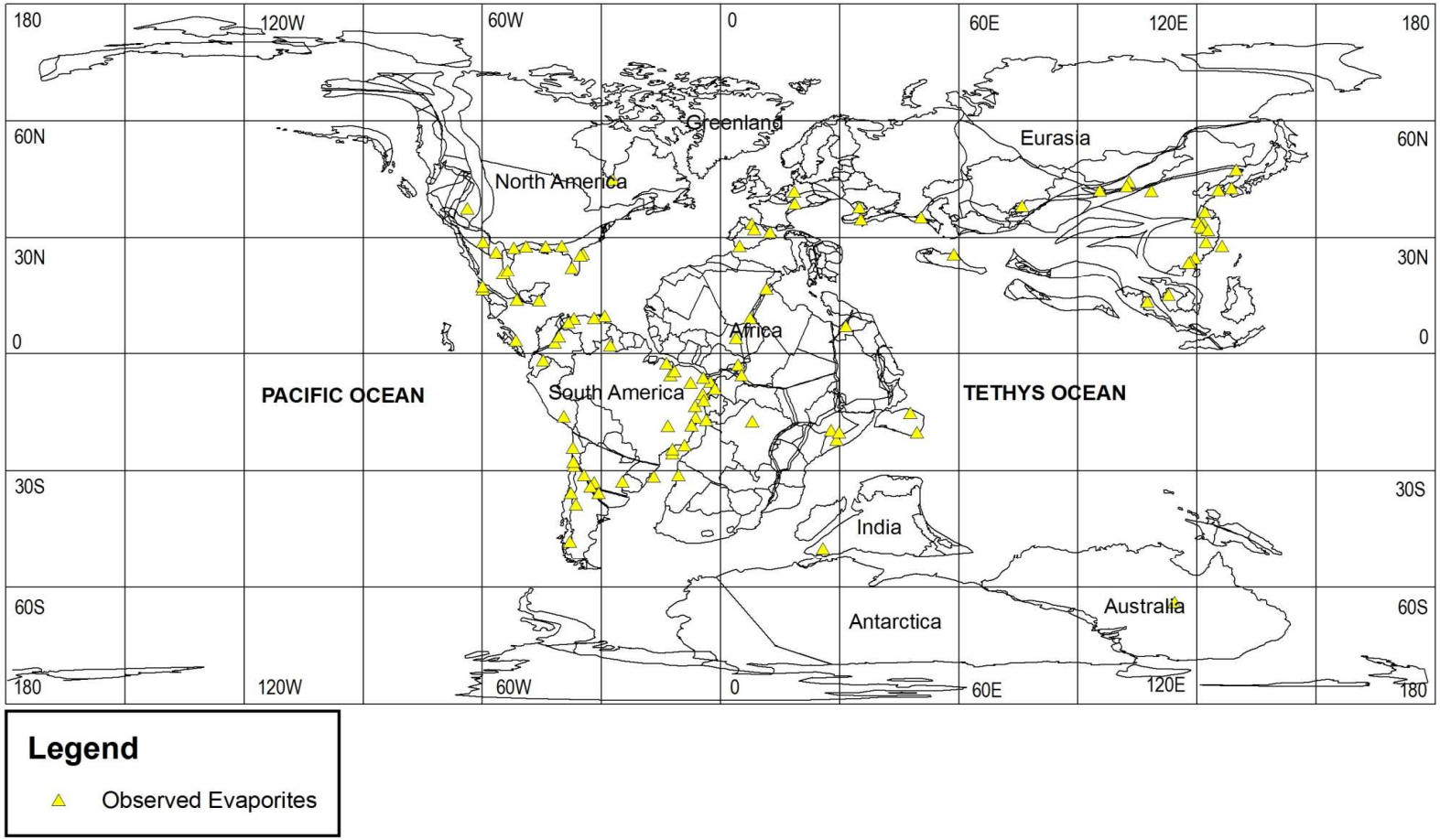

Figure 4.16: Paleoreconstruction showing the location of observed evaporites for the Aptian/Albian time period.

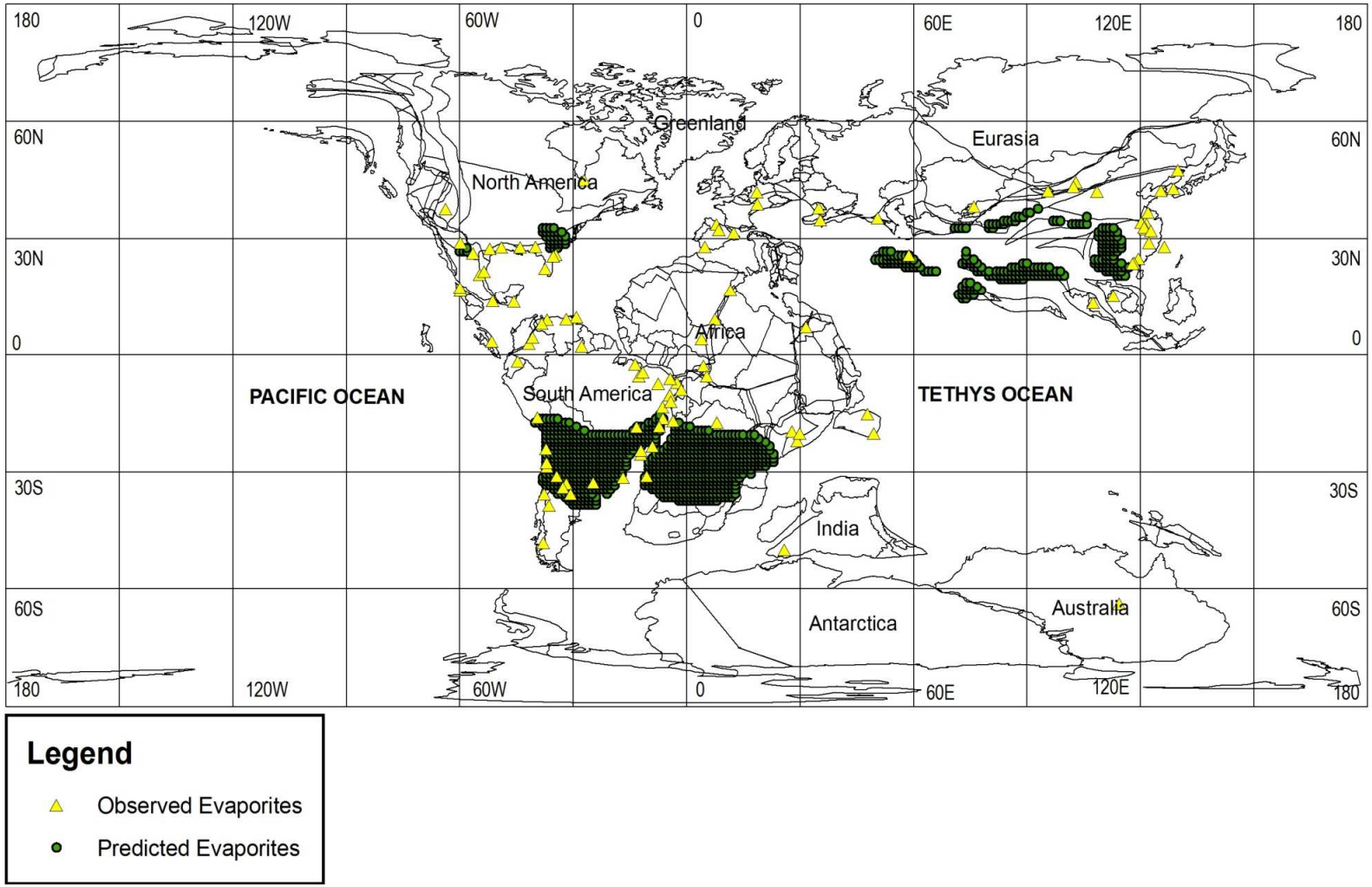

Figure 4.17: Paleoreconstruction showing the location of both the predicted and the observed evaporites for the Aptian/Albian time period.

4.4.1.1 Statistical Analyzes for the Aptian/Albian

A boundary representing the edge of the continental lithosphere for the Aptian/Albian was mapped and in Figure 4.18 is represented by a 5°x5° set of grid cells. For the Aptian/Albian, 1436 grid cells were obtained. 92 of these grid cells contained localities for the predicted evaporites. This represents 6.41% of the continental grid cells (Figure 4.19). 71 grid cells contained observed evaporite localities (Figure 4.20). 20 grid cells contained both predicted and observed evaporite localities which are designated as "hits" (Figure 4.21). According to the statistical procedure outlined in section 2.4, since the expected number of hits was 4.55 and the observed number of hits was 20, the probability that the number of hits is due to a random process is 6.28×10^{-8} (Table 4.1). This strongly suggests that the observed hits are not random and that the null hypothesis fails.

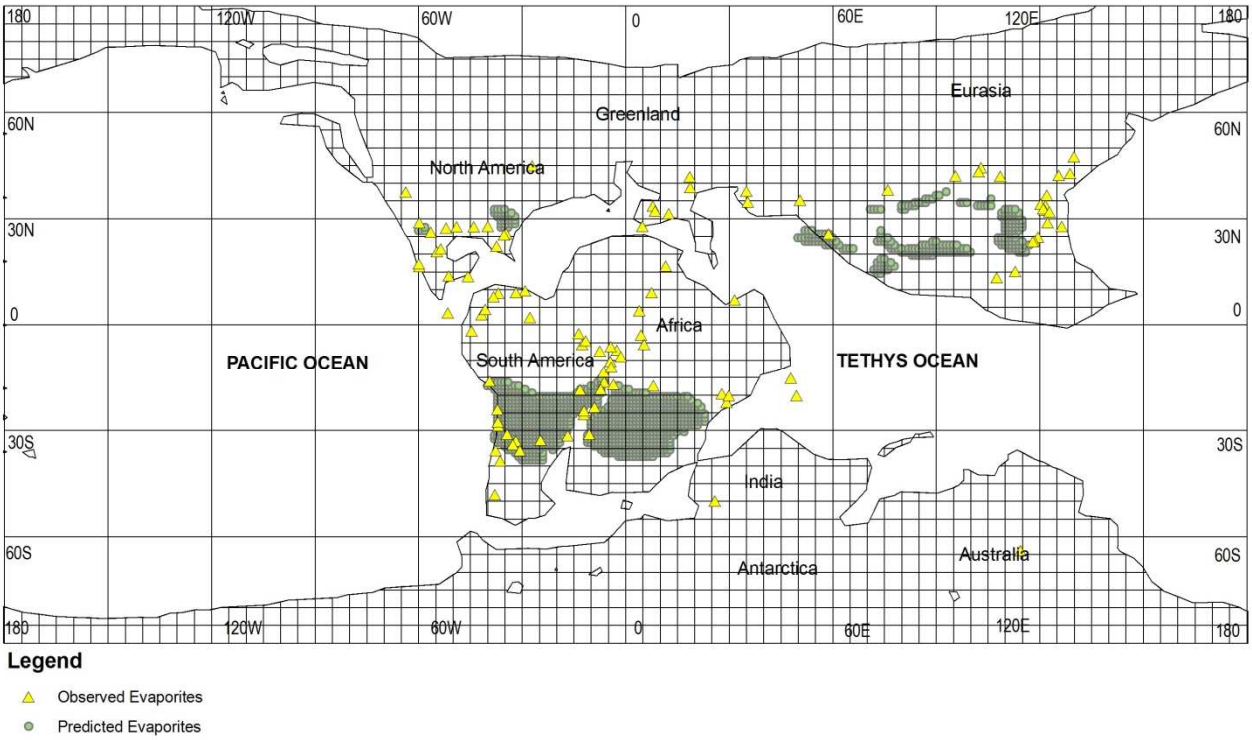

Figure 4.18: This map shows the 5°x5° latitude- longitude grids for the Aptian/Albian time period.

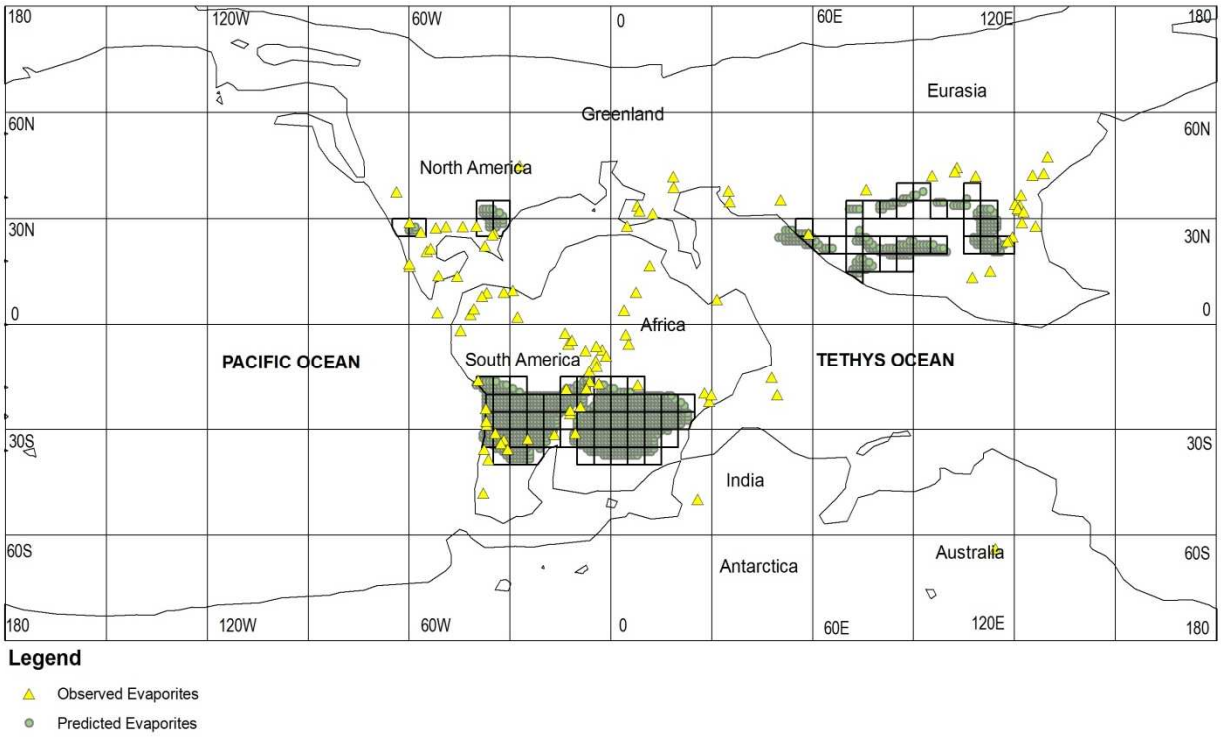

Figure 4.19: This map shows the 5°x5° latitude- longitude grid for the Aptian/Albian predicted evaporite localities.

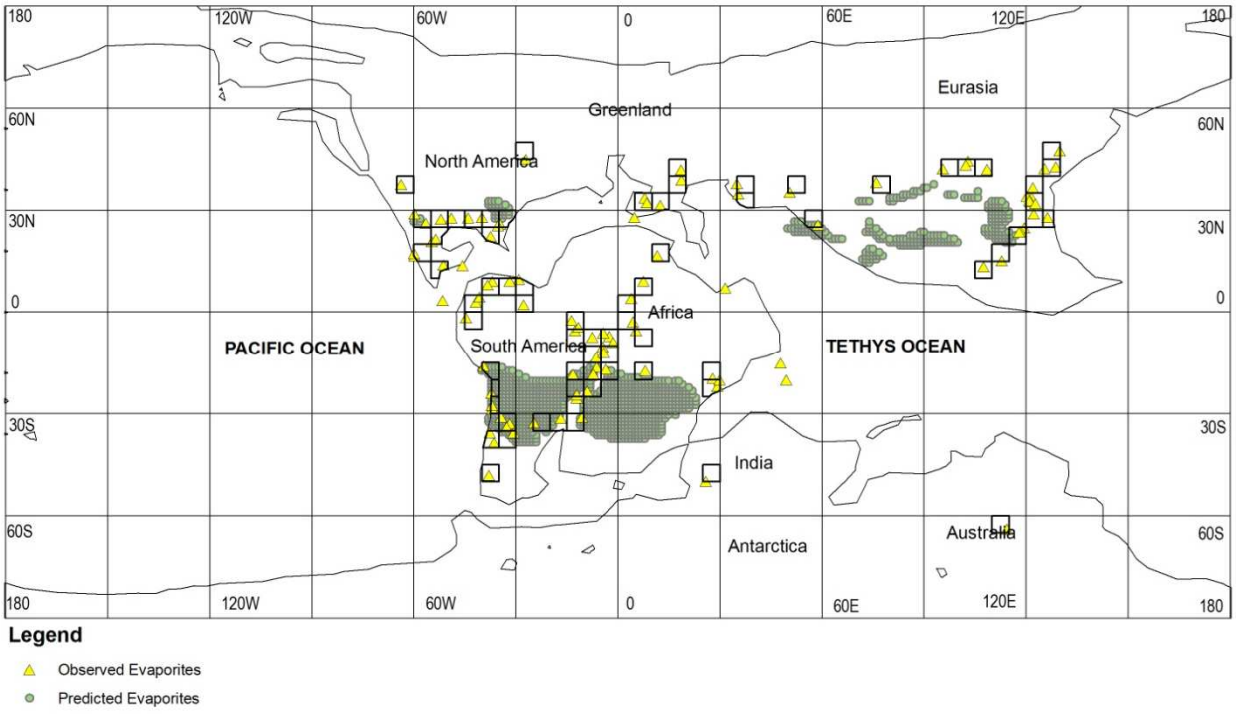

Figure 4.20: This map shows the 5°x5° latitude- longitude grids for the Aptian/Albian observed evaporite localities.

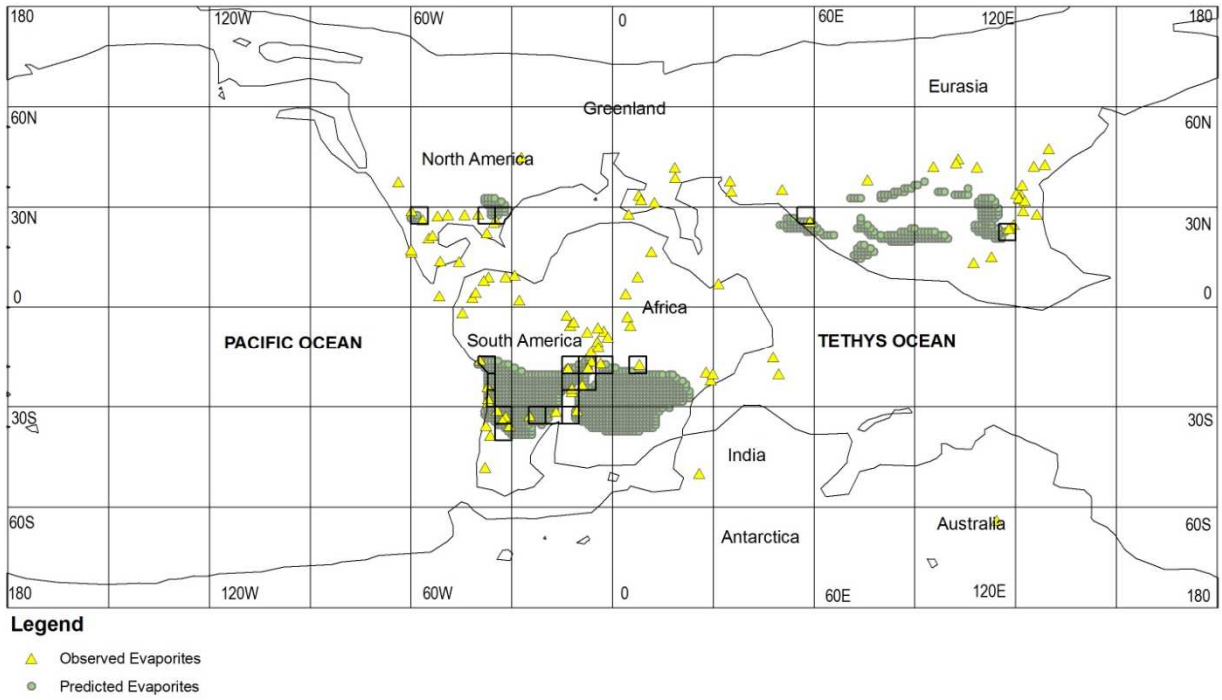

Figure 4.21: Thia map shows the "hits" obtained for the Aptian/Albian time period.

4.5 Early Cretaceous: Barremian/ Berriasian (~ 140 Ma)

4.5.1 Barremian/Berriasian Evaporites

The geographic distribution of predicted evaporites was obtained by intersecting the Evaporite Climate Envelope with precipitation and temperature estimates for the Early Cretaceous (Barremian/Berriasian) (Figure 4.22). A total of 2354 1°x1° localities fell within the Evaporite Climate Envelope for the Early Cretaceous. The predicted evaporites occur in North America, central and southern South America, parts of North Africa, southern Africa, and southern, eastern and central Asia.

The geographic distribution of actual (observed) evaporite localities was obtained from a compilation by Boucot et al (in press). Early Cretaceous evaporites occur in India, parts of central Africa, southern North America, northern South America, eastern South America,

southern South America, eastern Africa, central North Africa, and western, central and eastern Asia. A total of 103 evaporites are plotted on Figure 4.23.

"Hits" are observed in North Africa, southern North Africa, eastern and central Asia, western Africa and central South America (Figure 4.24). "Misses" are India, western Asia, northern South America and eastern South America.

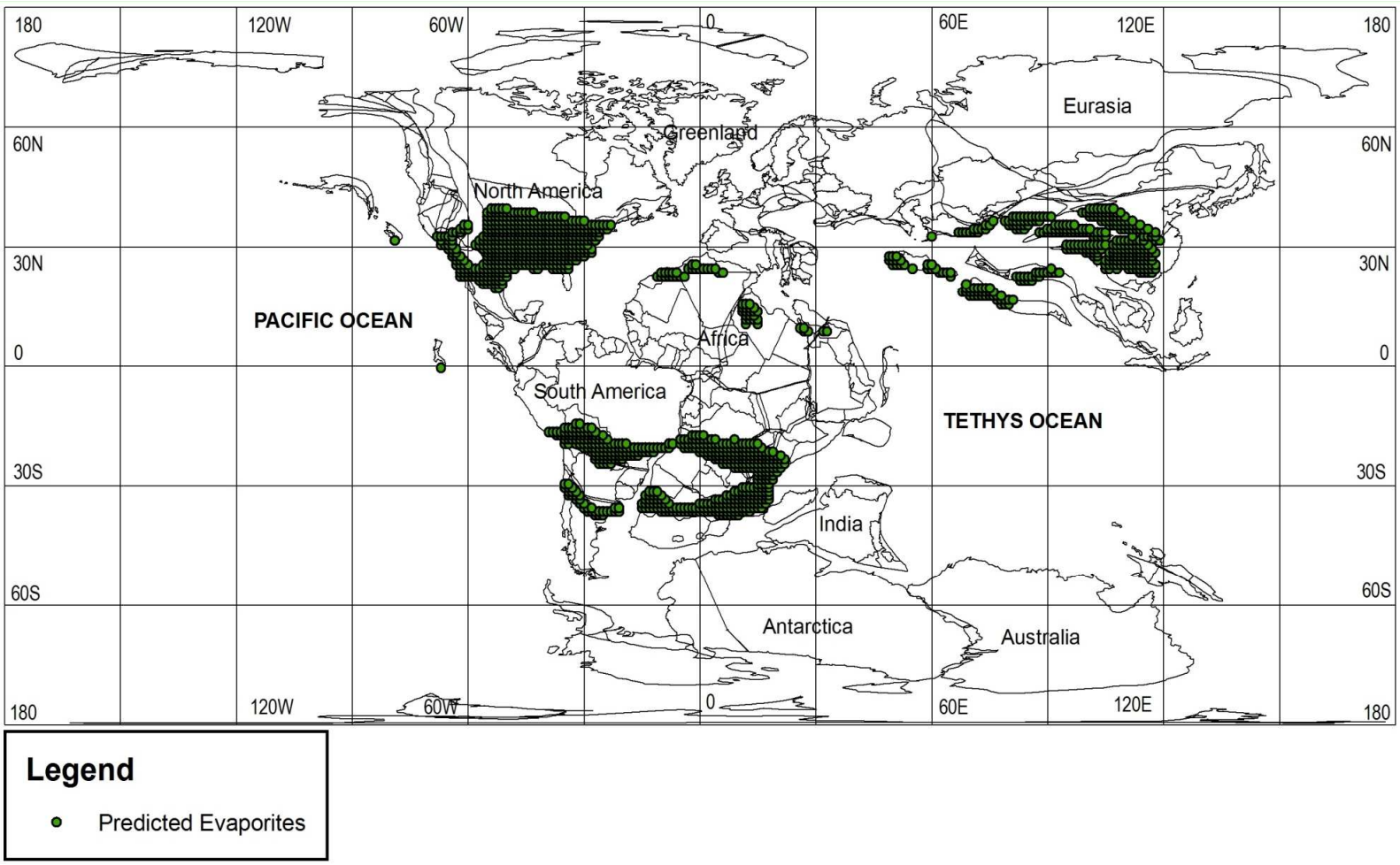

Figure 4.22: A map showing the location of the predicted evaporites for the Barremian/ Berriasian time period.

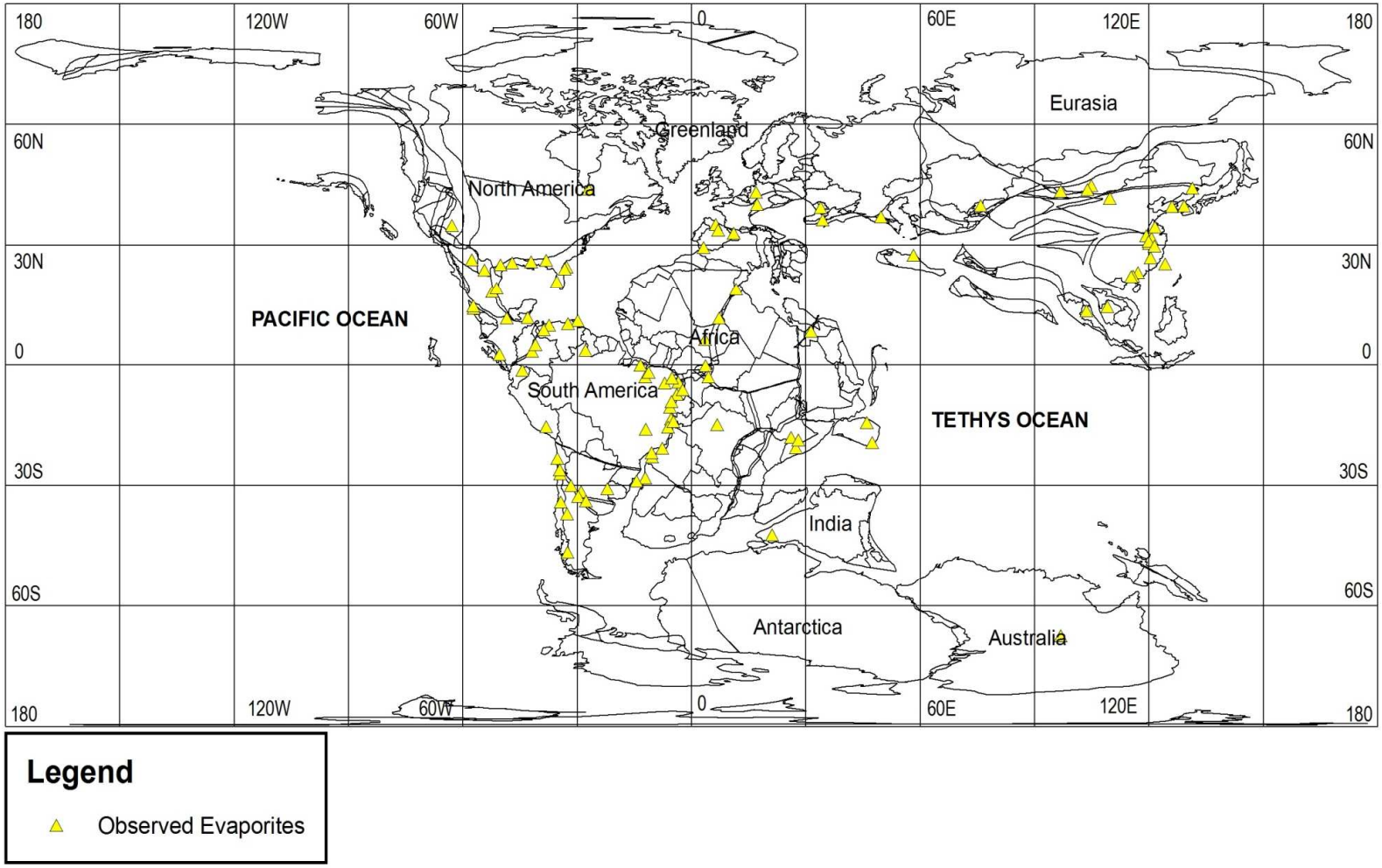

Figure 4.23: A map showing the location of the observed evaporites for the Barremian/ Berriasian time period.

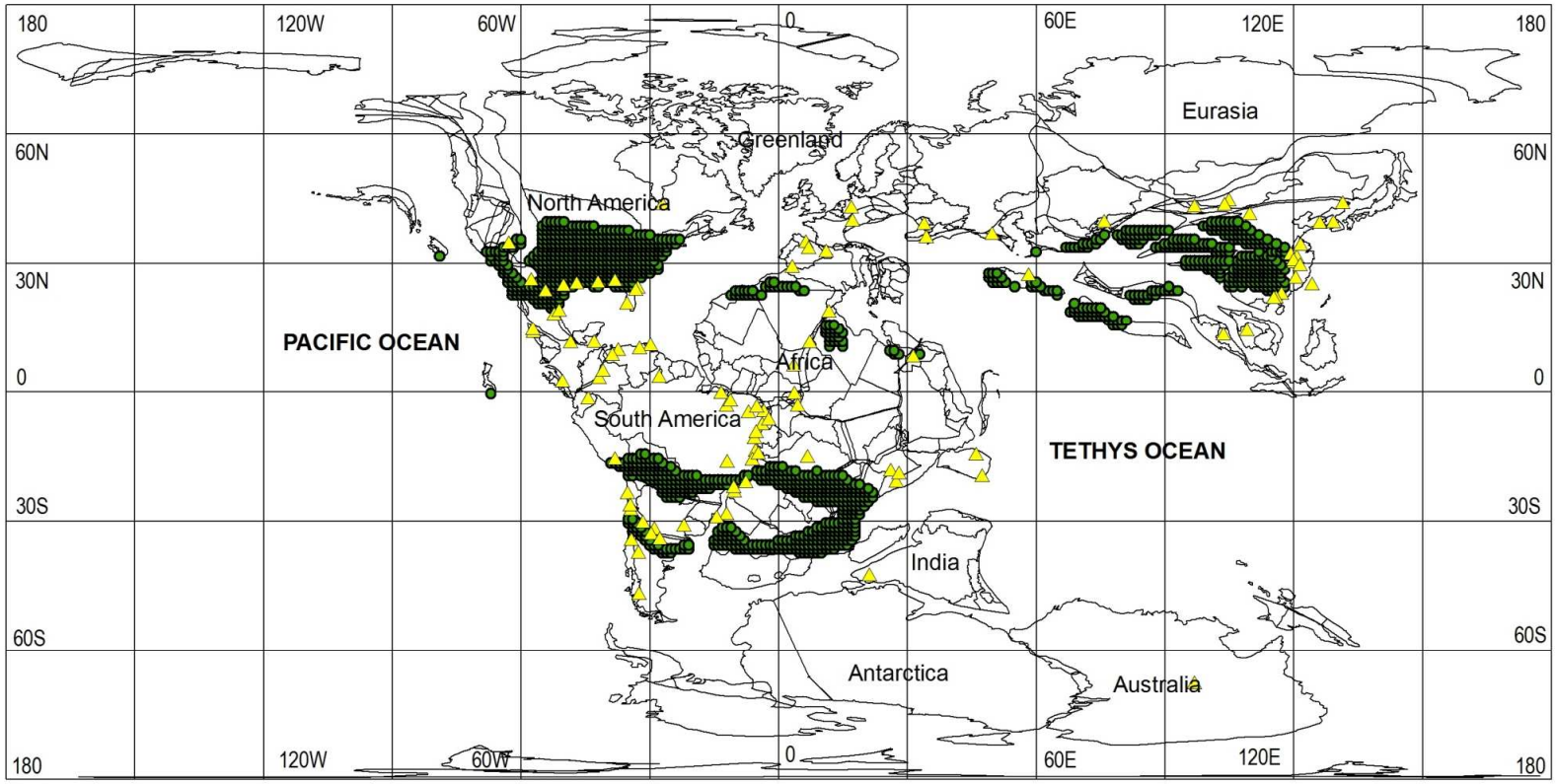

Figure 4.24: A map showing both the predicted and the observed evaporites for the Barremian/ Berriasian time period.

4.5.1.1 Statistical Analyzes for the Barremian/ Berriasian Age

A boundary representing the edge of the continental lithosphere for the Barremian/Berriasian was mapped and in Figure 4.25 is represented by a 5°x5° set of grid cells. For the Barremian/Berriasian, 1373 grid cells were obtained. 137 of these grid cells contained localities for the predicted evaporites. This represents 9.98% of the continental grid cells (Figure 4.26). 66 grid cells contained observed evaporite localities (Figure 4.27). 23 grid cells contained both predicted and observed evaporite localities which are designated as "hits" (Figure 4.28). According to the statistical procedure outlined in section 2.4, since the expected number of hits was 6.59 and the observed number of hits was 23, the probability that the number of hits is due to a random process is 3.63×10^{-7} (Table 4.1). This strongly suggests that the observed hits are not random and that the null hypothesis fails.

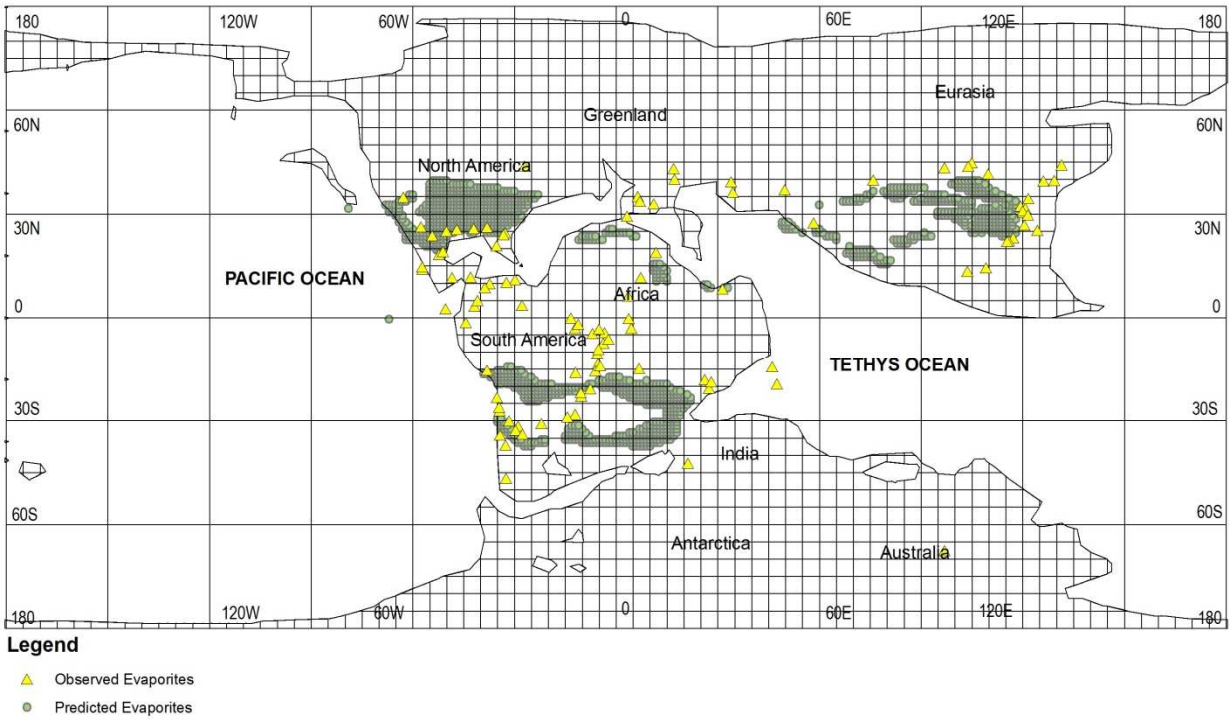

Figure 4.25: This map shows the 5°x5° latitude- longitude grids for the Barremian/ Berriasian time period.

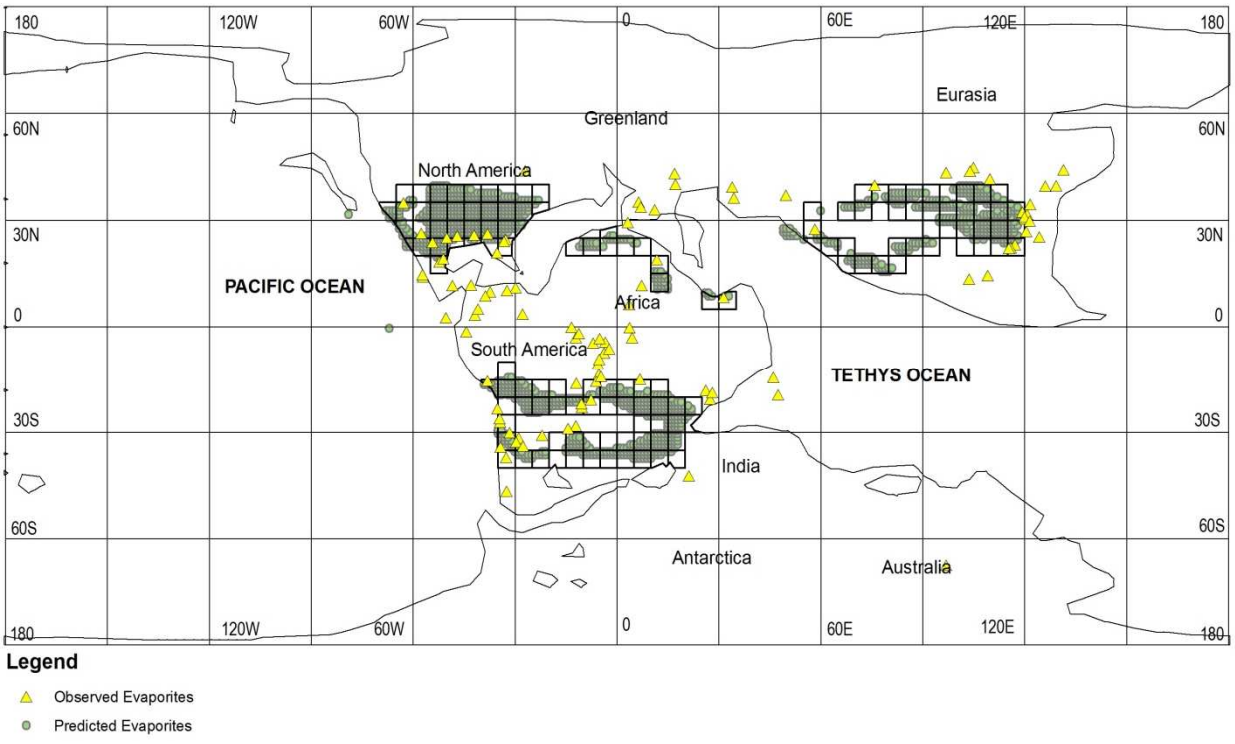

Figure 4.26: This map shows the 5°x5° latitude- longitude grids for the Barremian/ Berriasian predicted evaporite localities.

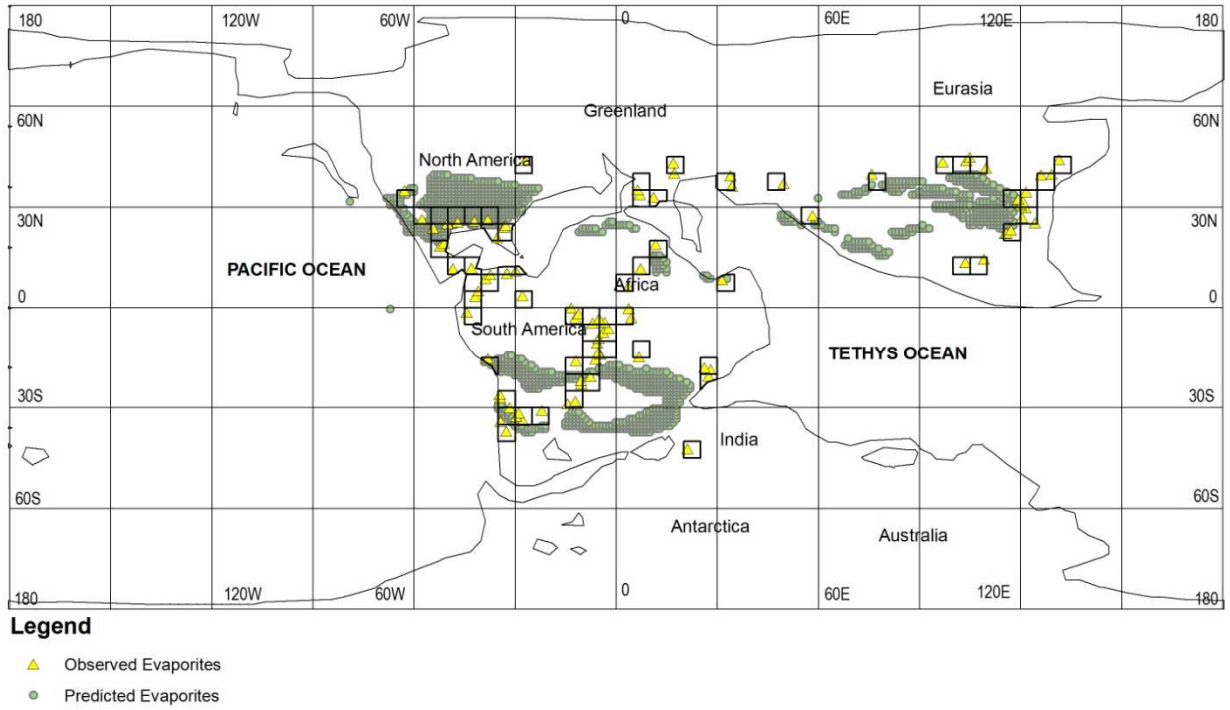

Figure 4.27: This map shows the 5°x5° latitude- longitude grids for the Barremian/ Berriasian observed evaporite localities.

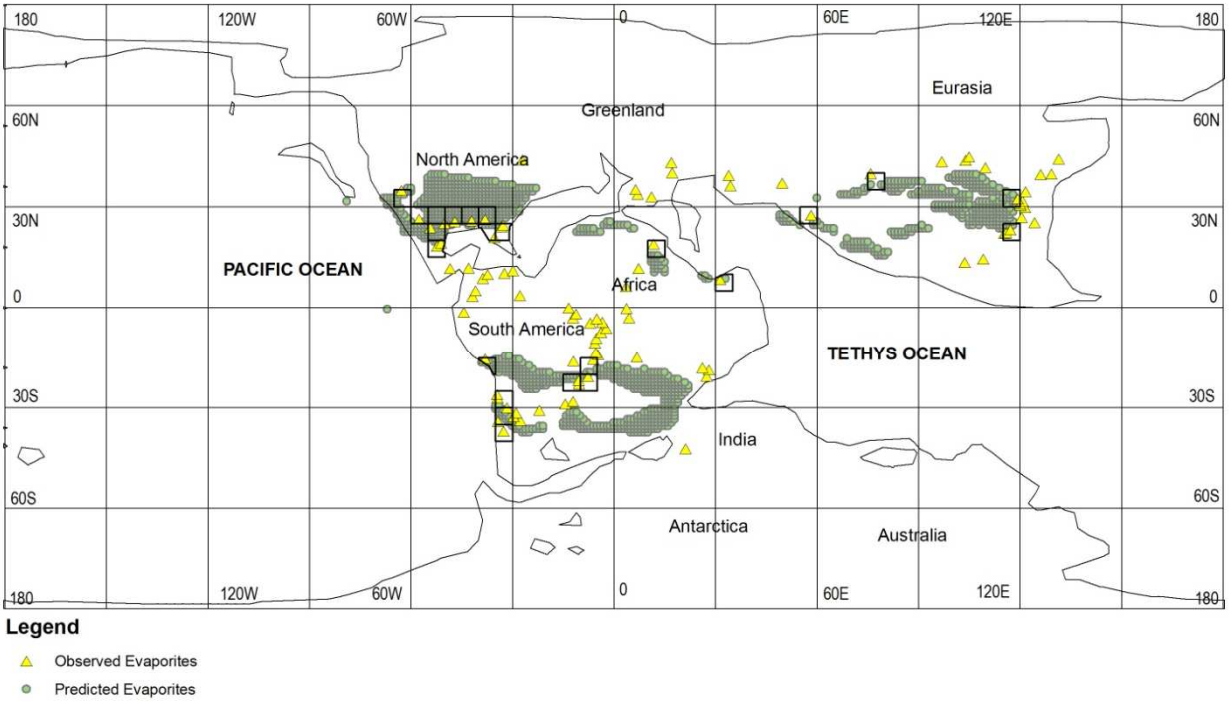

Figure 4.28: This map shows the "hits" obtained for the Barremian/ Berriasian time period.

4.6 Late Jurassic (~ 160 Ma)

4.6.1 Tectonics and Climate for the Jurassic Period

The supercontinent Pangea was still in existence by the Late Jurassic. South America which was partially still attached to Africa had begun to separate from southern Africa. Laurasia which consisted of North America and Asia had begun to move away from Africa and South America creating the Atlantic Ocean. Eurasia which consisted of Europe and Asia moved to the south and the Tethys Ocean had started to close (Crowley and North, 1990).

During the Late Jurassic, the landmass Pangea resulted in extreme continental climates (Parrish, 1982). The Late Jurassic is known for its warm and moist climate though it is believed that certain parts of the Jurassic were characterized by arid climates. The Jurassic is known to be much drier than the Triassic and it is believed that the evaporites in the Jurassic were less

abundant than in the Triassic (Frakes, 1979; Gordon, 1975). The Late Jurassic was also characterized by a sea- level lowstand (Grocke et al, 2003; Ziegler, 1990; Hallam, 2001). Oxygen- isotope data from Europe suggest warm, temperate climates in an arid Late Jurassic (Bowen, 1961, 1966; Price and Sellwood, 1994). There is no evidence of polar ice caps for the Jurassic period and the ocean surface stood higher than the continents with more extensive aridity on the continents (Hallam et al, 1982).

4.6.1.1 Late Jurassic Evaporites

The geographic distribution of predicted evaporites was obtained by intersecting the Evaporite Climate Envelope with precipitation and temperature estimates for the Late Jurassic (Figure 4.29). A total of 3255 1°x1° localities fell within the Evaporite Climate Envelope for the Late Jurassic. The predicted evaporites occur in North America, central and southern South America, western India, parts of North Africa, southern Africa, and southern, eastern and central Asia.

The geographic distribution of actual (observed) evaporite localities was obtained from a compilation by Boucot et al (in press). Late Jurassic evaporites occur in India, parts of central Africa, southern North America, northern South America, eastern South America, southern South America, eastern Africa, central North Africa, and western, central and eastern Asia. A total of 105 evaporites are plotted on Figure 4.30.

"Hits" are observed in North Africa, southern North Africa, eastern and central Asia, western Africa and central South America (Figure 4.24). "Misses" are India, western Asia, northern South America and eastern South America.

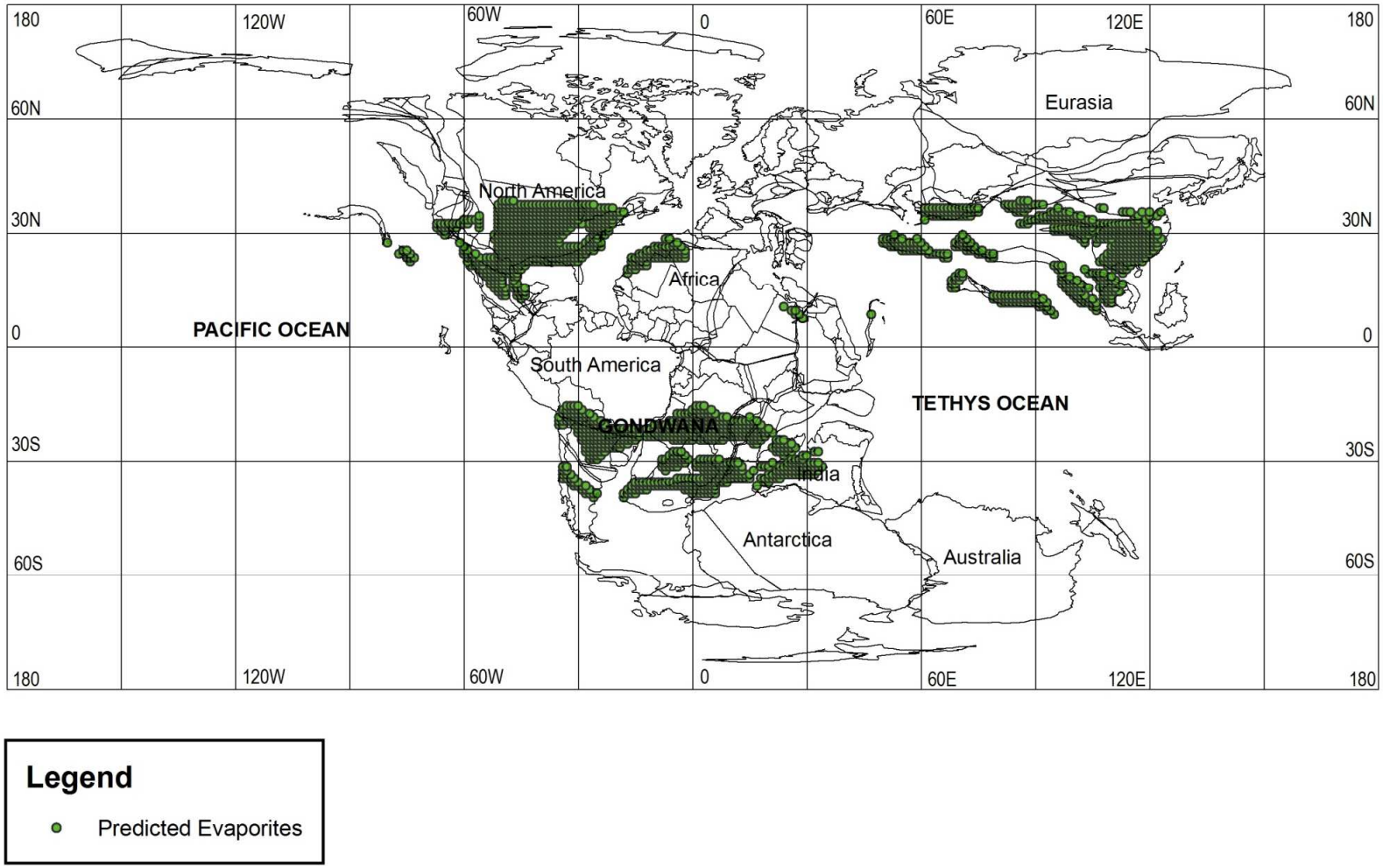

Figure 4.29: Paleoreconstruction for the Late Jurassic time period showing the location of the predicted evaporites.

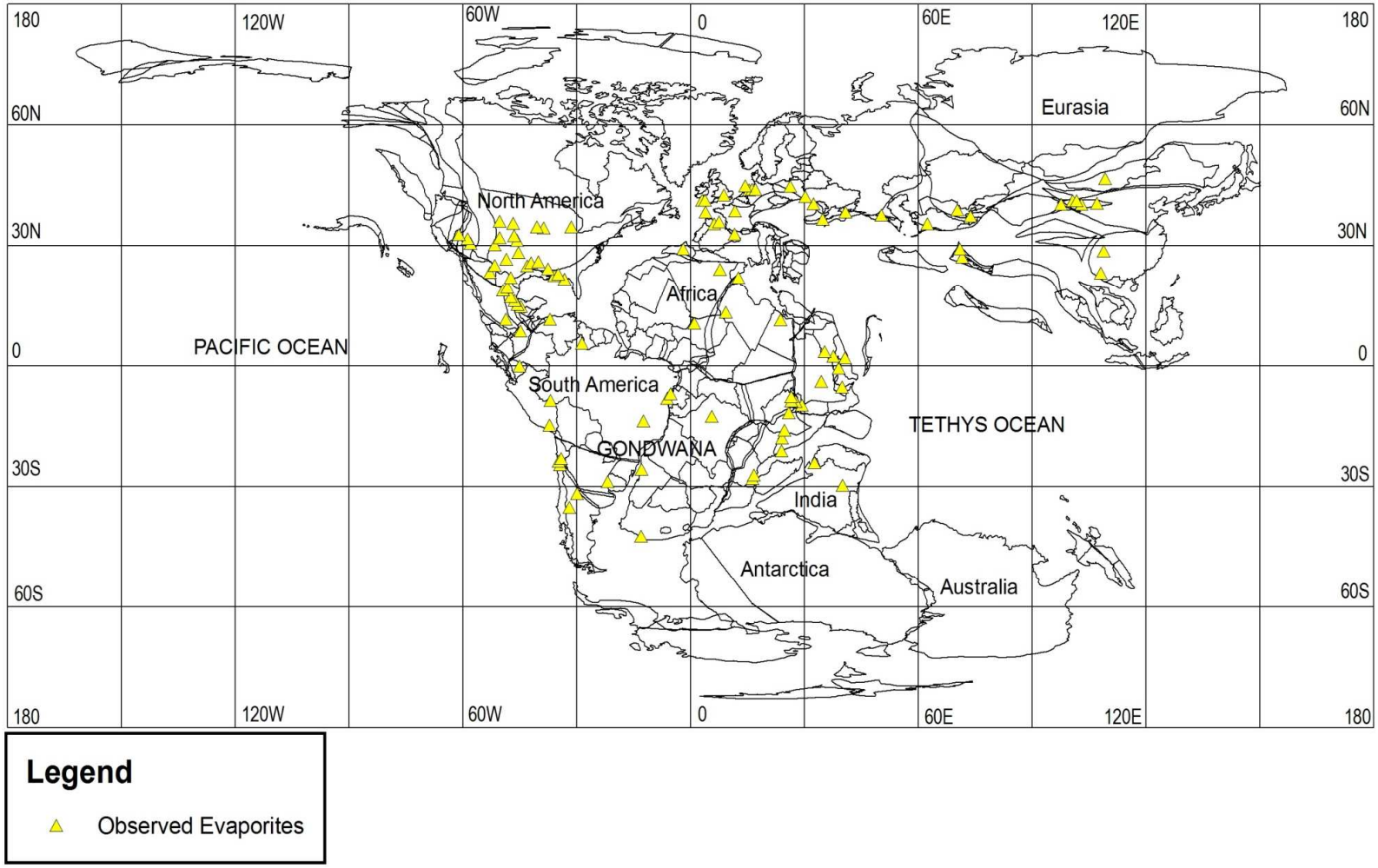

Figure 4.30: Paleoreconstruction for the Late Jurassic time period showing the location of the observed evaporites.

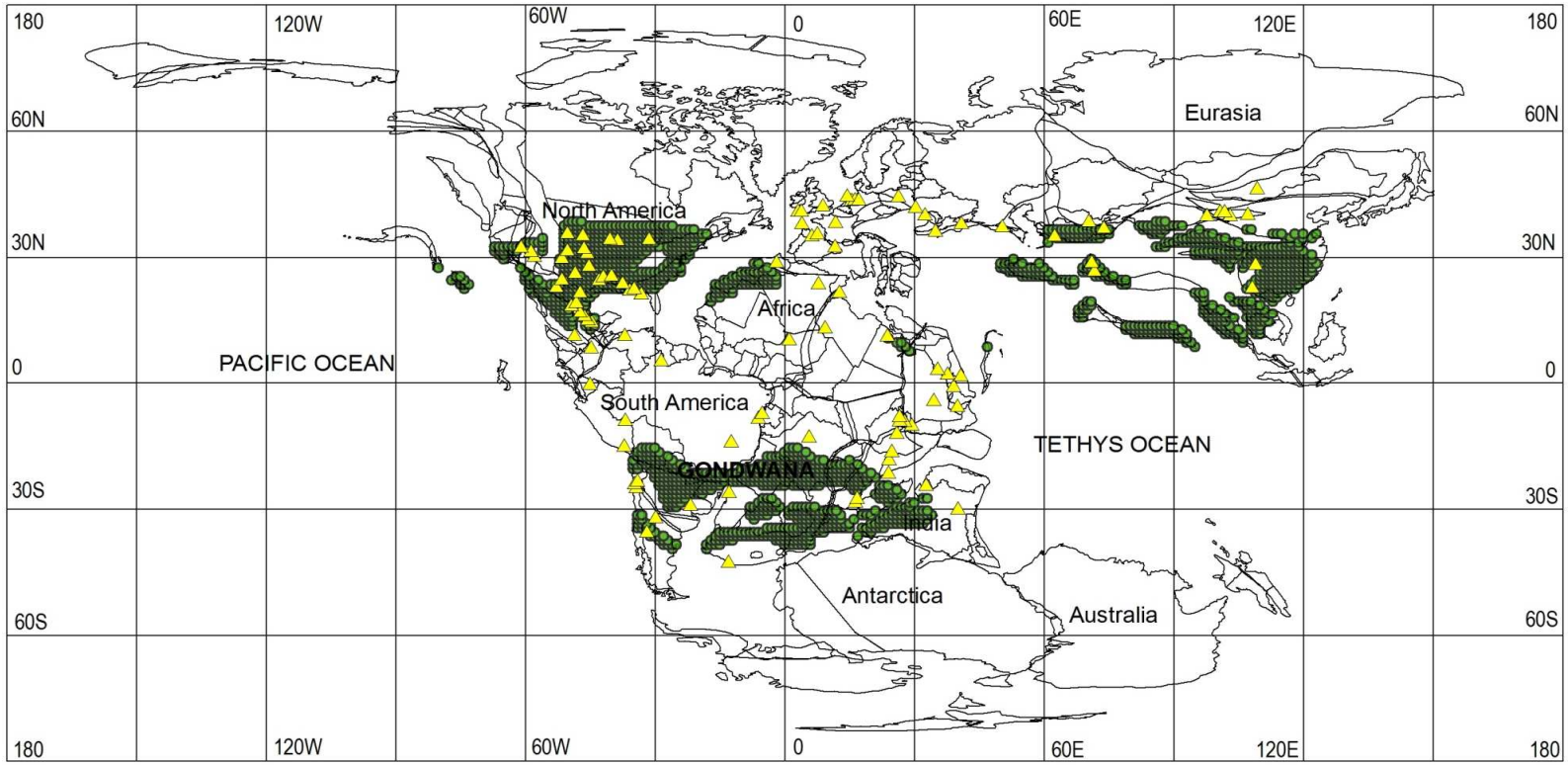

Figure 4.31: Paleoreconstruction for the Late Jurassic time period showing both the predicted and the observed evaporites.

4.6.1.1.1 Statistical Analyzes for the Late Jurassic

A boundary representing the edge of the continental lithosphere for the Late Jurassic was mapped and in Figure 4.32 is represented by a 5°x5° set of grid cells. For the Late Jurassic, 1198 grid cells were obtained. 168 of these grid cells contained localities for the predicted evaporites. This represents 14.02% of the continental grid cells (Figure 4.33). 73 grid cells contained observed evaporite localities (Figure 4.34). 31 grid cells contained both predicted and observed evaporite localities which are designated as "hits" (Figure 4.35). According to the statistical procedure outlined in section 2.4, since the expected number of hits was 10.24 and the observed number of hits was 31, the probability that the number of hits is due to a random process is 9.06×10^{-8} (Table 4.1). This strongly suggests that the observed hits are not random and that the null hypothesis fails.

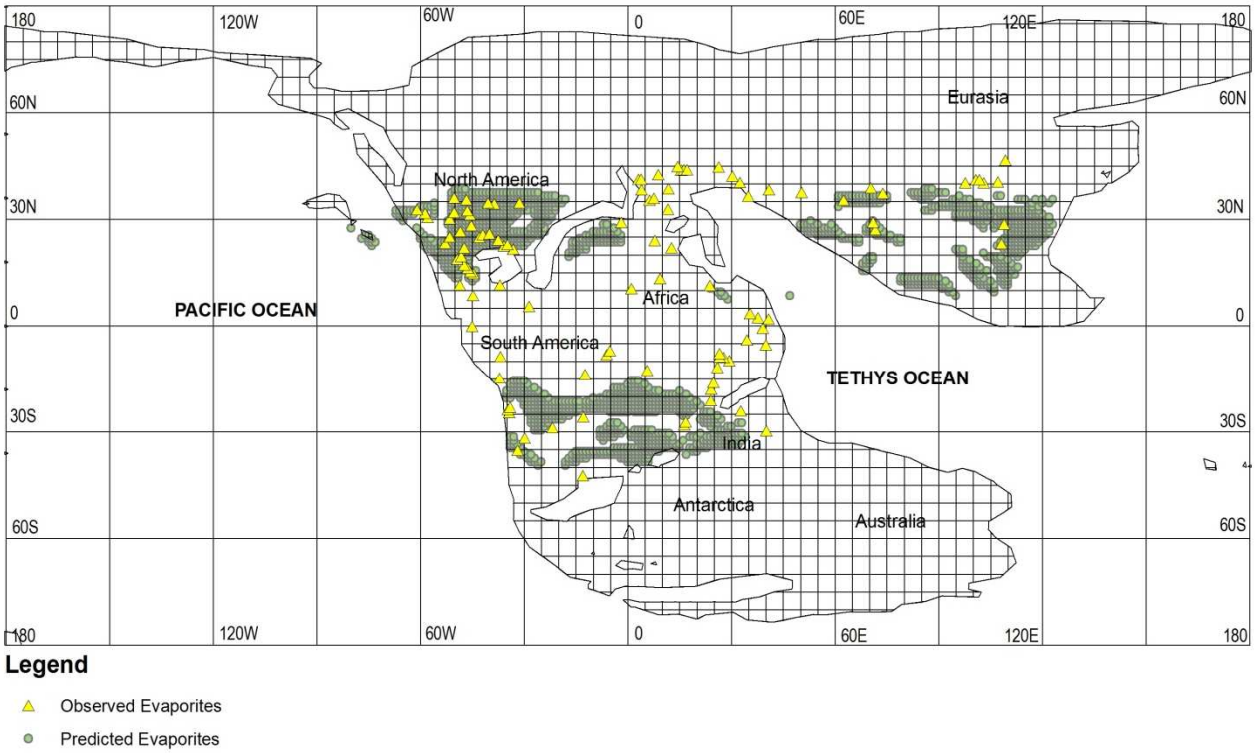

Figure 4.32: This map shows the 5°x5° latitude- longitude grids for the Late Jurassic time period.

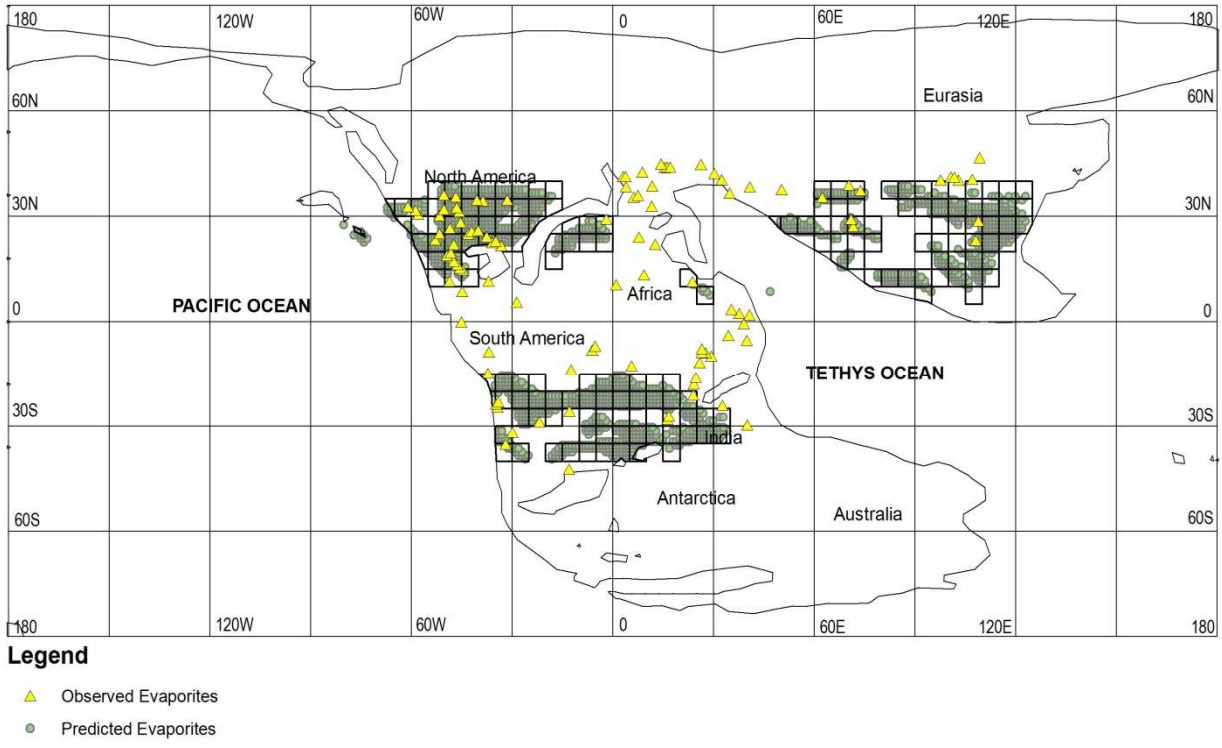

Figure 4.33: This map shows the 5°x5° latitude- longitude grids for the Late Jurassic predicted evaporite localities.

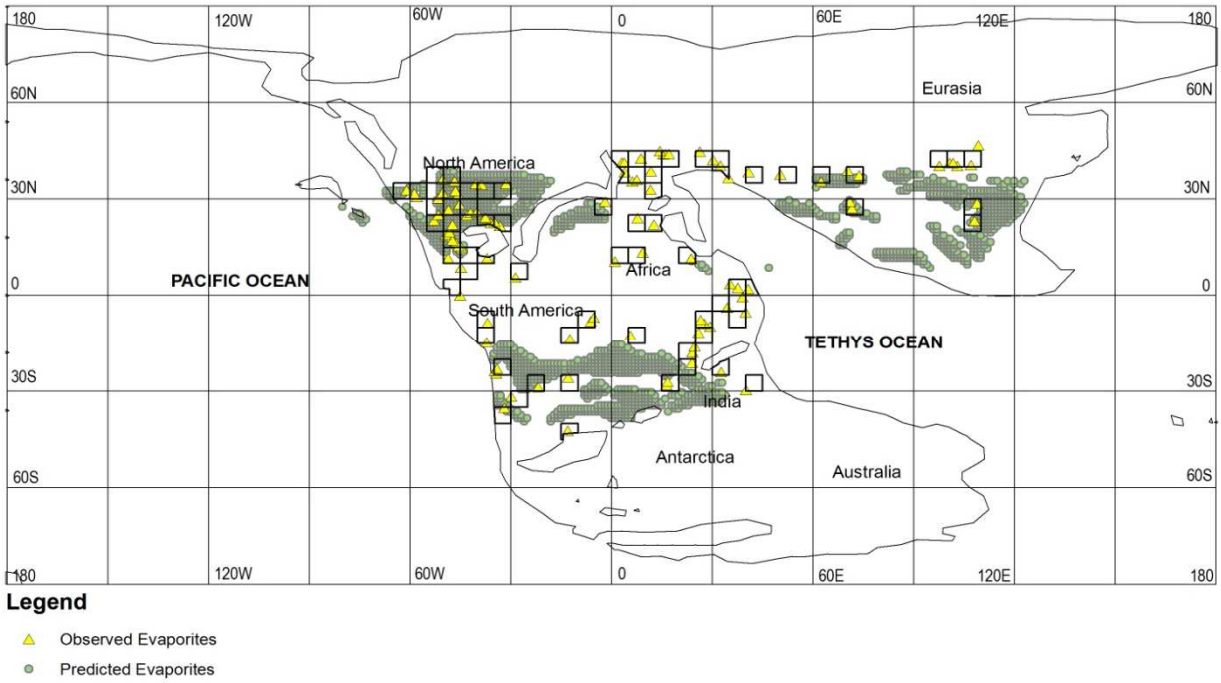

Figure 4.34: This map shows the 5°x5° latitude- longitude grids for the Late Jurassic observed evaporite localities.

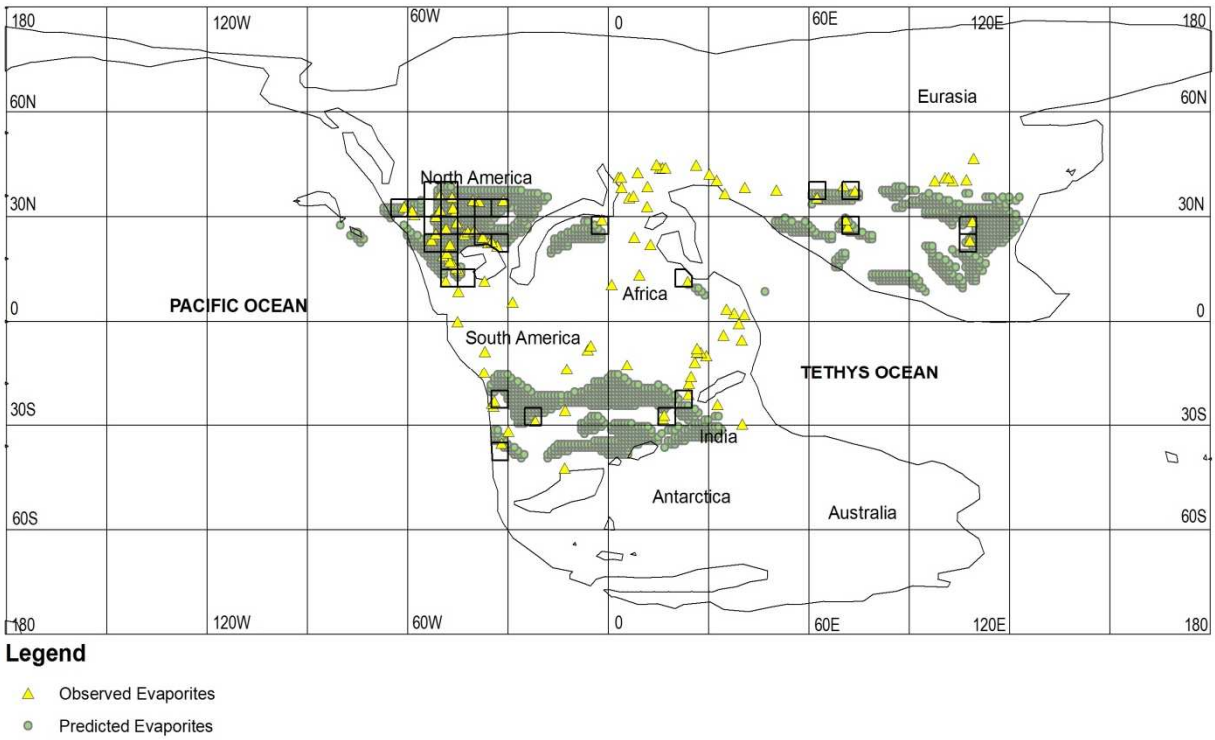

Figure 4.35: This map shows the "hits" obtained for the Late Jurassic.

4.7 Early Jurassic (~ 180 Ma)

4.7.1 Early Jurassic Evaporites

The geographic distribution of predicted evaporites was obtained by intersecting the Evaporite Climate Envelope with precipitation and temperature estimates for the Early Jurassic (Figure 4.36). A total of 2162 1°x1° localities fell within the Evaporite Climate Envelope for the Early Jurassic. The predicted evaporites occur in central North America, southern Eurasia, southern Africa and south of South America.

The geographic distribution of actual (observed) evaporite localities was obtained from a compilation by Boucot et al (in press). Early Jurassic evaporites occur in North Africa, East Africa with a few also occurring in South Africa. They also occur in western South America,

northern South America, southern North America, west central North America, southern Eurasia and south central Eurasia. A total of 104 observed evaporites are plotted on Figure 4.37.

"Hits" are observed in east central North America, west central North America, southeast and southwest Africa and southern Eurasia (Figure 4.38). "Misses" are North Africa, northeast and southeast Africa, south central Eurasia, southern North America, north and northwest South America.

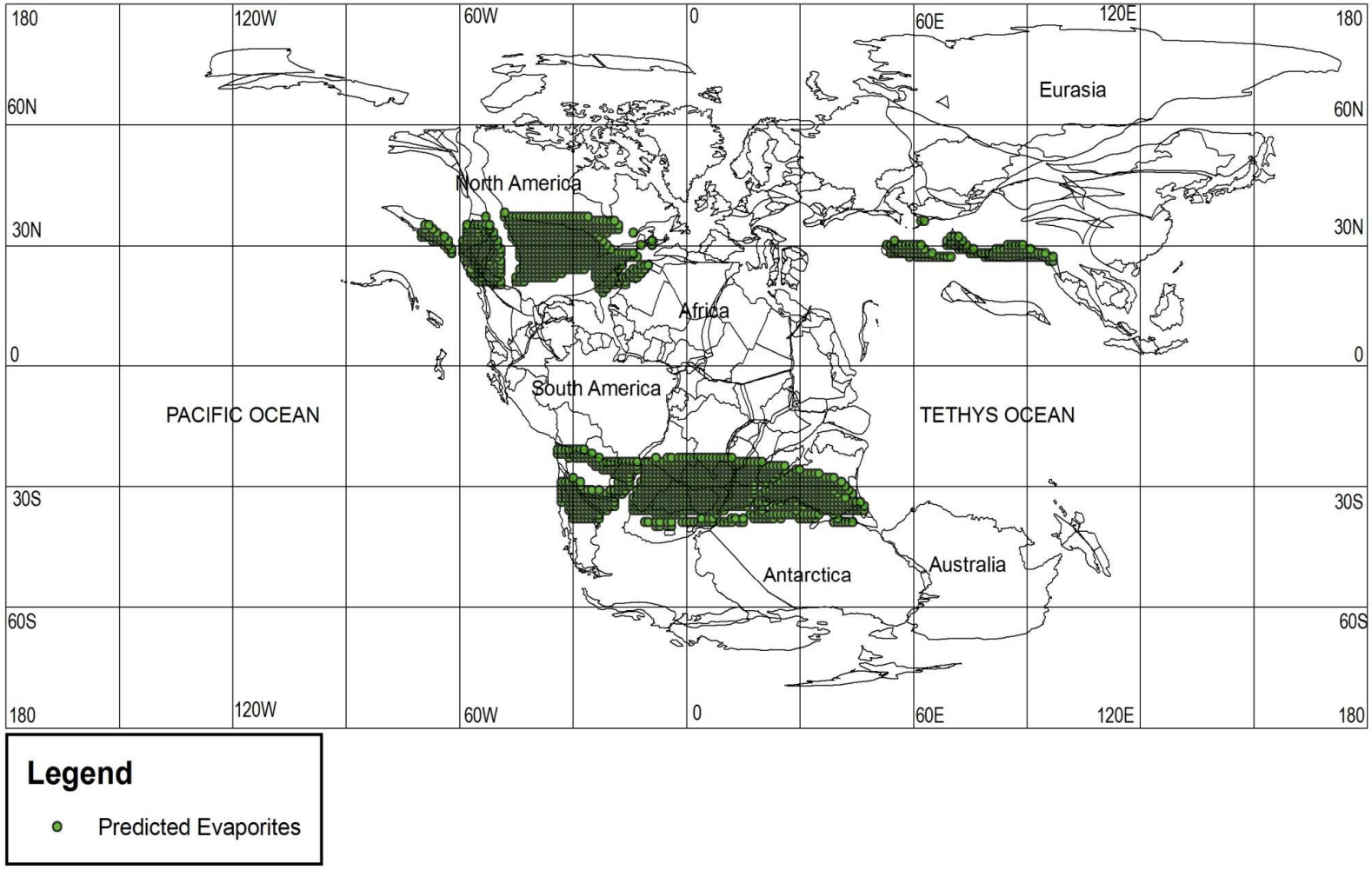

Figure 4.36: Paleoreconstruction for the Early Jurassic time period showing the location of the predicted evaporites.

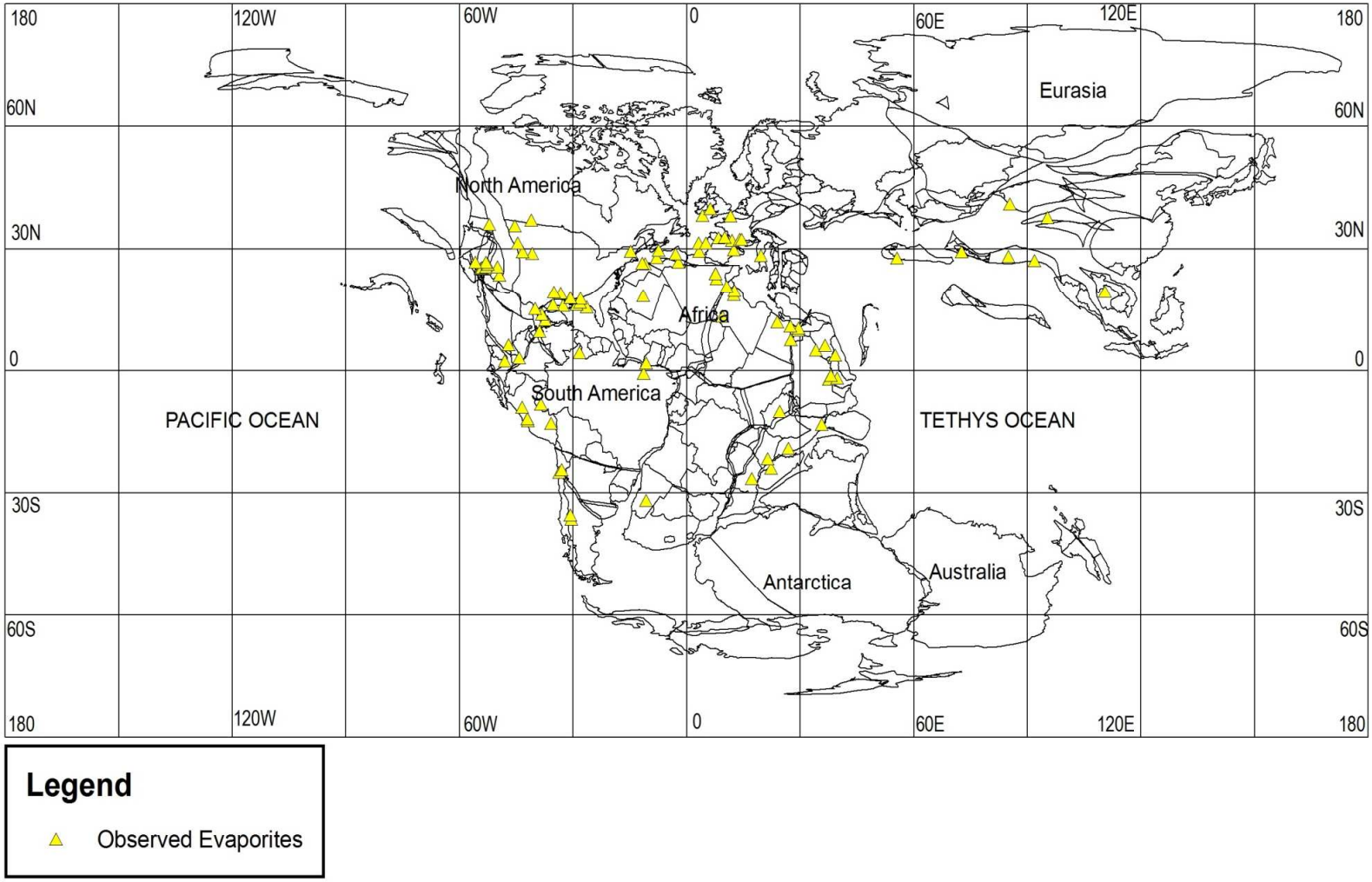

Figure 4.37: Paleoreconstruction for the Early Jurassic time period showing the location of the observed evaporites.

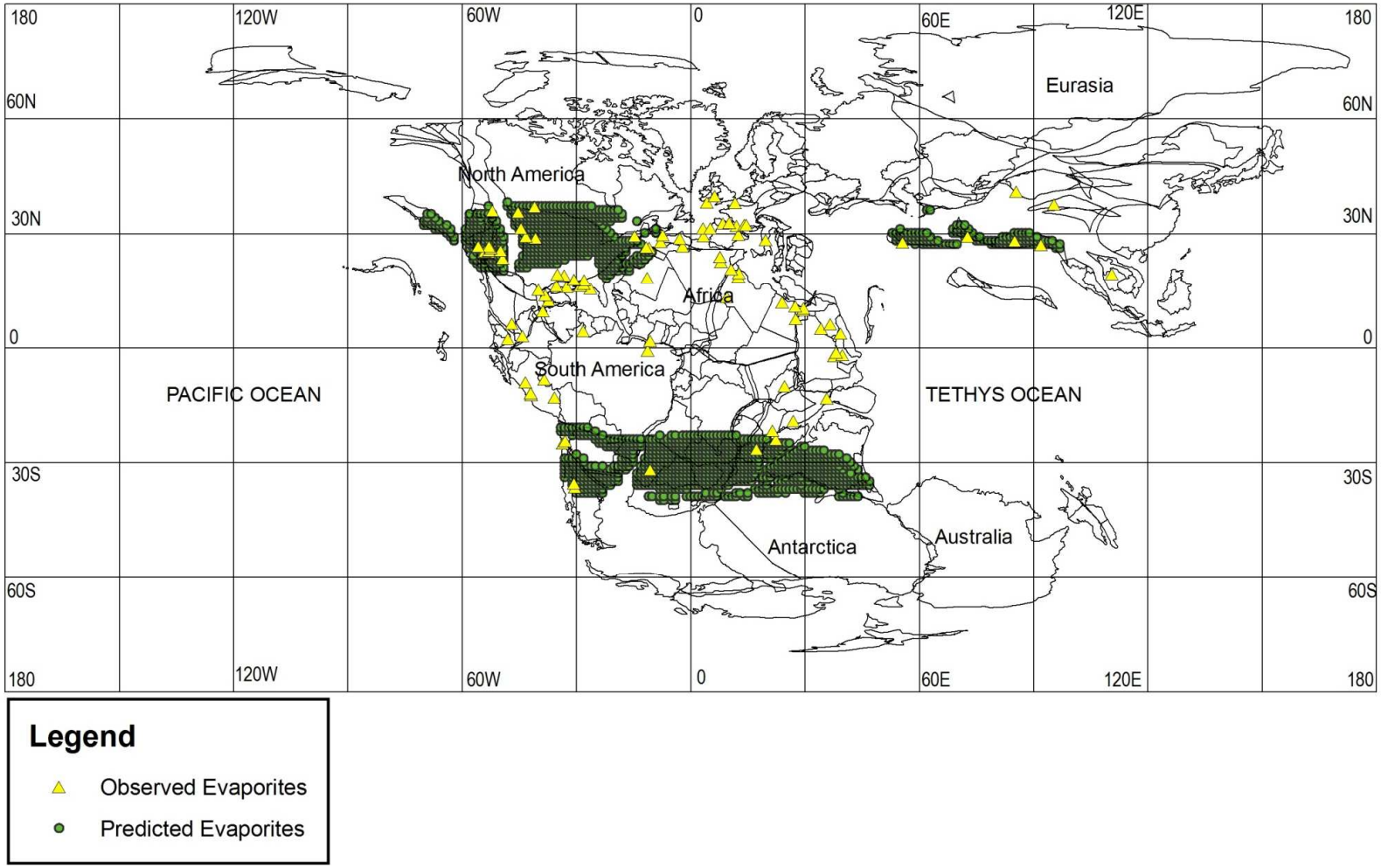

Figure 4.38: Paleoreconstruction for the Early Jurassic time period showing the location of both the predicted and the observed evaporites.

4.7.1.1 Statistical Analyzes for the Early Jurassic

A boundary representing the edge of the continental lithosphere for the Early Jurassic was mapped and in Figure 4.39 is represented by a 5°x5° set of grid cells. For the Early Jurassic, 1169 grid cells were obtained. 126 of these grid cells contained localities for the predicted evaporites. This represents 10.78% of the continental grid cells (Figure 4.40). 63 grid cells contained observed evaporite localities (Figure 4.41). 19 grid cells contained both predicted and observed evaporite localities which are designated as "hits" (Figure 4.42). According to the statistical procedure outlined in section 2.4, since the expected number of hits was 6.79 and the observed number of hits was 19, the probability that the number of hits is due to a random process is 5.91×10^{-5} (Table 4.1). This strongly suggests that the observed hits are not random and that the null hypothesis fails.

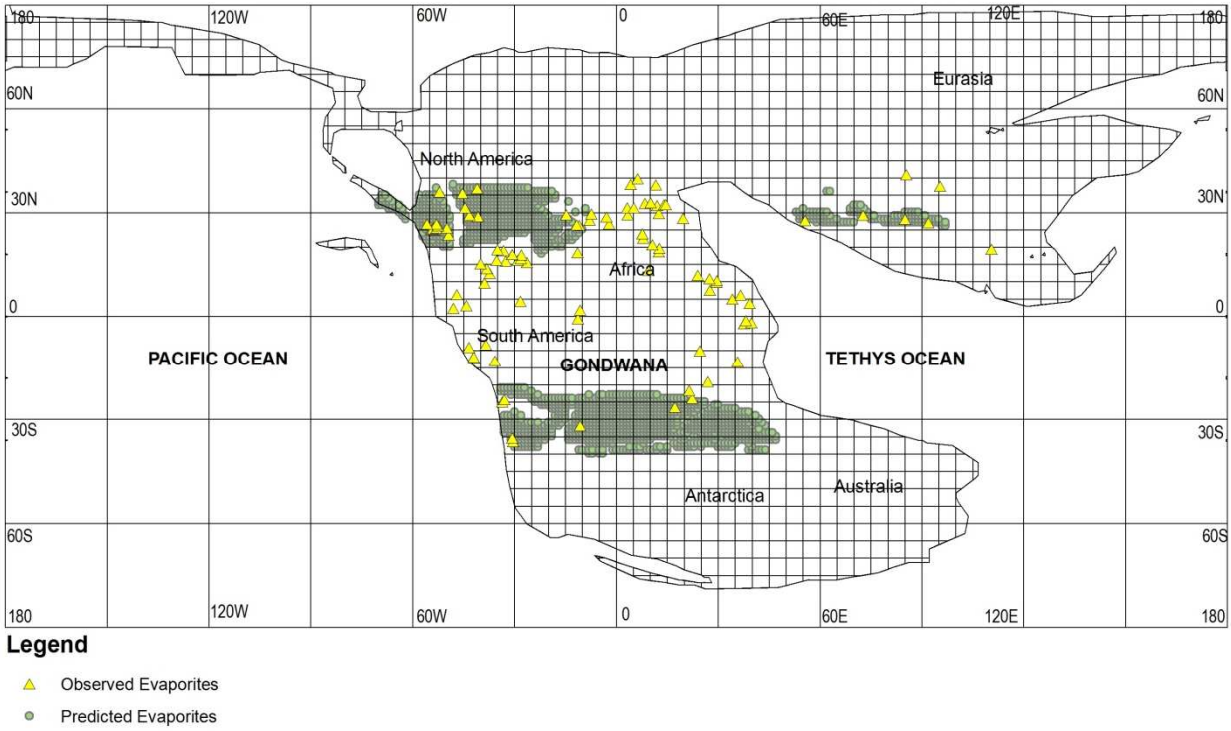

Figure 4.39: This map shows the 5°x5° latitude- longitude grids for the Early Jurassic time period.

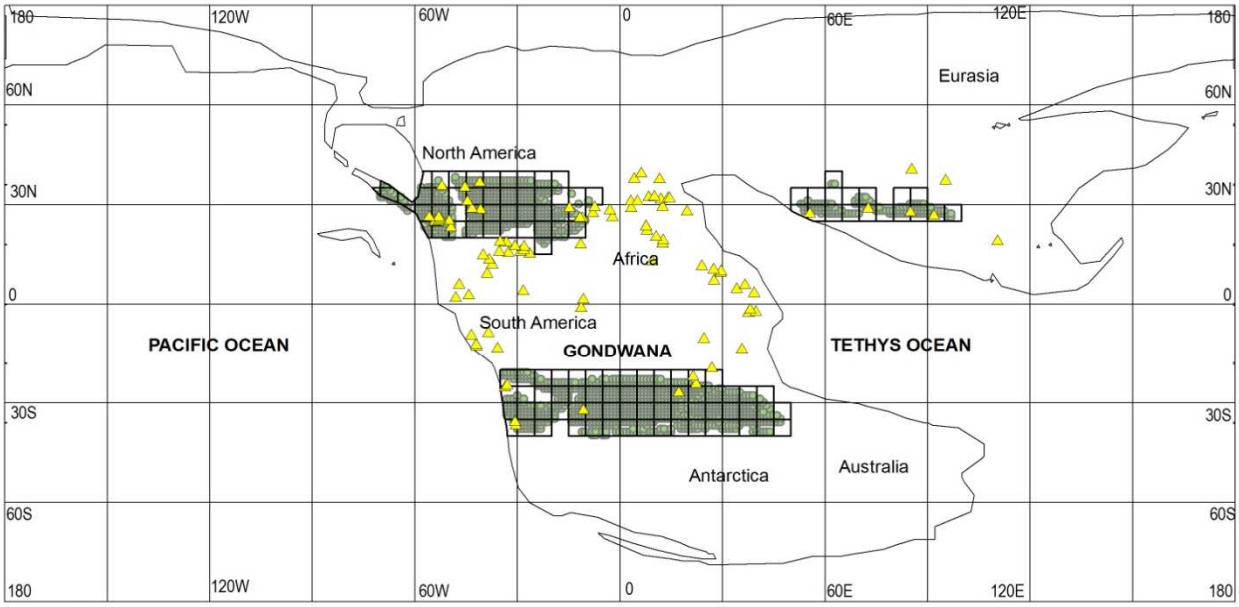

Figure 4.40: This map shows the 5°x5° latitude- longitude grids for the Early Jurassic predicted evaporite localities.

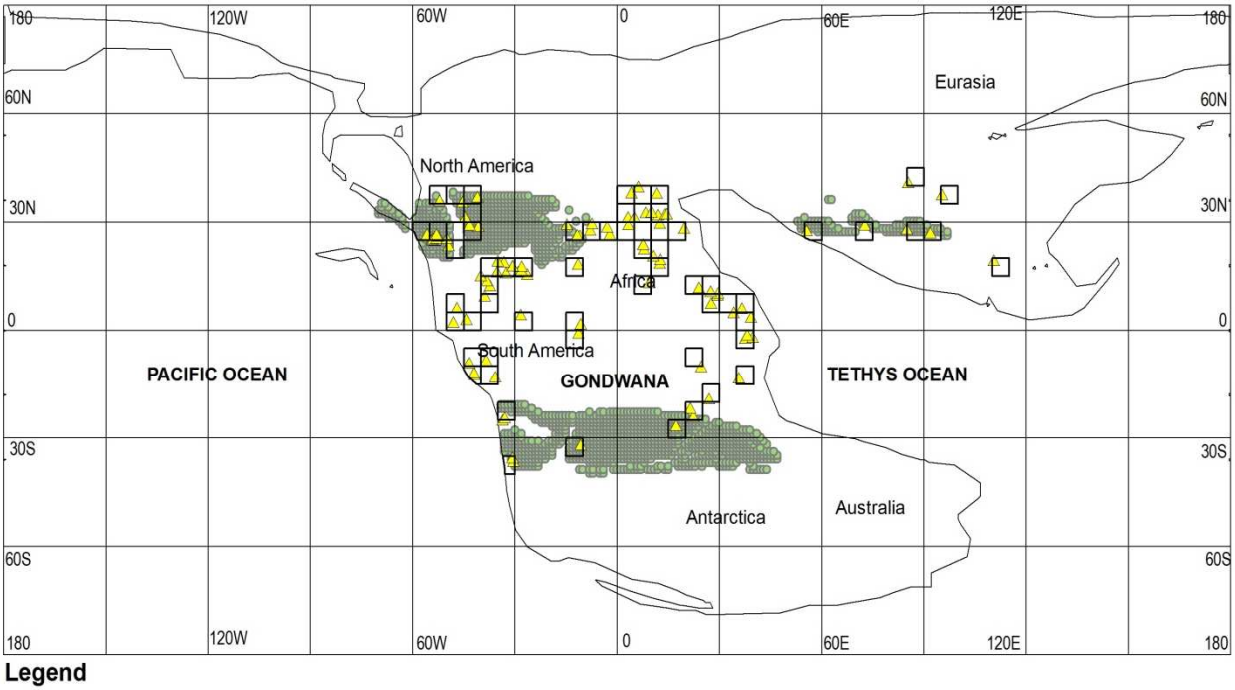

Figure 4.41: This map shows the 5°x5° latitude- longitude grids for the Early Jurassic observed evaporite localities.

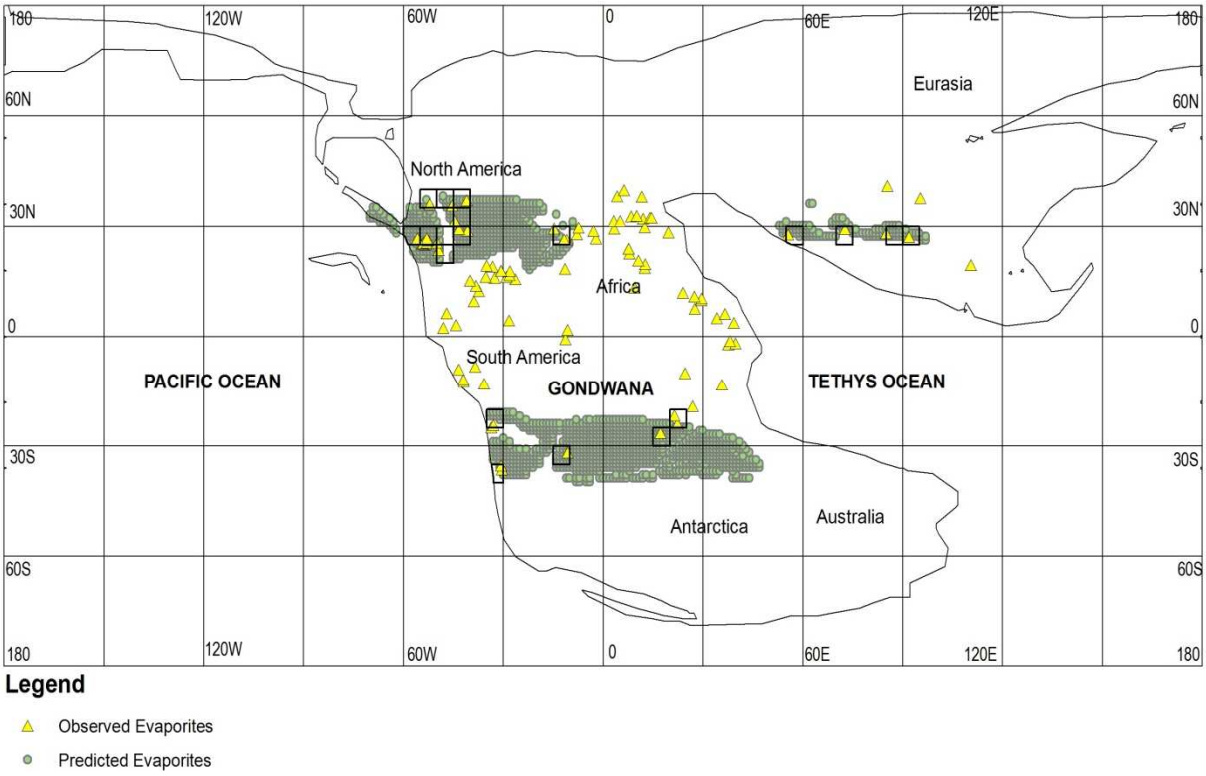

Figure 4.42: This map shows the "hits" obtained for the Early Jurassic time period.

4.8 Late Triassic (~ 220 Ma)

4.8.1 Tectonics and Climate of the Triassic

The Late Triassic was characterized by the initiation of the rifting of the supercontinent Pangea, the closure of the Palaeotethys Ocean and the Indosinian orogeny (Golonka, 2007). The Panthalassic Ocean and the Tethys Ocean were in existence during the Late Triassic (Crowley and North, 1990). The Triassic is considered to have had an arid climate with evaporites deposits that formed in the arid environments being more extensive than any other time (Gordon, 1975). Hay et al, 1982 noted in their paper, an increase in evaporite deposition in North America and in Europe and attributed it to the uplift of the Appalachian Mountains with enhanced aridity in the

lee side of the mountain. Frakes, 1979 reported that the Triassic climates were similar to those of the Late Permian which was arid and warm. The Early Triassic was characterized by very cool and humid climate and was later followed by warm and arid conditions during the Late Triassic which lasted until the Jurassic.

4.8.1.1 Late Triassic Evaporites

The geographic distribution of predicted evaporites was obtained by intersecting the Evaporite Climate Envelope with precipitation and temperature estimates for the Late Triassic (Figure 4.43). A total of 2000 1°x1° localities fell within the Evaporite Climate Envelope for the Late Triassic. The predicted evaporites occur in north and central North America, central and southern South America, western and central India, parts of North Africa, southern Africa, and southern Asia.

The geographic distribution of actual (observed) evaporite localities was obtained from a compilation by Boucot et al (in press). Late Triassic evaporites occur in western North America, western South America, North Africa, eastern Africa, and southern Europe. A total of 105 evaporites are plotted on Figure 4.44.

"Hits" are observed in North Africa, southern North Africa, eastern and central Asia, western Africa and central South America (Figure 4.45). "Misses" are India, western Asia, northern South America and eastern South America.

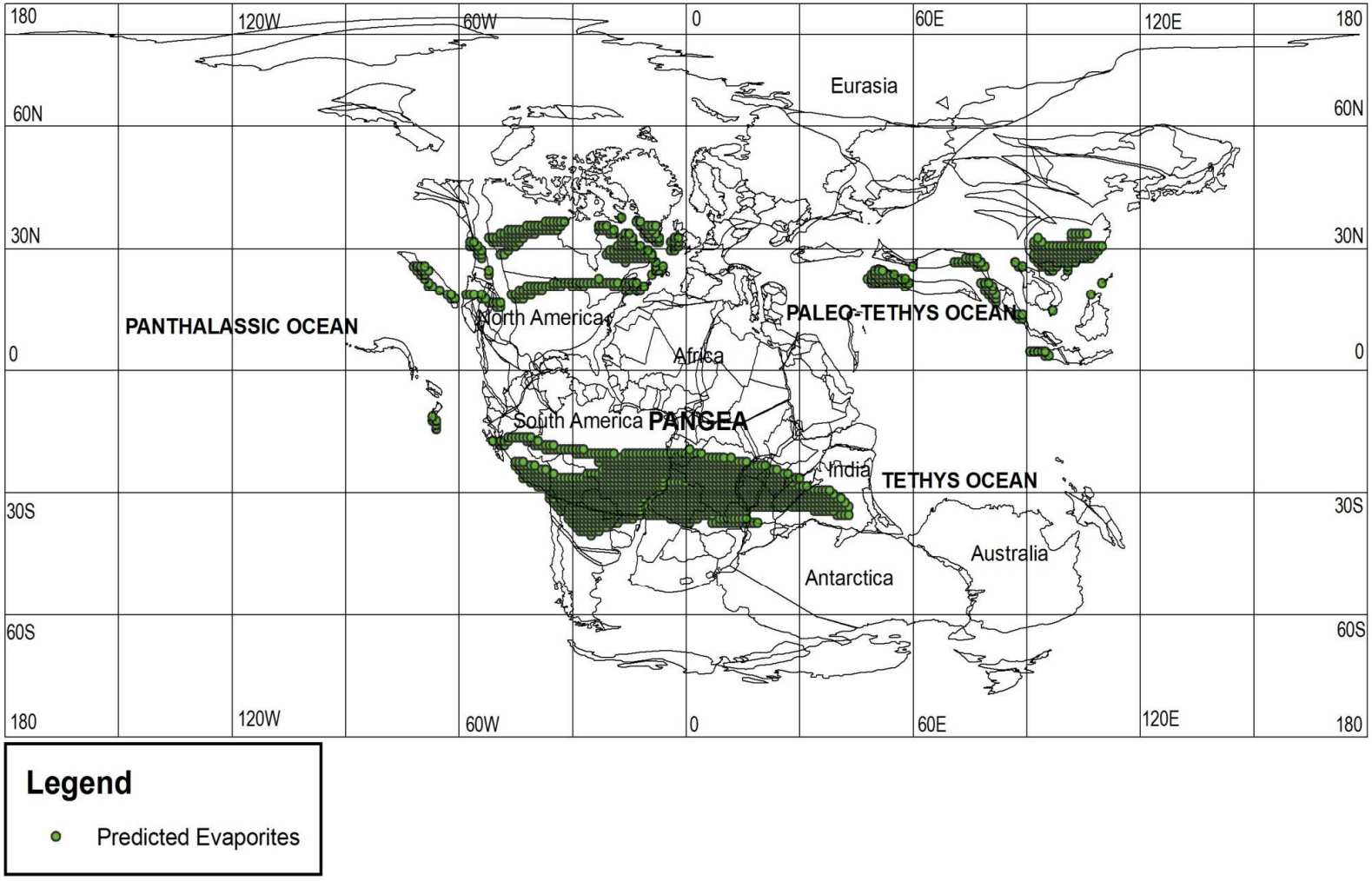

Figure 4.43: Paleoreconstruction for the Late Triassic showing the location of the predicted evaporites.

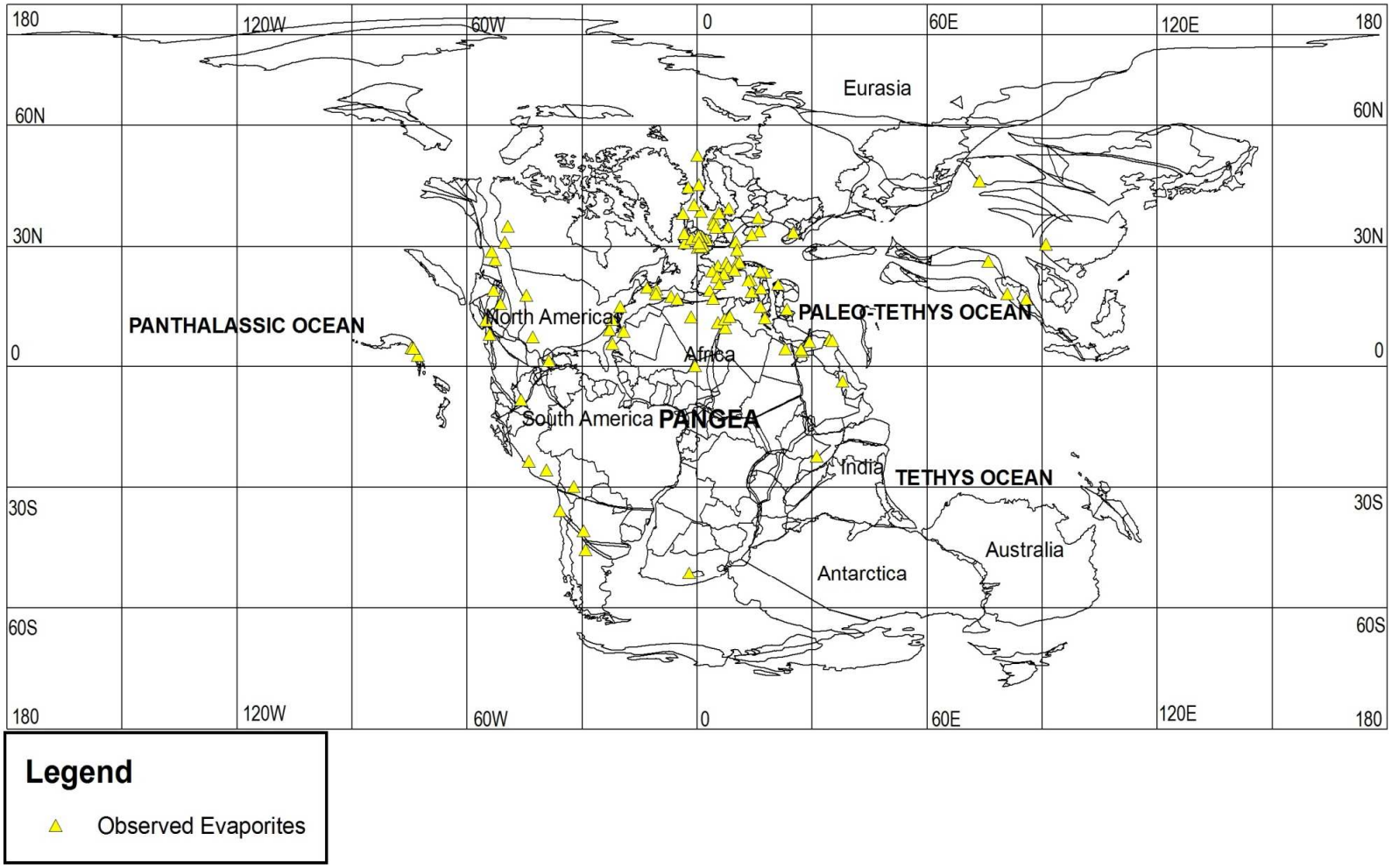

Figure 4.44: Paleoreconstruction for the Late Triassic showing the location of the observed evaporites.

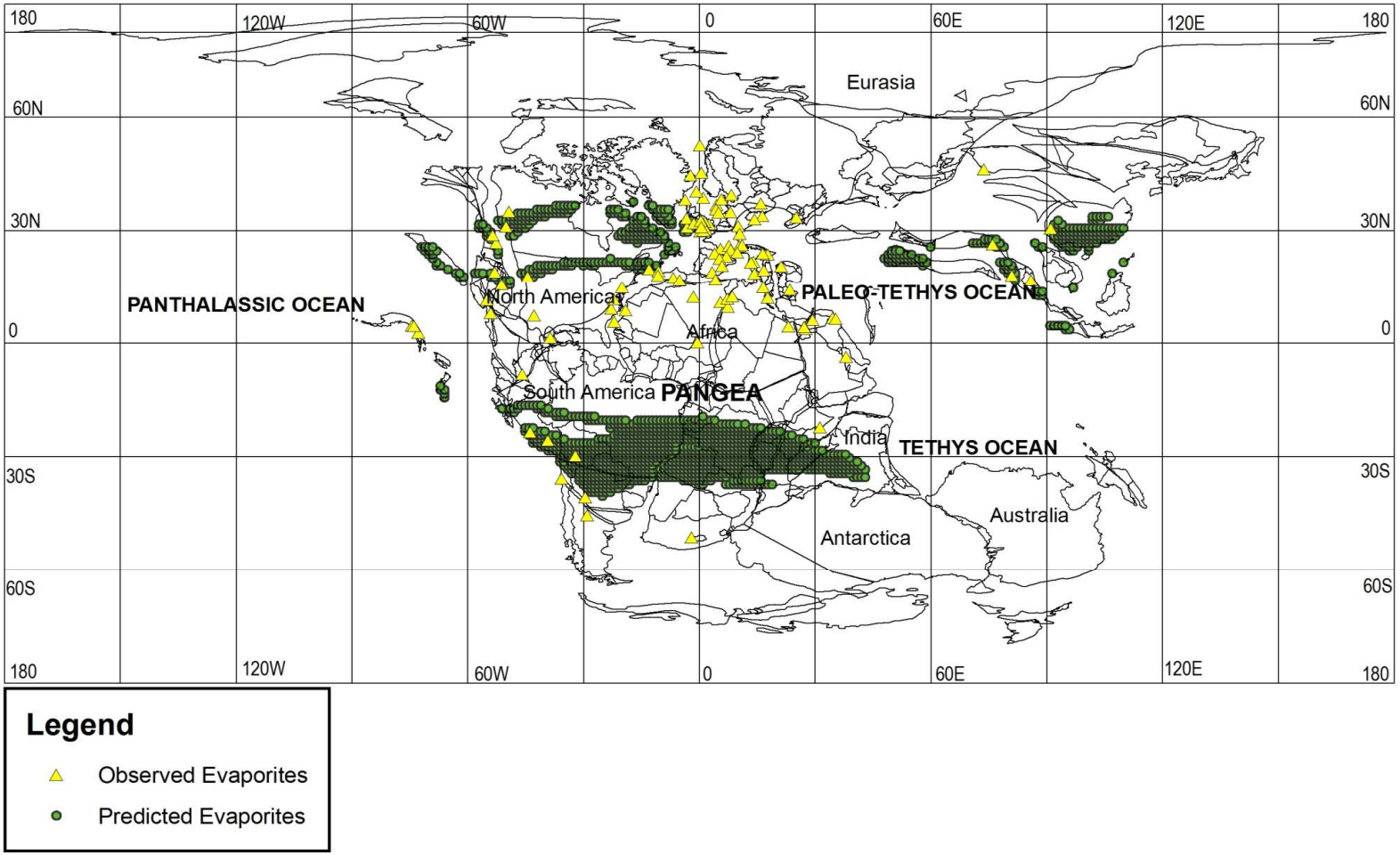

Figure 4.45: Paleoreconstruction for the Late Triassic showing the location of both the predicted and the observed evaporites.

4.8.2.1 Statistical Analyzes for the Late Triassic

A boundary representing the edge of the continental lithosphere for the Late Triassic was mapped and in Figure 4.46 is represented by a 5°x5° set of grid cells. For the Late Triassic, 1216 grid cells were obtained. 144 of these grid cells contained localities for the predicted evaporites. This represents 11.84% of the continental grid cells (Figure 4.47). 56 grid cells contained observed evaporite localities (Figure 4.48). 12 grid cells contained both predicted and observed evaporite localities which are designated as "hits" (Figure 4.49). According to the statistical procedure outlined in section 2.4, since the expected number of hits was 6.63 and the observed number of hits was 12, the probability that the number of hits is due to a random process is 0.0199 (Table 4.1). This strongly suggests that the observed hits are not random and that the null hypothesis fails.

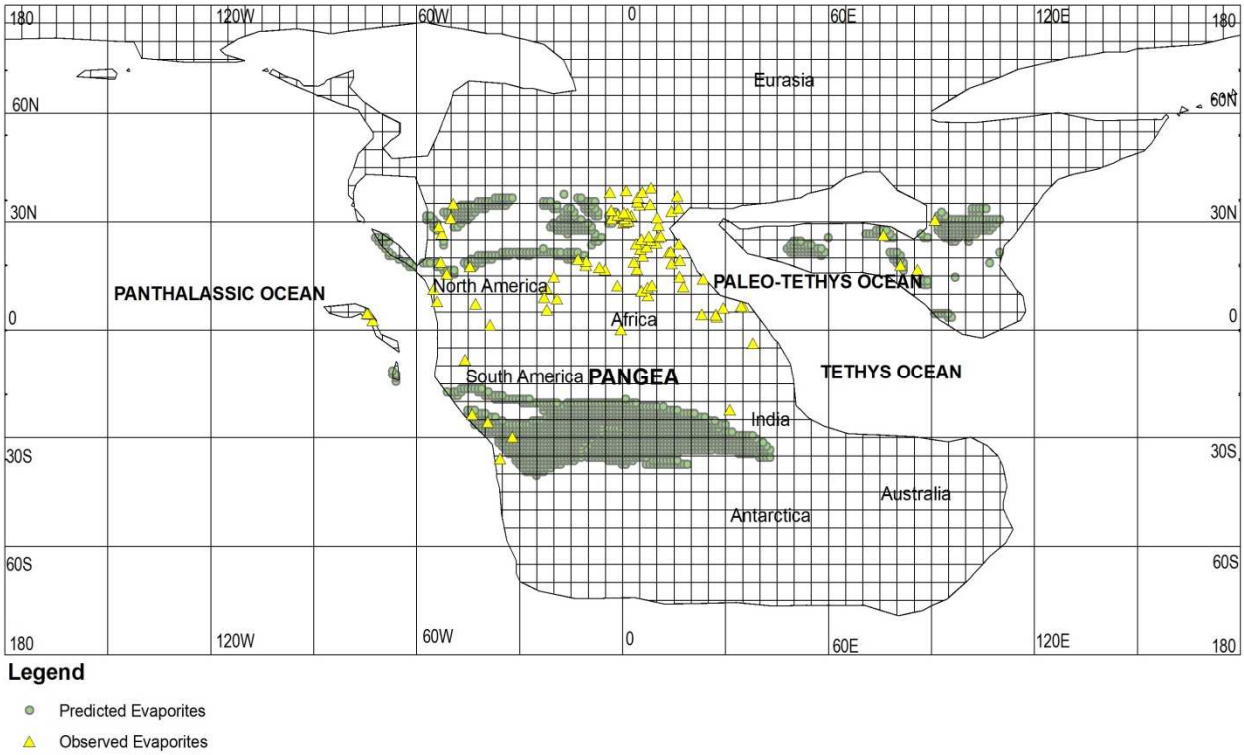

Figure 4.46: This map shows the 5°x5° latitude- longitude grids for the Late Triassic time period.

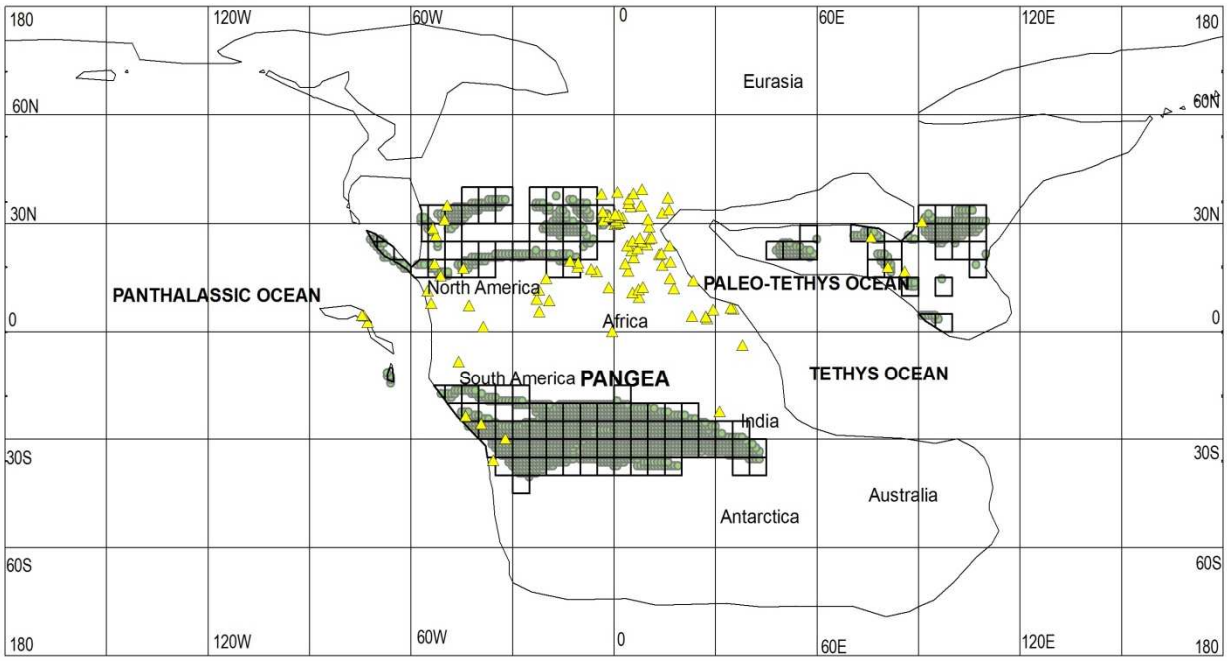

Figure 4.47: This map shows the 5°x5° latitude- longitude grids for the Late Triassic predicted evaporite localities.

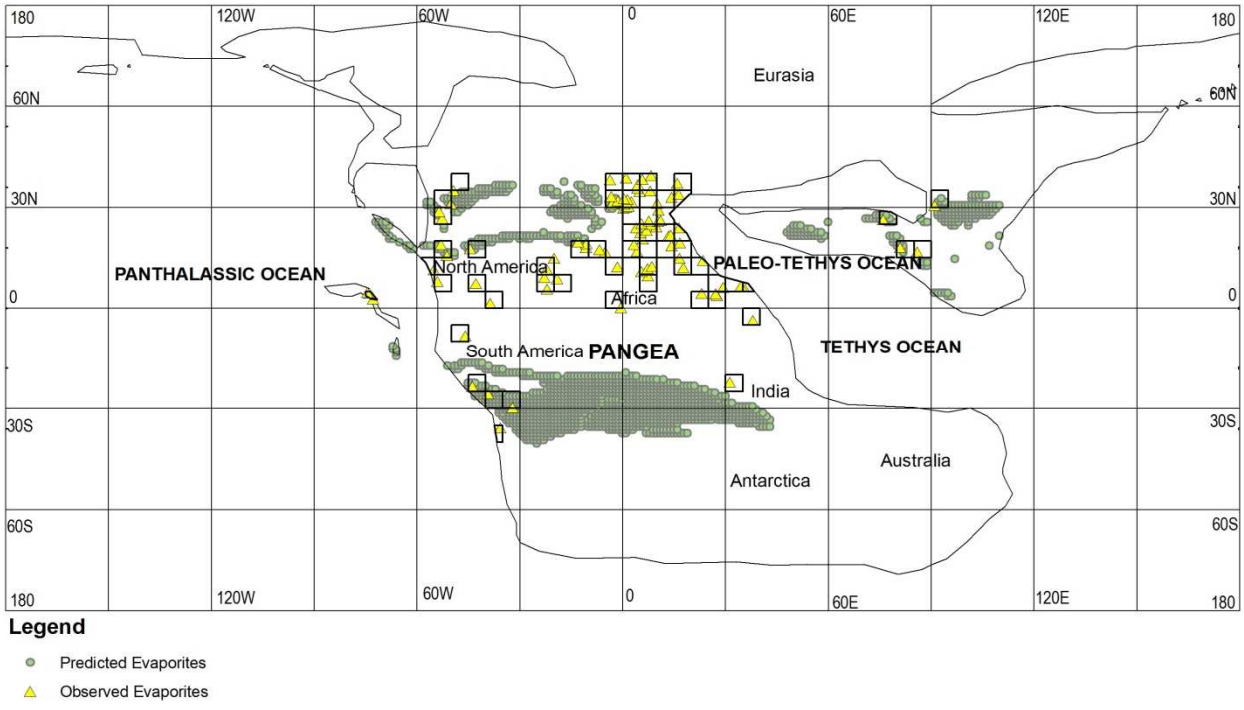

Figure 4.48: This map shows the 5°x5° latitude- longitude grids for the Late Triassic observed evaporite localities.

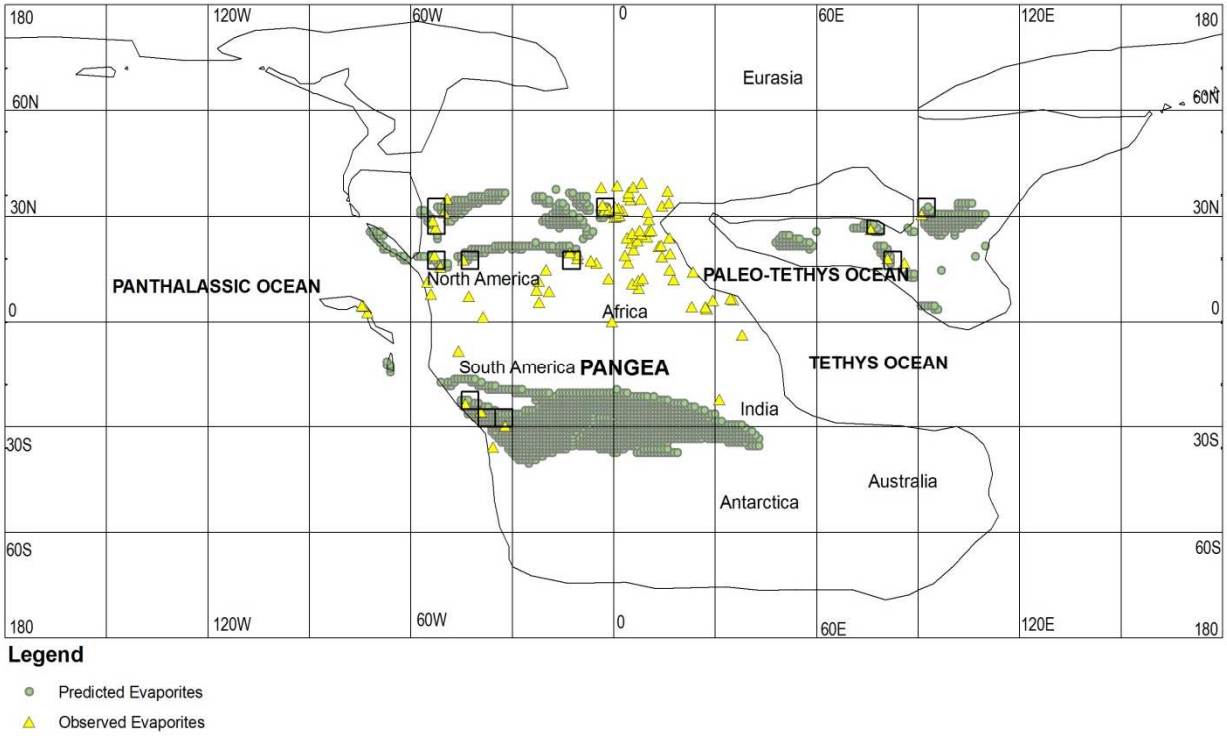

Figure 4.49: This map shows the "hits" obtained for the Late Triassic time period.

Table 4.1 Statistical Calculation for the Mesozoic Era

Geologic Time Period	Total Land	Number of Predicted Evaporites	%Total Land Occupied by Predicted Evaporites	Number of Observed Evaporites	Predicted Number of Hits	Hits	Misses	Probability that Hits are Random
Tertiary/Cretaceous Boundary (70 Ma)	1334	25	1.87	41	0.77	4	37	0.00678
Turonian/Cenomanian (90 Ma)	1403	104	7.41	55	4.08	24	31	1.23×10^{-11}
Aptian/Albian (120 Ma)	1436	92	6.41	71	4.55	20	51	6.28×10^{-8}
Barremian/Barresian (140 Ma)	1373	137	9.98	66	6.59	23	43	3.63×10^{-7}
Late Jurassic (160 Ma)	1198	168	14.02	73	10.24	31	42	9.06×10^{-8}
Early Jurassic (180 Ma)	1169	126	10.78	63	6.79	19	44	5.91×10^{-5}
Late Triassic (220 Ma)	1216	144	11.84	56	6.63	12	44	0.01988

CHAPTER 5

PALEOZOIC EVAPORITES

5.1 Introduction

The Paleozoic Era is the earliest of the three geologic eras and is subdivided into six geologic time periods based on the Gandolph time slice. These are the early Permo-Triassic Boundary (250 Ma), Early Permian (280 Ma), Mississippian (340 Ma), Late Devonian (360 Ma), Siluro-Devonian (400 Ma) and the Late Cambrian (480 Ma). This chapter will report on the climate, tectonics, results and statistics obtained for the predicted and the observed evaporites for all the time periods above.

5.2 Tectonics and Climates of the Paleozoic Era

The Paleozoic Era was characterized by varying tectonic and climatic conditions experiencing both Ice House and Hot House climates throughout the different geologic time periods. The further we travel back in time the more difficult it becomes to infer climate however, the Devonian, Silurian and Ordovician are known to have experienced greenhouse (Hot House) climates while the Cambrian, Carboniferous and Early Permian experienced Ice House climates (Crowley and North, 1991). The Cambrian climates have been reported to be slightly warmer than today's climate and the Late Silurian which was considered to have had a much cooler climate was preceded by a warm Early Silurian. The Early and Middle Devonian was characterized by warm and dry conditions. The Early Carboniferous was also

warm but more humid with a more extensive formation of coal. The Late Carboniferous had a much cooler climate with glaciations analogous to the Cenozoic era. The Early Permian was also characterized by a cool climate (Frakes, 1979; Fluteau et al, 2001; Crowley and North, 1991; Meyerhoff, 1970; Frakes et al, 1992; Copper, 1986; Stanley, 1988).

Brezinski et al, 2008 suggested that climate from the Early Silurian to the Middle/Early Carboniferous was characterized by a warm period. A warm climate also existed during the Late Devonian which was succeeded by a cooling episode. Glacial deposits from South America such as tillites were used as evidence for extensive cooling during the Late Devonian (Caputo, 1985; Scotese, 2001). Evaporites indicate aridity and a compilation by Gordon, 1975 of the abundance of evaporites through time shows evaporite accumulation during the Cambrian, Ordovician and Carboniferous with a culmination in the Permian and the Devonian.

5.3 Permo-Triassic Boundary(~ 250 Ma)

5.3.1 Permo-Triassic Boundary Evaporites

The geographic distribution (Figure 5.1) of predicted evaporites was obtained by intersecting the Evaporite Climate Envelope with precipitation and temperature estimates for the Permo-Triassic Boundary. A total of 1978 1°x1° localities fell within the Evaporite Climate Envelope for the Permo-Triassic Boundary. The predicted evaporite localities occur in central South America, central North Africa, parts of North America and southern Eurasia (Figure 5.1).

The geographic distribution of actual (observed) evaporite localities was obtained from a compilation by Boucot et al (in press). Permo- Triassic Boundary evaporites occur to the north of

South America, central North Africa, eastern North Africa and Eurasia. A total of 41 observed evaporites are plotted on Figure 5.2.

"Hits" are observed in Central Africa and Southern Eurasia (Figure 5.3). "Misses" are observed in northern Eurasia, eastern Eurasia, northern North America, central South America and parts of Central Africa.

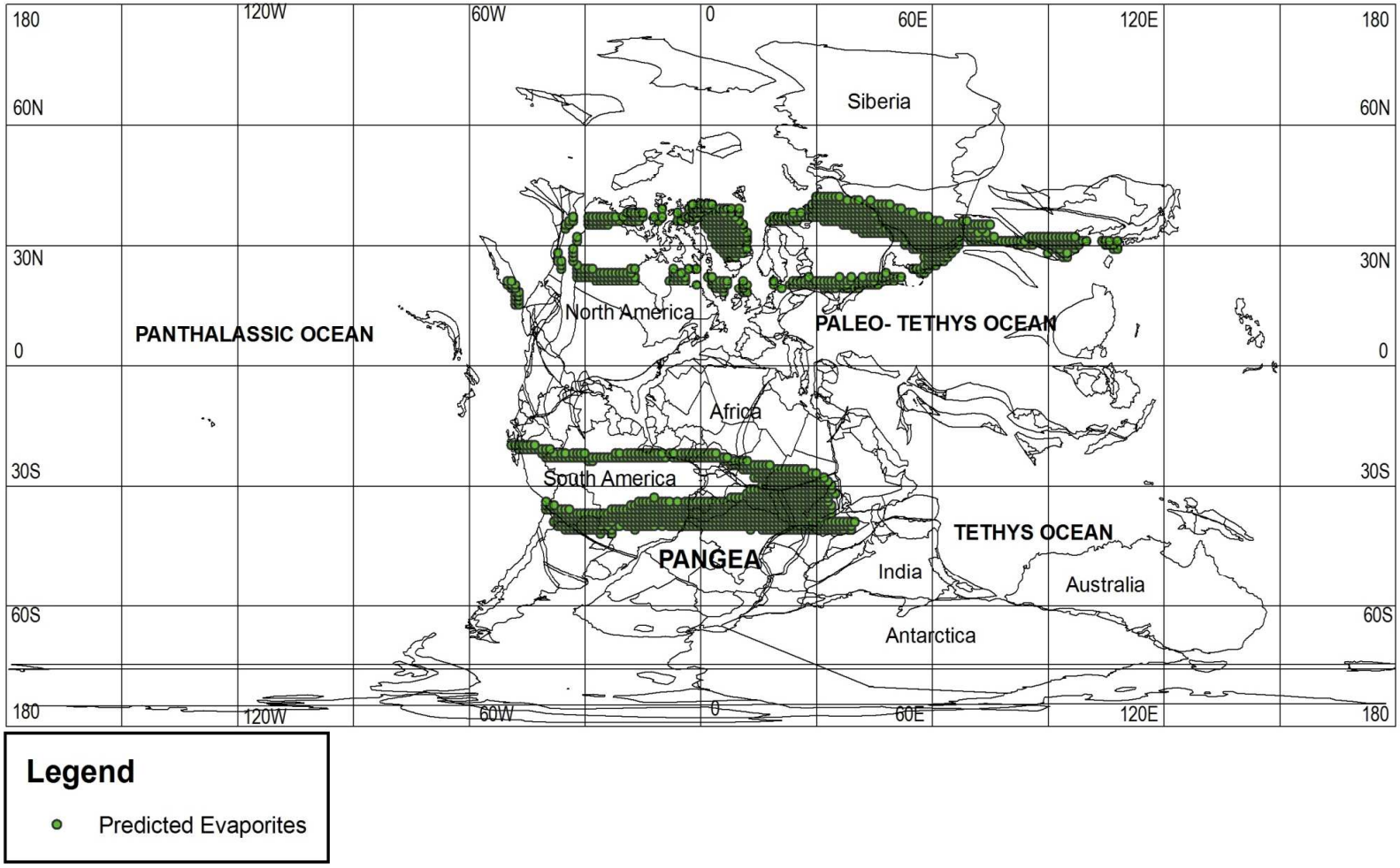

Figure 5.1: Paleoreconstruction for the Permo-Triassic Boundary showing the location of the predicted evaporites.

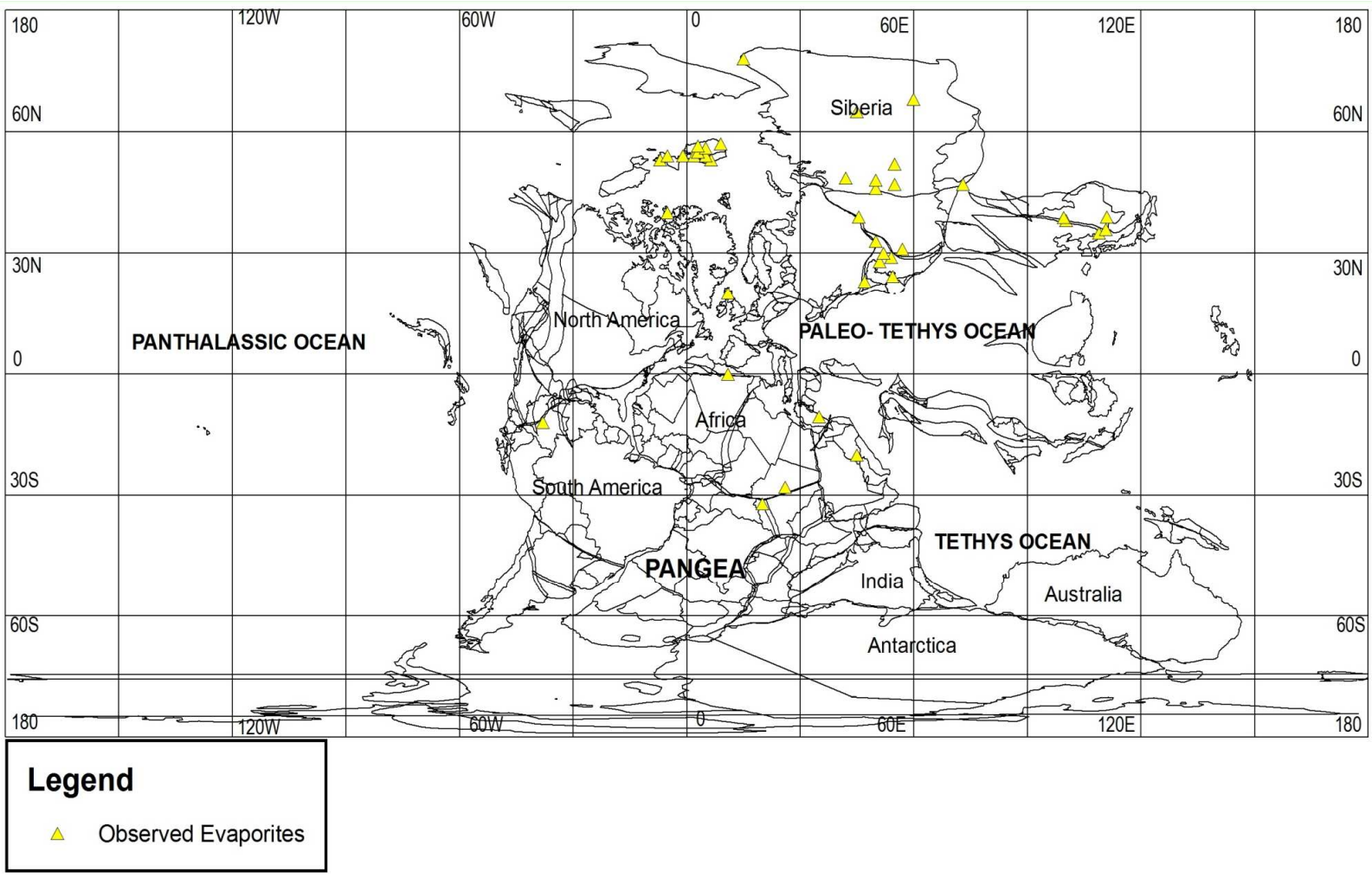

Figure 5.2: Paleoreconstruction for the Permo-Triassic Boundary showing the location of the observed evaporites.

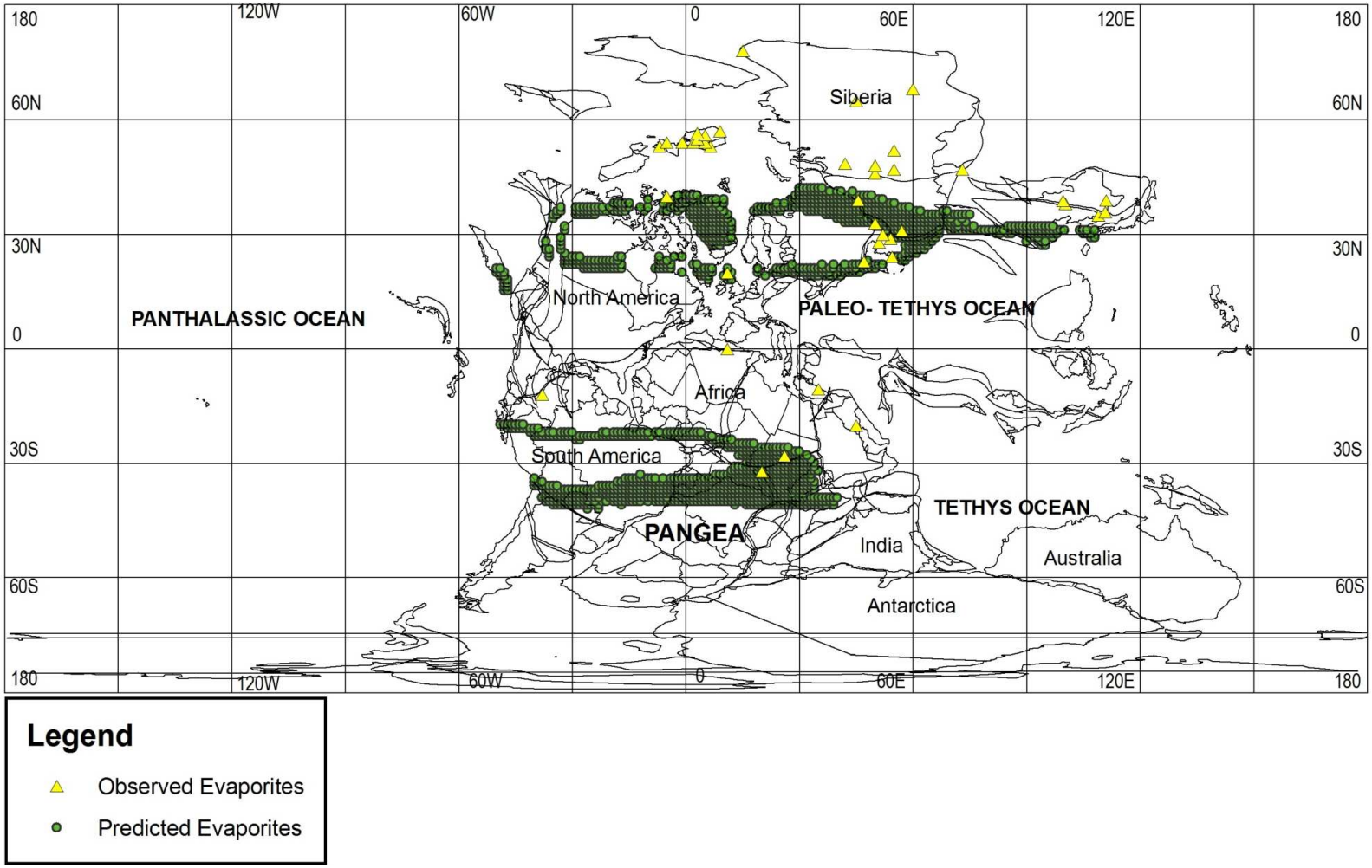

Figure 5.3: Paleoreconstruction for the Permo-Triassic Boundary showing the match between the predicted and the observed evaporites.

5.3.1.1 Statistical Analyzes for the Permo-Triassic Boundary

A boundary representing the edge of the continental lithosphere for the Permo-Triassic Boundary was mapped and in Figure 5.4 is represented by a 5°x5° set of grid cells. For the Permo-Triassic Boundary, 1162 grid cells were obtained. 150 of these 5°x5° grid cells contained localities for the predicted evaporites. This represents 12.91% of the continental grid cells (Figure 5.5). 30 grid cells contained observed evaporite localities (Figure 5.6). 16 grid cells contained both predicted and observed evaporite localities which are designated as "hits" (Figure 5.7). The variables used in the statistical analysis for the Permo-Triassic Boundary are given in Table 5.1. According to the statistical procedure outlined in section 2.4, since the expected number of hits was 3.87 and the observed number of hits was 16, the probability that the number of hits is due to a random process is 2.524×10^{-6}. This strongly suggests that the observed hits are not random and that the null hypothesis fails.

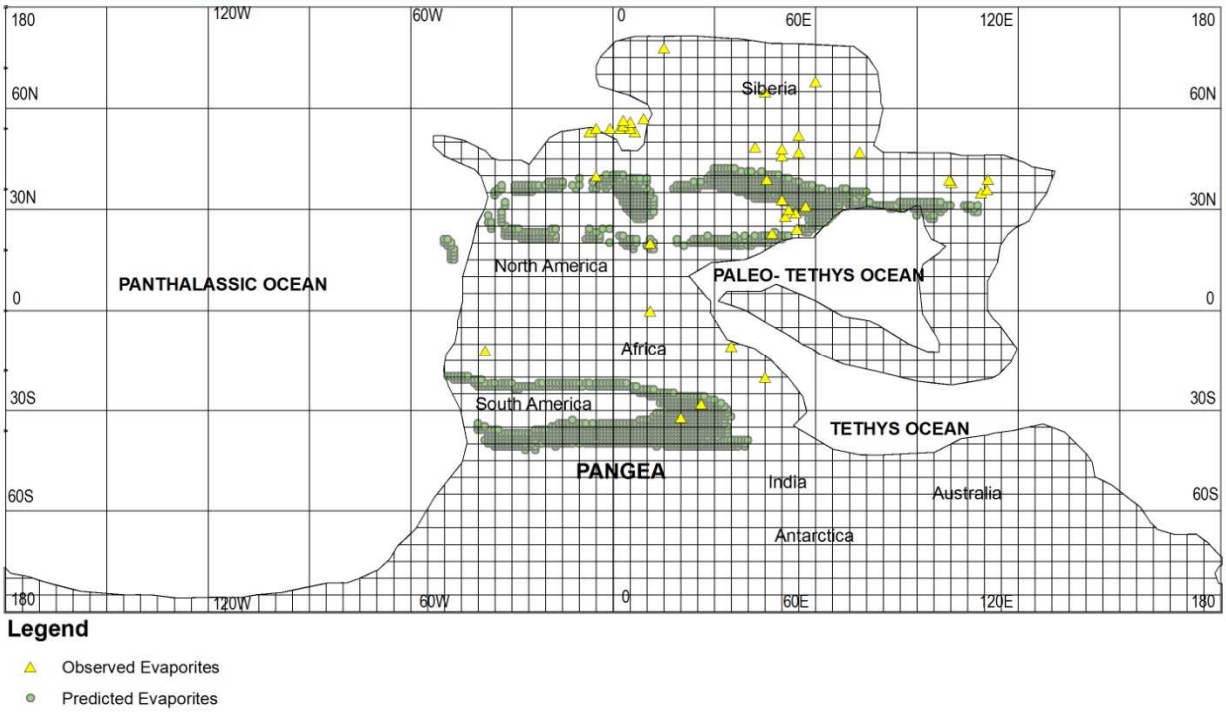

Figure 5.4: This map shows the 5°x5° latitude- longitude grids for the Permo-Triassic time period.

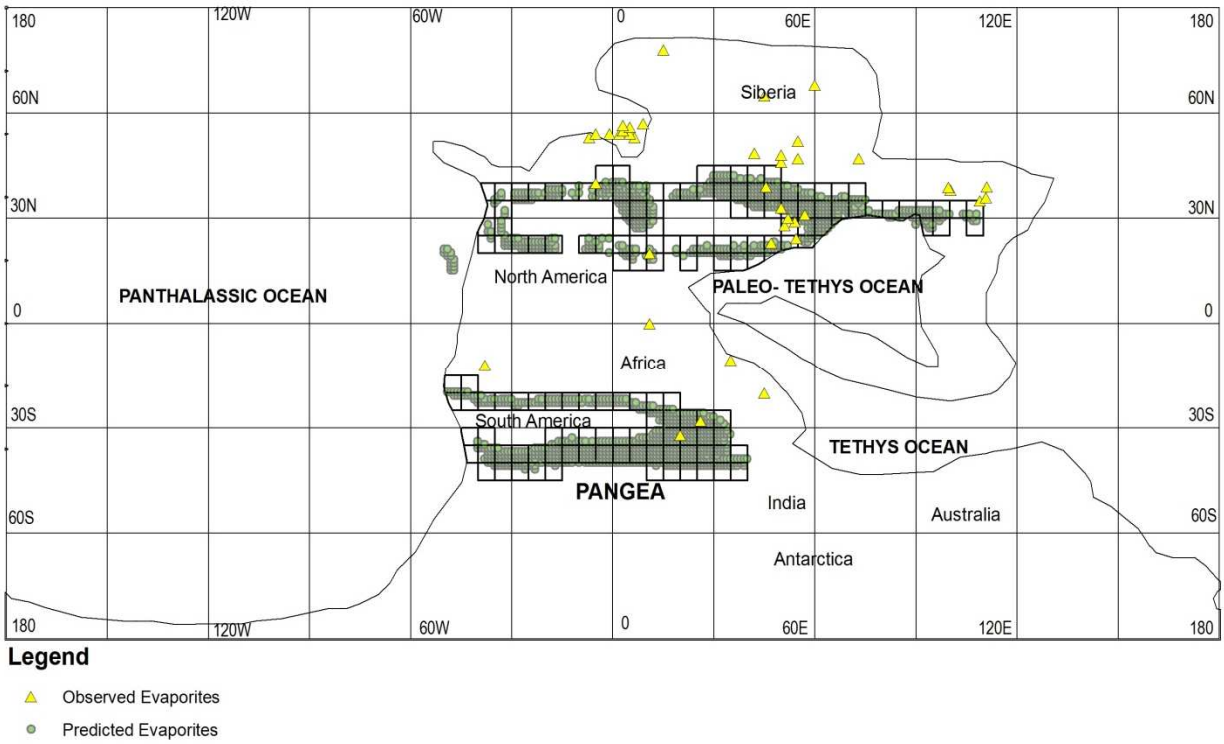

Figure 5.5: This map shows the 5°x5° latitude- longitude grids for the Permo-Triassic Boundary predicted evaporite localities.

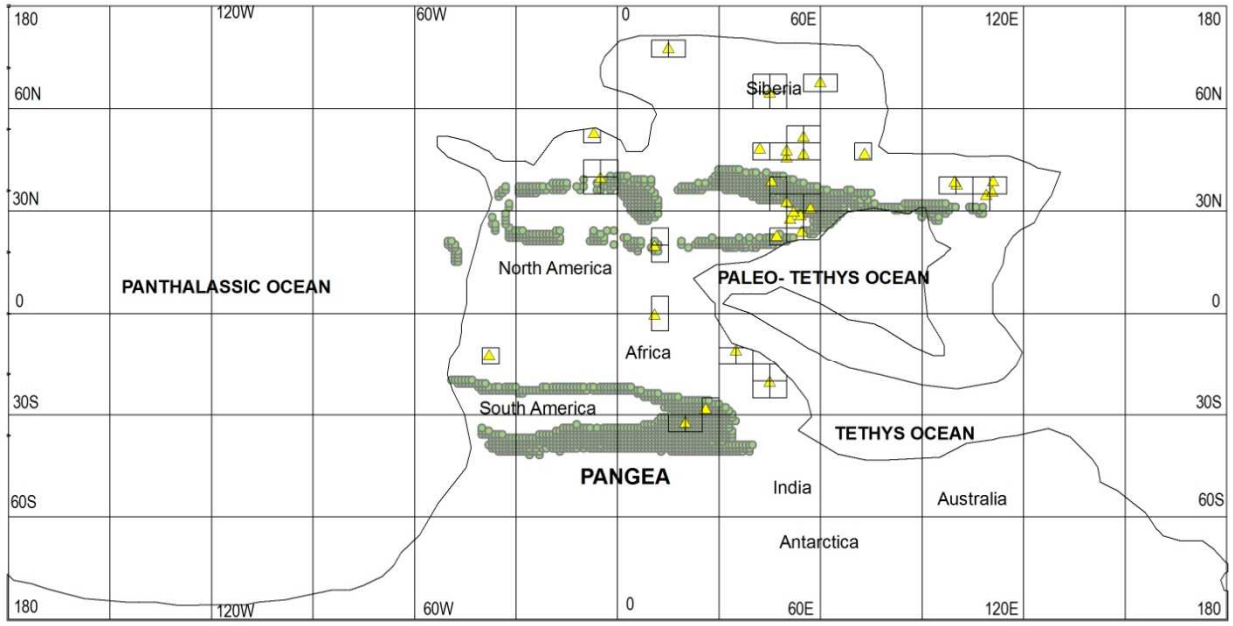

Figure 5.6: This map shows the 5°x5° latitude- longitude grids for the Permo-Triassic Boundary observed evaporite localities.

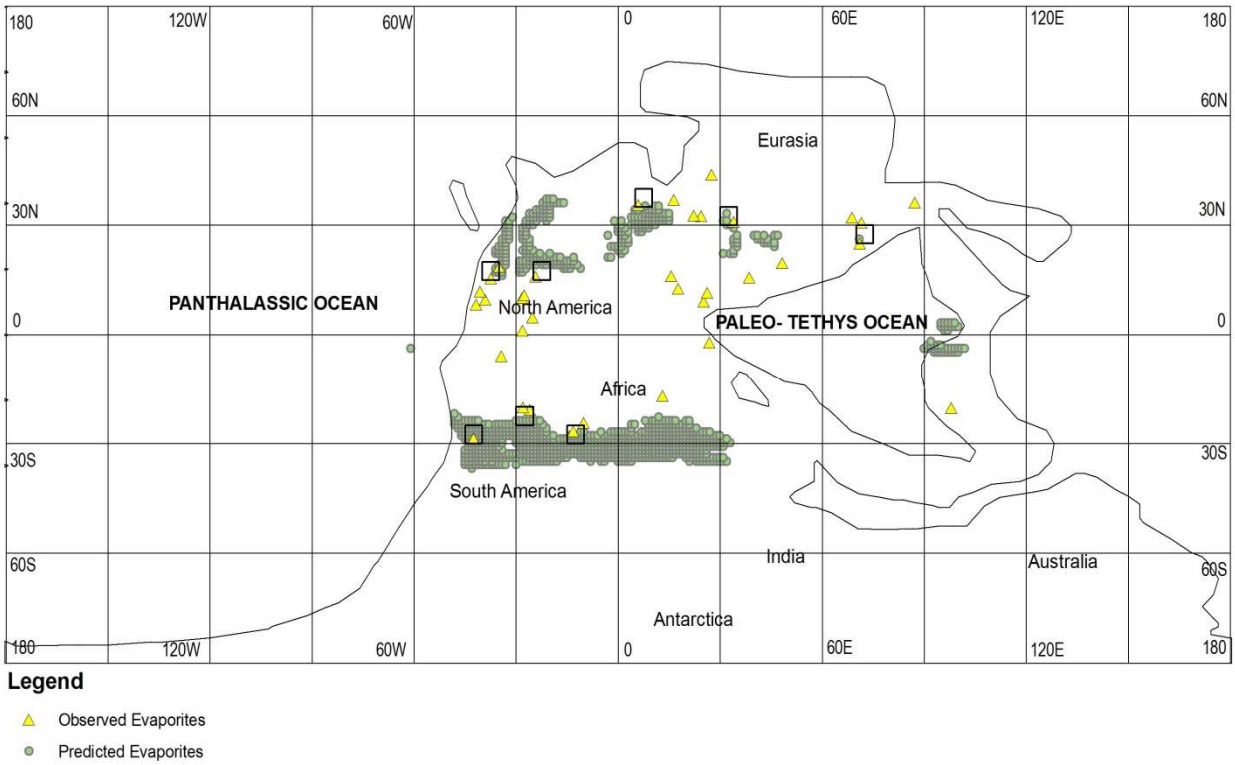

Figure 5.7: This map shows the "hits" obtained for the Permo-Triassic time period.

5.4 Early Permian (~280 Ma)

5.4.1 Early Permian Evaporites

The geographic distribution (Figure 5.8) of predicted evaporites was obtained by intersecting the Evaporite Climate Envelope with precipitation and temperature estimates for the Early Permian. A total of 1309 1°x1° localities fell within the Evaporite Climate Envelope for the Early Permian. The predicted evaporite localities occur in central South America, Central Africa forming an evaporitic belt across the two countries. They also occur in North America, northern Greenland and in South Asia (Figure 5.8).

The geographic distribution of actual (observed) evaporite localities was obtained from a compilation by Boucot et al (in press). Early Permian evaporites occur in South Asia, central and north South America, central North America and in parts of central Africa. A total of 37 observed evaporites are plotted on Figure 5.9.

"Hits" are observed in central North America, central South America and in South Asia (Figure 5.10). "Misses" are observed in Central Africa, parts of South Asia, central North America and in northern South America.

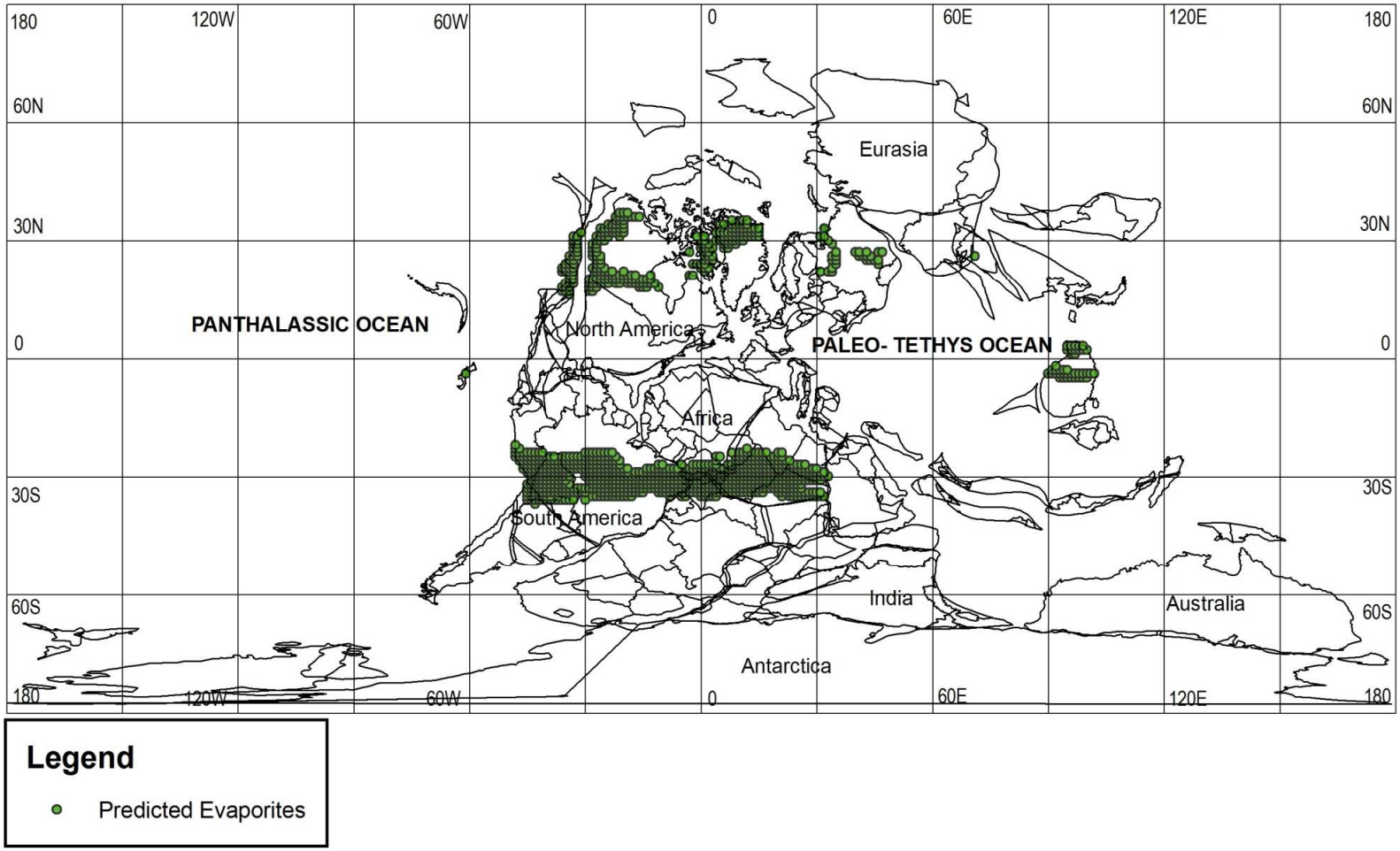

Figure 5.8: Early Permian predicted evaporites plotted on a 280 Ma paleoreconstruction.

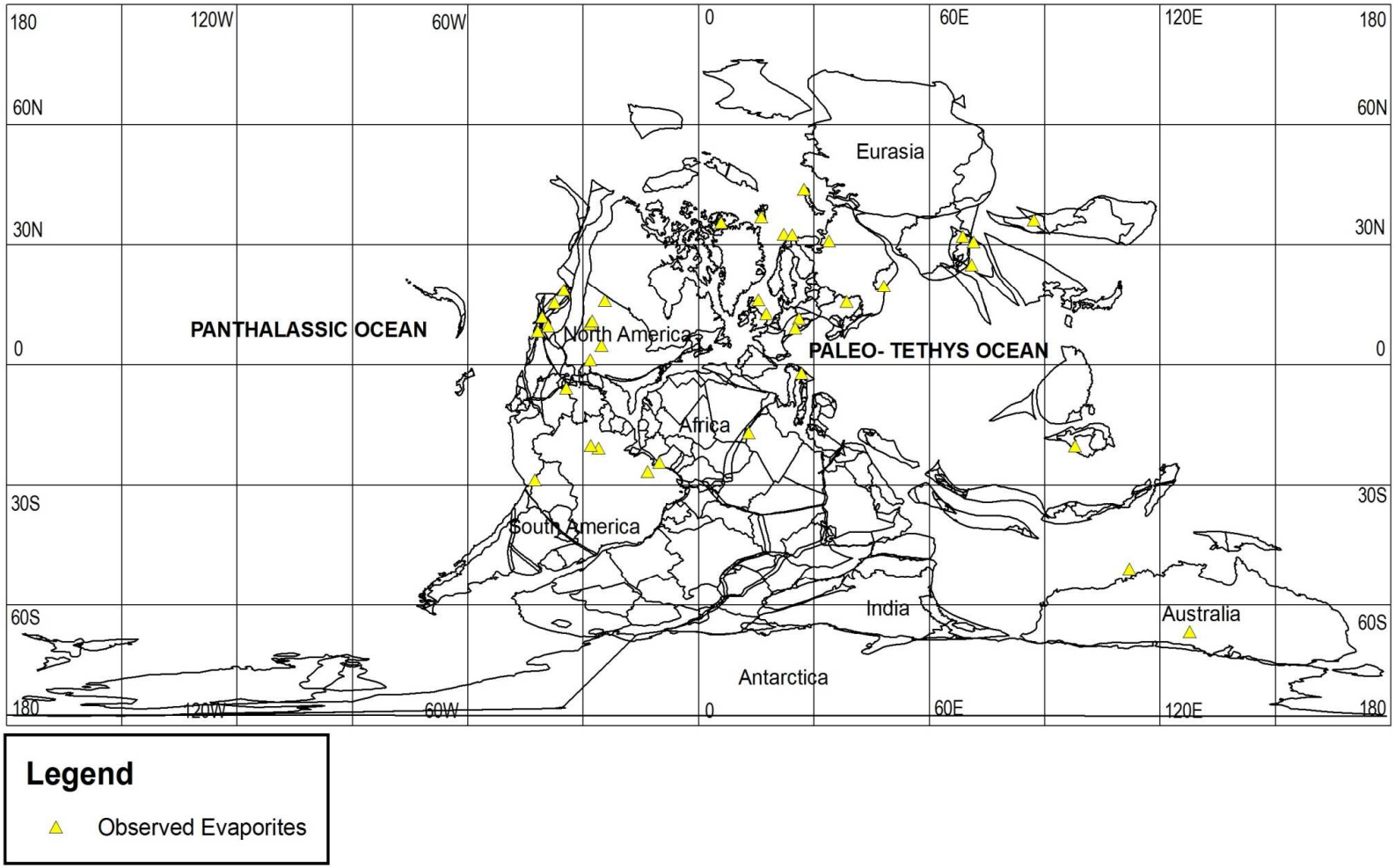

Figure 5.9: Early Permian observed evaporites plotted on a 280 Ma paleoreconstruction.

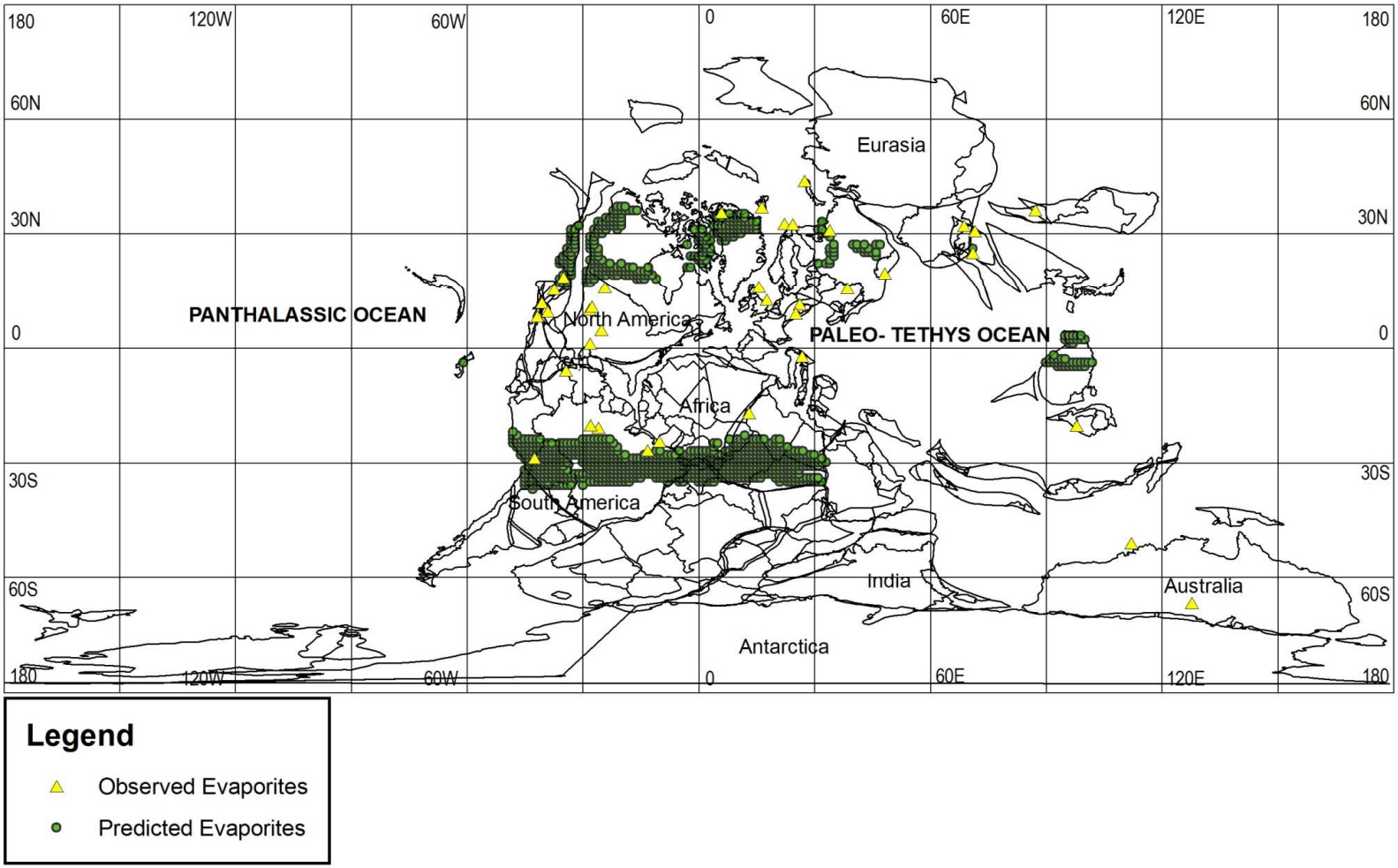

Figure 5.10: Early Permian predicted and observed evaporites plotted on a 280 Ma paleoreconstruction.

5.4.1.1 Statistical Analyzes for the Early Permian

A boundary representing the edge of the continental lithosphere for the Early Permian was mapped and in Figure 5.11 is represented by a 5°x5° set of grid cells. For the Early Permian, 1160 grid cells were obtained. 90 of these 5°x5° grid cells contained localities for the predicted evaporites. This represents 7.76% of the continental grid cells (Figure 5.12). 30 grid cells contained observed evaporite localities (Figure 5.13). 8 grid cells contained both predicted and observed evaporite localities which are designated as "hits" (Figure 5.14). The variables used in the statistical analysis for the Early Permian are given in Table 5.1. According to the statistical procedure outlined in section 2.4, since the expected number of hits was 2.33 and the observed number of hits was 8, the probability that the number of hits is due to a random process is 0.00209. This strongly suggests that the observed hits are not random and that the null hypothesis fails.

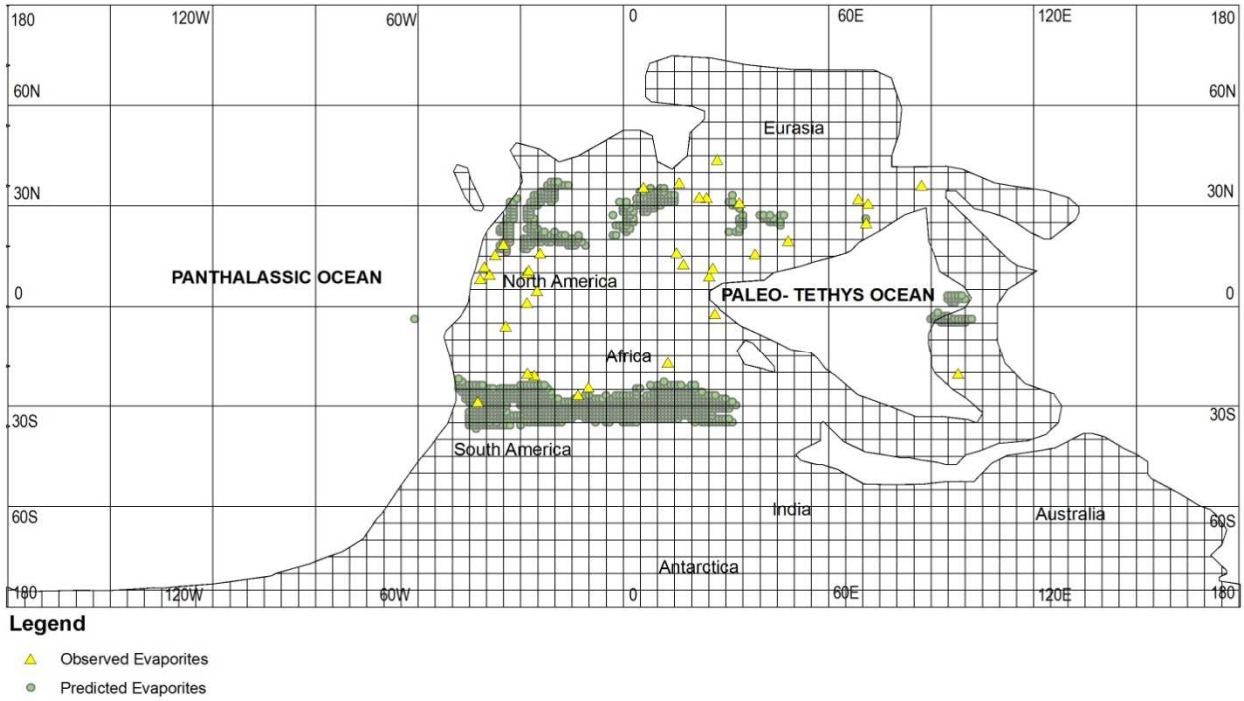

Figure 5.11: This map shows the 5°x5° latitude- longitude grids for the Early Permian time period.

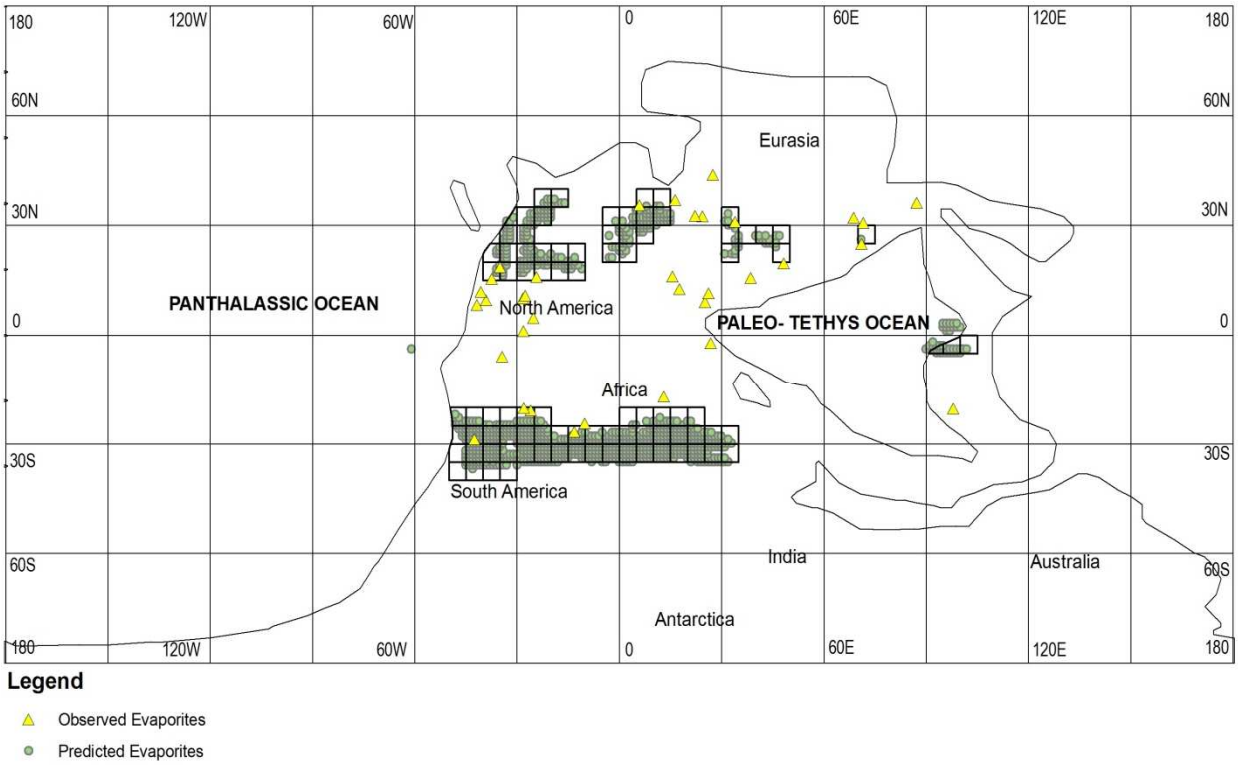

Figure 5.12: This map shows the 5°x5° latitude- longitude grids for the Early Permian predicted evaporite localities.

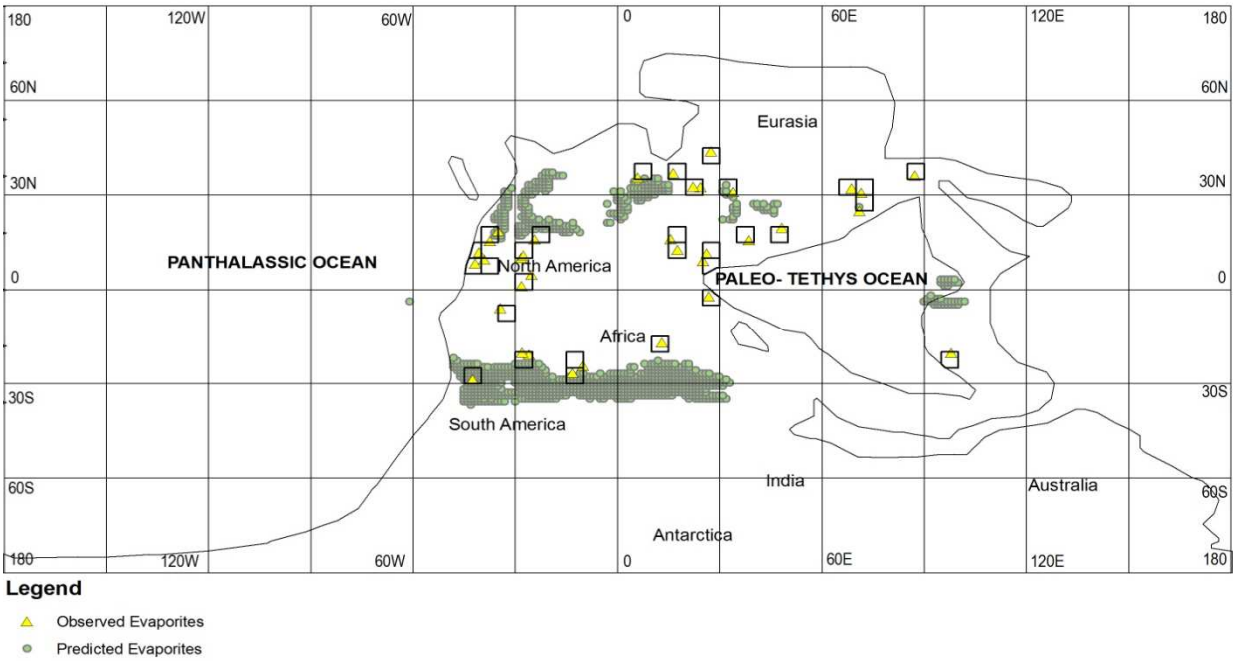

Figure 5.13: This map shows the 5°x5° latitude- longitude grids for the Early Permian observed evaporite localities.

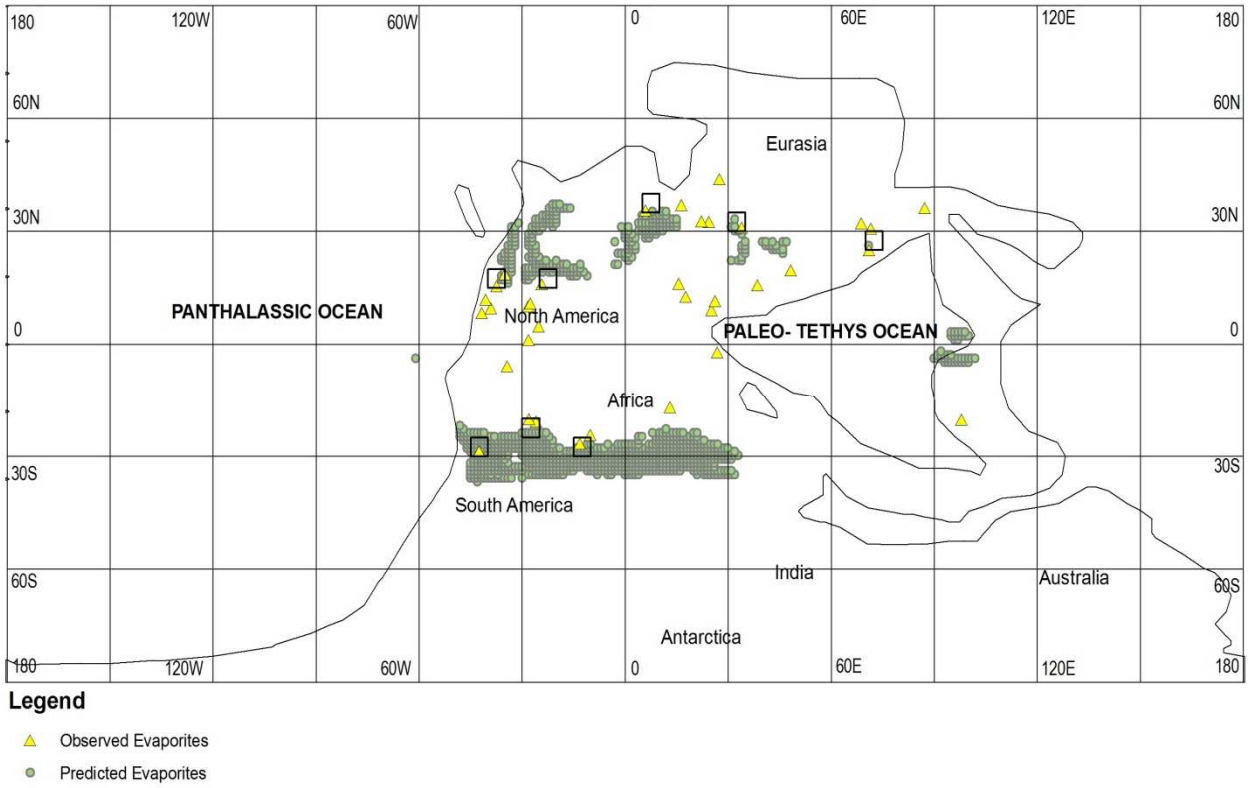

Figure 5.14: This map shows the "hits" obtained for the Early Permian.

5.5 Mississippian (~ 340 Ma)

5.5.1 Mississippian Evaporites

The geographic distribution (Figure 5.15) of predicted evaporites was obtained by intersecting the Evaporite Climate Envelope with precipitation and temperature estimates for the Mississippian. A total of 525 1°x1° localities fell within the Evaporite Climate Envelope for the Mississippian. The predicted evaporite localities occur in northern South America, North Africa, and southern North America and in parts of Asia (Figure 5.15).

The geographic distribution of actual (observed) evaporite localities was obtained from a compilation by Boucot et al (in press). Mississippian evaporites occur in northern Africa, North America and in Asia. A total of 105 observed evaporites are plotted on Figure 5.16.

"Hits" are observed in North Africa and in parts of Asia (Figure 5.17). "Misses" are observed in parts of Africa and South America, North America and in parts of Asia.

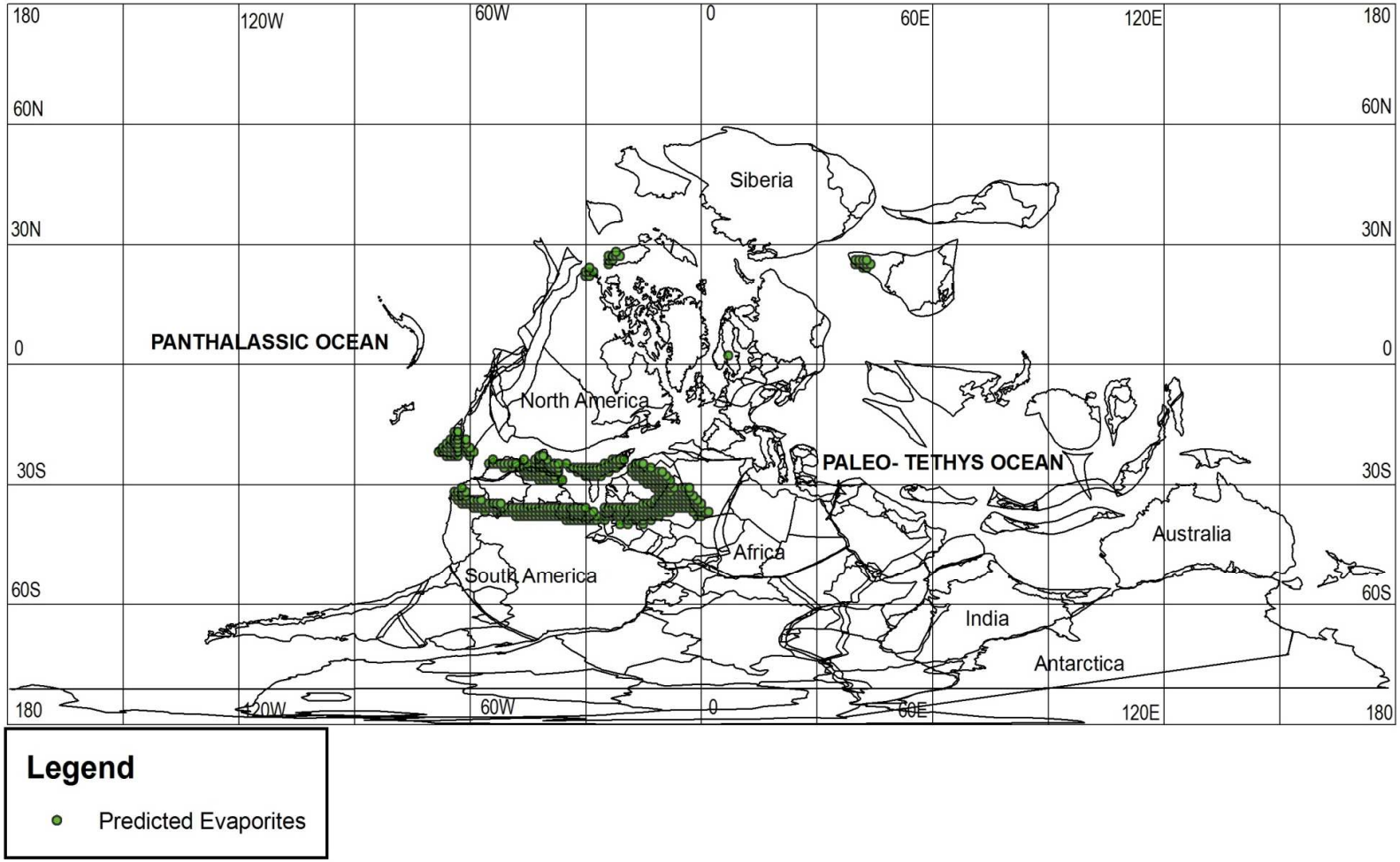

Figure 5.15: Mississippian predicted evaporites plotted on a 340 Ma paleoreconstruction.

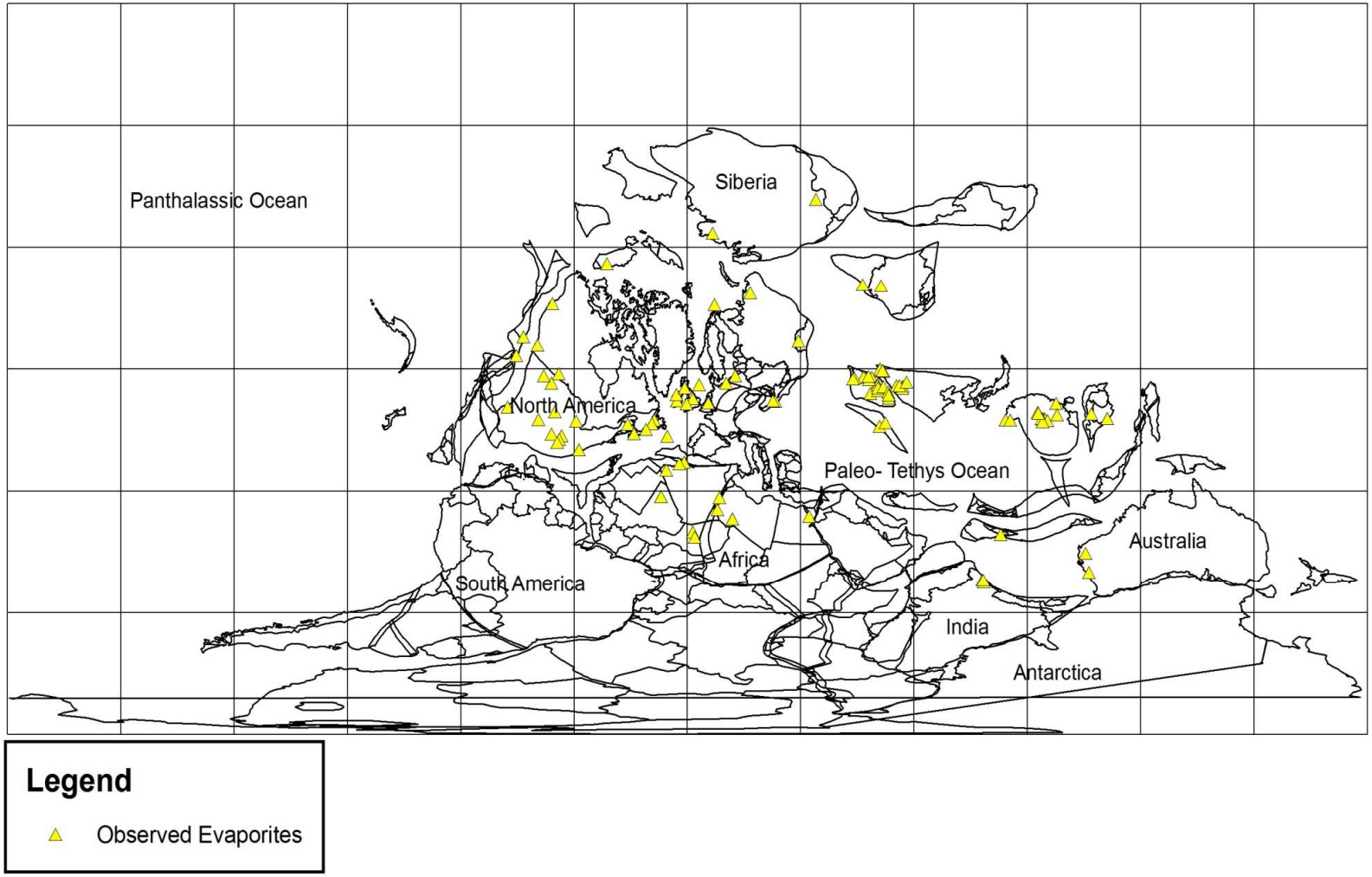

Figure 5.16: Mississippian observed evaporites plotted out on a 340 Ma paleoreconstruction.

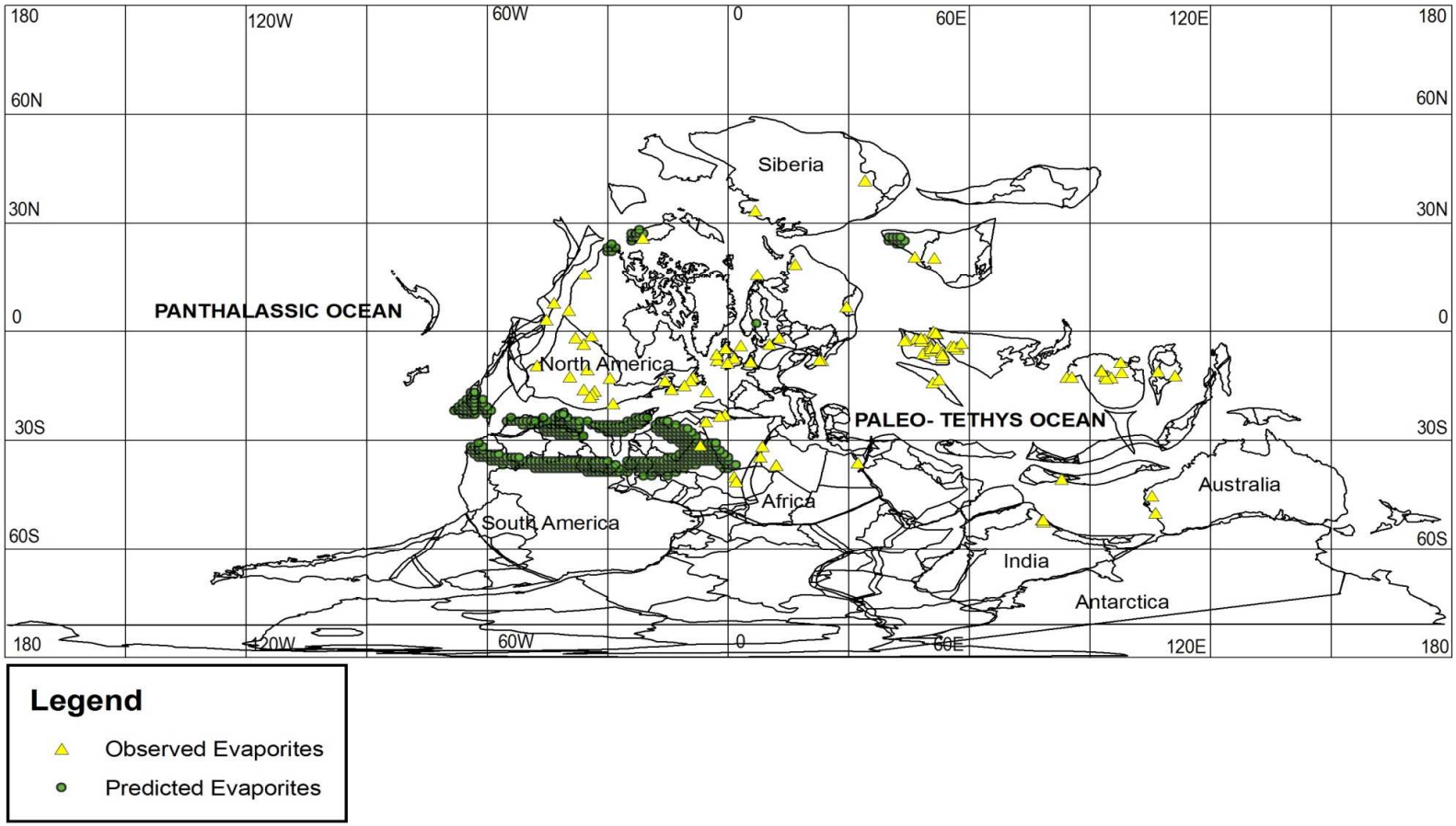

Figure 5.17: Mississippian predicted and observed evaporites plotted on a 340 Ma paleoreconstruction.

5.5.1.1 Statistical Analyzes for the Mississippian

A boundary representing the edge of the continental lithosphere for the Mississippian was mapped and in Figure 5.18 is represented by a 5°x5° set of grid cells. For the Mississippian, 1170 grid cells were obtained. 49 of these 5°x5° grid cells contained localities for the predicted evaporites. This represents 4.19% of the continental grid cells (Figure 5.19). 53 grid cells contained observed evaporite localities (Figure 5.20). 3 grid cells contained both predicted and observed evaporite localities which are designated as "hits" (Figure 5.21). The variables used in the statistical analysis for the Mississippian are given in Table 5.1. According to the statistical procedure outlined in section 2.4, since the expected number of hits was 2.22 and the observed number of hits was 3, the probability that the number of hits is due to a random process is 0.815. This suggests that the observed hits are random and that the alternative hypothesis fails.

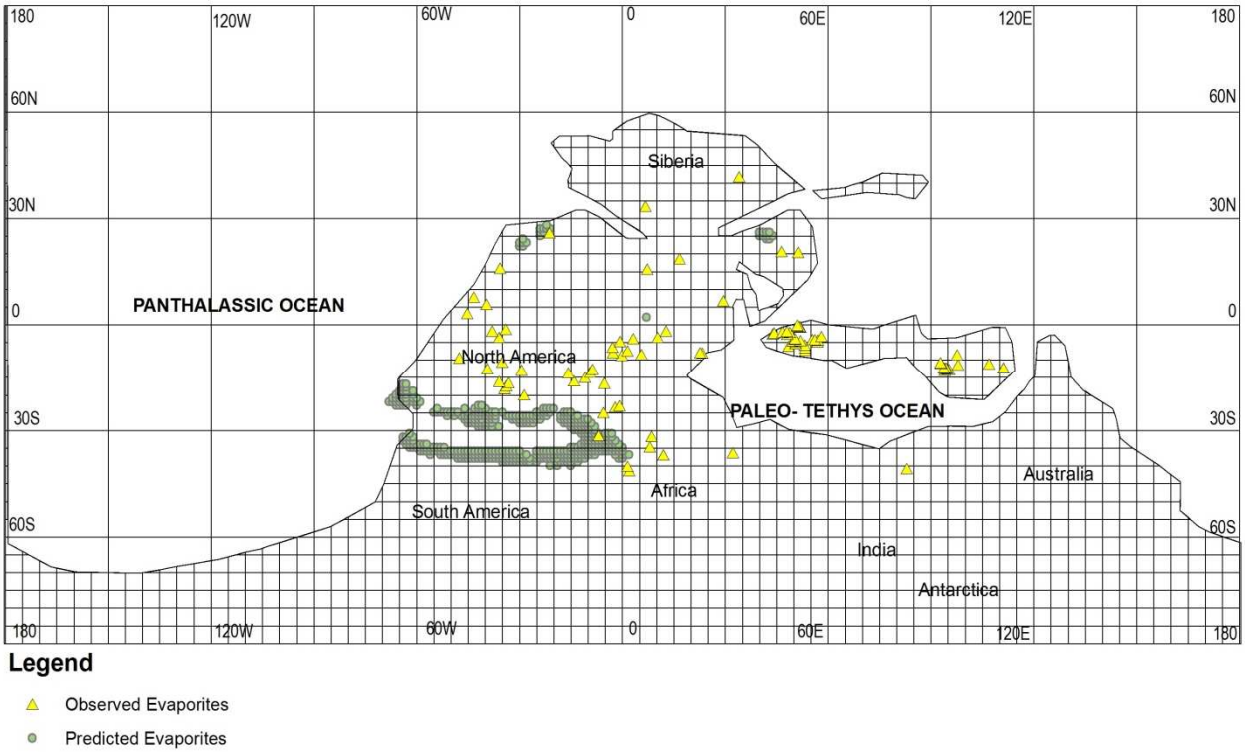

Figure 5.18: This map shows the 5°x5° latitude- longitude grids for the Mississippian time period.

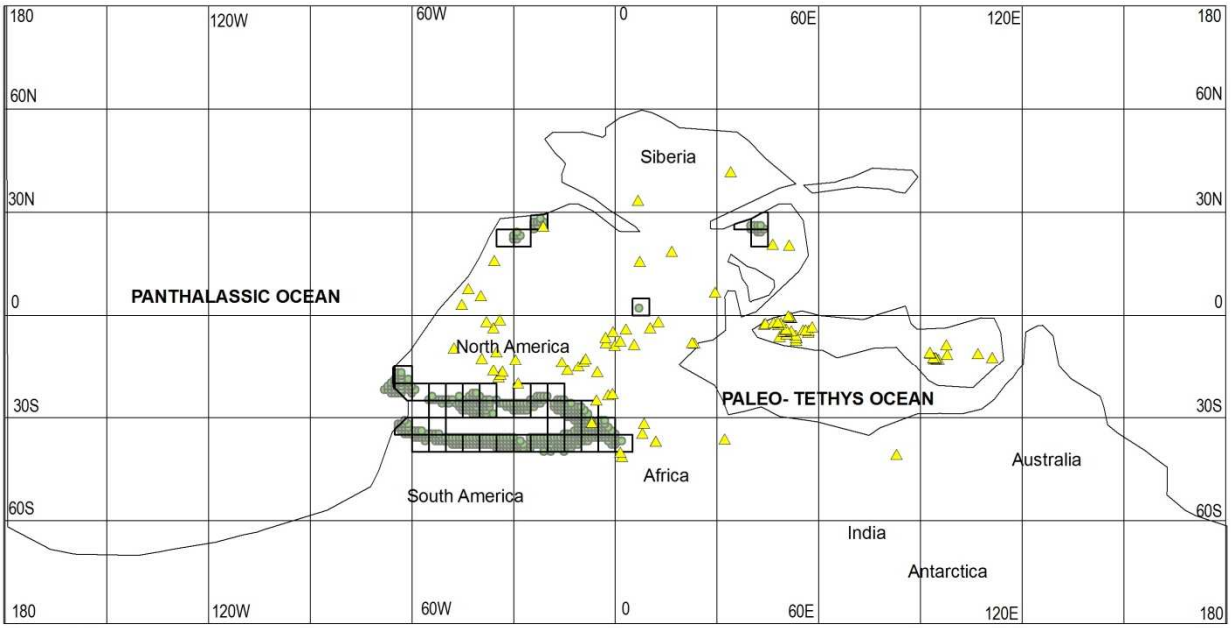

Figure 5.19: This map shows the 5°x5° latitude- longitude grids for the Mississippian predicted evaporite localities.

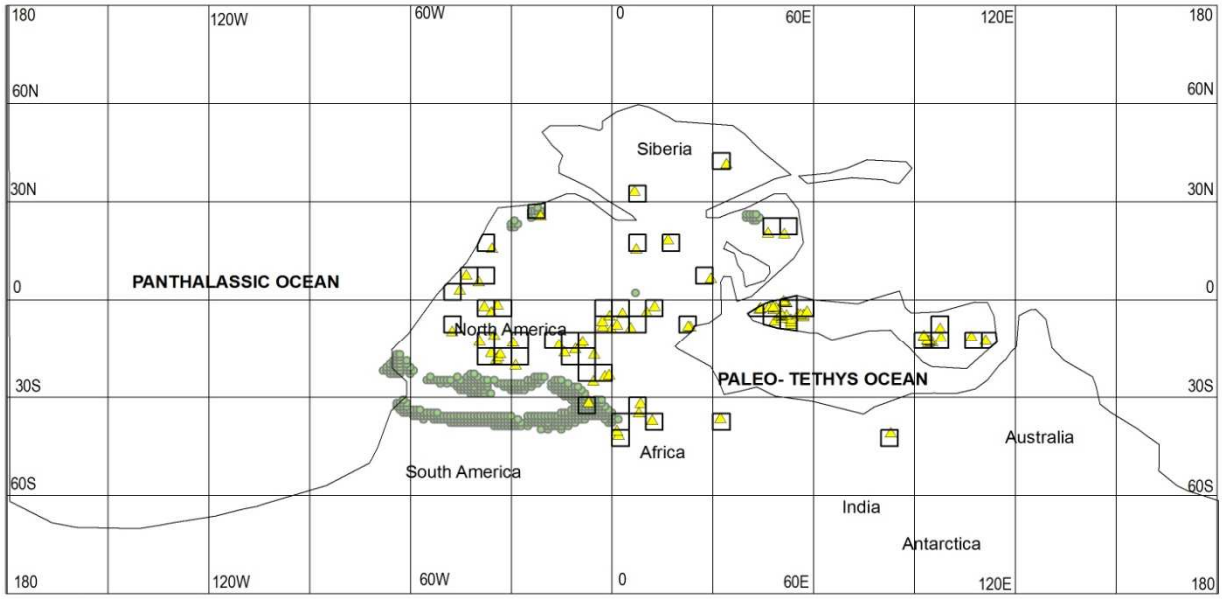

Figure 5.20: This map shows the 5°x5° latitude- longitude grids for the Mississippian observed evaporite localities.

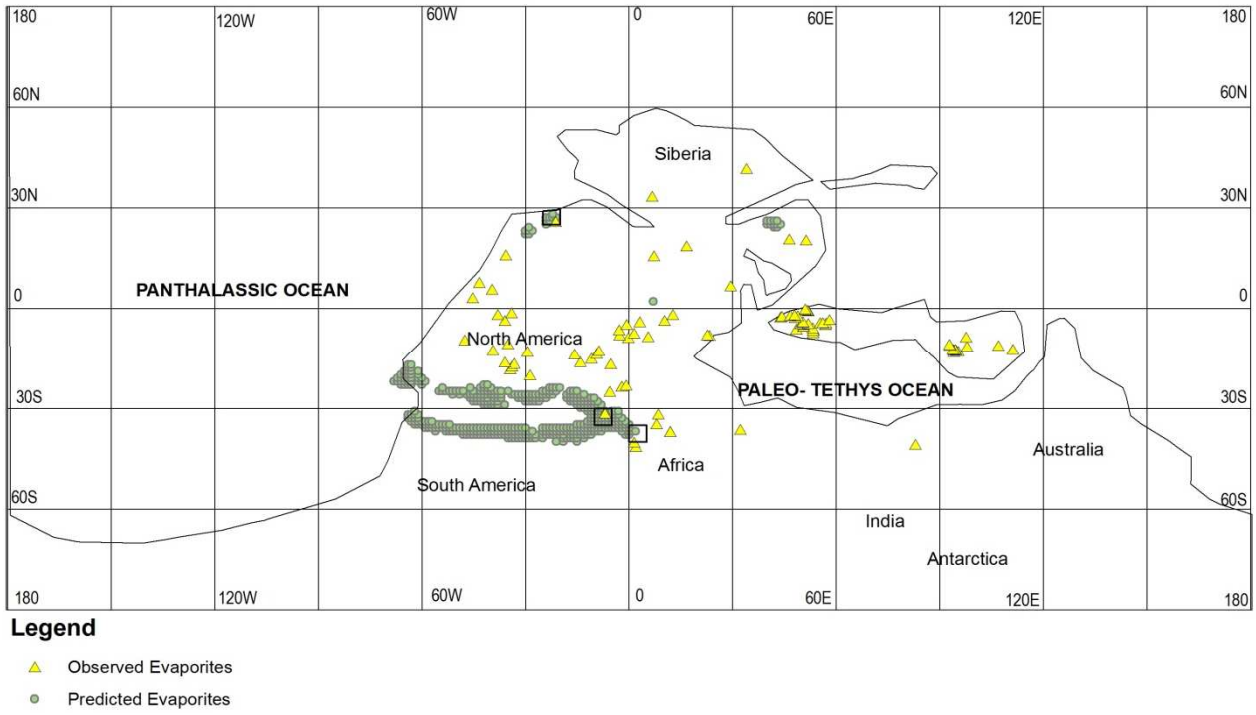

Figure 5.21: This map shows the "hits" obtained for the Mississippian.

5.6 Late Devonian (~ 360 Ma)

5.6.1 Late Devonian Evaporites

The geographic distribution (Figure 5.22) of predicted evaporites was obtained by intersecting the Evaporite Climate Envelope with precipitation and temperature estimates for the Late Devonian. A total of 69 1°x1° predicted localities fell within the Evaporite Climate Envelope for the Late Devonian. The predicted evaporite localities occur in Australia, Asia, eastern North America and in North Africa (Figure 5.22).

The geographic distribution of actual (observed) evaporite localities was obtained from a compilation by Boucot et al (in press). Late Devonian evaporites occur in Asia, North America, North Africa and in Australia. A total of 49 observed evaporites are plotted on Figure 5.23.

"Hits" are observed in Asia only (Figure 5.24). "Misses" are observed in North America, North Africa, Australia and in parts of Asia.

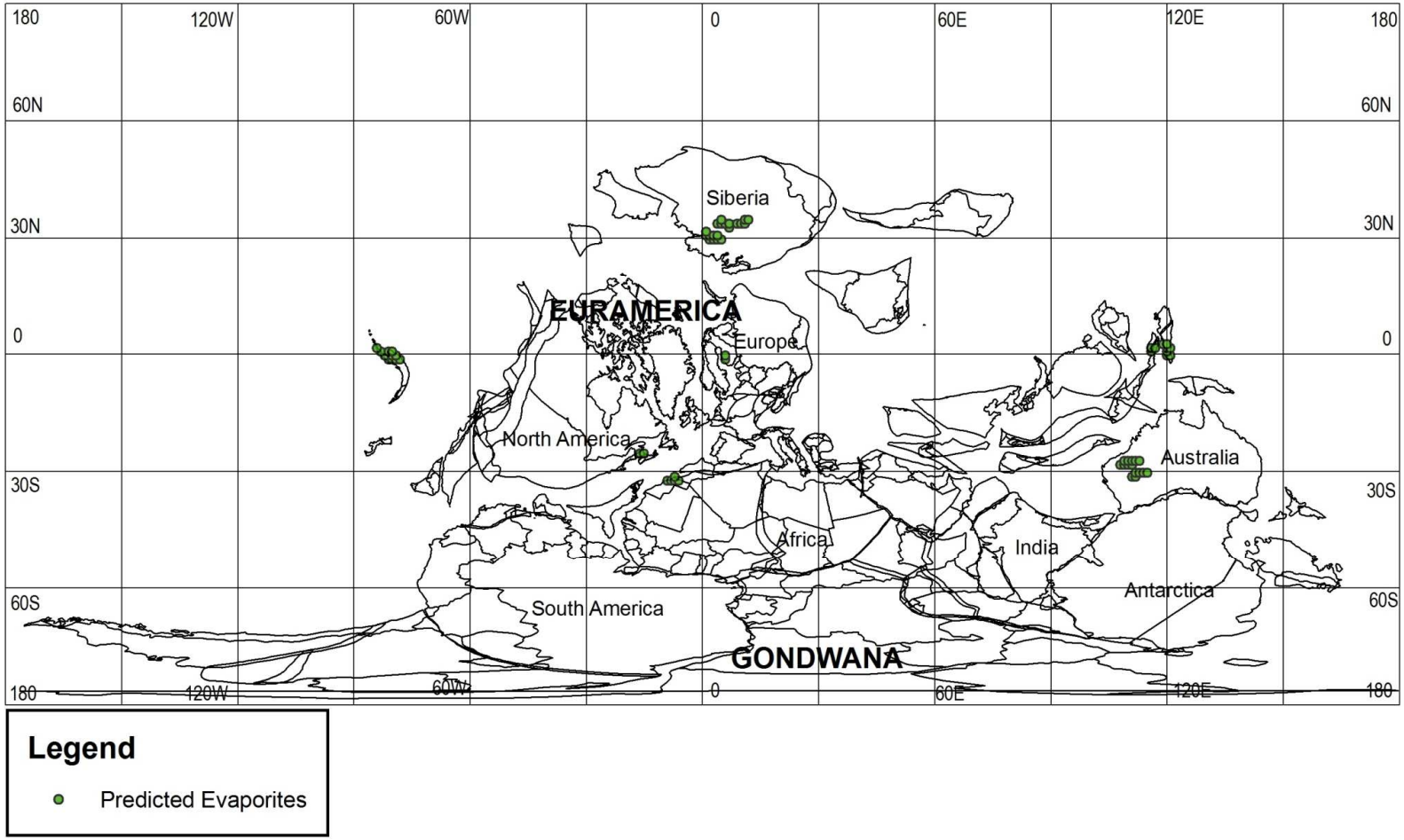

Figure 5.22: Late Devonian predicted evaporites plotted out on a 360 Ma paleoreconstruction.

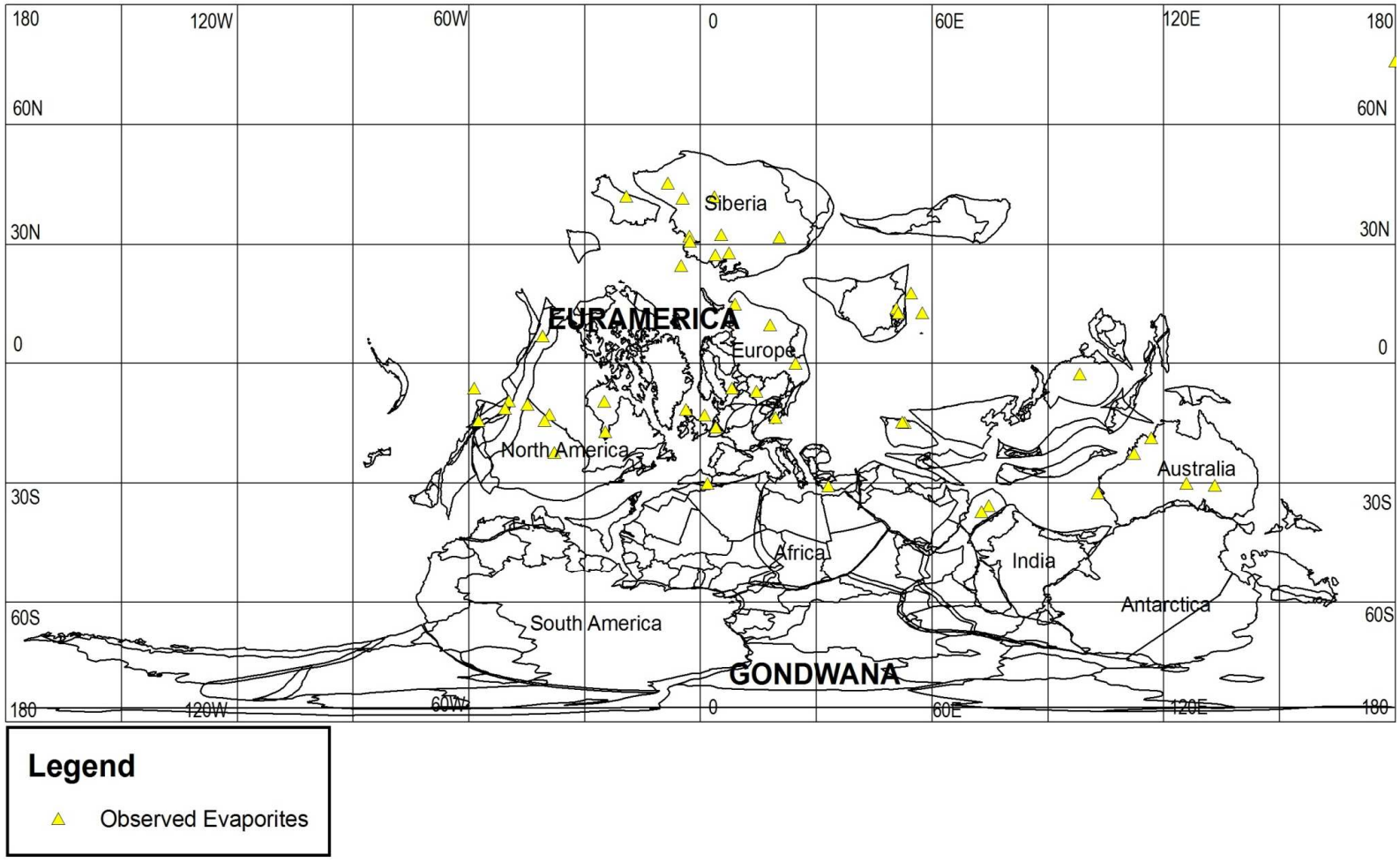

Figure 5.23: Late Devonian observed evaporites plotted out on a 360 Ma paleoreconstruction.

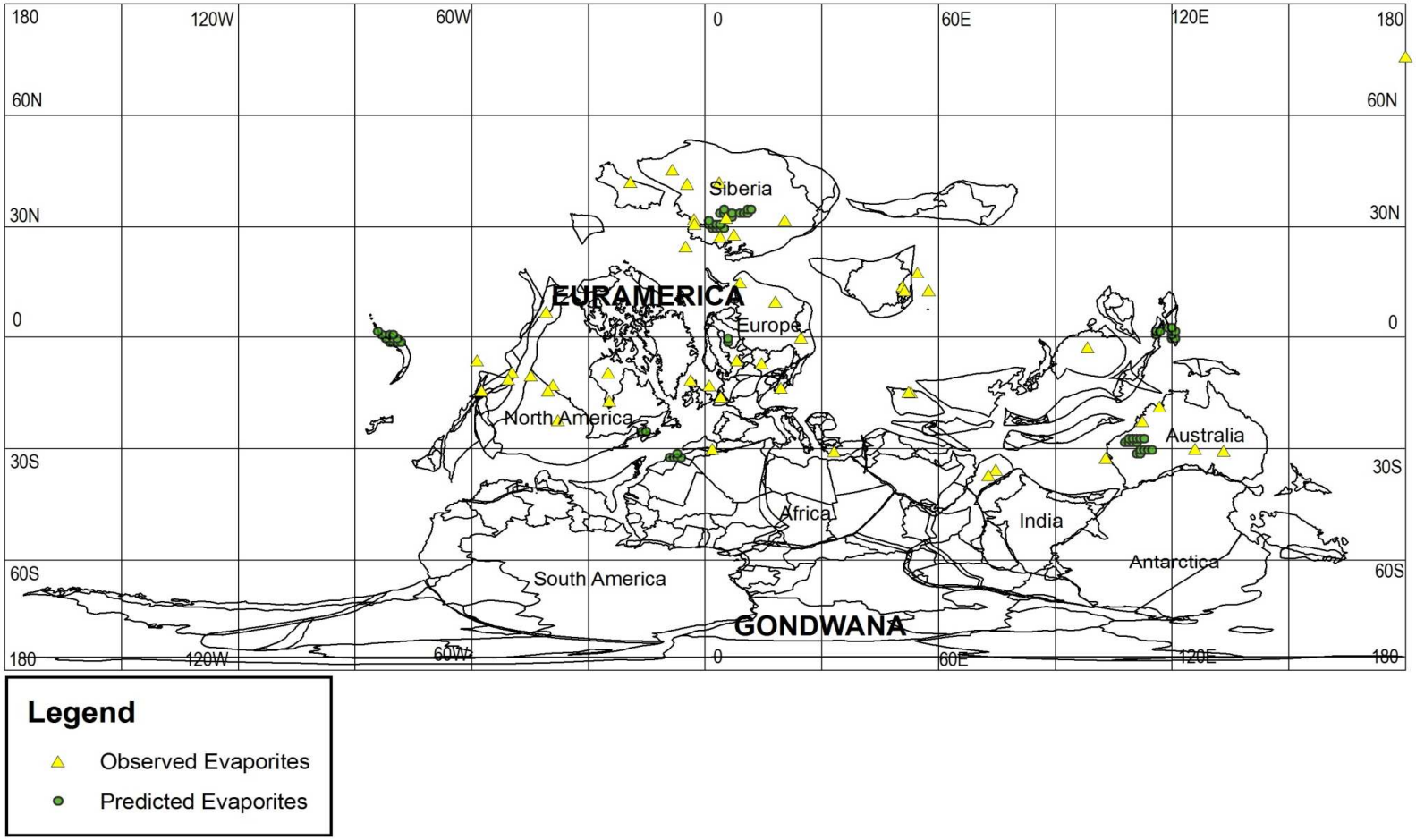

Figure 5.24: Late Devonian predicted and observed evaporites plotted out on a 360 Ma paleoreconstruction.

5.6.1.1 Statistical Analyzes for the Late Devonian

A boundary representing the edge of the continental lithosphere for the Late Devonian was mapped and in Figure 5.25 is represented by a 5°x5° set of grid cells. For the Late Devonian, 1162 grid cells were obtained. 14 of these 5°x5° grid cells contained localities for the predicted evaporites. This represents 1.20% of the continental grid cells (Figure 5.26). 39 grid cells contained observed evaporite localities (Figure 5.27). 2 grid cells contained both predicted and observed evaporite localities which are designated as "hits" (Figure 5.28). The variables used in the statistical analysis for the Late Devonian are given in Table 5.1. According to the statistical procedure outlined in section 2.4, since the expected number of hits was 1.50 and the observed number of hits was 2, the probability that the number of hits is due to a random process is 0.069. This suggests that the observed hits are random and that the alternative hypothesis fails.

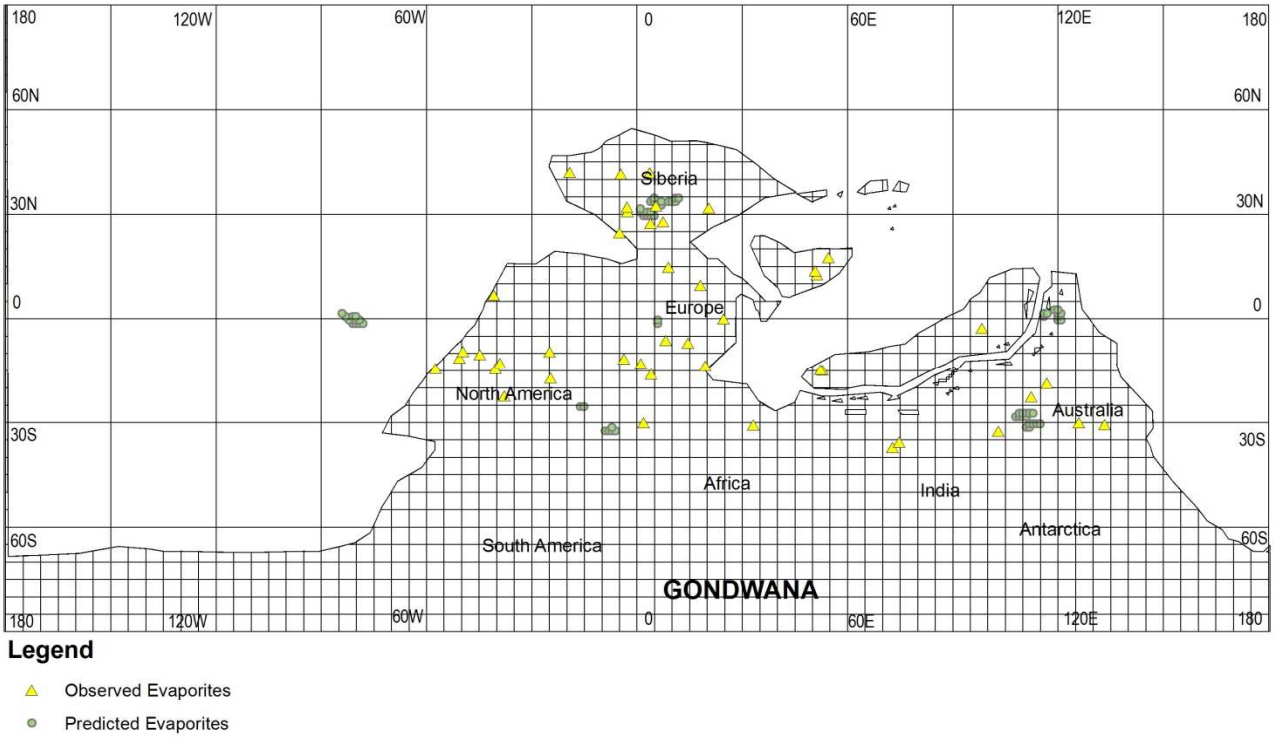

Figure 5.25: This map shows the 5°x5° latitude- longitude grids for the Late Devonian time period.

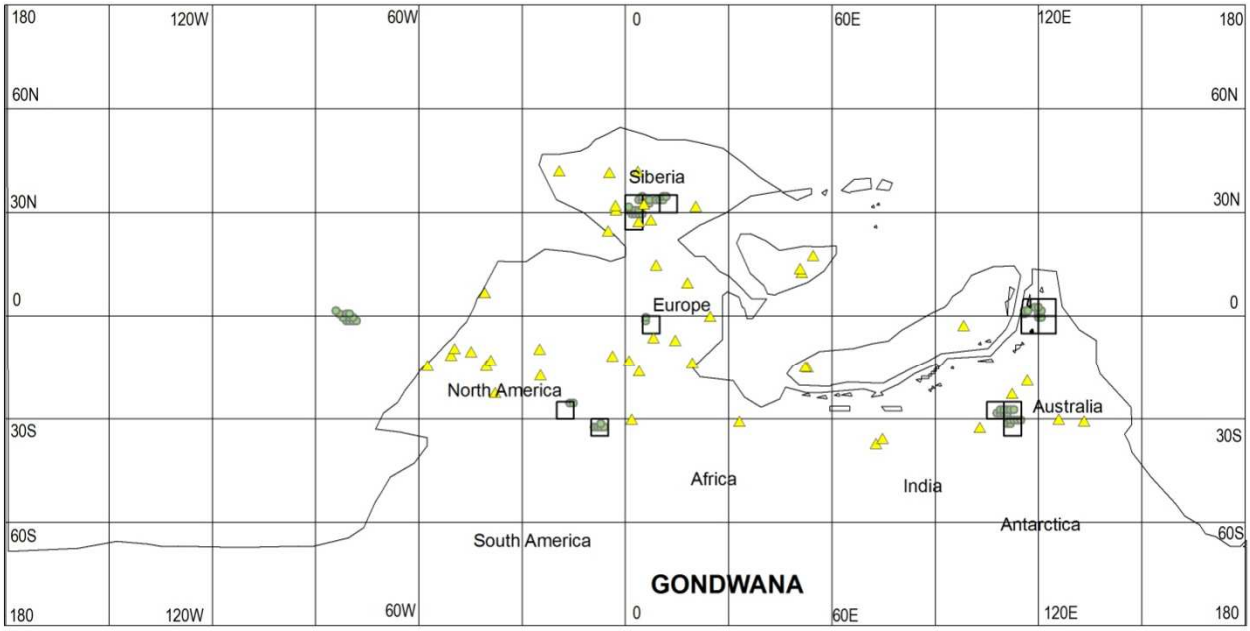

Figure 5.26: This map shows the 5°x5° latitude- longitude grids for the Late Devonian predicted evaporite localities.

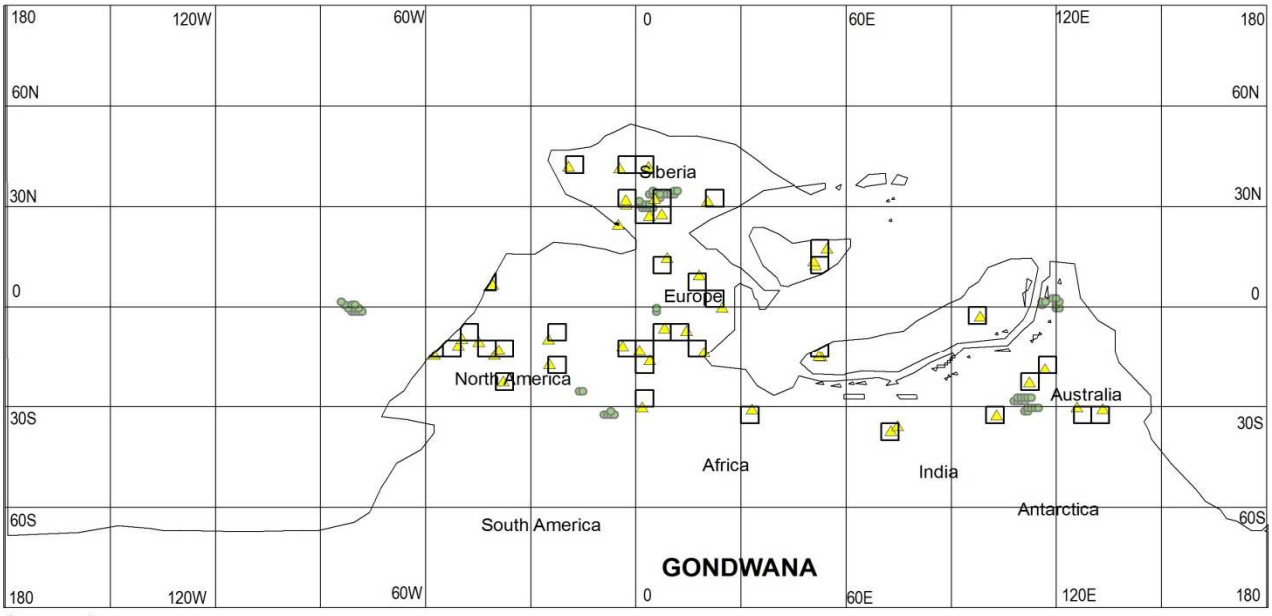

Figure 5.27: This map shows the 5°x5° latitude- longitude grids for the Late Devonian observed evaporite localities.

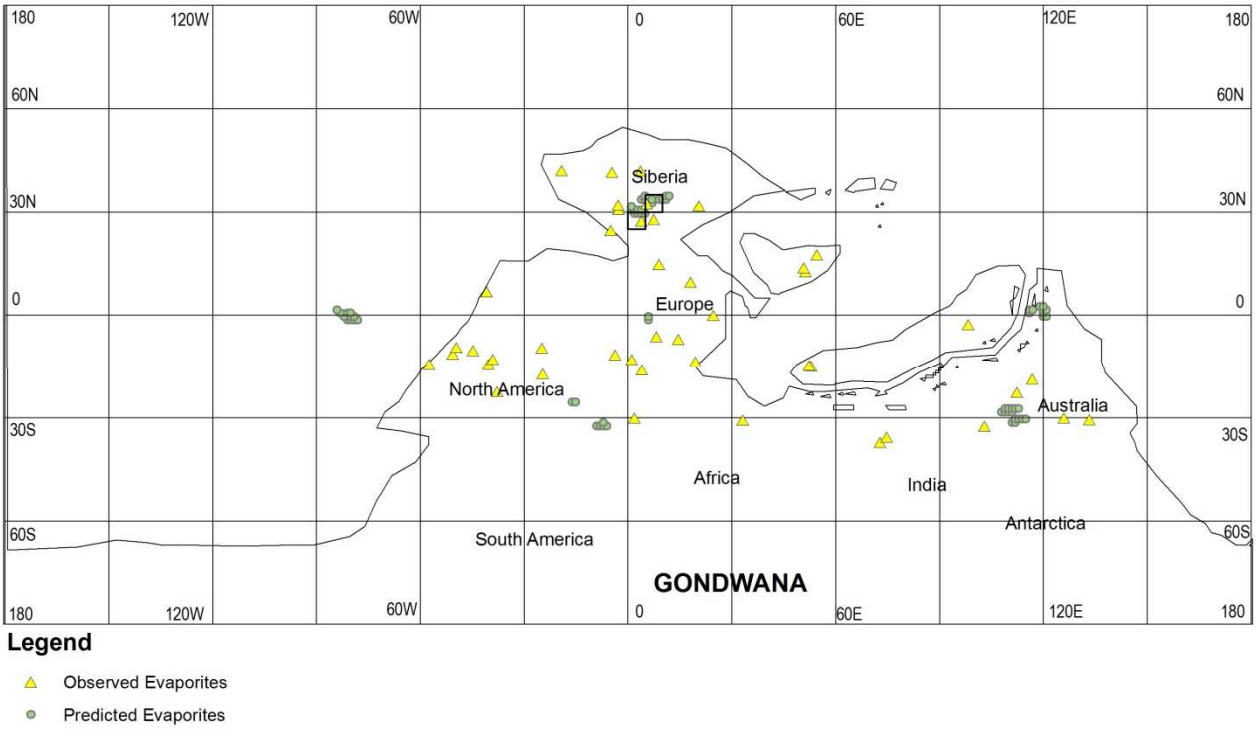

Figure 5.28: This map shows the "hits" obtained for the Late Devonian.

5.7 Siluro-Devonian (400 Ma)

5.7.1 Siluro-Devonian Evaporites

During the Siluro-Devonian time period, the continents were clustered in the southern hemisphere forming the continent Gondwana. The geographic distribution (Figure 5.29) of predicted evaporites was obtained by intersecting the Evaporite Climate Envelope with precipitation and temperature estimates for the Siluro-Devonian. The predicted evaporites mainly plotted out in the southern hemisphere between 0- 30° south latitude. A total of 467 1°x1° localities fell within the Evaporite Climate Envelope for the Siluro-Devonian. The predicted evaporite localities occur in northern Gondwana and in central North America (Figure 5.29).

The geographic distribution of actual (observed) evaporite localities was obtained from a compilation by Boucot et al (in press). Siluro-Devonian evaporites occur in Siberia, North America and in northern Gondwana. A total of 45 observed evaporites are plotted on Figure 5.30.

"Hits" are observed in central North America and northwest Gondwana (Figure 5.31). "Misses" are observed in Gondwana, parts of central North America and Siberia.

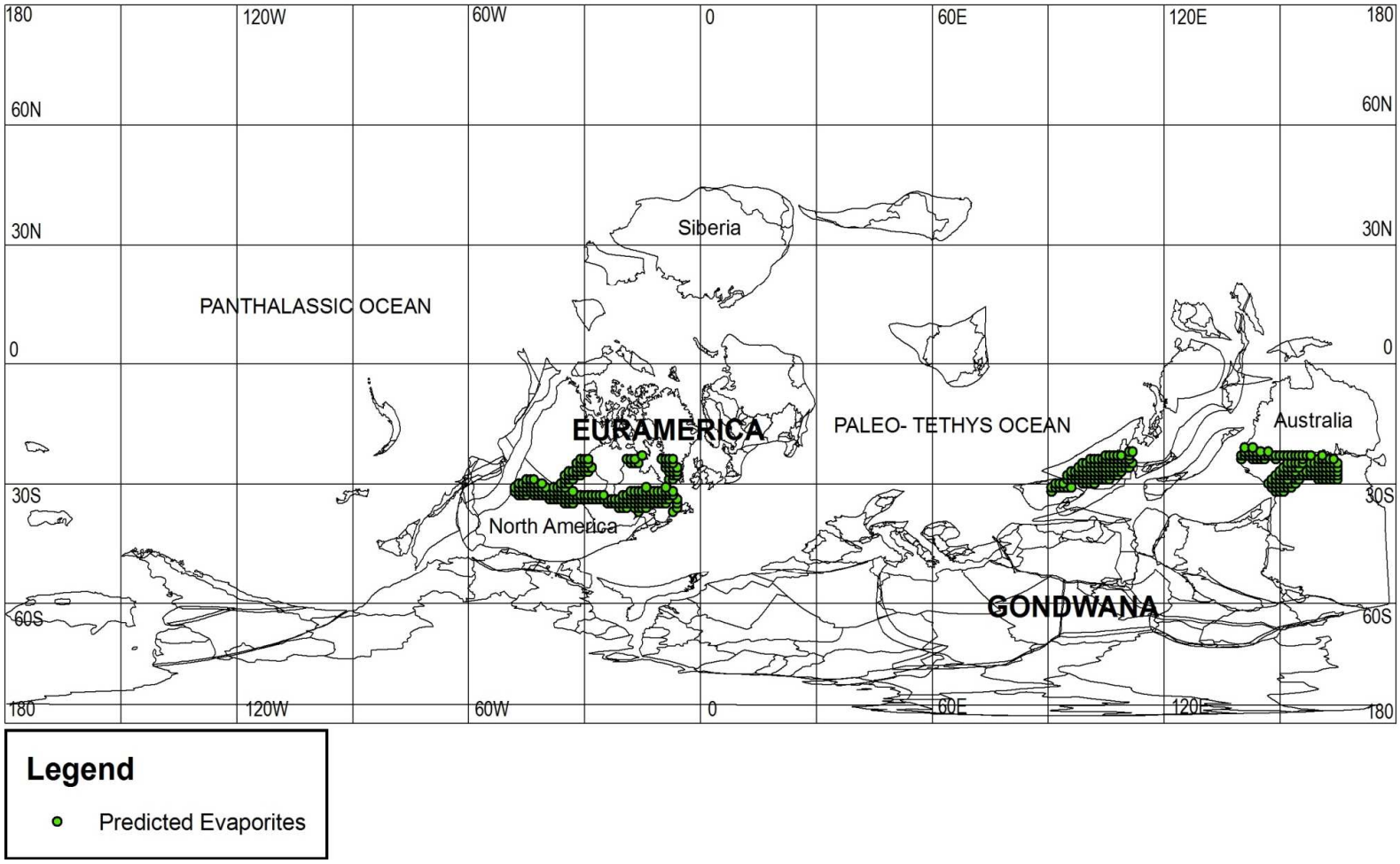

Figure 5.29: Siluro-Devonian predicted evaporites plotted out on a 400 Ma paleoreconstruction.

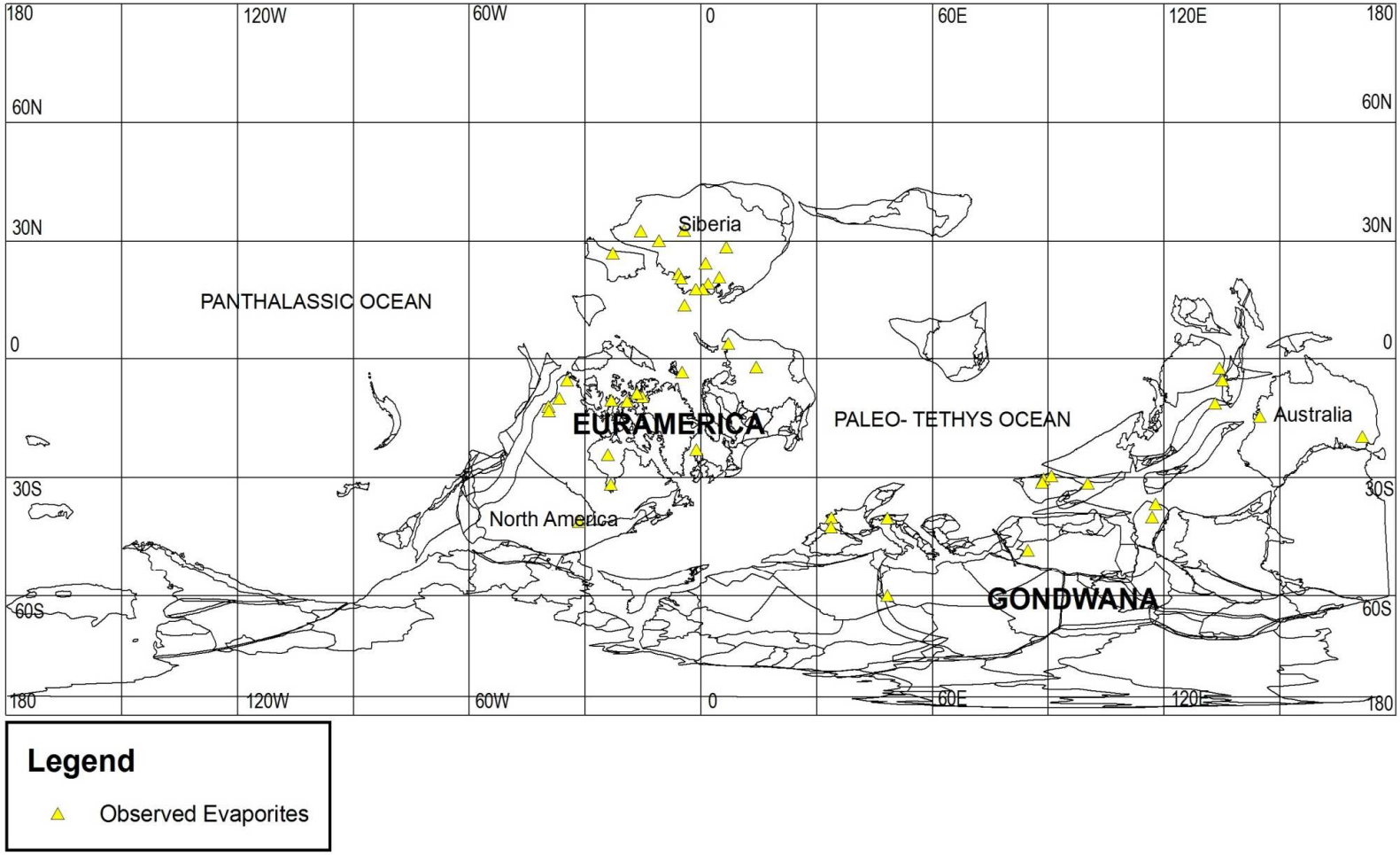

Figure 5.30: Siluro-Devonian observed evaporites plotted on a 480 Ma paleoreconstruction.

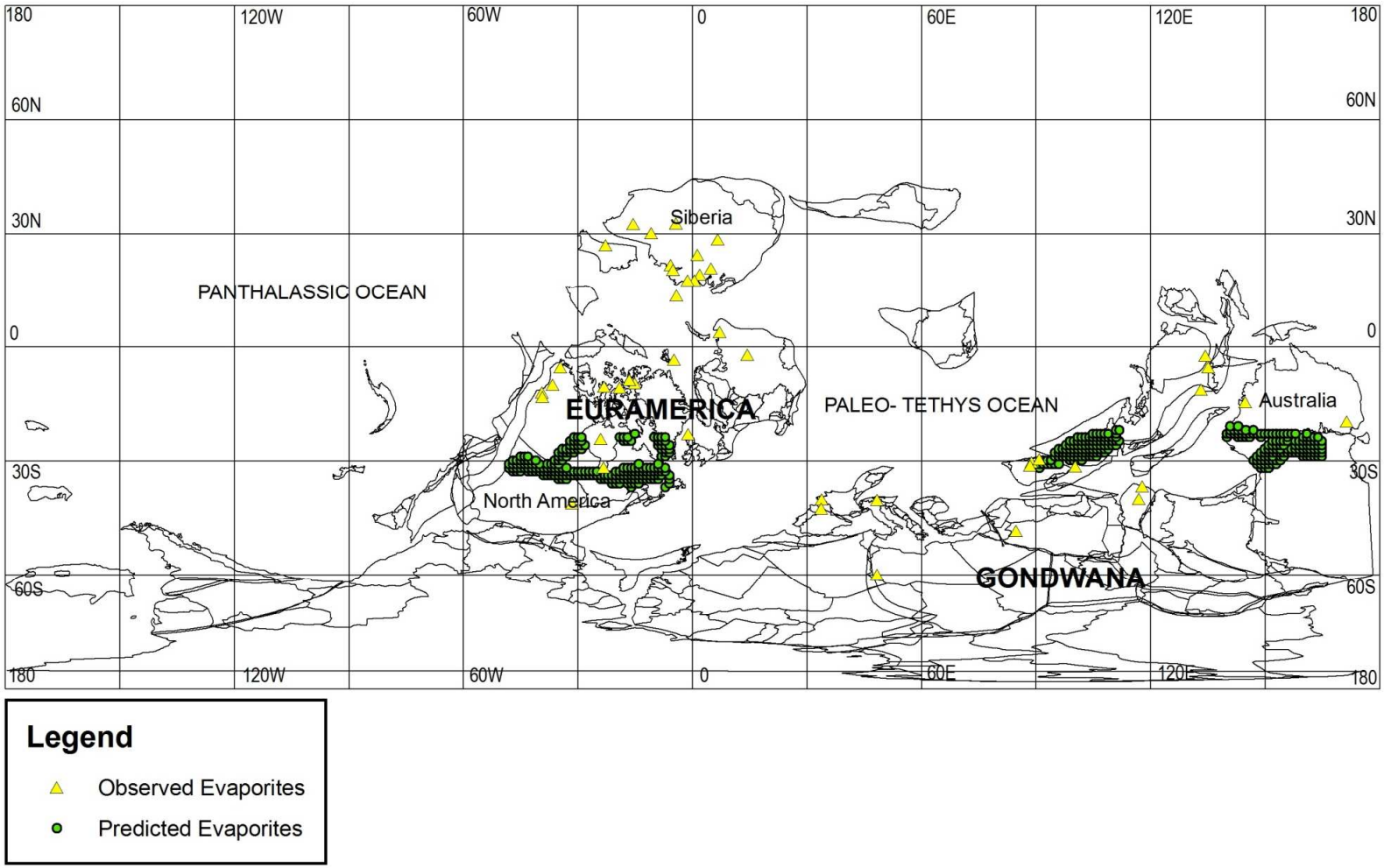

Figure 5.31: Siluro-Devonian predicted and observed evaporites plotted on a 400 Ma paleoreconstruction.

5.7.1.1. Statistical Analyzes for the Siluro-Devonian

A boundary representing the edge of the continental lithosphere for the Siluro-Devonian was mapped and in Figure 5.32 is represented by a 5°x5° set of grid cells. For the Siluro-Devonian, 1097 grid cells were obtained. 47 of these 5°x5° grid cells contained localities for the predicted evaporites. This represents 4.28% of the continental grid cells (Figure 5.33). 35 grid cells contained observed evaporite localities (Figure 5.34). 2 grid cells contained both predicted and observed evaporite localities which are designated as "hits" (Figure 5.35). The variables used in the statistical analysis for the Siluro-Devonian are given in Table 5.1. According to the statistical procedure outlined in section 2.4, since the expected number of hits was 1.50 and the observed number of hits was 2, the probability that the number of hits is due to a random process is 0.251. This suggests that the observed hits are random and that the alternative hypothesis fails.

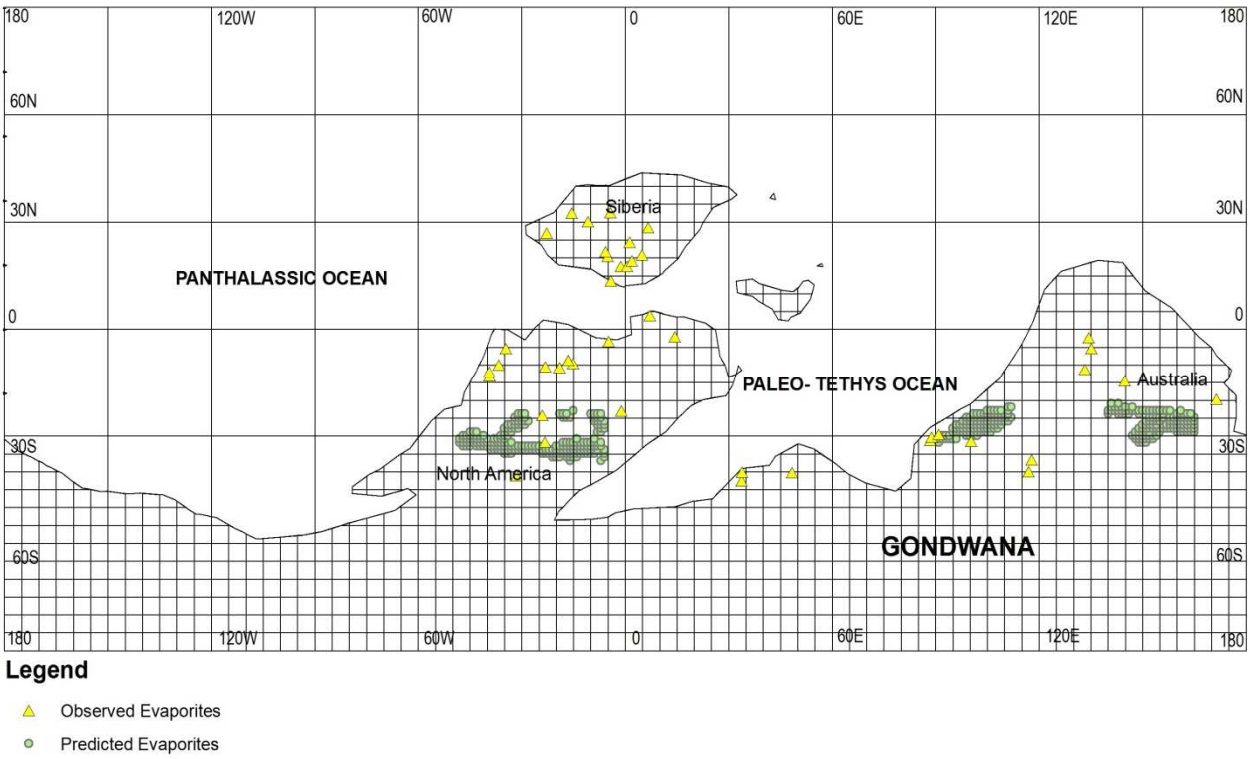

Figure 5.32: This map shows the 5°x5° latitude- longitude grids for the Siluro-Devonian time period.

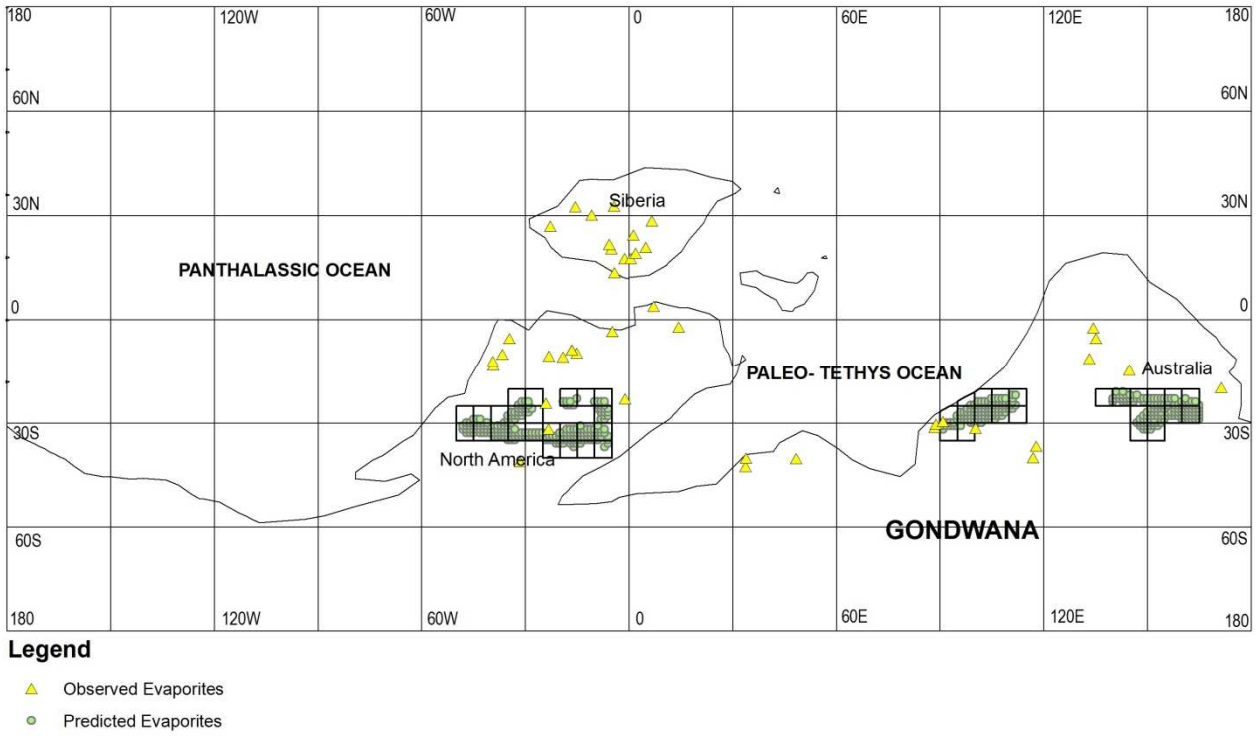

Figure 5.33: This map shows the 5°x5° latitude- longitude grids for the Siluro-Devonian predicted evaporite localities.

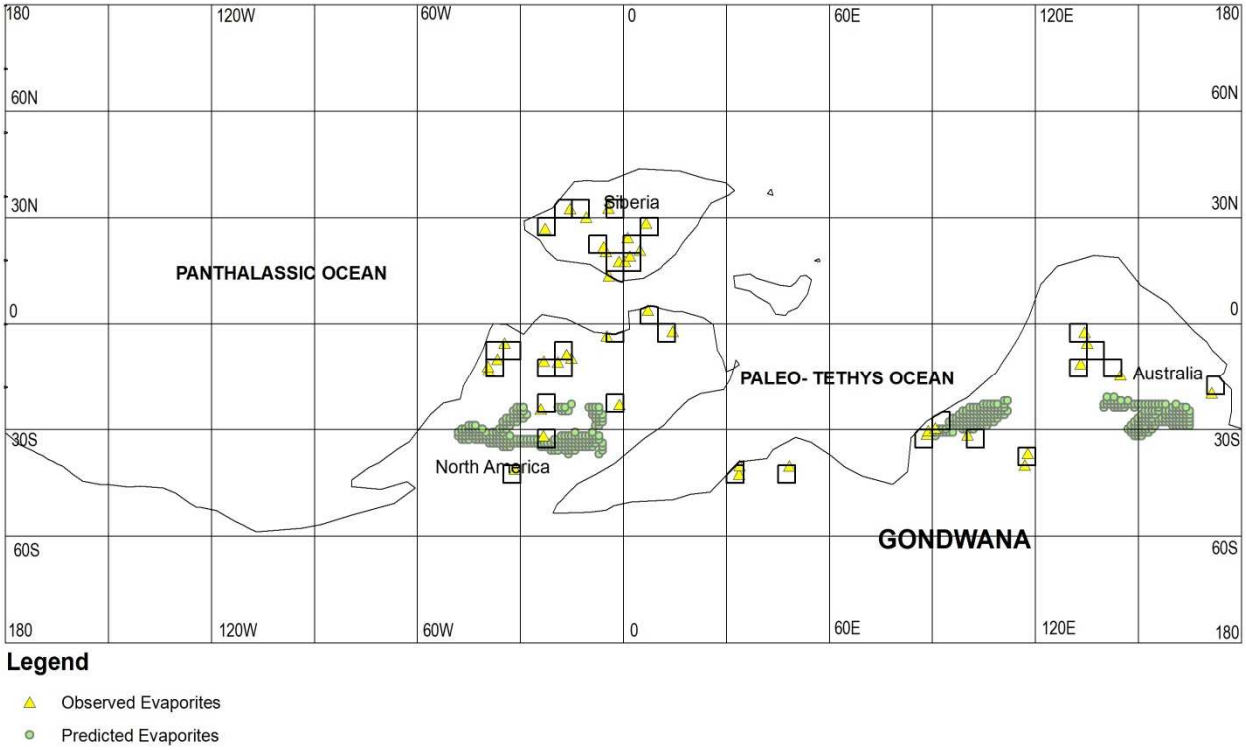

Figure 5.34: This map shows the 5°x5° latitude- longitude grids for the Siluro-Devonian observed evaporite localities.

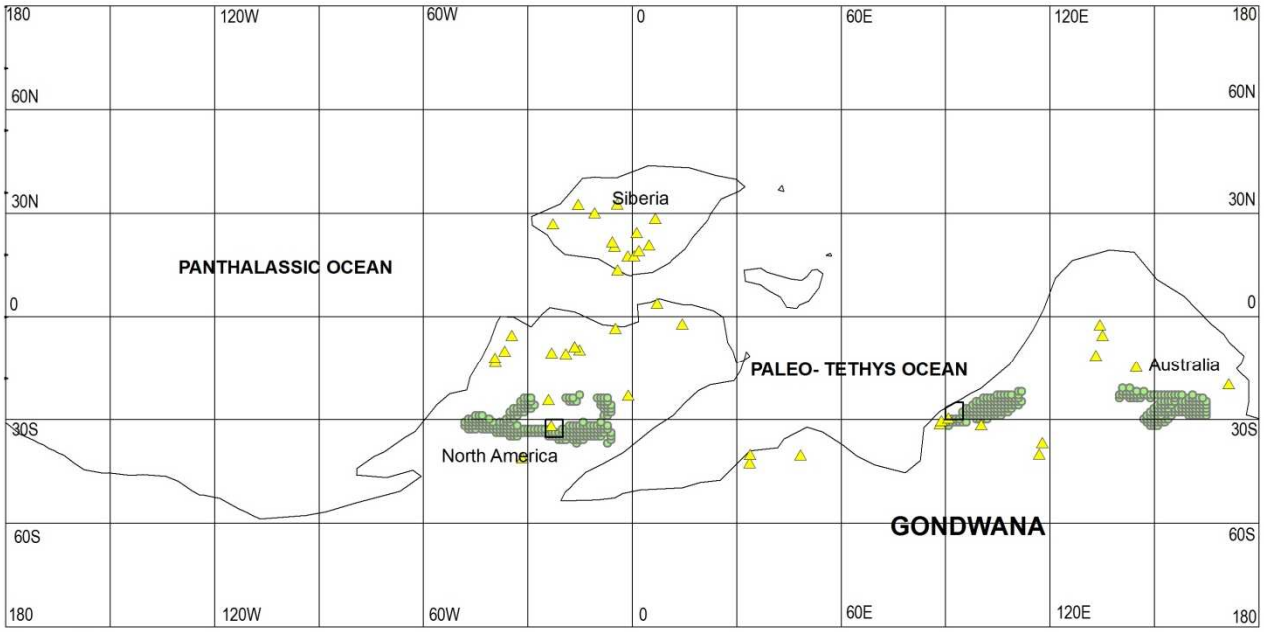

Figure 5.35: This map shows the "hits" obtained for the Siluro-Devonian.

5.8 Late Cambrian (~ 480 Ma)

5.8.1. Late Cambrian Evaporites

The Late Cambrian continents were clustered in the southern hemisphere forming the continent Gondwana. The geographic distribution (Figure 5.43) of predicted evaporites was obtained by intersecting the Evaporite Climate Envelope with precipitation and temperature estimates for the Late Cambrian. A total of 578 1°x1° localities fell within the Evaporite Climate Envelope for the Late Cambrian. The predicted evaporite localities occur in central Siberia and in central Gondwana (Figure 5.43).

The geographic distribution of actual (observed) evaporite localities was obtained from a compilation by Boucot et al (in press). Late Cambrian evaporites occur in Lauretia, central Siberia, western Gondwana and Australia. A total of 103 observed evaporites are plotted on Figure 5.44.

"Hits" are observed in Siberia only (Figure 5.45). "Misses" are observed in Lauretia, Gondwana and Australia.

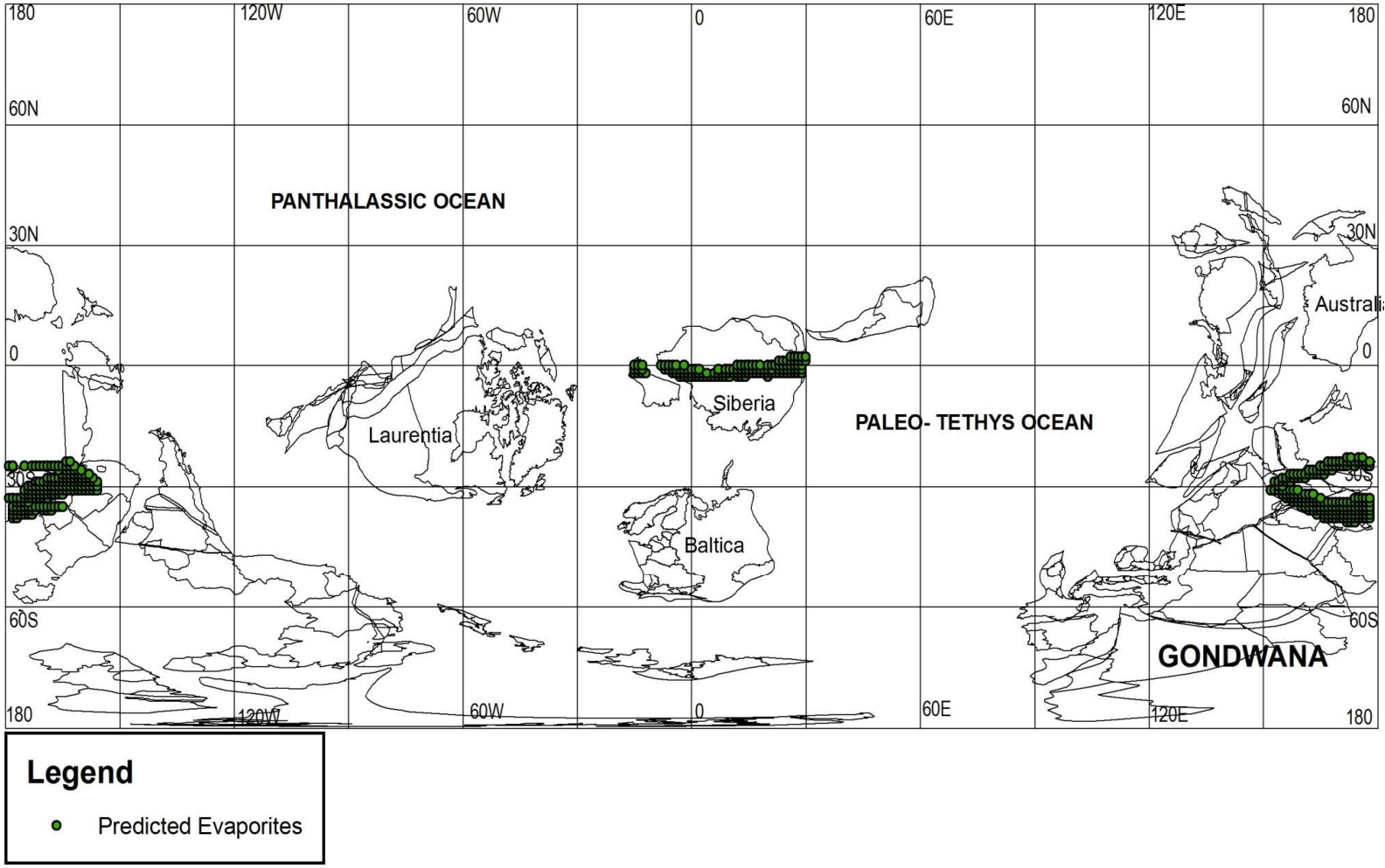

Figure 5.43: Late Cambrian predicted evaporites plotted on a 480 Ma paleoreconstruction.

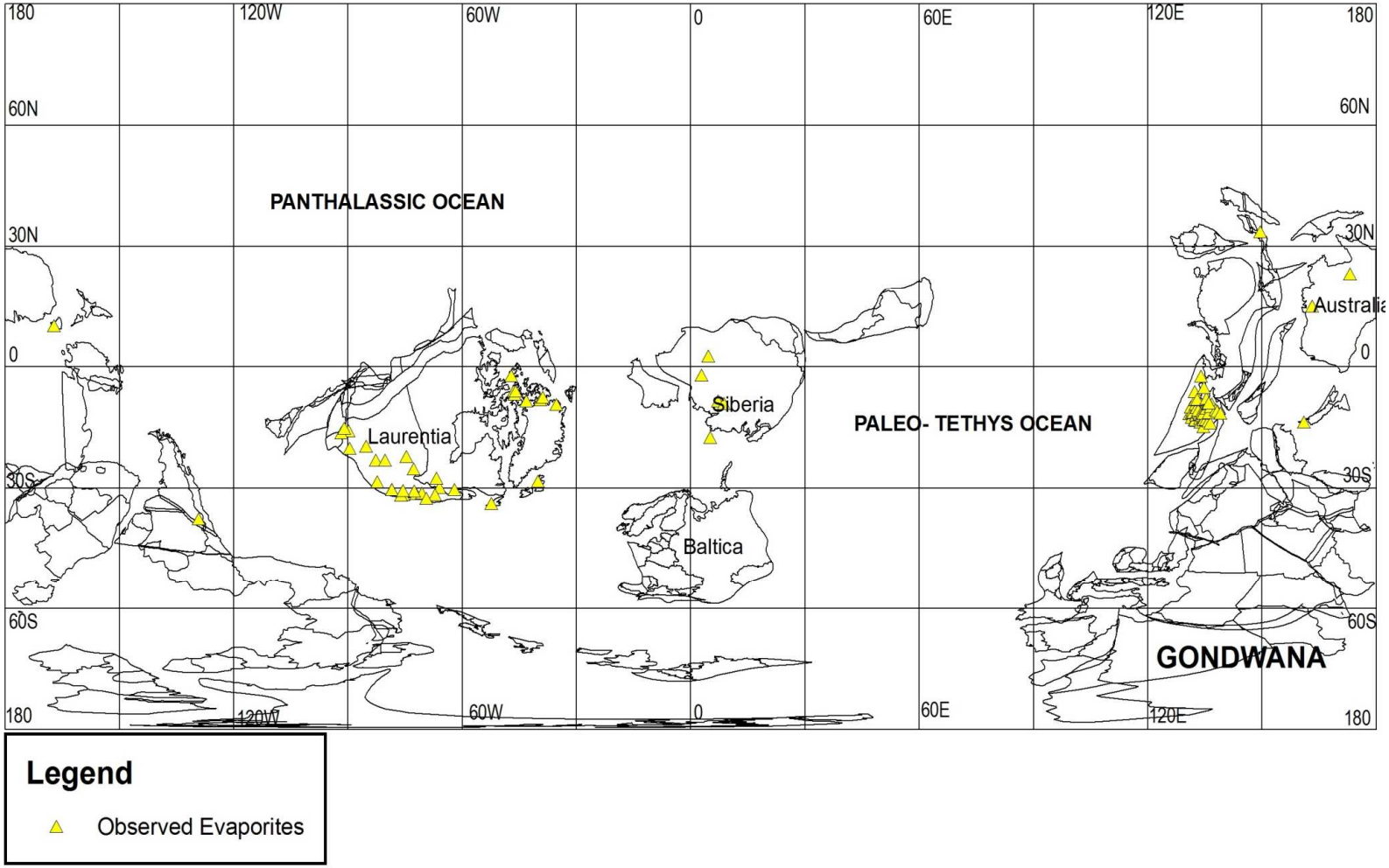

Figure 5.44: Late Cambrian observed evaporites plotted out on a 480 Ma paleoreconstruction.

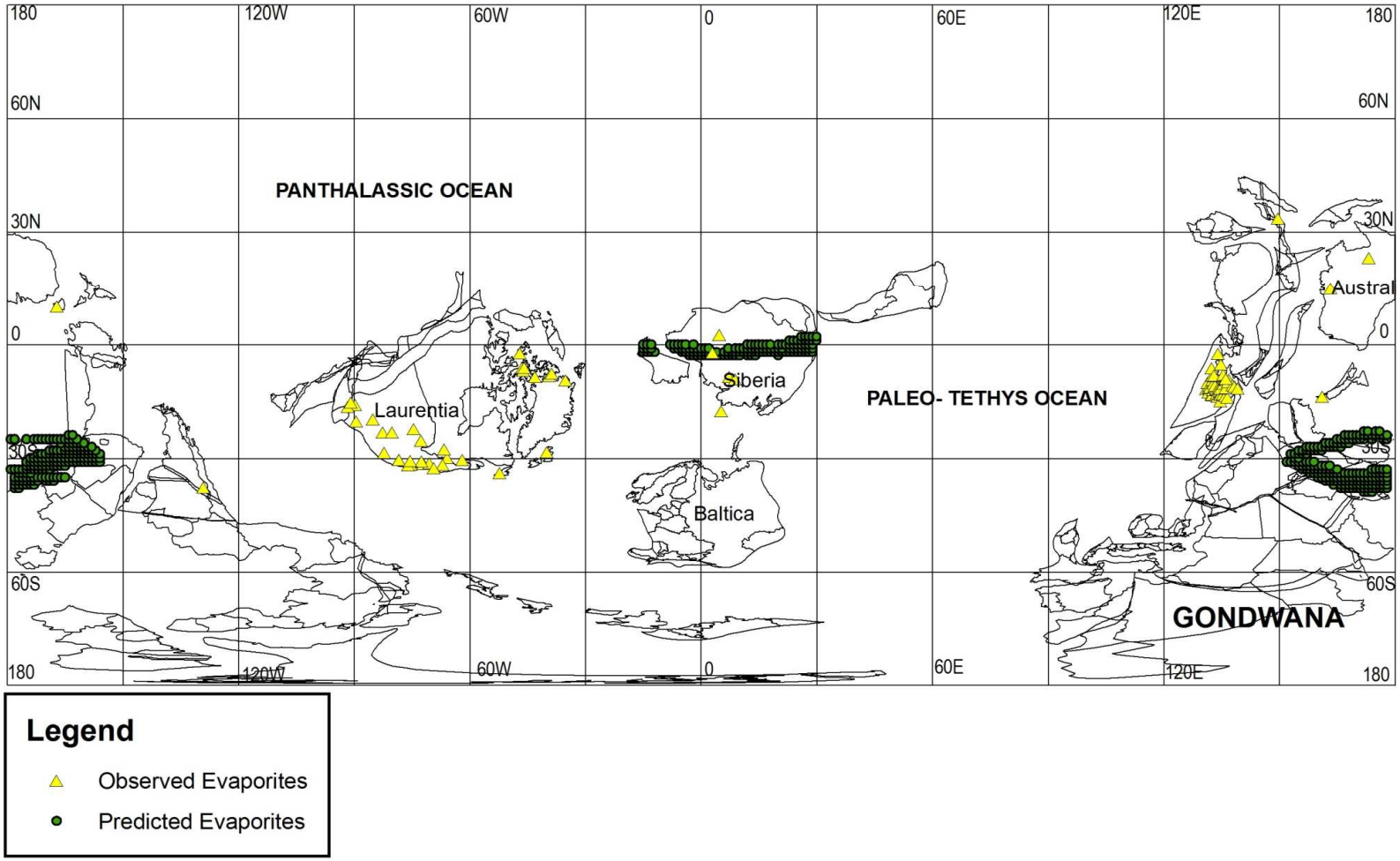

Figure 5.45: Late Cambrian predicted and observed evaporites plotted on a 480 Ma paleoreconstruction.

5.9.1.1 Statistical Analyzes for the Late Cambrian

A boundary representing the edge of the continental lithosphere for the Late Cambrian was mapped and in Figure 5.46 is represented by a 5°x5° set of grid cells. For the Late Cambrian, 1058 grid cells were obtained. 50 of these 5°x5° grid cells contained localities for the predicted evaporites. This represents 4.73% of the continental grid cells (Figure 5.47). 31 grid cells contained observed evaporite localities (Figure 5.48). 1 grid cell contained both predicted and observed evaporite localities which are designated as a "hit" (Figure 5.49). The variables used in the statistical analysis for the Late Cambrian are given in Table 5.1. According to the statistical procedure outlined in section 2.4, since the expected number of hits was 1.47 and the observed number of hits was 1, the probability that the number of hits is due to a random process is 0.338. This suggests that the observed hits are random and that the alternative hypothesis fails.

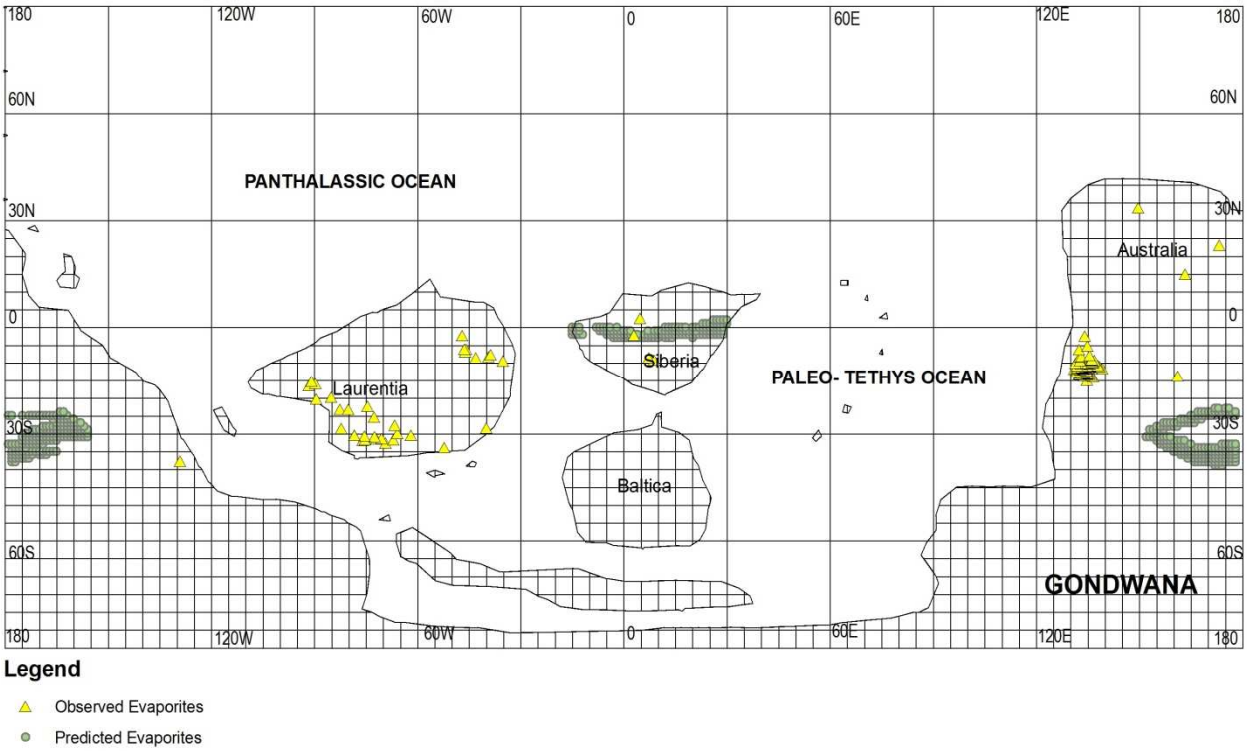

Figure 5.46: This map shows the 5°x5° latitiude- longitude grids for the Late Cambrian time period.

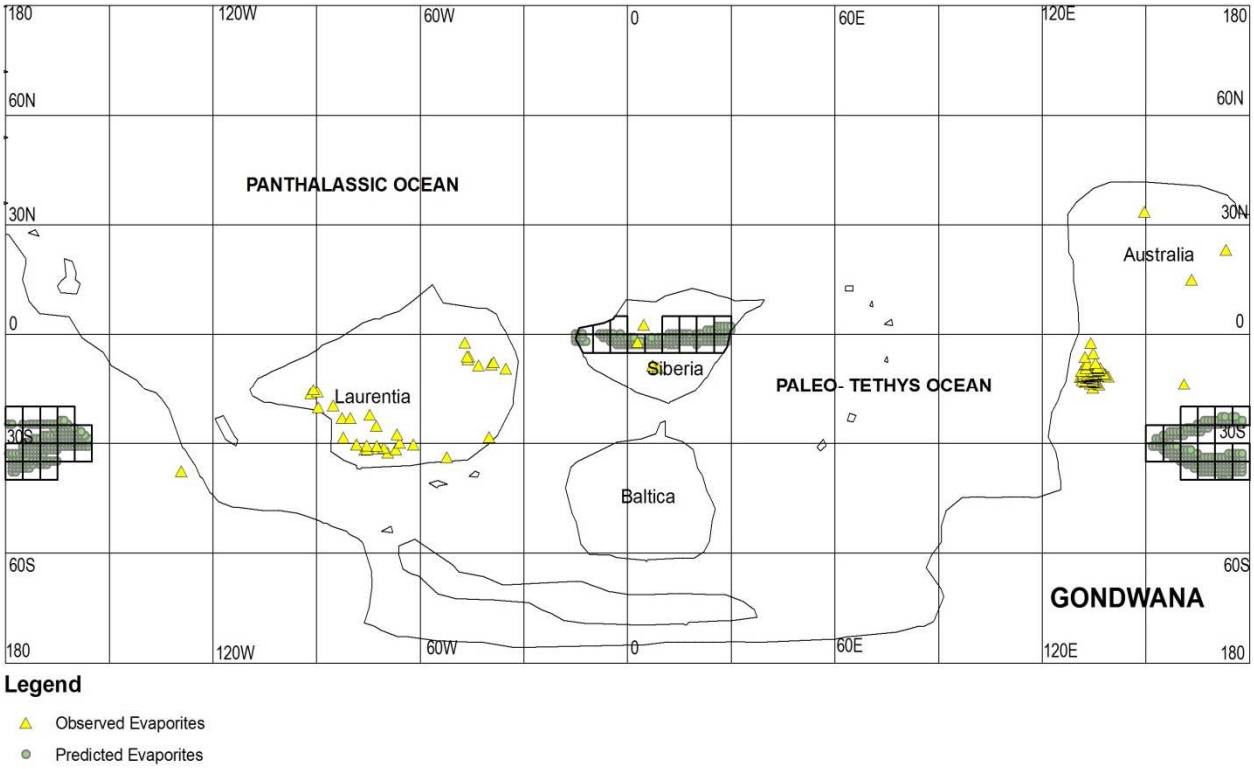

Figure 5.47: This map shows the 5°x5° latitude- longitude grids for the Late Cambrian predicted evaporite localities.

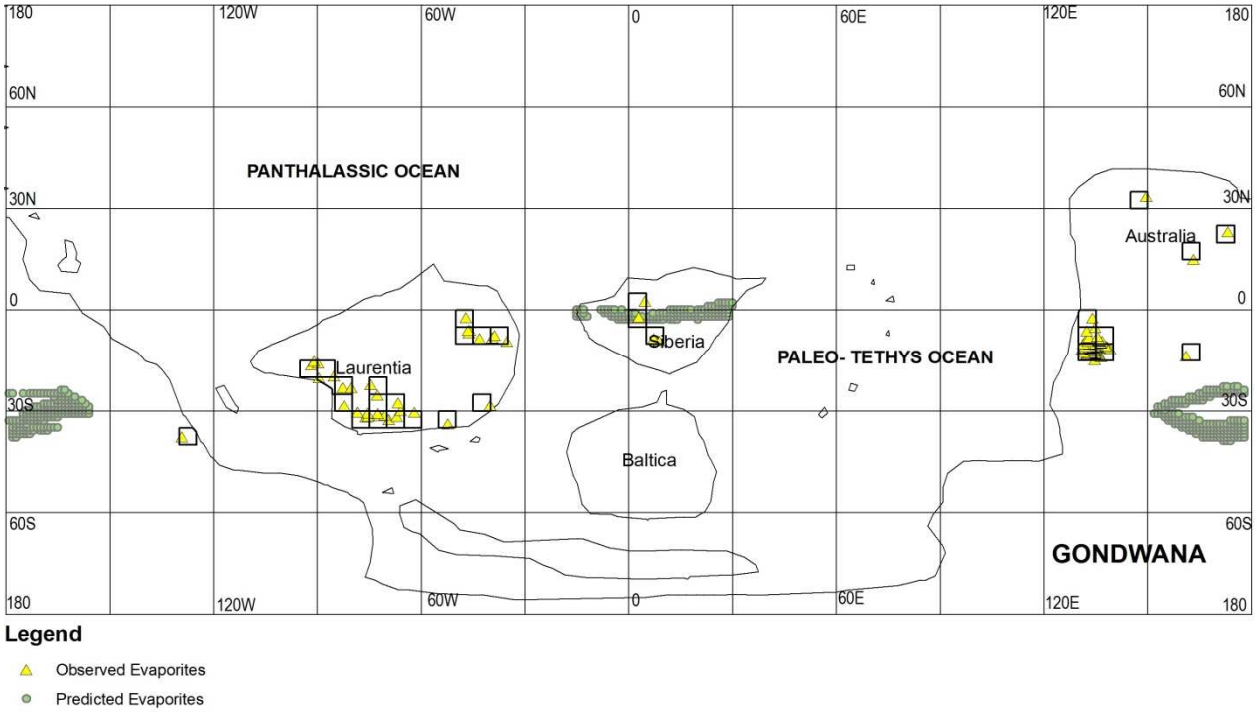

Figure 5.48: This map shows the 5°x5° latitude- longitude grids for the Late Cambrian observed evaporite localities.

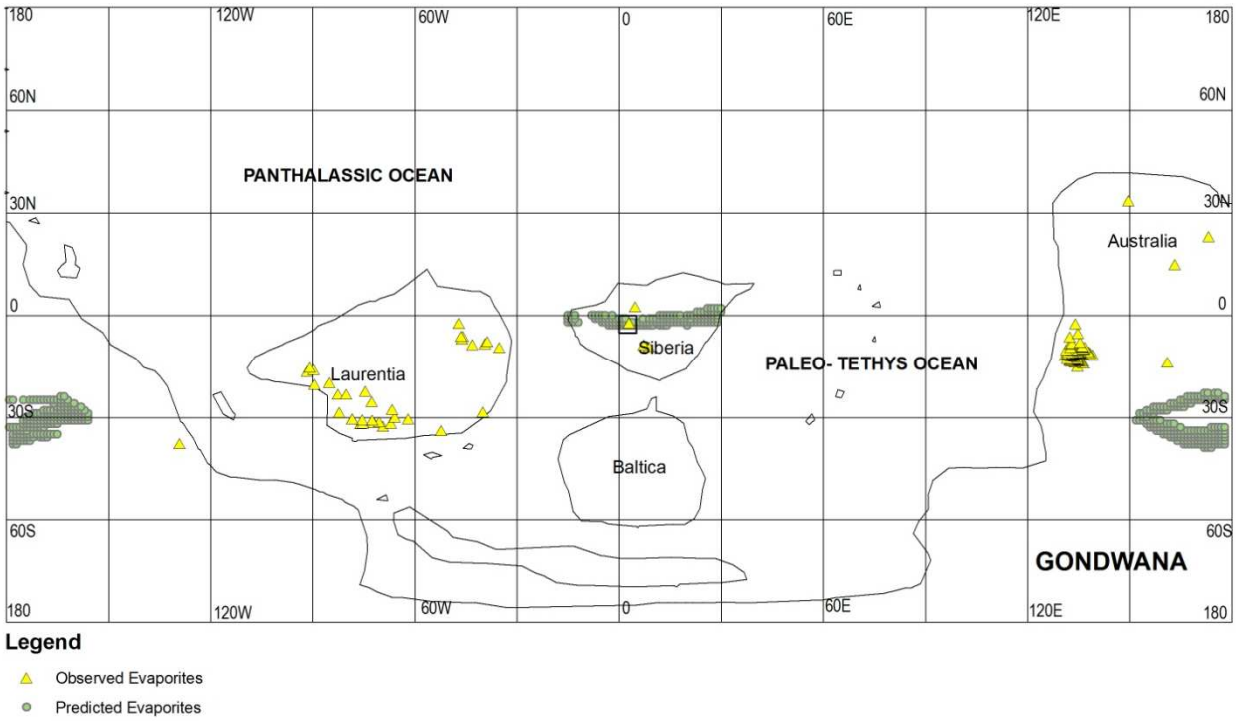

Figure 5.49: This map shows the "hits" obtained for the Late Cambrian.

Table 5.1 Statistical Calculation for the Paleozoic Era

Geologic Time Period	Total Land	Number of Predicted Evaporites	%Total Land Occupied by Predicted Evaporites	Number of Observed Evaporites	Predicted Number of Hits	Hits	Misses	Probability that Hits are Random
Permo-Triassic Boundary (250 Ma)	1162	150	12.91	30	3.87	16	14	2.52×10^{-6}
Permian (280 Ma)	1160	90	7.76	30	2.33	8	22	0.0021
Mississippian	1170	49	4.19	53	2.22	3	50	0.198
Late Devonian	1162	14	1.20	39	0.47	2	37	0.069
Siluro-Devonian	1097	47	4.28	35	1.50	2	33	0.251
Late Cambrian	1058	50	4.73	31	1.47	1	30	0.3379

CHAPTER 6

DISCUSSION AND CONCLUSION

The final chapter of this research discusses the results obtained from the prediction of the location of evaporites through geologic time, the match (hits) between the predicted and the observed evaporites for all three geologic Eras (Cenozoic, Mesozoic and Paleozoic) and an analysis of the goodness of fit between the predicted and the observed evaporites. The question raised in chapter 2 "What is the probability that the observed number of hits is due to a random process?" will be answered for each time period. The climate envelope model which was tested by comparing the predictions with the distribution of ancient evaporites will also be discussed.

Overall, the statistical results show that the observed number of hits obtained for each time period was not due to a random process. Exceptions are observed in the Paleozoic era where the Mississippian, Late Devonian, Siluro-Devonian and the Late Cambrian evaporites showed that the match between the predicted and the observed evaporites was random. Reasons for this exception will be discussed.

6.1. Analysis of Results obtained for the Cenozoic Era

6.1.1. Late Miocene Results

Climate of the late Miocene has been recorded as being mainly cool with high latitude climates being suggested to have been at their coolest. The equatorial regions however, recorded

a warmer climatic trend than observed at the high latitudinal regions (Frakes, 1979). This climatic trend reflects in the distribution of both the predicted and the observed evaporites.

The predicted evaporites could be found distributed close to the equatorial region (0-45°N and 0- 15°S). The observed evaporites were also distributed between 0- 45°N and S latitude (Appendix C). Both the predicted and the observed evaporites occur in regions that recorded warm climates for the Late Miocene. The average temperature and precipitation values recorded for the Late Miocene from the Climate Envelope were 17.25°C and 7.39 cm/month respectively (Figure 6.1 and Figure 6.2). "Hits" were mainly observed in North Africa (desert regions), Arabia and in parts of West Asia. The number of hits obtained for this time period was 15 (see Chapter 3).

A statistical calculation of the probability that the number of hits observed is due to a random process is 3.55×10^{-6}, which is a really low probability and indicates that the number of hits is not due to a random process. The null hypothesis predicts that 3.52 or 6.07% of the observed evaporites should be hits. However 15 hits were obtained which makes up 17.24% of the total number of predicted grid localities and 4 times the number of hits that were expected based on the "area" occupied by the predicted evaporites. This probability shows that the Late Miocene "hits" have a 99% chance of being due to a non- random process which is significant and implies that the null hypothesis has failed. The results obtained for the Late Miocene shows that there is a reasonably good fit between the predicted evaporite localities and the observed evaporite localities.

6.1.2. Oligocene Results

The climate of the Oligocene period was mainly characterized by low temperatures and during the Early and Late Oligocene was truncated by two warming events (Frakes, 1979). The average temperature and precipitation obtained from the Climate Envelope was 20.52°C and 2.39 cm/month respectively (Figure 6.1 and Figure 6.2). The Oligocene predicted evaporites were distributed close to the equatorial region in a similar manner to the Late Miocene evaporites and could mainly be found between 0- 45°N and S latitude. The observed evaporite localities could also be found between 0- 45°N latitude with a few evaporites distributed within the 0- 45°S latitude (Appendix C).

The hits for this time period as mentioned in Chapter 3 could mainly be seen in North Africa and in the central parts of Eurasia. The hits obtained for the Oligocene time period specifically in Eurasia could mainly be observed on the lee side of the Tibetan Plateau. The uplift of the Tibetan Plateau during the Late Cenozoic is believed to have had a profound effect on atmospheric circulation leading to an overall global cooling (Raymo et al, 1988; 1991; 1992).

A statistical calculation of the probability that the number of hits observed is due to a random process is 6.50×10^{-7}, which is a really low probability and indicates that the number of hits is not due to a random process. The null hypothesis predicts that 3.04 or 6.76% of the observed evaporites should be "hits". However 15 hits were obtained which makes up 15.46% of the total number of predicted grid localities and 4 times the number of hits that were expected based on the "area" occupied by the predicted evaporites. This probability shows that the Oligocene "hits" have a 99% chance of being due to a non- random process which is significant and implies that the null hypothesis has failed. The results obtained for the Oligocene shows that

there is a reasonably good fit between the predicted evaporite localities and the observed evaporite localities.

6.1.3. Middle Eocene Results

The final epoch considered in this research for the Cenozoic Era is the Middle Eocene. The Eocene climate was mainly characterized by strong seasonal wet conditions which were later succeeded by cool and humid conditions in the middle Eocene (Dingle et al, 1998). Climate during the Eocene was much cooler than modern temperatures (Pearson et al, 2006). Majority of the Middle Eocene predicted and observed evaporites could be found distributed between 0-45°N latitude. The predicted evaporites obtained from the Climate Envelope for this time period were relatively few with a count of 485 as compared to the Oligocene that had a count of 1049 and the Late Miocene that had a count of 1243 however, the average temperature obtained from the Climate Envelope was 18.97°C and average precipitation was 0.59 cm/month showing conditions that are highly favorable for the formation of evaporites (Figure 6.1 and Figure 6.2).

A statistical calculation of the probability that the number of hits observed is due to a random process is 2.17×10^{-8}, which is a really low probability and indicates that the number of hits is not due to a random process. The null hypothesis predicts that 1.09 or 2.48% of the observed evaporites should be "hits". However 11 hits were obtained which makes up 10 times the number of hits that were expected based on the "area" occupied by the predicted evaporites. This probability shows that the Middle Eocene "hits" have a 99% chance of being due to a non-random process which is significant and implies that the null hypothesis has failed. The results

obtained for the Middle Eocene shows that there is a reasonably good fit between the predicted evaporite localities and the observed evaporite localities.

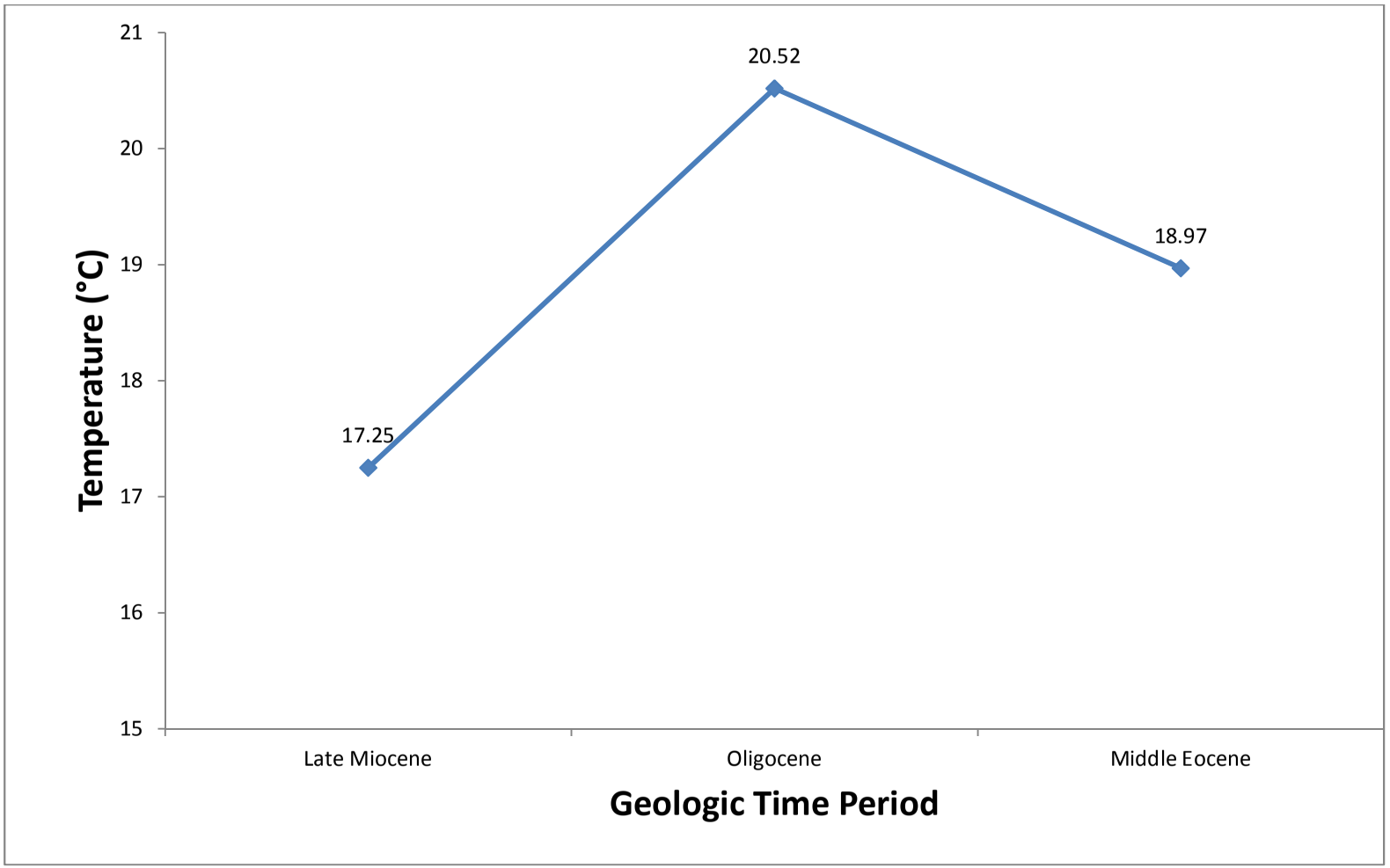

Figure 6.1: This graph shows the average temperatures recorded across the Cenozoic Era. Temperatures fluctuated throughout the Cenzoic Era with the lowest average temperature being for the Climate Envelope being recorded for the Late Miocene. The highest average temperature is observed for the Oligocene which experienced two warming events.

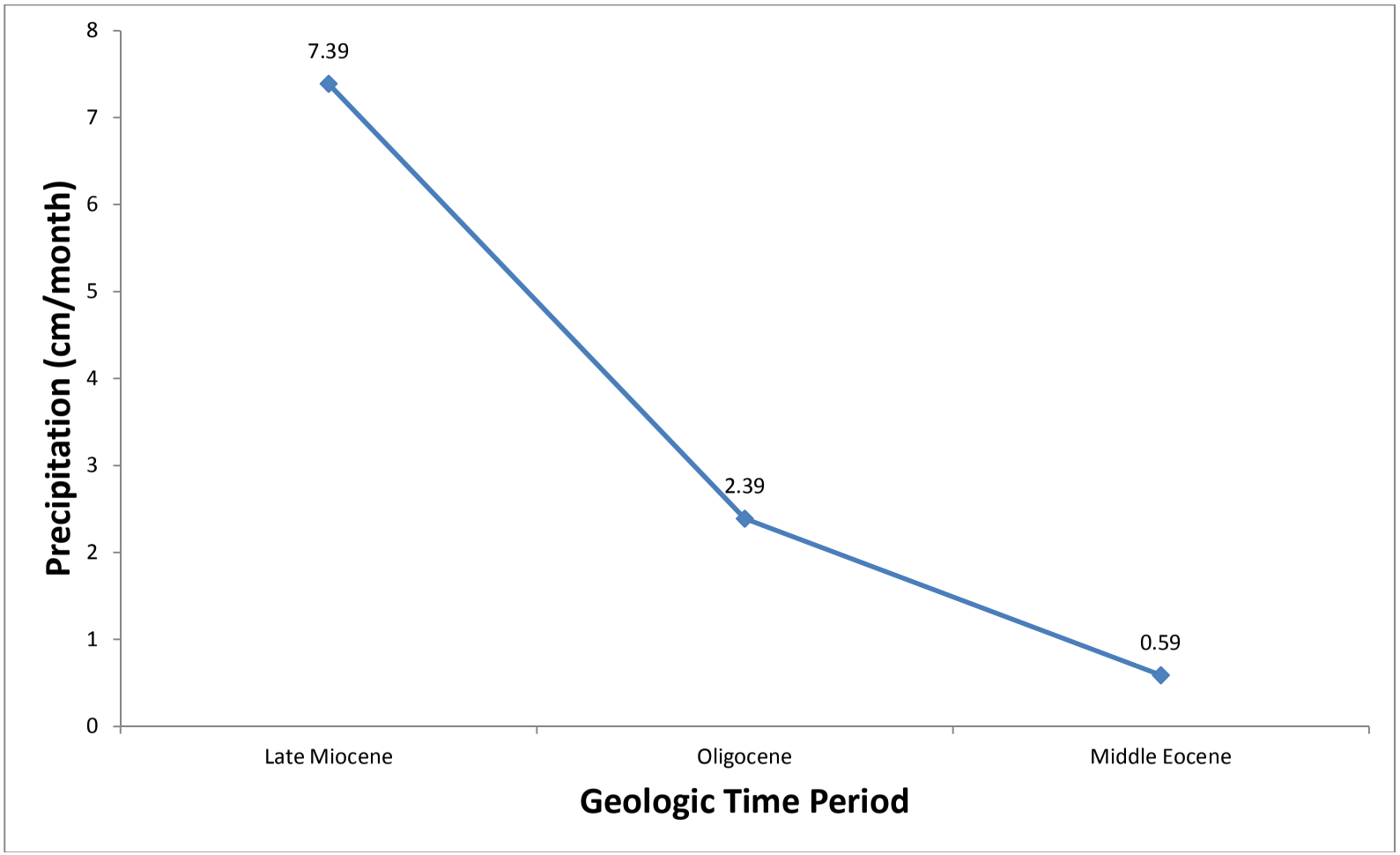

Figure 6.2: This graph shows the average precipitation in cm/month across the Cenozoic Era. Precipitation decreased across time periods with the lowest average precipitation being recorded for the Middle Eocene.

6.2. Analysis of Results obtained for the Mesozoic Era

6.2.1 Cretaceous Results

6.2.1.1 Cretaceous/Tertiary Boundary Results

The Cretaceous/Tertiary Boundary climate was characterized by warm conditions. Late Cretaceous global climate was warmer than today's climate (Scotese, 2001). The predicted and the observed evaporite localities were between 0- 40°N and 0-55°S. The average temperature and precipitation obtained for this time period were 20.41°C and 0.66cm/month respectively (Figure 6.3 and 6.4). This reflects in the distribution of evaporite localities for this time period.

A statistical calculation of the probability that the number of hits observed is due to a random process is 0.0067, which is a low probability and indicates that the number of hits is not due to a random process. The null hypothesis predicts that 0.77 or 1.87% of the observed evaporites should be hits. However 4 hits were obtained which is 5 times the number of hits that were expected based on the "area" occupied by the predicted evaporites. This probability shows that the Cretaceous/Tertiary Boundary "hits" have a 99.32% chance of being due to a non-random process which is significant and implies that the null hypothesis has failed. The results obtained for the Cretaceous/Tertiary Boundary shows that there is a reasonably good fit between the predicted evaporite localities and the observed evaporite localities.

6.2.1.2 Cenomanian/Turonian Results

The Late Cretaceous which encompasses the Cenomanian/Turonian had mostly warm climate. Temperatures were higher across the globe from the equator to the pole (equable climates). The global climate for the Late Cretaceous was much warmer than today's (Frakes,

1979; Scotese, 2001; Barron, 1983). This warm climate is evident in the results obtained for the Cenomanian/Turonian time period. The average temperature and precipitation for the Cenomanian/Turonian was 21.32°C and 0.38cm/month respectively (Figure 6.3 and 6.4). The distribution of both the predicted and the observed evaporite localities was between 0- 45°N and S latitude (Appendix C).

A statistical calculation of the probability that the number of hits observed is due to a random process is 1.23×10^{-11}, which is a really low probability and indicates that the number of hits is not due to a random process. The null hypothesis predicts that 4.08 or 7.41% of the observed evaporites should be hits. However 24 hits were obtained which makes up 23.07% of the total number of predicted grid localities and 5 times the number of hits that were expected based on the "area" occupied by the predicted evaporites. This probability shows that the Cenomanian/Turonian "hits" have a 99.99% chance of being due to a non- random process which is significant and implies that the null hypothesis has failed. The results obtained for the Cenomanian/Turonian shows that there is a reasonably good fit between the predicted evaporite localities and the observed evaporite localities.

6.2.1.3 Aptian/Albian Results

The Aptian/Albian was characterized by climate which was identical to that of the Cenomanian/Turonian. Climate for this age was mostly warm and this warmth was distributed globally (Frakes, 1979; Scotese, 2001). This warm climatic trend is evident in the results obtained for this time period. The average temperature and precipitation for the Aptian/Albian was 22.64°C and 0.20 cm/month respectively (Figure 6.3 and 6.4). The distribution of the

predicted evaporite localities for this time period was similar to that of the Cenomanian/Turonian with majority of the evaporite localities in South America and Africa. The distribution of the observed evaporite localities were also similar to that of the Cenomanian/Turonian with the overall distribution of both the predicted and the observed evaporites being between 0-45°N and 0-50°S latitude (Appendix C).

A statistical calculation of the probability that the number of hits observed is due to a random process is 6.28×10^{-8}, which is a really low probability and indicates that the number of hits is not due to a random process. The null hypothesis predicts that 4.55 or 6.41% of the observed evaporites should be hits. However 20 hits were obtained which makes up 21.74% of the total number of predicted grid localities and 4 times the number of hits that were expected based on the "area" occupied by the predicted evaporites. This probability shows that the Albian/Aptian "hits" have a 99% chance of being due to a non- random process which is significant and implies that the null hypothesis has failed. The results obtained for the Albian/Aptian shows that there is a reasonably good fit between the predicted evaporite localities and the observed evaporite localities.

6.2.1.4 Barremian/ Berriasian Results

The Barremian/Berriasian age is known to have been characterized by mostly warm and humid conditions (Frakes, 1979). The average temperature and precipitation for the Barremian/Berriasian was 18.92°C and 0.37 cm/month respectively (Figure 6.3 and 6.4). This reflects in the distribution of both the predicted and the observed evaporite localities which were between 0- 45°N and S latitude (Appendix C).

A statistical calculation of the probability that the number of hits observed is due to a random process is 3.63×10^{-7}, which is a low probability and indicates that the number of hits is not due to a random process. The null hypothesis predicts that 6.59 or 9.98% of the observed evaporites should be hits. However 23 hits were obtained which makes up 16.79% of the total number of predicted grid localities and 3 times the number of hits that were expected based on the "area" occupied by the predicted evaporites. This probability shows that the Barremian/Berriasian "hits" have a 99% chance of being due to a non- random process which is significant and implies that the null hypothesis has failed. The results obtained for the Barremian/Berriasian shows that there is a reasonably good fit between the predicted evaporite localities and the observed evaporite localities.

6.2.3 Jurassic Results

6.2.3.1 Late Jurassic Results

Climate of the Late Jurassic period was known to be very warm and moist with an abundant distribution of evaporites and possibly much drier than the Triassic (Frakes, 1979). Evidence from paleontology suggests a broad zone of warm and arid climates (Beauvais, 1973). The climate of the Late Jurassic was characterized by high atmospheric CO_2 levels leading to greenhouse conditions and was also characterized by a monsoonal rainfall pattern (Weissert et al, 1996). The average temperature and precipitation for the Late Jurassic was 19.58°C and 0.32 cm/month respectively (Figure 6.3 and 6.4) reflecting the dry conditions that existed during this time period. This is evident in the distribution of evaporites for this time period. The predicted and the observed evaporites are more abundant for this time period with the highest number of

hits being recorded in the Late Jurassic. The predicted and the observed evaporites are distributed between 0- 40°N and S latitude (Appendix C).

A statistical calculation of the probability that the number of hits observed is due to a random process is 9.06×10^{-8}, which is a low probability and indicates that the number of hits is not due to a random process. The null hypothesis predicts that 10.24 or 14.02% of the observed evaporites should be hits. However 31 hits were obtained which makes up 18.45% of the total number of predicted grid localities and 3 times the number of hits that were expected based on the "area" occupied by the predicted evaporites. This probability shows that the Late Jurassic "hits" have a 99.99% chance of being due to a non- random process which is significant and implies that the null hypothesis has failed. The results obtained for the Late Jurassic shows that there is a reasonably good fit between the predicted evaporite localities and the observed evaporite localities.

6.2.3.2 Early Jurassic Results

Though the Early Jurassic climate was warm and similar to that of the Late Jurassic, there was a mega- monsoon which characterized the Early Jurassic supercontinent Pangea. The interior of Pangea was very arid and hot (Scotese, 2001). It has been suggested that the Early Jurassic climate was more arid than the present climate (Frakes, 1979; Gordon, 1975). The average temperature and precipitation for the Early Jurassic was 9.84°C and 0.35 cm/month respectively (Figure 6.3 and 6.4). This is once again evident in the abundant distribution of predicted evaporites localities for the Early Jurassic time period. Both the predicted and the observed evaporite localities are distributed between 0- 40°N and S latitude (Appendix C).

A statistical calculation of the probability that the number of hits observed is due to a random process is 5.91×10^{-5}, which is a low probability and indicates that the number of hits is not due to a random process. The null hypothesis predicts that 6.79 or 10.78% of the observed evaporites should be hits. However 19 hits were obtained which makes up 15.08% of the total number of predicted grid localities and 2 times the number of hits that were expected based on the "area" occupied by the predicted evaporites. This probability shows that the Early Jurassic "hits" have a 99.99% chance of being due to a non- random process which is significant and implies that the null hypothesis has failed. The results obtained for the Early Jurassic shows that there is a reasonably good fit between the predicted evaporite localities and the observed evaporite localities.

6.2.4 Late Triassic Results

Climate of the Late Triassic was arid however; wet monsoonal climates are believed to have prevailed during this time period (Frakes, 1979; Barron, 1983). Global climate was warm during the Late Triassic and there was no ice at either North or South Poles. Warm Temperate conditions extended towards the poles (Scotese, 2001). The average temperature and precipitation for the Late Triassic was 11.32°C and 0.34 cm/month respectively (Figure 6.3 and 6.4). This climatic pattern reflects in the distribution of evaporites for the Late Triassic with the evaporite localities extending as for as 55°N and S latitude for the observed evaporites. The predicted evaporite localities mostly fell within 0- 40°N and S latitude (Appendix C).

A statistical calculation of the probability that the number of hits observed is due to a random process is 0.019, which is a low probability and indicates that the number of hits is not

due to a random process. The null hypothesis predicts that 6.63 or 11.84% of the observed evaporites should be hits. However 12 hits were obtained which makes up twice the number of hits that were expected based on the "area" occupied by the predicted evaporites. This probability shows that the Late Triassic "hits" have a 98.01% chance of being due to a non-random process which is significant and implies that the null hypothesis has failed. The results obtained for the Late Triassic shows that there is a reasonably good fit between the predicted evaporite localities and the observed evaporite localities.

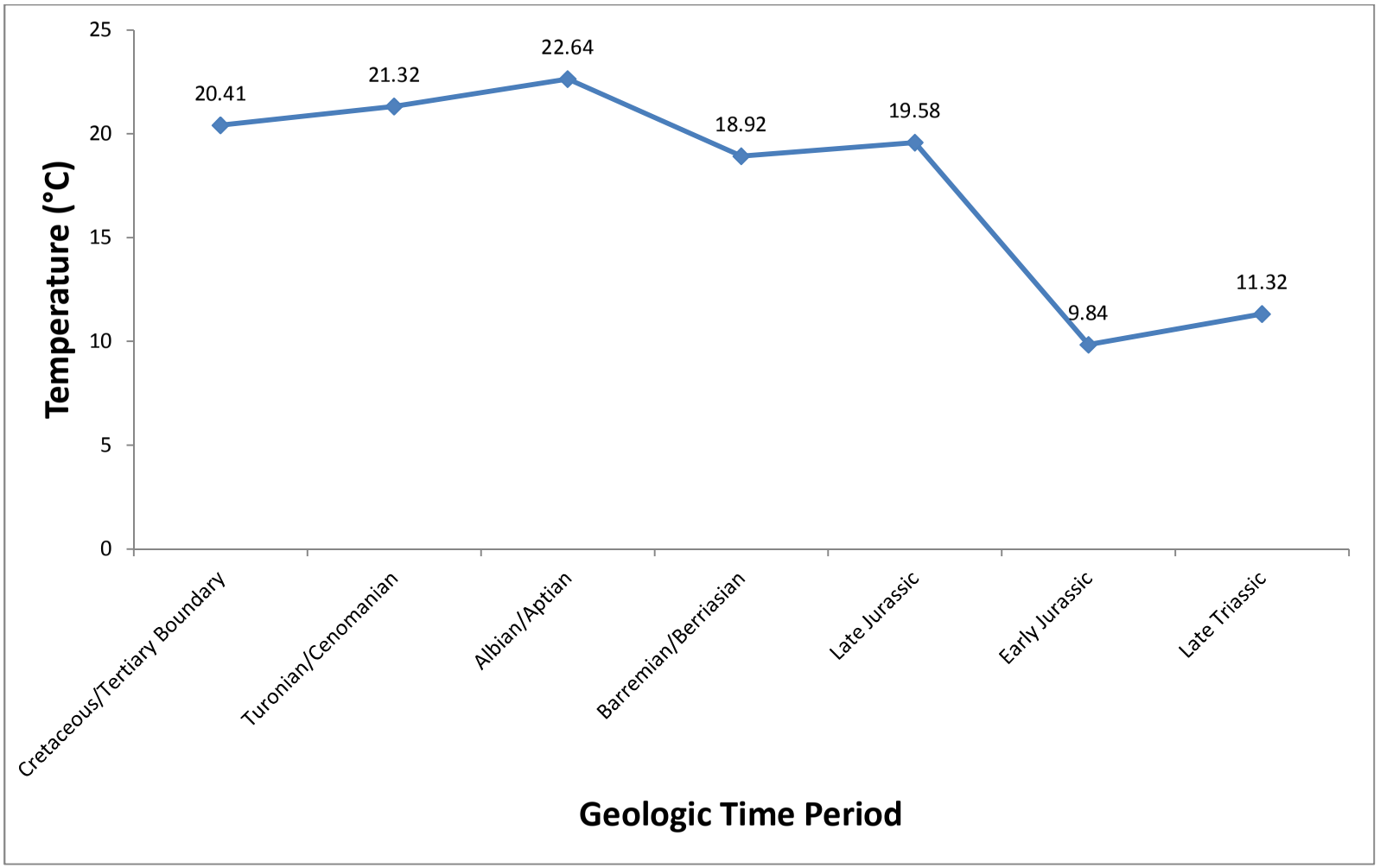

Figure 6.3: Graph showing the average temperature for the Mesozoic Era. The Albian/Aptian time period shows the highest average temperature and the Early Jurassic showed the lowest average temperature for the Mesozoic Era.

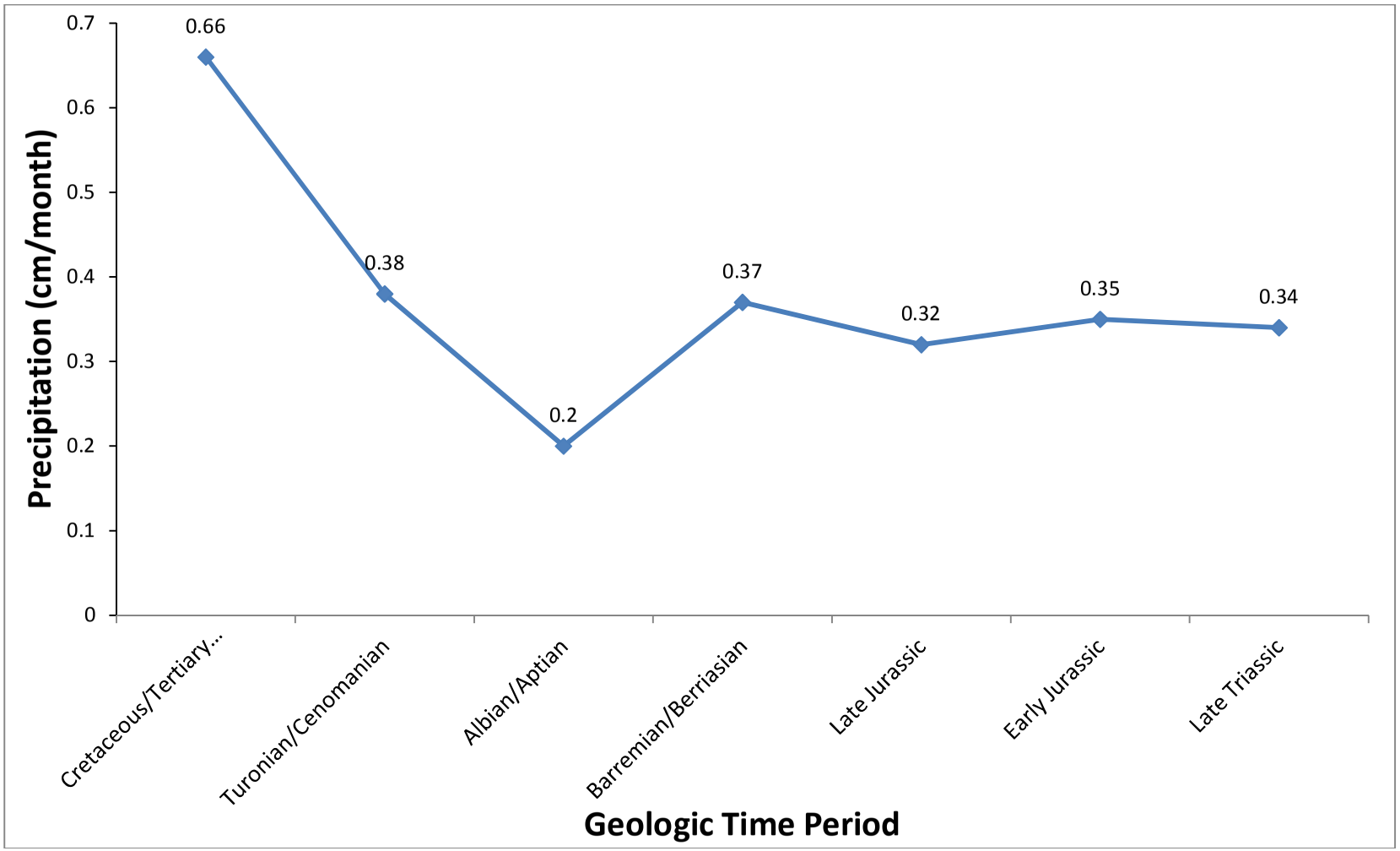

Figure 6.4: Graph showing the average precipitation for the Mesozoic Era. The Cretaceous/Tertiary Boundary time period shows the highest average precipitation and the Albian/Aptian showed the lowest average precipitation for the Mesozoic Era.

6.3 Analysis of Results obtained for the Paleozoic Era

6.3.1 Permo-Triassic Boundary Results (250 Ma)

Climate of the latest Permian through to the earliest Triassic has been suggested to have been hot (Dickins, 1984). No sign of glaciations has been reported for the Permo-Triassic Boundary (Dickins, 1983, 1984). The Late Permian may have been characterized by rapid global warming which extended to the Permo-Triassic Boundary (Scotese, 2001). The average temperature and precipitation recorded for the Permo-Triassic Boundary was 13.4°C and 0.48 cm/month respectively.

The distribution of predicted evaporites for the Permo-Triassic Boundary is extensive with the predicted evaporite localities forming an evaporite belt between 25- 45°N and S latitude. The observed evaporites were distributed between 0- 70°N and 0-45°S. The extensive distribution of evaporite localities towards the poles may be as a result of global warming conditions that existed for this time period.

A statistical calculation of the probability that the number of hits observed is due to a random process is 2.52×10^{-6}, which is a low probability and indicates that the hits are not due to a random process. The null hypothesis predicts that 3.87 or 12.91% of the observed evaporites should be hits. However 16 hits were obtained which makes up 4 times the number of hits that were expected based on the "area" occupied by the predicted evaporites. This probability shows that the Permo- Triassic Boundary "hits" have a 99.99% chance of being due to a non- random process. This number is significant and implies that the null hypothesis has failed. The results obtained for the Permo- Triassic Boundary shows that there is a reasonably good fit between the predicted evaporite localities and the observed evaporite localities.

6.3.2 Early Permian Results (280 Ma)

The Permian was mainly characterized by varying climatic conditions; however the Early Permian climate was arid to semi- arid. Evidence of global warming during the Early Permian has been obtained from oxygen isotopes. Asia may have experienced wet climates throughout the Permian with the deposition of coal and the southern hemisphere was mainly covered by glaciers (Frakes 1979; Drewry et al, 1974; Scotese, 2001). The arid to semi- arid conditions would have favored the formation of evaporites. The average temperature and precipitation obtained for this time period from the intersection of the climate envelope with FOAM data from this time period was 9.26°C and 0.30 cm/month respectively.

This climatic trend reflects in the results obtained for the early Permian. As reported by Frakes, 1979 and also observed in this data both the predicted and the observed evaporites are limited to 40°N and S latitude. The predicted evaporites are mainly distributed across South America, Asia and North America while the observed evaporites can be found on all continents except India.

A statistical calculation of the probability that the number of hits observed is due to a random process is 2.1×10^{-3}, which is a low probability and indicates that the number of hits is not due to a random process. The null hypothesis predicts that 2.33 or 7.76% of the observed evaporites should be hits. However 8 hits were obtained which makes up 4 times the number of hits that were expected based on the "area" occupied by the predicted evaporites. This probability shows that the Early Permian "hits" have a 99.79% chance of being due to a non-random process. This number is significant and implies that the null hypothesis has failed. The

results obtained for the Early Permian shows that there is a reasonably good fit between the predicted evaporite localities and the observed evaporite localities.

6.3.3 Mississippian Results (340 Ma)

The Mississippian climate was characterized by alternating wet and warm to dry conditions (Wright, 1980). Frakes, 1979 also noted that the Mississippian was characterized by increased precipitation and generally high humid conditions seem to characterize the intervals after glaciations. The average temperature and precipitation obtained from the intersection of the Climate Envelope with FOAM was 13.17°C and 0.46cm/month respectively.

Majority of the predicted evaporites plotted out in South America and in Africa with a few in North America while the observed evaporites plotted out between 0-35°N and 0- 40°S.

A statistical calculation of the probability that the number of hits observed is due to a random process is 0.198, which is a high probability and indicates that the number of hits between the predicted and the observed evaporites is due to a random process. The null hypothesis predicts that 2.22 or 4.19% should be hits, however 3 hits were obtained. This probability shows that the Mississippian "hits" have an 80.19% chance of being due to a random process. This number is not significant and implies that the null hypothesis is true. The results obtained for the Mississippian shows that there is not reasonably good fit between the predicted evaporite localities and the observed evaporite localities.

6.3.4 Late Devonian (360 Ma)

Climate for the Late Devonian is known to be generally dry and warm to very warm (Dickins, 1993; Joachimski et al, 2009). Evaporites were typically uncommon during the Late Devonian with much of the Devonian aridity being represented by red beds (Frakes, 1979). The average temperature and precipitation obtained from the intersection of the Climate Envelope and FOAM was 14.28°C and 0.77cm/month respectively. The supercontinent Pangea is believed to have begun its assembly during this time (Scotese, 2001).

The climatic trend recorded for the Late Devonian reflects once again in the distribution of the predicted evaporites. Few evaporites where predicted for this time period with majority of the predicted evaporites being found in Australia and Siberia. The observed evaporites are also distributed in North America, Siberia, Europe and Australia were dry conditions are known to have prevailed.

A statistical calculation of the probability that the number of hits observed is due to a random process is 0.069, which is a high probability and indicates that the number of hits is due to a random process. The null hypothesis predicts that 0.47 or 1.20% of the observed evaporites should be hits, however 2 hits were obtained. This probability shows that the Late Devonian "hits" have a 93.09% chance of being due to a random process. This number is not significant and implies that the null hypothesis is true. The results obtained for the Late Devonian shows that there is not reasonably good fit between the predicted evaporite localities and the observed evaporite localities.

6.3.5 Siluro-Devonian (400 Ma)

The Siluro-Devonian climate was generally warm and semi-arid to arid (Wright, 1980, Frakes, 1979). Generally dry conditions prevailed across much of North America, Siberia, China and Australia during the Early Devonian. South America and Africa were covered by cool, temperate conditions. The arid belt stretched across North America and northern Europe and glacial conditions prevailed at the South Pole seas (Scotese, 2001). The average temperature and precipitation obtained from the Climate Envelope and FOAM for this time period was 14.85°C and 0.57cm/month respectively.

The climate reflects in the distribution of both the predicted and the observed evaporites with evaporites occurring on the continents where dry conditions are known to have prevailed with no evaporites being found in the South Pole where glacial conditions are known to have existed.

A statistical calculation of the probability that the number of hits observed is due to a random process is 0.25, which is a high probability and indicates that the number of hits is due to a random process. The null hypothesis predicts that 1.50 or 4.28% of the observed evaporites should be hits, however 2 hits were obtained. This probability shows that the Siluro-Devonian "hits" have a 74.84% chance of being due to a random process. This number is not significant and implies that the null hypothesis is true. The results obtained for the Siluro-Devonian shows that there is not reasonably good fit between the predicted evaporite localities and the observed evaporite localities.

6.3.6 Late Cambrian (480 Ma)

Climate of the Late Cambrian is not well known and well documented however, it has been suggested that the Late Cambrian was characterized by falling sea levels and the onset of cooler global temperatures. There has been no evidence of glaciations at the poles (Scotese, 2001). The average temperature and precipitation obtained for this time period were 16.07°C and 0.61 cm/month respectively. The distribution of evaporites for the Late Cambrian was mainly concentrated in the southern latitude.

A statistical calculation of the probability that the number of hits observed is due to a random process is 0.33, which is a high probability and indicates that the number of hits is due to a random process. The null hypothesis predicts that 1.47 or 4.73% of the observed evaporites should be hits, however 1 hit was obtained. This probability shows that the Late Cambrian "hit" has a 66.2% chance of being due to a random process. This number is not significant and implies that the null hypothesis is true. The results obtained for the Late Cambrian shows that there is not a reasonably good fit between the predicted evaporite localities and the observed evaporite localities.

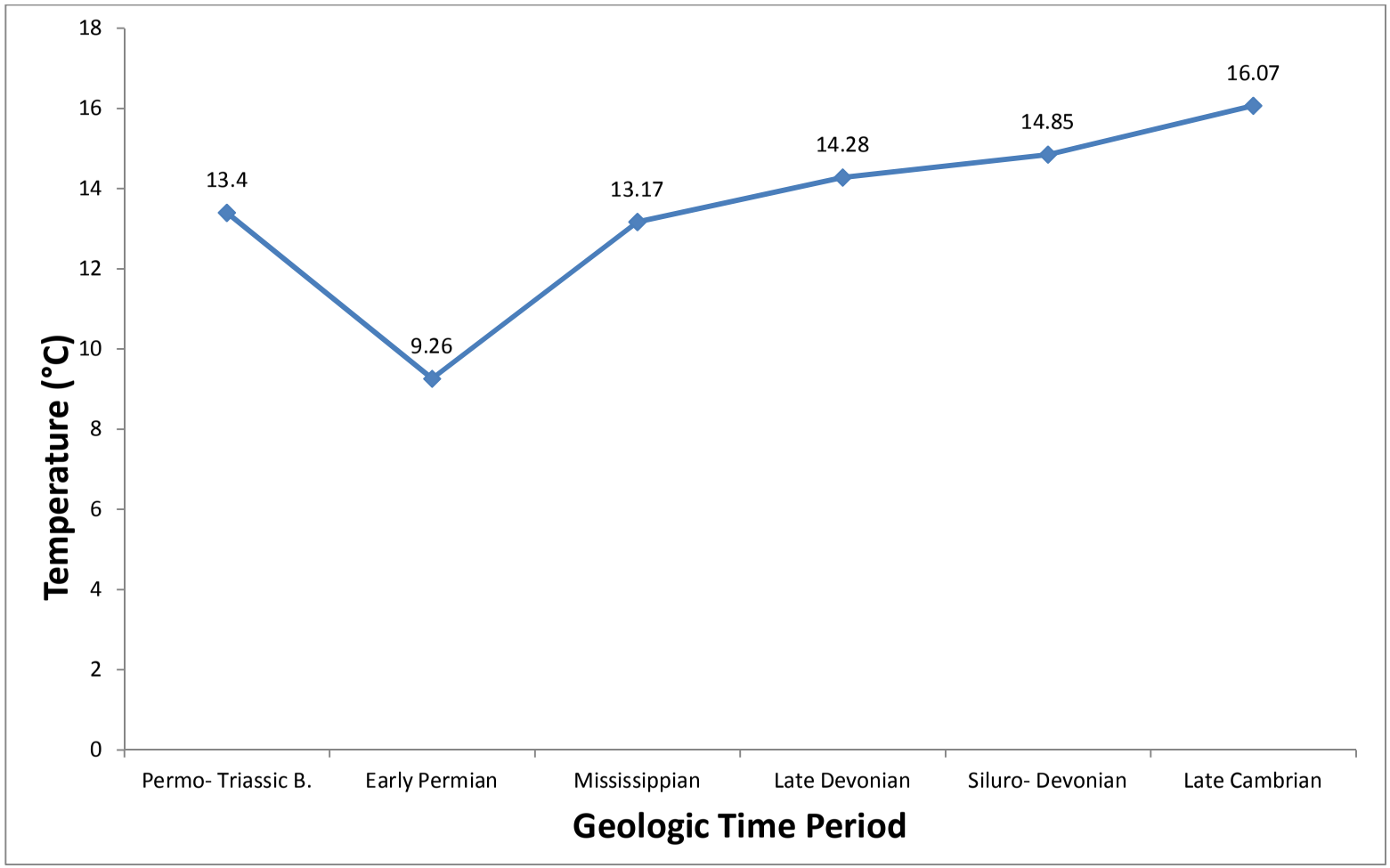

Figure 6.5: This graph shows the average temperatures recorded across the Paleozoic Era. Temperatures ranged between 9.26- 16.07 with the lowest temperature being recorded during the Early Permian and the highest tempearutes during the Late Cambrian. (Inconsistencies are observed between general climatic conditions during the time periods and the average temperatures obtained from the intersection).

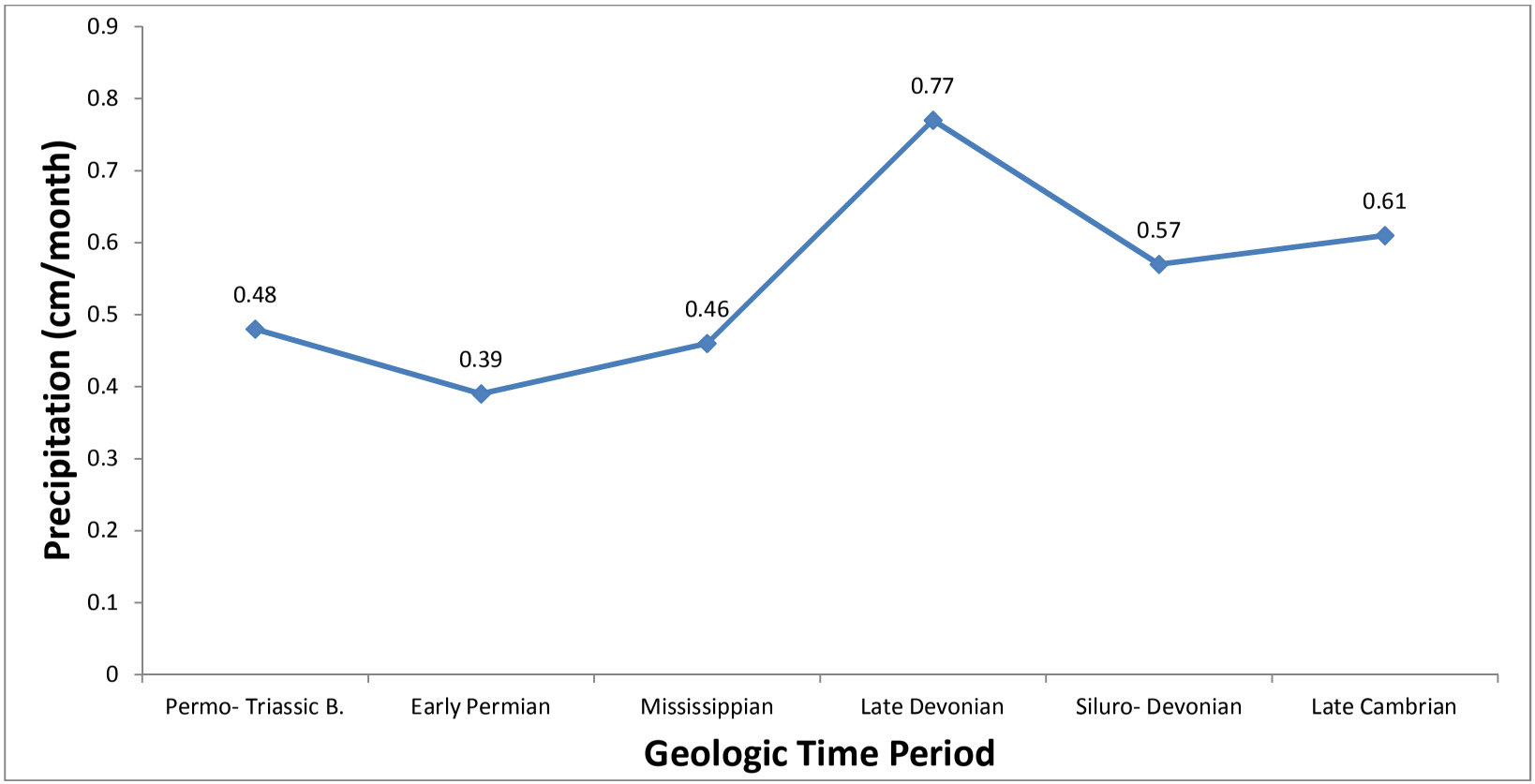

Figure 6.6: This graph shows the average precipitation in cm/month across the Paleozoic Era. Precipitation fluctuated across time periods with the lowest average precipitation being recorded for the Early Permian and the highest precipitation for the Late Devonian.

6.4 Distribution of Hits across Time Periods

6.4.1 Cenozoic, Mesozoic and Paleozoic distribution of hits

The distribution of evaporite localities varied across all the time periods. Figure 6.7 shows the distribution of the actual hits obtained for each time period. It is observed that the number of hits decreases across the Cenozoic Era with the lowest number of hits (11) being observed for the Middle Eocene. The Mesozoic Era recorded a high number of hits as compared to the Cenozoic and Paleozoic eras with the Late Jurassic recording the highest number of hits (31). The Cenomanian/Turonian recorded 24 hits which is the next highest to the Late Jurassic. The Late Triassic however, recorded a low number of hits (12) while the Cretaceous/Tertiary Boundary recorded the lowest number of hits (4) for the Mesozoic Era. The Paleozoic Era recorded high hits at the Permo-Triassic Boundary (16) and in the Early Permian (8). The Mississippian, Late Devonian, Siluro-Devonian and Late Cambrian all recorded very low hits (3, 2, 2 and 1 respectively).

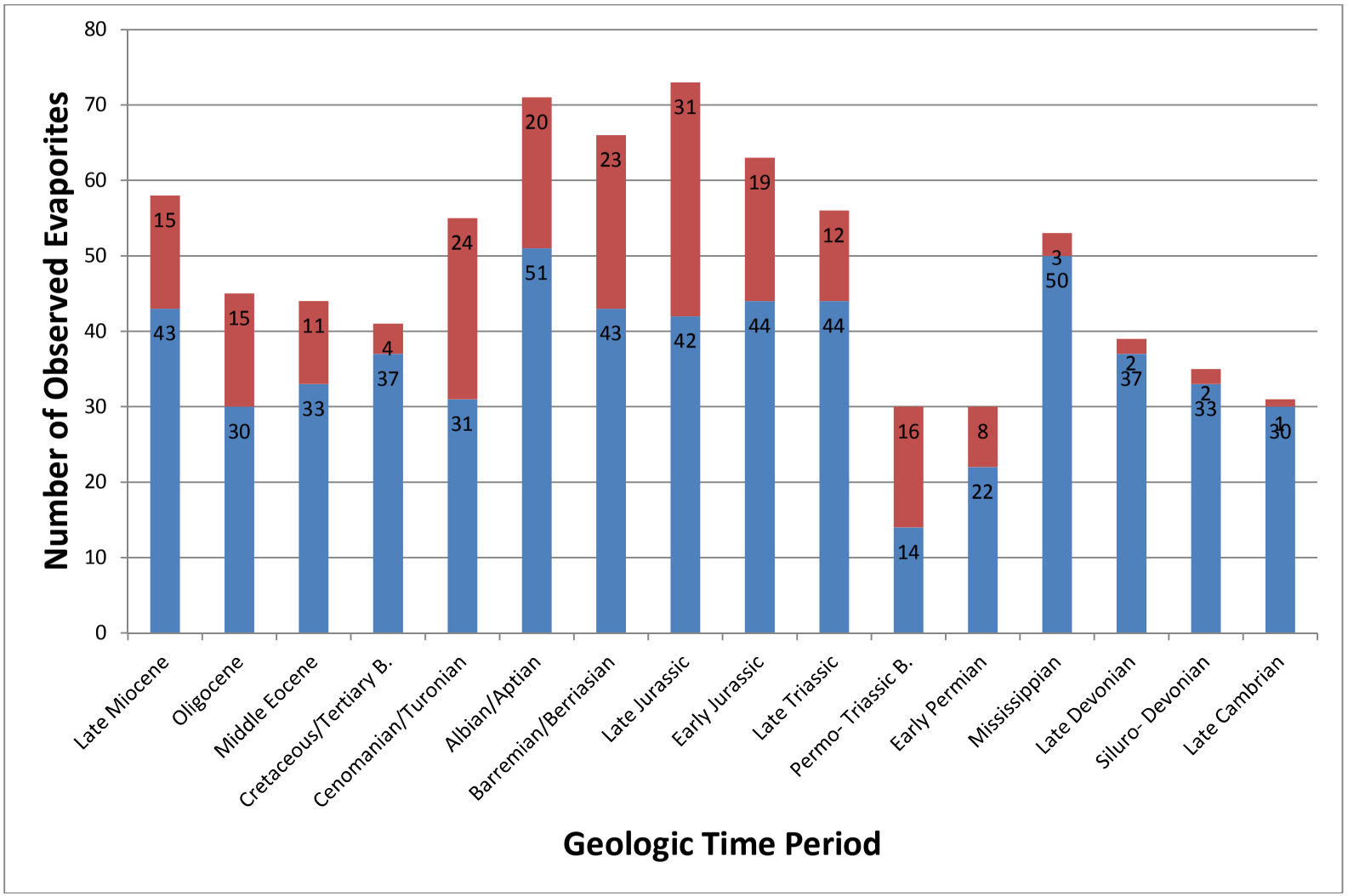

Figure 6.7: Distribution of the actual number of hits for all 16 time periods.

Figure 6.8 is a graph that compares both the actual number of hits and the predicted number of hits for all the geologic time periods used in this research. The graph shows that, the actual number of hits exceeds the predicted number of hits with exceptions being observed in the Mississippian, Late Devonian, Siluro-Devonian and the Late Cambrian. For the Mississippian, Late Devonian and the Siluro-Devonian, the predicted number of hits is less than twice the actual number of hits obtained which when compared to the previous time periods presents very poor statistical results. The Late Cambrian has the expected number of hits being more than the actual number of hits obtained.

A graph of the abundance of evaporites through geologic time obtained from Gordon (1975) compared with a compilation from the study shows that abundance of evaporites was very low during the Siluro-Devonian and Cambro-Ordovician. Evaporite abundance was relatively high during the Devonian and at its highest peak during the Triassic and Jurassic time periods (Figure 6.9).

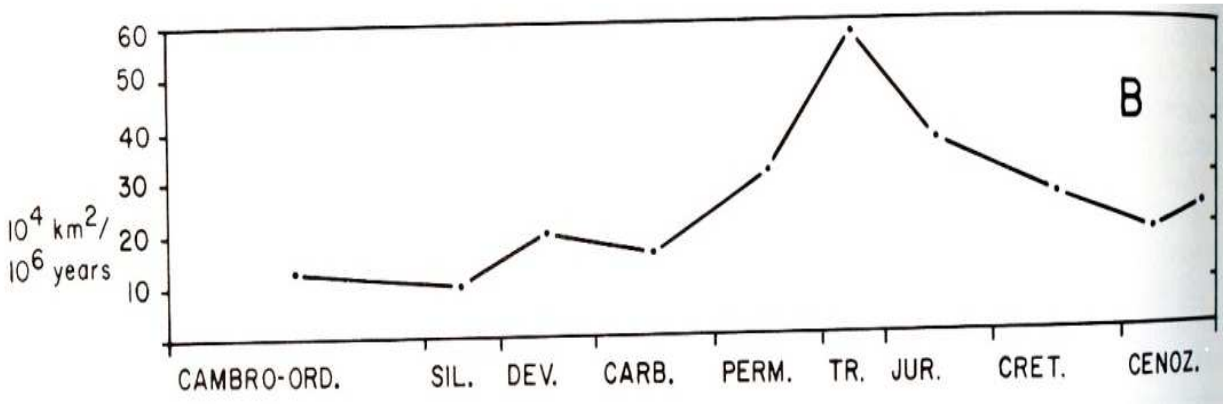

Figure 6.8: A graph showing evaporite abundance during the Phanerozoic with a greatest peak during the Jurassic and Triassic (Gordon, 1975).

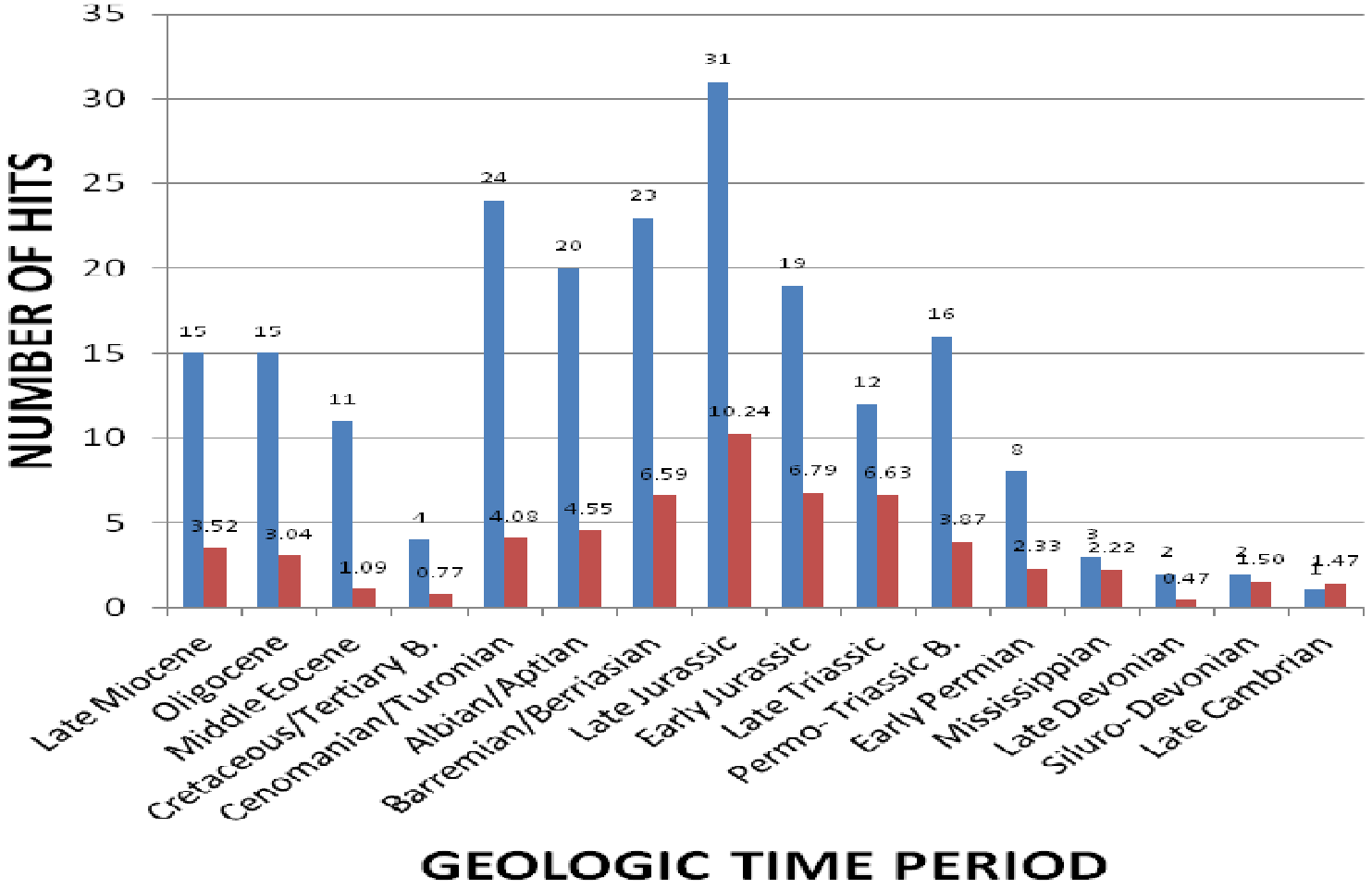

Figure 6.9: A graph showing both the actual and predicted number of hits for all the time periods. The blue histogram represents the actual number of hits and the red histogram represents the predicted number of hits.

The probabilities obtained from the Poisson distribution reflects these observations with Figure 6.10 showing a plot of the probabilities plotted against time. Very low probabilities were observed for the following time periods: Late Miocene, Oligocene, Middle Eocene, Cenomanian/Turonian, Aptian/Albian, Barremain/Barresian, Late Jurassic, Permo-Triassic Boundary, Early Permian, Cretaceous/Tertiary Boundary and the Late Triassic which indicate that the "hits" obtained for these time periods is not due to a random process. On the contrary high probabilities were observed for the following time periods: Mississippian, Late Devonian, Siluro-Devonian and Late Cambrian all of which supported the null hypothesis and shows that the "hits" obtained for these time periods was due to a random process.

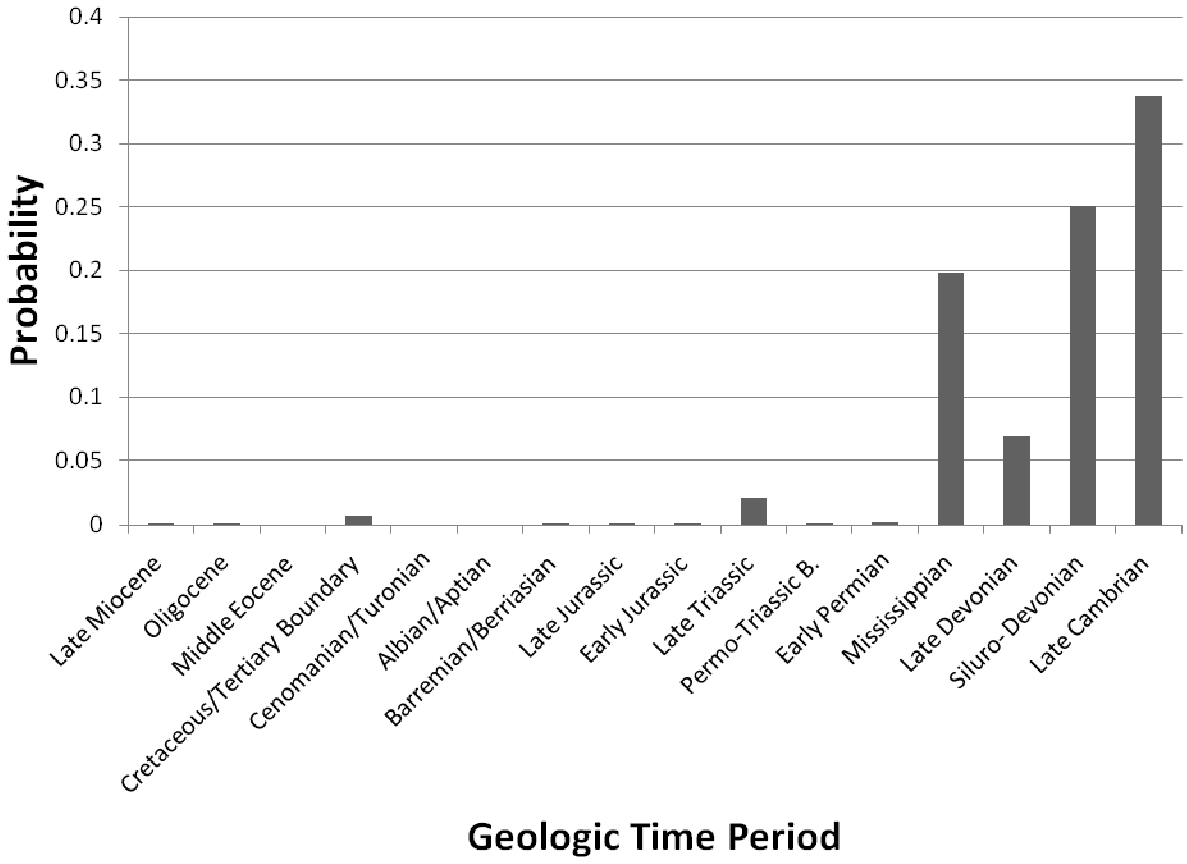

Figure 6.10: Graph showing a histogram of the probabilities that the observed number of hits were random for all the time periods.

This observation shows the accuracy in the predictions for the Cenozoic and Mesozoic Era's. The Paleozoic Era which had some exceptions in the trend of the overall data may be due to the fact that not enough predictions were made for these time periods. The climatic conditions that existed during those time periods may also have resulted in the low statistics obtained. This is because the climate envelope constructed was based on modern temperature and precipitation data which was then intersected with FOAM simulations for the various time periods. Climate of the Mississippian, Siluro-Devonian and the Late Cambrian predicted by FOAM may have differed greatly from the modern climate hence resulting in the low number of predicted evaporite localities and hence the low number of hits and significance level for these time periods.

Figure 6.11 is a graph of the average latitude for the predicted and observed evaporite localities. The average latitude for the predicted evaporites of the Cenozoic Era was around 25.85° while that for the Mesozoic Era was around 27.51°. The Paleozoic Era had its average predicted evaporite latitude around 26.62°. The average latitude for the observed evaporites of the Cenozoic Era was around 32.66° while that for the Mesozoic Era was around 26.23°. The Paleozoic Era had its average observed evaporite latitude around 20.67°.

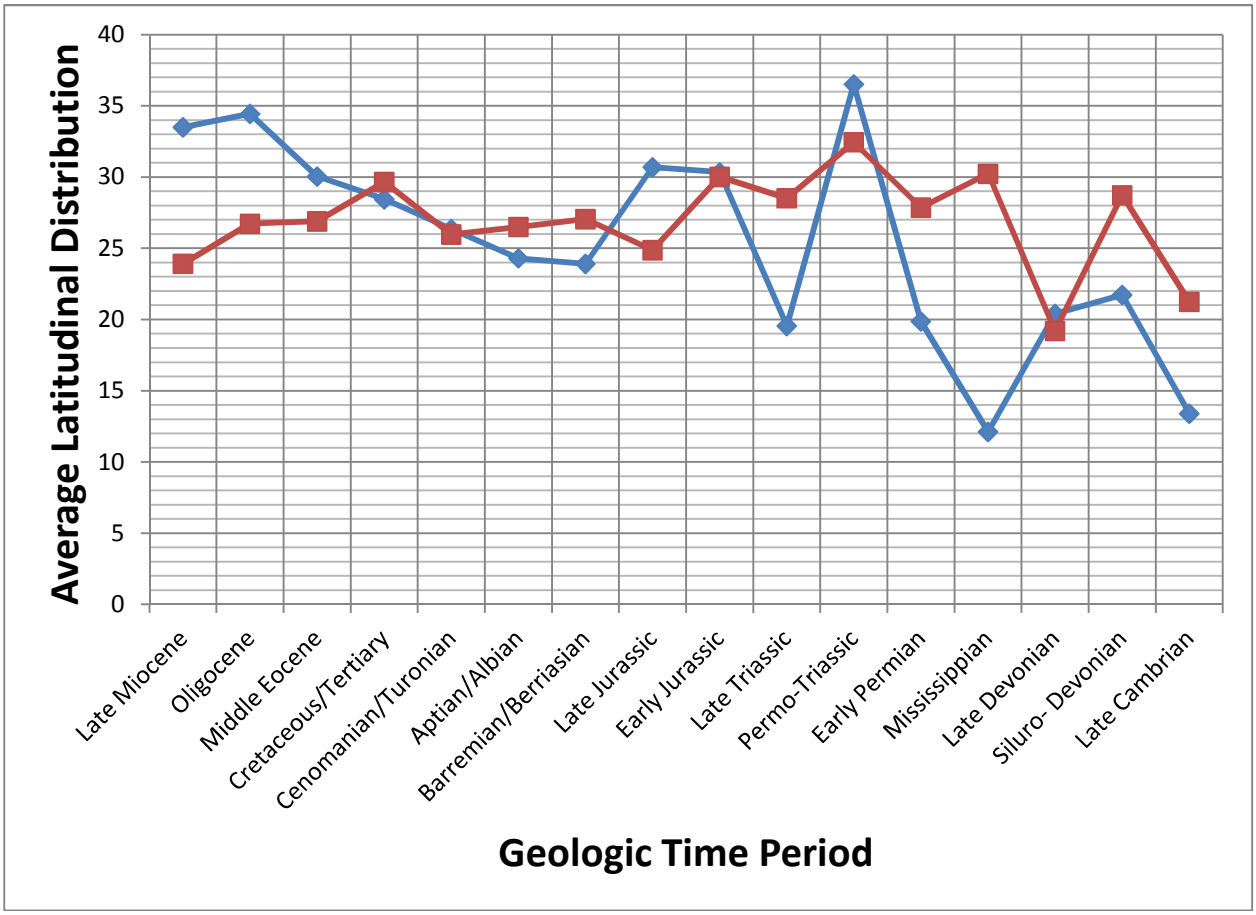

Figure 6.11: Graph showing the average latitudinal distribution of observed and predicted evaporite localities. The blue graph represents the average latitudinal distribution for the observed evaporites and the red graph represents the average latitudinal distribution for the predicted evaporites.

The average latitudinal distribution of the predicted evaporites ranges from 24 to 32°N and S latitude. The Late Devonian and Late Cambrian however, show a lower latitudinal distribution occurring at 19° and 21° respectively and mostly in the south. The average latitudinal distributions of the observed evaporites seem to occur at slightly higher latitudes and ranges from 24 to 37°N and S latitude. For the observed evaporites, exceptions are observed in Late Triassic, Early Permian, Mississippian, Late Devonian, Siluro-Devonian and Late Cambrian. These show much lower average latitudinal distributions ranging from 12 to 22° N and S latitude. The higher

latitudinal distributions may be due to the fact that some time periods (Mesozoic, parts of Paleozoic and parts of Cenozoic) recorded very warm temperatures with very little glaciations at the poles.

The average latitudinal distribution of the predicted evaporites seems to be in conformity with the Hadley cell circulation. The exceptions observed for the predicted latitudinal distributions especially in the Late Devonian and Late Cambrian may be due to the arrangements of the continents during these times. Very little predictions were made by the climate envelope for these periods which may suggest that either 1) climate during these time periods were very different from modern climate or that 2) the climate envelope needs to be expanded in order to be able to obtain more predictions and hence have a better overview of the distribution of predicted evaporites for these times.

6.5 Conclusions

From this study it can be concluded that climate greatly influences the distribution and extent of evaporite distribution. It is also clear that there was a reasonable good fit between the predicted and the observed evaporites for all the time periods in the Cenozoic and Mesozoic Eras and for some time periods in the Paleozoic (Early Permian and Late Devonian). The Mississippian, Siluro-Devonian and Late Cambrian did not fail the null hypothesis and this shows that the hits that were obtained for these time periods are likely due to a random process

or that the climatic assumption we have made for the Cenozoic and Mesozoic Eras do not apply to the Paleozoic.

In previous research, generally low evaporite accumulation has been observed for the Cambrian, Ordovician and the Carboniferous in the Paleozoic Era with the Paleozoic maxima for evaporite accumulation being observed only in the Permian and Devonian (Gordon, 1975; Frakes, 1979). According to Gordon's data generally humid conditions existed for these time periods which may have resulted in the low prediction.

It can also be concluded that the hits obtained from the comparison of the predicted and the observed evaporite localities is not due to a random with a relatively high significance for most of the time periods. Finally, we conclude that because the number of hits indicated that the predicted location of evaporites for majority of the times was not random that the climate envelope tool is a good predictive tool for climatic sensitive sediments such as evaporites.

APPENDIX A

YERMOSOL DATABASE

SEE SUPPLEMENTARY FILE

APPENDIX B

STATISTICAL TABLES

Geologic Time Period	Total Land	Number of Predicted Evaporites Cells	% Total Land Occupied by Predicted Evaporites	Number of Observed Evaporites Cells	Actual Number of Hits	Predicted Number of Hits	Misses	Probability	Significance
Late Miocene (10 Ma)	1434	87	6.07	58	15	3.52	43	3.5721E-06	99.99%
Oligocene (30 Ma)	1434	97	6.76	45	15	3.04	30	6.40249E-07	99.99%
Middle Eocene (45 Ma)	1489	37	2.48	44	11	1.09	33	2.17348E-08	99.99%
Cretaceous/Tertiary Boundary (70 ma)	1334	25	1.87	41	4	0.77	37	0.006781799	99.32%
Turonian/ Cenomanian (90 Ma)	1403	104	7.41	55	24	4.08	31	1.23372E-11	99.99%
Albian/Aptian (120 Ma)	1436	92	6.41	71	20	4.55	51	6.2815E-08	99.99%

Barremian / Berriasian (140 ma)	1373	137	9.98	66	23	6.59	43	3.62969E-07	99.99%
Late Jurassic (160 Ma)	1198	168	14.02	73	31	10.24	42	9.05944E-08	99.99%
Early Jurassic (180 Ma)	1169	126	10.78	63	19	6.79	44	5.90978E-05	99.99%
Late Triassic (220 Ma)	1216	144	11.84	56	12	6.63	44	0.01988167 5	98.01%
Permo-Triassic Boundary (250 Ma)	1162	150	12.91	30	16	3.87	14	2.52369E-06	99.99%
Permian (280 Ma)	1160	90	7.76	30	8	2.33	22	0.00209614 2	99.79%
Mississippian (340 Ma)	1170	49	4.19	53	3	2.22	50	0.19804957 9	80.19%
Late Devonian (360 Ma)	1162	14	1.20	39	2	0.47	37	0.06903150 1	93.09%

Siluro-Devonian (400 Ma)	1097	47	4.28	35	2	1.50	33	0.25102143	74.89%
Late Cambrian (480 Ma)	1058	50	4.73	31	1	1.47	30	0.337990463	66.21%

REFERENCES

Barron, E.J. "A warm, equable Cretaceous: The nature of the problem." *Earth Science Reviews* 19 (1983): 305-338.

Barron, E.J. "Climatic implications of the varibale obliquity explanation of Cretaceous-Paleogene high- latitude floras." *Geology* 12 (1984): 595-598.

Barron, E.J., J.L. Sloan, and C.G.A. Harrison. "Potential significance of land- sea distribution and surface albedo variations as a climatic forcing factor; 180my to the present." *Palaeogeography, Palaeoclimatology, Palaeoecology* 30 (1980): 17-40.

Barron, Eric J. "Explanations of the Tertiary Global Cooling Trend." *Palaeogeography, Palaeoclimatology, Palaeoecology* 50 (1985): 45-61.

Beauvais, L. "Upper Jurassic hermatypic corals." In *Atlas of Palaeogeography*, by A. Hallam, 317-328. Amsterdam: Elsevier, 1973.

Bell, F.G. *Environmental Geology Principles and Practice.* London: Blackwell Science Ltd, 1998.

Boucot, A.J., X. Chev, and C.R. Scotese. "Phanerozoic Atlas of Climate Indicators." *SEPM*, in press.

Boul, B.W., F.D. Hole, R.J. McCraken, and R.J. Southard. *Soil Genesis and classification.* Ames, Iowa: Iowa State University Press, 1997.

Bowen. *Paleotemperature Analysis.* Amsterdam: Elsevier, 1966.

Bowen. "Paleotemperature analysis of belemnoidea and Jurassic paleoclimatology." *Journal of Geology* 69 (1961): 309-320.

Brezinski, D.K., C.C. Blaine, V.W. Skema, and R. Stamm. "Late Devonian glacial deposits from the eastern United States signal an end of the mid-Paleozoic warm period." *Palaeogeography, Palaeoclimatology, Palaeoecology*, 2008: 143-151.

Brezinski, David K., C. Blaine Cecil, Viktoras W. Skema, and Robert Stamm. "Late Devonian glacial deposits from the eastern United States signal an end of the mid-Paleozoic warm period." *Palaeogeography, Palaeoclimatology, Palaeoecology* 268 (2008): 143-151.

Caputo, M.V. "Late Devonian glaciation in South America." *Palaeogeography, Palaeoclimatology, Palaeoecology* 51 (1985): 291-317.

Chamley, H. "North Atlantic clay sedimentation and paleoenvironment since the Late Jurassic In:." *America Geophysical Union* 3 (1979): 342-361.

Cocks, P. A. Walker, K. D. "HABITAT: A Procedure for Modelling a Disjoint Environmental Envelope for a Plant or Animal Species." *Global Ecology and Biogeography Letters* 1 (1991): 108-118.

Copper, P. "Frasmian/Fammenian mass extinction and cold water oceans." *Geology* 14 (1986): 835-839.

Crowley, T.J., and G.R., North. *Paleoclimatology: Oxford Monographs on Geology and Geophysics.* Vol. 18. New York: Oxford University Press, 1991.

Crowley, T.J., and J.C. Zachos. "Warm climates in Earth History." 50-76. New York: Cambridge University Press, 2000.

D.R., Grocke, Price G.E., Ru¡ell A.H., Mutterlose J., and Baraboshkin E. "Isotopic evidence for Late Jurassic- Early Cretaceous." *Palaeogeography, Palaeoclimatology, Palaeoecology* 202 (2003): 97-118.

Dickins, J.M. *Palaeogeography, Palaeoclimatology, Palaeoecology*, 1993: 89-94.

Dickins, J.M. "Evolution and climate in the upper Paleozoic: ." In *In Fossils and Climate ed P. Brenchvy*, 317-327. John Wiley and Sons, 1984.

Dickins, J.M. "Permian to Triassic changes in life." *Association of Australian Paleontology Memoir* 1 (1983): 297-303.

Dingle, R.V., S.P. Marensti, and M. Lavelle. "High Latitude Eocene Climate deterioration: evidence from North Antarctic Peninsula." *Journal of South American Earth Sciences* 11 (1998): 571-579.

Donn, W.L., and D.M. Shaw. "Model of climate evolution based on continental drift an dpolar wandering." *Geological Society of America Bulletin* 88 (1977): 390-396.

Douglas, R.G., and S.M. Savin. "Oxygen and carbon isotope analyses of Cretaceous and tertiary microfossils from Shatsky Rise and other sites in the North Pacific Ocean." *Initial Reports of the Deep Sea Drilling Project* (U.S. Government Printing Office) 32 (1975): 509-520.

Downing, D., and J. Clark. "Statisitcs the easy way." 100-103. Barron's educational series, 1989.

Drewry, G.E., A.T.S. Ramsay, and A.G. Smith. "Climatically controlled sediments, the geomagnetic field, and trade wind belts in Phanerozoic time." *Journal of Geology* 82 (1974): 531-553.

Ewing, W.M, J.L Worzel, and C.A. Burk. "Regional aspects of deep water drilling in the Gulf of Mexico, east of the Bahama Platform, and on the Bermuda Rise. In: Ewing,W.M.,Worzel, J.L., Beall, A.O., Berggren, W.A., Bukry, J.D., Burk, C.A., Fischer, A G., Pessagno Jr., E.A. (Eds.),." *Initial Report of the Deep Sea Drilling Project* 1 (1969): 624-640.

Fluteau, F., G. Ramstein, J. Besse, R. Giuraud, and J.R. Masse. "Impacts of palaeogeography and sea level changes on Mid-Cretaceous climate." *Palaeogeography, Palaeoclimatology, Palaeoecology*, 2007: 357-381.

Frakes, L.A.,. *Climates Throughout Geologic Time.* Amsterdam: Elsevier Scientific , 1979.

Frakes, L.A., J.E. Francis, and J.I. Syktus. *Climate models of the Phanerozoic.* Cambridge University Press, 1992.

Gordon, W.A.,. "Distribution by latitude of Phanerozoic evaporite deposits." *Journal of Geology* 83 (1975): 671-684.

Grunau, H.R. "A worldwide look at the cap- rock problem." *Journal of Petroleum Geology* 10 (1987): 245-265.

Hallam, A. "A review of the broad pattern of Jurassicnext term sea-level changes and their possible causes in the light of current knowledge." *Palaeogegraphy, Palaeoclimatology, Palaeoecology* 167 (2001): 23-37.

Hallam, A. "The Jurassic Climate In: ." In *Climate in Eath History*, 159-163. Washington, D.C: Natinal Academy Press, 1982.

Hay, W.W., Jr. Behensky, E.J. Barron, and J.L. Sloan. "Late Triassic-Liassic paleoclimatology of the proto-central North Atlantic rift system." *Palaeogeography, Palaeoclimatology, Palaeoecology* 40 (1982): 13-30.

Hay, William W. "Evolving ideas about the Cretaceous climate and ocean circulation." *Cretaceous Research* 29 (2008): 725–753.

Hay, William W., Areg Migdisov, Alexander N. Balukhovsky, Christopher N. Wold, Sascha Flögel, and Emanuel Söding. "Evaporites and the salinity of the ocean during the Phanerozoic: Implications for climate, ocean circulation and life." *Palaeogeography, Palaeoclimatology, Palaeoecology* 240 (2006): 3-46.

J., Golonka. "Late Triassic and Early Jurassic palaeogeography of the world." *Palaeogeography, Palaeoclimatology, Palaeoecology* 244 (2007): 297–307.

Jacob, R., C. Schafer, I. Foster, M. Tobis, and J. Anderson. "Computational Design and Performance of the Fast Ocean Atmosphere Model, Version One." In *International Conference*

on Computational Science, by V. N. Alexandrov, J. J. Dongarra and C. J. K. Tan, 175-184. Springer-Verlag, 2001.

Joachimskia, M.M., et al. "Devonian climate and reef evolution: Insights from oxygen isotopes in apatite." *Palaeogeography, Palaeoclimatology, Palaeoecology*, 2009: 599-609.

Keller, Gerta. "Cretaceous climate, volcanism, impacts, and biotic effects." *Cretaceous Research* 29 (2008): 754–771.

Kendall, Christopher G. C., Paul Lake, H. Dallon Weathers III, and Venkat Lakshmi. "Evidence of rain shadow in the geologic record: repeated evaporite accumulation at extensional and compressional plate margins." *INTERNATIONAL CONFERENCE ON DESERTIFICATION.* Dubai, 2002.

Kraus, Mary J., and Susan Riggins. "Transient drying during the Paleocene–Eocene Thermal Maximum (PETM): Analysis of paleosols in the bighorn basin, Wyoming." *Palaeogeography, Palaeoclimatology, Palaeoecology* 245 (2007): 444–461.

Kring, David A. "The Chicxulub impact event and its environmental consequences at the Cretaceous–Tertiary boundary." *Palaeogeography, Palaeoclimatology, Palaeoecology*, no. 255 (2007): 4- 21.

Legates, D.R., and C.J. Willmott. "Mean seasonal and spatial variability in gauge gaugecorrected,global precipitation." *International Journal of Climatology* 10 (1990a): 111-127.

Legates, D.R., and C.J. Willmott. "Mean seasonal and spatial variability in global surface air temperature." *Theoretical and Applied Climatology* 41 (1990b): 11-21.

Lu, Jian, Gabriel A. Vecchi, and Thomas Reichler. "Expansion of the Hadley cell under global warming." *GEOPHYSICAL RESEARCH LETTERS* 34 (2007): 1-5.

Meyerhoff, A.A. "Continental Drift High- latitude evaporite deposits and geologic history of Arctic and North Atlantic Oceans." *Journal of Geology* 78 (1970): 406-444.

Moore, T.L., E.P.Roy, M. Perlmutter, and J.T. Parrish. "Evalauating paleoclimate indicators using climate envelopes." *AAPG Annual Convention.* Long Beach California, 2007.

Parrish, T.J., A.M. Ziegler, and C.R. Scotese. "Rainfall patterns and the distribution of coals and evaporites in the Mesozoic and Cenozoic." *Palaeogeography, Palaeoclimatology, Palaeoecology* 40 (1982): 67-101.

Pearson, P.N., et al. "Stable warm tropical climate through the Eocene epoch." *Journal of Geology*, 2006: 211-214.

Pope, K.O. "Energy, volatile production and climatic effects of the Chicxulub Cretaceous/Tertiary impact." *Journal of Geophysical Research*, 1997: 21645-21664.

Potter, Paul Edwin, and Peter Szatmari. "Global Miocene tectonics and the modern world." *Earth-Science Reviews* 96 (2009): 279–295.

Raymo M.E., Ruddiman W.F. "Tectonic forcing of late Cenozoic climate." *Nature* 359 (1992): 117-122.

Raymo, M.E., and W.F. Ruddiman. "Tectonic Forcing of the late Cenozoic Climate." *Nature*, 1992: 117-122.

Raymo, M.E., W.F. Ruddiman, and P.N. Froelich. "Influence of late Cenozoic montain building on ocean geochemical cycles." *Geology* 16 (1988): 649-653.

Raymo, M.E., W.F. Ruddiman, and P.N. Froelich. "Influence of late Cenozoic montain building on ocean geochemical cycles." *Geology*, 1988: 649-653.

Rea, D.K., S.A. Hovan, and T.R. Janecek. "Late Quatenary bflux of eolian dust to the pelagic ocean." *Global Geoflux Study*, 1990: Natinal Researchj Council, in press.

Retallack, Gregory J. *Soils of the Past: An Introduction to Paleopedology.* London: Blackwell Science Ltd, 2001.

Ronov, A.B. *Osadochnaya Obolochka Zemli (Kolichestvennoe Zakonomernosti Stroeniya, Sostava y Evoliutsii. Izdatelstvo "Nauka".* Moskva, 1980.

Ruddiman, W.F. *Earth's Clamate: Past and Future.* New York: W.H. Freeman and Company, 2008.

Ruddiman, William F., and John E. Kutzbach. "Forcing of late Cenozoic Northern Hemisphere Climate by Plateau Uplift in Southern Asia and the American West." *Journal of Geophysical Research* 94 (1989): 18409-18427.

Ruddiman, William F., and John E. Kutzbach. "Plateau Uplift and Climatic Change." *Scientific American*, 1991: 66-75.

Scotese, C.R. *Atlas of Earth History.* Vol. 1, in *Paleogeography, PALEOMAP project*, 52. Arlington, 2001.

Scotese, C.R., Illich, H., Zumberge, J, and Brown, S. The GANDOLPH Project: Year One Report: Paleogeographic and Paleoclimatic Controls on Hydrocarbon Source Rock Deposition, A Report on the Methods Employed, the Results of the Paleoclimate Simulations (FOAM), and Oils/Source Rock Compilation for the Late Cretaceous (Cenomanian/Turonian; 93.5 Ma), Late Jurassic (Kimmeridgian/Tithonioan; 151 Ma), Early Permian (Sakmarian/Artinskian; 284 Ma), and Late Devonian (Frasnian/Femennian; 372 Ma), Conclusions at the End of Year One, February, 2007. GeoMark Research Ltd, Houston, Texas, 2007: 142 pp.

Scotese, C.R., Illich, H., Zumberge, J, and Brown, S., and Moore, T. The GANDOLPH Project: Year Two Report: Paleogeographic and Paleoclimatic Controls on Hydrocarbon Source Rock Deposition, A Report on the Methods Employed, the Results of the Paleoclimate Simulations (FOAM), and Oils/Source Rock Compilation for the Miocene (10 Ma), Early Cretaceous (Aptian/Albian; 120 Ma and Berriasian/Barremian (140 Ma), Late Triassic (220 Ma), and Early Silurian (430 Ma), Conclusions at the End of Year Two, July, 2008. GeoMark Research Ltd, Houston, Texas, 2008: 177 pp.

Scotese, C.R., Illich, H., Zumberge, J, and Brown, S., and Moore, T. The GANDOLPH Project: Year Three Report: Paleogeographic and Paleoclimatic Controls on Hydrocarbon Source Rock Deposition, A Report on the Methods Employed, the Results of the Paleoclimate Simulations (FOAM), and Oils/Source Rock Compilation for the Eocene (45 Ma), Early/Middle Jurassic (180 Ma), Mississippian (340 Ma), and Neoproterozoic (600 Ma), Conclusions at the End of Year Three, August, 2009. GeoMark Research Ltd, Houston, Texas, 2009: 154 pp.

Scotese, C.R., Illich, H., Zumberge, J, and Brown, S., and Moore, T. The GANDOLPH Project: Year Four Report: Paleogeographic and Paleoclimatic Controls on Hydrocarbon Source Rock Deposition, A Report on the Methods Employed, the Results of the Paleoclimate Simulations (FOAM), and Oils/Source Rock Compilation for the Oligocene (30 Ma), Cretaceous/Tertiary (70 Ma), Permian/Triassic (250 Ma), Silurian/Devonian (400 Ma), and Cambrian/Ordovician (480 Ma), Conclusions at the End of Year Four, April 2011. GeoMark Research Ltd, Houston, Texas, 2011: 219 pp.

Sellwood, B.W., and G.D. Price. "Sedimentary facies as indicators of Mesozoic paleoclimate in." In *Paleoclimate and their modelling with special reference to the Meosozoic Era*, by J.R.L. Allan, B.J. Hoskins, B.W. Sellwood and R.A. Spicer and P.J. Valds, 17-26. London: Chapman and Hall, 1994.

Stanley, S.M. "Climate cooling and mass extinction of Paleozoic reef." *Palaios* 3 (1988): 228-232.

Trappe, Jorg. "Pangea: extravagant sedimentary resource formation during supercontinent configuration, an overview." *Palaeogeography, Palaeoclimatology, Palaeoecology* 161 (2000): 35-48.

W., Hay William. "Can humans force a return to a ‘Cretaceous’ climate?" *Sedimentary Geology* 235 (2011): 5-26.

Warren, J. "Evaporites: Their Evolution and Economics." 63-68. London: Blackwell Science, 1999.

Warren, J. "Evaporties Sedimentation." 2-20. New Jersey: Prentice Hall, 1989.

Weissert, H., and Mohr H. "Late Jurassic climate and its impact on carbon cycling." *Palaeogeography, Palaeoclimatology, Palaeoecology* 122 (1996): 27-43.

Wright, V.P. "Climatic Fluctuation in the Lower Carboniferous." *Naturwissenschaften*, 1980: 252-253.

Zanazzi, A., M.J. Kohn, B.J. McFadden, and D.O. Terry. "Large temperature drop across the Eocene- Oligocene transition in Central North America." *Nature* 445 (2007): 639-642.

Zharkov, M.A. *History of Palaeozoic Salt Accumulation.* Berlin: Springer Verlag, 1981.

Zharkov, M.A. "Paleozoic Saline bearing formations of the world." 427. Berlin Heidelberg: Springer Verlag, 1984.

Ziegler, A.M., et al. "Paleozoic biogeography and climatology In:." In *Paleobotany, Paleoecology and Evolution*, 231-266. New York: K.J. Niklas(Ed.) Praeger, 1981.

Ziegler, P.,. "Geological Atlas of Western and Central Europe. second ed., Shell Internationale Petroleum Maatschappy." *The Hague.*, 1990: 239 pp.+56 pl.

Zobler, L. "A World Soil File for Global Climate Modelling." In *NASA Technical Memorandum 87802*. New York: NASA Goddard Institute for Space Studies. "Global Soil Types." *Oak Ridge National Laboratory Active Distribution Archive.* 1999. www.daac.ornl.gov.

BIOGRAPHICAL INFORMATION

Amiratu Yamusah earned a Bachelor's Degree from the University of Ghana in 2005. She went on to work with the Ghana National Petroleum Corporation for three years. She then earned her Master's Degree at the University of Texas at Arlington after which she intends to pursue a full time career as a petroleum geologist in the Oil and Gas industry and to play a key role in the newly discovered petroleum deposits in Ghana.